MODIFICATION OF CARBON ELECTRODE MATERIALS WITH ANTHRAQUINONE AND DIHYDROXYBENZENE FUNCTIONALITIES FOR SUPERCAPACITORS

ZAHER ALGHARAIBEH

Modification of Carbon Electrode Materials with Anthraquinone and Dihydroxybenzene Functionalities for Supercapacitors

by

Zaher Algharaibeh

A thesis submitted to the

School of Graduate Studies

in partial fulfillment of the requirements for the degree of

Doctor of Philosophy

Department of Chemistry

Memorial University of Newfoundland

April, 2013

St. John's Newfoundland

Abstract

The main purpose of this thesis was to study the modification of carbon materials with anthraquinone (AQ) and dihydroxybenzene (DHB) functionalities, via diazonium chemistry and electrochemical oxidative polymerization of their amines, and to examine their usefulness as new electrode materials for supercapacitor applications.

High surface area carbon materials have been widely used as electrode materials for supercapacitors. They store charges primarily through an electrostatic double layer charging mechanism which limits their energy density. The need for cost effective supercapacitors with high power and energy densities is crucial for many potential new applications.

Modified electrodes were investigated by one or more of the following techniques: cyclic voltammetry, galvanic cycling, electrochemical impedance spectroscopy, scanning electron microscopy, attenuated total reflectance Fourier transform infrared spectroscopy and elemental analysis.

The performances of the supercapacitors were evaluated by cyclic voltammetry and constant current discharging chronopotentiometry. Ragone plots were used to determine energy and power densities.

Various diazonium coupling approaches were successfully implemented to attach anthraquinone, 3,4-dihydroxybenzene and 3,4-dimethoxybenzene to different types of

carbon electrode materials including carbon fabric (Spectrocarb 2225), Vulcan XC72, Black Pearls 2000 and glassy carbon.

AQ modified carbon fabric was used as a negative electrode with Ru oxide as a positive electrode in a 1 M H_2SO_4 (aq) asymmetric supercapacitor. Better energy and power densities were achieved from this device using 64% less Ru compared to an expensive symmetric Ru oxide device of the same mass as a result of the extended cell voltage and the higher specific capacitance that the AQ modification provides. Replacing the Ru oxide electrode with DHB modified carbon fabric electrode resulted in doubling the energy densities compared to the symmetric unmodified carbon fabric device.

An electrochemical oxidative polymerization approach was successfully used to prepare the following conducting polymers; poly(1-aminoanthraquinone), poly(aniline-co-1-aminoanthraquinone), poly(dimethoxyaniline) on carbon electrodes.

Interestingly, poly(1-aminoanthraquinone) films prepared from 6 M H_2SO_4 (aq) solution showed unusual electrochemical behaviour. These films were extensively studied by cyclic voltammetry and impedance spectroscopy and it was found that the AQ electrochemical activity was strongly affected by the conductivity of the polyaniline-like backbone. Accordingly, a charge trapping phenomenon was recognized.

Acknowledgements

I would like to thank my supervisory committee Dr. Chris Flinn and Dr. Paris Georghiou for their valuable guidance and advice. I would also like to thank all Pickup group members for their useful discussion. My special thanks are extended to Lee Stewart and David Murphy for helping me solve some computer problems.

I wish to acknowledge the help provided by the Centre for Chemical Analysis, Research and Training (C-CART) and the Core Research Equipment and Instrument Training network (CREAIT) to analyse my samples and to get valuable instrumental analysis training.

I highly appreciate the financial support from Memorial University, Defence Research and Development Canada (DRDC) and the Natural Sciences and Engineering Research Council of Canada (NSERC).

I am particularly grateful to my parents, brothers and sisters for their encouragement and support. My grateful thanks are also extended to my friends who made the difficulties insignificant in my eyes.

Finally, I would like express my very great appreciation to my supervisor Dr. Peter Pickup for his support, guidance and sharing his extensive knowledge to make my goals achievable.

Table of Contents

Contents

List of Tables

List of Figures

List of Schemes

List of Abbreviations and Symbols

1,5-DAAQ	1,5-diaminoanthraquinone
1-AAQ	1-aminoanthraquinone
A	ampere
ABA	4-aminobenzylaniline
AQ	anthraquinone
ATR FTIR	attenuated total reflectance Fourier transform infrared
BQ	benzoquinone
C	capacitance
C-AQ	carbon fabric modified with AQ
CB	carbon black
C_{cell}	total electrochemical cell capacitance
C-DHB	carbon fabric modified with DHB
C_{dl}	double layer capacitance
CFP	carbon fiber paper
C_L	film capacitance
CME	chemically modified electrode
CNT	carbon nanotubes
CPEs	carbon paste electrodes
C_{sp}	Specific capacitance
$C_{sp\text{-}2E}$	specific capacitance of 2-electrode cell
$C_{sp\text{-}3E}$	specific capacitance of 3-electrode cell

CV	cyclic voltammetry
DHA	3,4-dihydroxyaniline
DHB	1,2-dihydroxybenzene
DMB	dimethoxybenzene
E'	amplitude of the potential oscillation
$E^{\circ\prime}$	formal potential
EA	elemental analysis
ECDL	electrochemical double-layer
EIS	electrochemical impedance spectroscopy
E_{pa}	anodic peak potential
ESR	equivalent series resistance
F	farad
H_2AQ	reduced form of anthraquinone
i	current
I'	amplitude of current oscillation
i_C	charging current
ICPs	intrinsically conducting polymers
i_F	Faradaic current
IPE	ideal polarized electrode
o-BQ	*o*-benzoquinone
ORR	oxygen reduction reaction
PANI	polyaniline

p-BQ	*p*-benzoquinone
PME	polymer-modified electrode
PVDF	polyvinylidene difluoride
Q	electric charge
R	gas constant
R_{ct}	charge transfer resistance
R_e	electronic resistances
R_i	ionic resistances
R_Σ	sum of R_e and R_i
R_{un}	uncompensated resistance
SCE	saturated calomel electrode
SEM	scanning electron microscope
SWCNT	single-wall carbon nanotube
TMCs	transition metal compounds
V	applied potential across the electrode
v	scan rate
Vulc-ABA	Vulcan XC72 modifed with 4-aminobenzylaniline
Vulc-ABA-BQ	Vulcan XC72 modifed with 4-aminobenzylaniline followed by benzoquinone
Vulcan-DHB	Vulcan XC72 modifed with dihydroxybenzene
Z'	real impedance
Z''	imaginary impedance

Ω	ohm
φ	phase angle between the potential-current oscillations

Chapter 1

Introduction

1.1. Background

Over the past few decades, issues like global warming, environmental pollution, fossil fuel depletion and their effect on the economy have lead scientists to pay more attention to natural energy sources such as the sun and the wind as cheap, environmentally safe and renewable energy resources.[1-7] However, these resources are not effectively available in all regions all the time. Therefore, alternative energy/power devices that store energy when it is available and retrieve it on demand have become of practical importance.[2,8]

There are three promising electrochemical energy devices which are currently being developed to store and/or convert energy in a sustainable and environmentally friendly way. These include fuel cells, batteries and supercapacitors.[1,6,7,9,10] Each of these is an electrochemical cell that consists of two electrodes immersed in an electrolyte solution and are separated from each other by a porous separator that allows ions to pass, but not electrons.

A common feature among these devices is that the transport of electrons and ions is necessarily separated from each other in a closed electric circuit.[1,3,11] Electrons are

transported to or from an electrode via external conductors while positive and negative ions are transported within the electrolyte solution and through the separator to the oppositely charged electrode. In such a cell the energy storage or consumption occurs at the electrode/electrolyte interface.[1,12]

These devices use different materials and have different mechanisms for energy storage and conversion.[1,9,10] Consequently, they have different performances. Fuel cells and batteries are excellent energy storage devices, but they suffer from low power characteristics. However, supercapacitors are excellent power devices with lower energy storage characteristics than batteries and fuel cells. Moreover, supercapacitors can store much higher energy compared to conventional capacitors.[1,12]

Practically, the performance for any given energy storage system can be predicted from its Ragone plot (Figure 1.1.[1]) which relates the specific energy to the corresponding specific power of that system. This figure shows that the combustion engine dominates over the electrochemical devices in terms of both specific energy and specific power. This difference inspires researchers to improve each electrochemical system individually or in combination to compete with combustion engines or to become even better. From the consumer and the industrial point of view, these systems need to have high efficiency, low volume, low mass, and be inexpensive.[8]

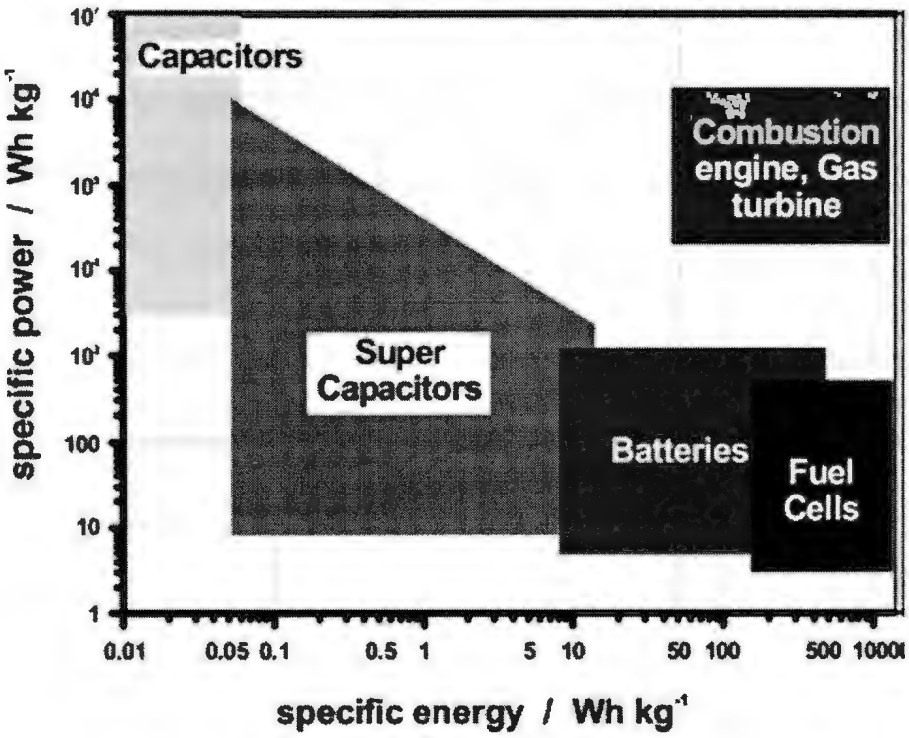

Figure 1.1: Ragone plot shows a performance comparison between capacitors, electrochemical devices and the combustion engine. *Reprinted with permission from ref 1. Copyright 2004 Chemical Review.*

The differences observed between these electrochemical devices are related directly to the physical and chemical properties of their electrodes.[1-3,12] The high energy encountered in fuel cells and batteries is related to the transformation of full electron(s) per atom of the electroactive electrode material during the bulk redox reactions.[4] The occurrence of the redox reactions within the bulk electrode is responsible for the low power densities in both devices.[2]

On the other hand, the energy and power density of supercapacitors are related to their fast capacitive and/or pseudocapacitive characteristics. Considering that the average charge density for a planar electrode is 30 $\mu C\ cm^{-2}$ and an atom density of 10^{15} atoms per

cm^2 then the charge density will be 0.18 moles of electrons per moles of atoms (i.e. 0.18 electron per atom) can be stored at 1V potential in a double layer mechanism.[4] However, pure capacitive electrodes show the highest power density and the longest cycle lives of *ca.* 10^6 cycles.[4,13,14] Pseudocapacitance electrodes have lower power density than pure capacitance electrodes due to the relatively slower kinetics of the redox reaction involved.

For comparison, redox reactions can be present in both supercapacitors and batteries. However, in contrast to batteries, the redox reactions in supercapacitors are not concomitant with phase changes,.[15] In addition, power densities for supercapacitors are higher than that for batteries because the charge delivery process from the surface (in supercapacitors) is always faster than that from the bulk (in batteries).[2]

1.2. Applications of supercapacitors

Since the first commercially available supercapacitors by the NEC Company appeared in Japan in 1971, the application of supercapacitor technology becomes an increasingly growing area.[2] Some examples are: mobile electronics,[2,16] pulse laser technology[2,16] and power tools.[3] Recently, due to environmental issues, supercapacitors have been introduced to the field of transportation such as in hybrid electric vehicles and electric vehicles.[17]

1.3. Definitions and equations

A *Supercapacitor,* also known as an *electrochemical capacitor,* is an electrochemical device that has very high specific capacitance compared to a

conventional capacitor, and has the ability to store and deliver charges very rapidly as a result of ion adsorption and/or fast surface redox reaction(s) at the electrode/electrolyte interfaces.[4]

An *Electrolyte* is any ionic material which maintains a pure ionic conductivity between electrodes in a given electrochemical cell.[1]

A *Separator* is a porous barrier that allows ionic species to pass between electrodes but does not allow electrons to pass. That is, it allows ionic conductivity to be established without the danger of electrical shorting.[1]

An *Ideal polarized electrode* (IPE) is an electrode in which changing the potential across it, within a certain potential window, does not allow charge to pass across the electrode-electrolyte interface.[18] Consequently, charges are accumulated at the electrode/electrolyte interface in the same manner as they do in conventional capacitors.[18]

Current (*i*) is the rate of flow of electrons (or coulombs) that pass through a given point in a conductor, and has a unit of ampere (A), where one ampere is equivalent to one coulomb per second (C/s).[18] The current can flow within electronic conductors, ionic conductors and/or across the interface between them.[15]

The current across an interface, which consists of two different conductors, may refer to a charging current and/or faradaic current.[15]

Charge transport is a macroscopic movement of charges within a single phase only.

Charge transfer is a microscopic process and it represents the flow of faradaic current within a single phase or at the interface between two boundaries and results in a change in the oxidation state of the corresponding species.[15] This process can occur at any interface between two phases: solid-liquid, solid-solid, and solid-gas.[15] The redox reaction that is involved in a charge transfer step may result in neutralization, formation of ions from neutral species, or simply alteration between two different oxidation states.[15] According to this process, diffusion generally occurs to and/or from the electrode interface due to either consumption of the reactants or formation of the products.[15] An exception is when the electroactive groups are part of modified electrode films.

Faradaic current (i_F) is the current passed due to the occurrence of a reduction or oxidation reaction at the electrode/electrolyte interface, i.e. it represents the rate of the redox reaction.[18]

Charging current (i_C) is the current that occurs due to changes in the accumulation of charges electrostatically at the electrode/electrolyte double-layer interface upon changing the potential. Generally, one electrode has an excess of electrons while the other electrode has a deficiency of electrons.[18] The amount of charging current is proportional to the capacitance of the electrode.

Charging occurs when the positive terminal of a DC power source is connected to one electrode of a supercapacitor, while its negative terminal is connected to the second electrode. The flow of charges in this process allows the potential of the negative electrode to move to a more negative limit and the potential of the positive electrode to move to a more positive limit.[1]

Capacitance (C) is a measure of the ability of the supercapacitor to store electric charge (Q) when a potential difference (ΔV) is applied between the two electrodes. It has units of farad (F) and is given by Eq. 1.1. [15]

$$C = \frac{\Delta Q}{\Delta V} \qquad \text{Eq. 1.1}$$

In fact each electrode-interface behaves as a capacitor. Therefore, a supercapacitor is effectively two capacitors connected in series to each other and according to that the total capacitance is given by Eq. 1.2, where C_{cell} is the total capacitance for supercapacitor, C_1 and C_2 are the individual capacitance for each electrode[11].

$$\frac{1}{C_{cell}} = \frac{1}{C_1} + \frac{1}{C_2} \qquad \text{Eq. 1.2}$$

Specific capacitance (C_{sp}) is the capacitance in farad per mass of material in grams (F/g). For a two-electrode cell, the total mass of the two electrodes is considered while in a three-electrode cell only the mass of the working electrode is considered. In general the (specific) capacitance can be elucidated experimentally from cyclic voltammetry, constant current discharge, or impedance techniques.[11]

Cyclic voltammetry (CV) is a transient electrochemical technique in which the potential of a stationary working electrode that is immersed in an unstirred solution is scanned linearly with time until it reaches a certain potential where the scan is reversed linearly.[18]

A *Cyclic voltammogram* is the observed current versus potential plot that is obtained in a cyclic voltammetry experiment.[18] The capacitance can be determined at any instant by Eq. 1.3. where, i is the current in amperes (A) at any given potential and v is the scan rate in volts per second (V/s).

$$C = \frac{i}{v} \qquad \text{Eq. 1.3}$$

Constant current discharging is a chronopotentiometric technique used to discharge the cell at constant current from one potential value to a lower one.

Energy is the ability of a physical system to do work. It is determined by Eq. 1.4.

$$E = \frac{1}{2}CV^2 \qquad \text{Eq. 1.4}$$

E, C, and V are the energy, capacitance and initial voltage, respectively.

Energy density indicates the ability of a single electrode or the whole supercapacitor to do work. It is normally expressed as gravimetric watt-hours per kilogram ($W.h.kg^{-1}$) or volumetric watt-hours per litre.

Power indicates how quickly stored energy can be delivered from a supercapacitor.

Power density indicates how quickly stored energy can be delivered from a single electrode or the whole supercapacitor. It is normally expressed as gravimetric watt per kilogram ($W.kg^{-1}$) or volumetric watt per litre.

A *Ragone plot* is plot of power density versus energy density.

Electrochemical impedance spectroscopy (EIS) is a technique in which the electrochemical cell is exposed to a small-amplitude perturbing sinusoidal voltage signal and measuring the corresponding sinusoidal current over a selected range of frequencies.[18] It is represented mathematically as a complex quantity (Z) given by Eq. 1.5.[15]

$$Z = \frac{E'}{I'} e^{-j\varphi} \qquad \text{Eq. 1.5}$$

$$j = \sqrt{-1} \qquad \text{Eq. 1.6}$$

Where, E' is the amplitude of the potential oscillation, I' is the amplitude of current oscillation, j shown in Eq. 1.6 is an imaginary unit, and φ is the phase angle between the potential-current oscillations. This complex formula can be written in terms of two real quantities Z′ and Z″ as in Eq. 1.7 and Eq. 1.8.[15]

$$Z' = \frac{E'}{I'} \cos\varphi \qquad \text{Eq. 1.7}$$

$$Z'' = -\frac{E'}{I'}\sin\varphi \qquad \text{Eq. 1.8}$$

Where, Z' and Z'' are also called real and imaginary impedance, respectively. Moreover, the absolute value of impedance is evaluated by Eq. 1.9.[15]

$$|Z| = \sqrt{(Z')^2 + (Z'')^2} = \frac{E'}{I'} \qquad \text{Eq. 1.9}$$

The phase angle is given by Eq. 1.10.[15]

$$\varphi = \tan^{-1}(Z''/Z') \qquad \text{Eq. 1.10}$$

A *Nyquist plot* also known as a *complex plane impedance plot* is a plot of the imaginary impedance versus the real impedance for a given electrode or cell.

1.4. Mechanisms of supercapacitors

There are two types of mechanisms that control the charge storage in supercapacitors. These include electrochemical double-layer (ECDL) capacitance and pseudocapacitance. Practically, a given electrode may have one or both mechanisms.[4]

1.4.1. Electrochemical double-layer (ECDL) capacitance mechanism

Electrochemical double-layer (ECDL) capacitance is based on a pure electrostatic (non-faradaic) accumulation of charges (electrons and ions) at the electrode/electrolyte interface (e.g. carbon double-layer interface). This process is very fast and highly reversible because it causes no chemical changes. Consequently, excellent cycle life (*ca.*

10^6 cycles) and power density are achievable.[4] The double-layer interface at any electrode consists of either an excess of electrons with an excess of positive ions or a deficiency of electrons with an excess of negative ions.[13,14] The source of such phenomena is the application of an external potential that causes charge to flow to, or from, the electrode. The capacitance of these kinds of capacitors is generally independent of the applied potential.[15] ECDL behavior is typically characterized by a rectangular shape cyclic voltammogram as shown for glassy carbon (GC) electrode in nonaqueous media, see Figure 1.2.[12]

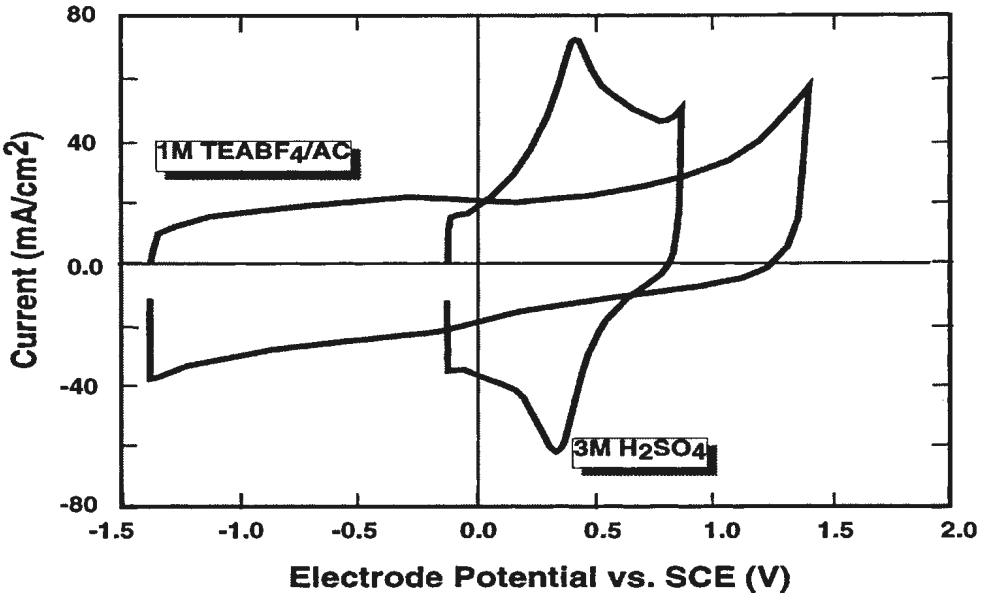

Figure 1.2: Cyclic voltammetry of a bare GC electrode in aqueous and nonaqueous media. *Reprinted with permission from ref 12. Copyright 2000 J. Electrochimica Acta.*

A simplified sketch of an electrochemical double-layer (ECDL) capacitor in the charged state is shown in Figure 1.1. Positive and negative ions are evenly distributed in the electrolyte solution before charging. As the terminals of the capacitor connected to the

power supply, the charging process begins quickly. The positive ions in the electrolyte solution are attracted electrostatically to the high surface area carbon electrode that is connected to the negative terminal of the power supply and the negative ions are attracted to the second carbon electrode which is connected to the positive terminal.

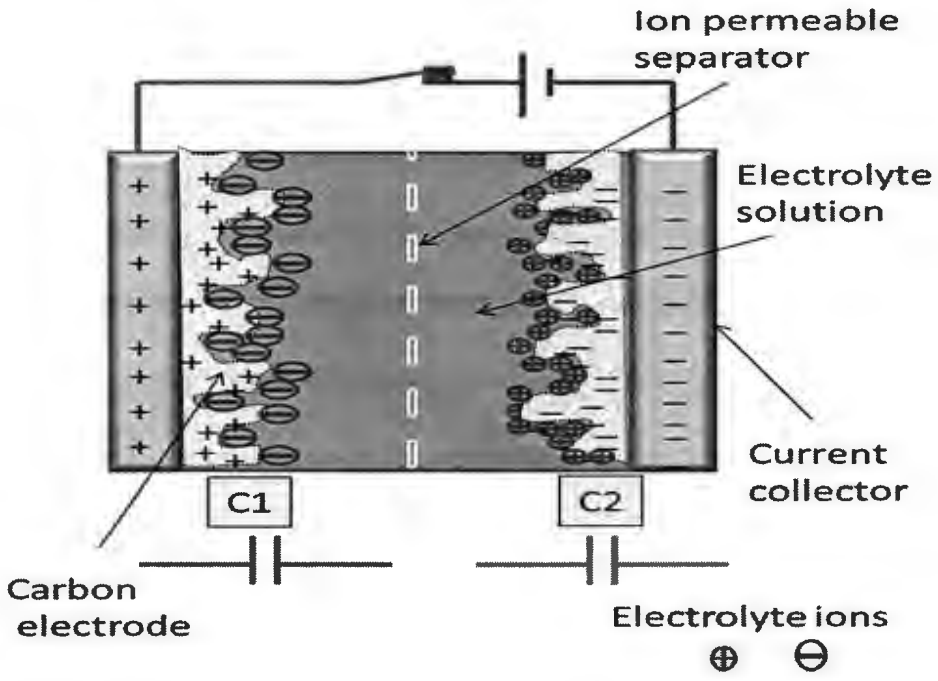

Figure 1.3: Schematic diagram of an electrochemical double layer (ECDL) capacitor in the charged state.

1.4.2. Pseudocapacitance mechanism

Pseudocapacitance is based on surface electron transfer (faradaic) process at an electrode (e.g. metal oxides or conducting polymers).[4] However, it is different from the electron-transfer mechanism that normally occurs in batteries. This is because there is no

phase change accompanying the electron-transfer reaction.[15] Moreover, it is distinguishable from pure capacitance because there is no physical charge accumulation on the electrode/electrolyte interface due to this electron-transfer reaction.

1.5. Classification of supercapacitors

There are different ways to classify supercapacitors. The first way is according to the electrode material, which can be generally one of the following: carbons, metal oxides, metal nitrides,[2] or conducting polymers.[2,4,19-21] A second way is according to the electrolyte used, which can be aqueous, organic, or ionic liquid.[12,13] A third way is according to the electrode configuration, which can be either symmetric or asymmetric. The asymmetric configuration, where the two electrodes are made of different materials, is generally better than the symmetric one in terms of energy and power densities. This is because each electrode can be designed for operation over its optimum potential range to maximize the cell voltage.[5,22-28]

1.6. Materials for supercapacitors

There are some key features that must be fulfilled in any material to be a practical candidate as an electrode material for supercapacitors. These include a high specific surface area of *ca.* more than 1000 $m^2 g^{-1}$, with an optimized pore size distribution and minimum internal resistance, high cycle life, high electrochemical stability during cycling, wide operating potential window, high conductivity, good wettability and good mechanical properties.[2,4,29]

These features are generally present in a wide range of materials such as carbons, metal oxides, metal nitrides, and conducting polymers. Examples are given in Table 1.1. Sarangapani *et al.* [29] reviewed some common electrode materials and made some comparisons between their experimental and theoretical performances.[29] Carbon-based electrodes have been extensively investigated in the literature.[2,11,13,14,30-36] Recently, Simon and coworkers reported the benefit of combining a battery-like electrode, such as a lithium electrode, with a carbon electrode to obtain a high energy supercapacitor.[2] Zhao *et al.* addressed the role of nanostructured materials and their composites in the redox-based supercapacitors.[8]

Table 1.1: Comparison of theoretical and experimental specific capacitance (C_{sp}) values of some electrode materials.

Material	Theoretical C_{sp}, F/g	Experimental C_{sp}, F/g	References
Polyaniline	2000	160 - 815	37-40
Polypyrrole	620	530	21
Polythiophene	485	--	21
PEDOT	210	92	21
Mn oxide	1370	1145	41, 42
Ru oxide	2000	716	35, 43
Ru oxide/CNT	2977	1715	8
CNT	977	20-180	35

1.6.1. Carbon materials

The electronic configuration of elemental carbon determines its physical, chemical and electrochemical properties.[44] There are four different solid allotropes for pure carbon with different hybridizations. These include diamond (tetrahedral, sp^3 hybridization), graphite (hexagonal sheets, sp^2), carbyne (linear, sp^1), and fullerene (spherical, tubular, or ellipsoidal, distorted sp^2).[11] Carbons with sp^2 and distorted sp^2 hybridization have been widely used, and commercially available, as synthetic electrode materials due to their inherent electrical conductivity resulting from π-electron delocalization.[11,45] Moreover, the presence of π-electrons indicates the possibility of chemical modification without losing the entire skeleton structure.[45] However, graphitic-type carbons are electrochemically stable, and behave as ideally polarizable electrodes in aqueous and non-aqueous electrolyte solutions, see Figure 1.2.[12] In practice, the presence of some unavoidable oxygenated groups on the surface of the carbon electrode lead to reversible redox reactions in aqueous media, see Figure 1.2. The ideally polarizable carbon electrodes are ideal for electrochemical double-layer ECDL capacitors in which high reversibility and high cycle stability (*ca.* 10^6 cycles) are desirable for maintenance-free devices[4,12] such as those operating in deep oceans.[3,4,12]

There are many other reasons that make graphitic carbon useful for supercapacitors. These include: high surface area, controlled pore structure,[13,14] good corrosion resistance,[11] high temperature stability,[11,46-48] and relatively low cost.[4,46] One

major limitation of carbon materials is that their specific capacitance is low compared to pseudocapacitance materials such as metal oxides or conducting polymers.[12]

Many forms of engineered porous graphitic carbons have been investigated as electrode materials for supercapacitors.[13,14,46,47] These fall between amorphous forms (disordered hexagonal layers) to graphite (ordered hexagonal layers).[11] Examples are activated carbon,[11] carbon black,[13,14] carbon nanotubes,[8,32] fullerene,[2,30] graphene,[8,30,31,48-50] carbon aerogel,[2] template carbon,[8] onion-like carbon,[2] and carbon fabric.[2,13,30] These materials can be utilized as powder, felt, woven cloth, fiber or as carbon paste made from one form of the carbon mentioned above and a liquid binder such as mineral oil (paraffin oil).[2,11,13,14,51]

Carbon paste electrodes (CPEs) are of interest because they have unique physicochemical and electrochemical properties. CPEs are easy to make and have high stability and conductivity. Although the mineral oil which is used as a binder has a massive resistivity (20-50 ohms), the corresponding carbon paste is highly conductive.[51-53] The reason for this phenomenon is unknown.[51] More importantly, CPEs have versatile and controllable electrochemical behavior. First, the polarization characteristic of CPE can be controlled by controlling the nature and/or the ratio of the paste components. Second, CPEs have a small background current over a potential window of -1 V to +1 V vs. SCE. Finally, CPEs surfaces can be modified to alter their kinetic properties.[51-53]

1.6.1.1. Activated carbons

As mentioned above, various forms of carbon have been widely investigated as supercapacitor materials. The most widely used form is activated carbon because it can be easily produced,[2,11,13,14] with high surface areas (i.e. up to 2500 m^2/g),[11] and at a relatively low cost.[13,14] The particle size of activated carbon is relatively large, ca 20-30 μm in diameter.[45] However, due to the activation process, the particles are highly porous with various pore sizes forming a mixture of micropores (< 2 nm), mesopores (2- 50 nm) and macropores (> 50 nm).[14,15] Controlling the pore size distribution is crucial to the performance of the ECDL capacitors. Practically, this can be carried out by controlling the carbon precursor, the activation method (i.e. chemical or physical)[13] and the activation conditions such as temperature, time, and pressure.[11,13,14] However, the best ways to control the pore size distribution are procedures using templates such as the use of silica templates.[13,14,54] Commercially, activated carbon-based electrodes have limited thickness due to their relatively low conductivity.[2] Therefore, carbon black, which has lower specific area, is generally added to increase their conductivity.[2]

1.6.1.2. Carbon black

Carbon black is produced by thermal decomposition of any carbon precursor in an inert atmosphere.[45] As a result, amorphous spherical particles having diameters of *ca.* 50 nm are formed which may aggregate to form higher particle sizes of about 250 nm.[45,55] Depending on the carbon precursor and decomposition conditions a number of different

forms of carbon black are commercially available, such as Vulcan X72R and Black Pearls 2000.[45]

1.6.1.3. Nanostructured carbon

Recently, a new trend in improving supercapacitors is to utilize nanostructured carbons such as carbon nanotubes,[2,32,56] carbon aerogels,[47,48] graphene[8,48-50] and carbon nanotemplates.[8]

1.6.1.3.1. Carbon nanotubes (CNTs)

Although carbon nanotubes (CNTs) have moderate specific surface areas of *ca.* 200 to 2000 m^2 g^{-1}, they are considered to be promising as electrode materials for supercapacitors.[8] They yield flexible, open porous structures with narrow pore size distribution ranges.[8] As a result, low ionic resistivity and high power density electrodes are obtained.[8] Recently, Futaba *et al.* fabricated a high-density single-wall carbon nanotubes (SWCNT) solid to form flexible micro-electrochemical devices.[56]

There are three major achievable benefits from CNT composites with pseudocapacitance materials such as metal oxides or conducting polymers.[8,13,14] First, they protect the electrode from volume changes during charging/discharging cycles, because they are flexible.[8] Second, the addition of a conducting binder with high weight loading such as carbon black is not necessary.[8] Finally, CNT can be used without a current collector.[8]

1.6.1.3.2. Carbon aerogel

Carbon aerogels are low-density continuous carbon networks[15] prepared from polycondensation of resorcinol and formaldehyde utilizing a sol-gel process followed by pyrolysis.[11] They can be produced as monoliths, thin films, and powders.[11] As continuous network aerogels, they can be used as electrode materials without a binder which allows aerogel carbon electrodes to have lower ionic[47] and electronic resistance[13,47] than activated carbon and carbon black electrodes.[8]

1.6.1.3.3. Graphene

Graphene consists of one atom-thick carbon sheets.[31,48,50] It has very high surface area >2600 m^2 g^{-1} [48,50] and small resistivity compared to activated carbons.[47,48,50] These two significant properties are responsible for the high energy and power density of graphene-based electrode supercapacitors. The thickness is not problematic because the electrical conductivity of *ca.* $2x10^2$ S m^{-1} is high enough.[31,50] Recently, high performance supercapacitors were obtained by covalently bonding aminoanthraquinone to graphene.[52]

1.6.1.3.4. Carbon nanotemplates

CNTs, aerogels, and graphene, are fairly expensive nanomaterials.[2,8] Therefore, as cheaper alternatives, hard nanotemplates made of silica,[8] metal oxides[2,4,8] or polymer beads are used to obtain carbons with controllable pore size distribution.[8]

1.6.2. Transition metal compounds (TMCs)

Transition metal compounds (TMCs) are promising candidates for supercapacitor applications due to their variable oxidation states.[4,42,43,57-60] Hydrous ruthenium oxide is considered to be the best material for supercapacitors with the highest theoretical capacitance of about 2000 F g^{-1} over a wide potential window of *ca.* 1.4 V.[8] In addition, it has a metallic electric conductivity and high chemical stability.[2,4,8,43] However, its widespread application is limited by the high cost of ruthenium itself.[2,4,43] Recently, Liu and Pickup studied and optimized a variety of preparation methods of some potential ruthenium-based materials.[43,57,59,60] Other inexpensive metal oxides and metal nitrides have been widely investigated.[2,4,8]

1.6.3. Intrinsically conducting polymers (ICPs)

In 2000, the Nobel Prize in chemistry was given to Alan G. MacDiarmid, Alan J. Heeger, and Hideki Shirakawa for their efforts in the discovery and development of intrinsically conducting polymers.[19,61-66] Plastic materials were considered insulators before the discovery of conducting polyacetylene by Shirakawa and coworkers in 1977.[61] ICPs, also known as synthetic metals or plastic electronics, have since become widely used in electrochemical studies and applications such as supercapacitors,[2,4,20,21,63] fuel cells,[63,65,68-71] batteries,[63,72,73] sensors[73-76] and solar cells.[77]

The electrical conductivity in CPs can be changed from low to high depending on their doping properties. Fortunately, these properties can be tuned and controlled.[63,66,73,79]

In aromatic-type CPs, the electronic conductivity can be explained through the movement of polarons (radical cations) and bipolarons (dications) along the polymer chain.[72,73]

In a supercapacitor cell composed of two ICP electrodes, π electrons are accepted and are released for one of the electrodes during the charging while the opposite occurs for the other electrode resulting in a reversible doping-undoping process.[4,63,66,73] There are two doping processes in CPs named p-doping and n-doping.[63,64]

p-doping:

$$(\text{Polymer}) + xA^- \leftrightarrow [(\text{Polymer})^{x+}\, xA^-] + xe^- \qquad \text{Eq. 1.11}$$

n-doping:

$$(\text{Polymer}) + yC^+ + ye^- \leftrightarrow [(\text{Polymer})^{y-}\, yC^+] \qquad \text{Eq. 1.12}$$

Aromatic-type CP have several advantages that make them promising as electrode materials in supercapacitors. They have high theoretical capacitance,[4,21] high conductivity, are easy to prepare, and are relatively cheap.[21]

On the other hand, there are two major disadvantages for CPs. First, the cycle life of CP is poor compared to carbon-based electrodes, due to doping or undoping of anions or cations which result in volume change over a few thousand charge/discharge cycles.[4,21,63] Second, the charge/discharge rate is low even for nanostructured CPs.

1.6.3.1. Polymer-modified electrode (PME)

A polymer-modified electrode (PME) is an electrode in which a polymer phase exists between ionically- and electronically-conducting phases (i.e. the electrode and the electrolyte system).[15] Consequently, there are six main regions that must be considered when studying conducting polymer films.[78] Three of them represent the pure bulk regions which include the electrode, the bulk electrolyte system, and the bulk polymer film.[78] The other three regions are the interfacial regions between the electrode/electrolyte, electrode/polymer, and polymer/electrolyte. A proper utilization of any modified electrode depends on understanding the charge transport and transfer that can occur in the bulk regions and at the interfacial regions. Moreover, controlling film thickness and tuning oxidation states of the polymer can be done by electrochemical techniques.[63,64] For example, PANI polymers have a wide range of specific capacitance (*ca.* 44-270 F g^{-1}) depending on the morphology, preparation conditions, and film thickness.

A unique characteristic feature of polymer modified electrodes is that there is no mass transfer of reactant and product to or from the electrode since the electroactive species are inherent components of the polymer chains.[80] Thus, studying such electrodes will give a deep understanding of the charge transfer and charge transport within the electrode films.

1.7. Chemically modified electrodes (CME)

A chemically modified electrode (CME) is an electrode whose surface is modified with a thin film, usually in the range of *n*m to μm thickness, of selected chemicals in order to alter the chemical, electrochemical, optical, or other properties as desired.[15,18,80,81]

There are two main reasons behind modifying a particular electrode. First, it is essential in some applications to alter the inherent electrode properties with more favorable ones.[15,18,80,81] Second, it is helpful in fundamental studies to understand some interfacial properties of certain systems.[15]

Generally, an electrode can be modified by one of the following: covalent bonding, adsorption of insoluble materials or polymer coating, or chemisorption.[81] Murray addressed some of the benefits of using electroactive molecules attached chemically and/or non-chemically to an electrode in his 1980 paper.[81] The most stable modified electrodes are obtained via covalent bonding. A general way to achieve a covalent carbon-carbon bond is via diazonium coupling.[82-85]

Our interest in this work is to modify carbon materials with quinone moieties for supercapacitor applications.[22,28] There are many other potential applications for quinone modified carbons, such as catalysis of the oxygen reduction reaction[86-89] and as anticorrosion coatings.[19]

1.7.1. Carbon electrodes modified via diazonium coupling

It is highly desirable to modify carbon electrodes to improve their mechanical, chemical, and electrochemical properties.[83-85] Carbon electrode materials with sp^2 hybridization can be readily modified with a wide range of organic species through covalent bonding, if a suitable organic modifier is used.[90,91]

1.7.1.1. Chemical diazonium coupling

The formation of a new carbon-carbon bond between two compounds through the reactions of aromatic diazonium salts is well known.[90-93] This idea can be extended to react the aromatic diazonium salt with graphitic-type carbon electrode to modify it with the desired functional group. In general, the modification of the electrode surface can be carried out as desired by changing the functional group in the *p*-position of a phenyl diazonium ion.[90]

The formation of a diazonium salt is based on the reaction between nitrous acid and any salt of a primary aromatic amine; see Eq. 1.13.[92,93]

$$Ar\text{-}NH_2 + 2\,HX + NaNO_2 \rightarrow Ar\text{-}N_2X + NaX + 2\,H_2O \qquad \text{Eq. 1.13}$$

Where X = Cl, Br, HSO_4, NO_3, etc. The "Ar" refers to a mono- or poly-nuclear aromatic unit, and "HX" refers to any mineral or organic strong acid. Sparingly soluble arylamines can be diazotized in a mixture of glacial acetic acid and a mineral acid.[92] Theoretically, two equivalents of mineral acid is a minimum requirement to accomplish a diazotization reaction. Practically, however, an excess is used to prevent the formation of

a triazene (Ar-NHN=N-Ar) due to the reaction of the resulting diazonium ion with the arylamine.[92,93]

The first diazonium salt was prepared by Griess in 1858.[93] Since then a vast number of diazonium salts have been prepared as intermediates for further reactions, or have been separated as final products.[92-94] Aryl diazonium salts are an excellent alternatives to the use of silanes and thiols for covalent binding of species to electrodes.[83,94]

The formation of mono- or multi-layers through diazonium coupling depends on the experimental conditions.[83] Adenier *et al.* reported that dipping a glassy carbon electrode into a solution of 4-nitrobenzene diazonium tetrafluoroborate leads to the spontaneous formation of a multilayer coating.[95] Other systematic studies to modify carbon black under various conditions via chemical diazonium coupling revealed the formation of less than one layer.[96]

Surfaces modified with aryl diazonium salts have some common features such as the formation of covalent bonding, the formation of mono or multilayers and the presence of the azo groups within the layers.[94] However, diazonium coupling starting from an amine instead of a diazonium salt can also result in the formation of a C-N covalent bond as reported by Buttery in 1999.[97] Both the pre-synthesized diazonium salts and the *in situ* preparation of diazonium salts provide similar results in terms of formation of covalent bonding, which addresses the advantage of using the *in situ* approach.[94]

There are five main methods to perform diazotization. These include the direct method, indirect method, Witt method, Griess method, and Knoevenagel method.[92,93] Moreover, diazotization of substituted primary amines can also be conducted in dilute or concentrated acidic media, depending on the basicity of the corresponding arylamine. Weaker basic arylamines need a more concentrated acid than do stronger basic arylamines.[92,93] Diazotization reactions can be carried out in aqueous or organic media.[92,93]

1.7.1.2. Electrochemical diazonium coupling

In 1992, Delamar *et al.* reported a new strategic approach for the modification of carbon materials through electrochemical reduction to overcome the drawbacks of the previously known oxidation approach.[82] The oxidation approach resulted in a high background current due to the corrosion of the carbon modified electrode.

This corrosion was explained as being due to the formation of some undesirable functional groups- such as quinone, ketone, hydroxyl, and carboxylic acid - upon oxidation. Unfortunately, the reaction of these groups with the organic modifier is often uncontrolled, leading to corrosion.[82]

In contrast, the electrochemical reduction of the aryl diazonium salts approach forms stable covalent bonding with the surface and provides a highly resistant surface towards corrosion. Pinson *et al.* reviewed the attachment of organic layers to carbon electrodes via reduction of diazonium salts and discussed the mechanism of such

attachment.[83] The authors also highlighted that the formation of mono or multilayers is controlled by the experimental conditions. Recently, Ceccato *et al.* reported that the formation of conducting organic films of high thickness is possible if the aryl diazonium salt contains an electroactive group such as anthraquinone or a nitro group, probably due to their mediating effect during the electroreduction.[98]

1.7.1.3. Diazonium coupling followed by Michael addition reactions

The reaction of a primary diamine with excess benzoquinone in the presence of an oxidizing agent such as peroxyacetic acid is known to form polyaminoquinone via a Michael addition reaction. [99] In addition, the primary diamine can be covalently bonded to a carbon electrode through diazonium coupling.[100] Therefore, a promising methodology to obtain covalently bonded benzoquinone moieties to a carbon electrode can be carried out by a two-step approach. In the first step, one end of the primary diamine is attached to a carbon electrode through diazonium coupling.[109] This step leaves the other end of the diamine available to react with benzoquinone via a Michael addition reaction in the second step.

1.7.2. Carbon electrodes modified with quinone polymers

Many publications concerning polymer modified electrodes have appearedsince the first that report in 1978.[101] Exploiting different types of electroactive polymers as modified electrodes is based on the electrochemical behavior of the electroactive site(s) in

the respective polymer. This redox behavior may resemble that of the monomer precursor or may be significantly changed due to the polymer structure as a whole.[102,103]

Quinones are organic compounds that contain an unsaturated six-membered ring with two *ortho-* or *para-* carbonyl groups. Examples are: *p*-benzoquinone (*p*-BQ), *o*-benzoquinone (*o*-BQ), naphthaquinone (NQ), anthraquinone (AQ) and phenanthraquinone (PQ).[104] The simplest electroactive unit among organic molecules is the BQ/H_2BQ couple. Introducing this couple to a polymer chain is of considerable importance to many potential applications.[104-114]

Here are some potential applications and findings. For example, Degrand and Miller successfully bound dopamine chemically to poly(methacryloyl chloride) to form a pyridine-soluble quinone polymer which was irreversibly adsorbed on a carbon electrode and showed a catalytic effect towards the oxidation of nicotinamide adenine dinucleotide (NADH).[115] They found that the catalytic efficiency was maximum at critical film thickness and was relatively independent of pH.[115] The thicker polymer film was experimentally observed to have a slower catalytic electron transfer with additional diffusion processes. However, the outermost layers can be charged when using a mixture of aqueous/organic media instead of only aqueous media which facilitates the polymer chain movement leading to easier quinone desorption from the electrode so new H_2BQ sites can reach the electrode.[115]

Kinetics and theoretical modeling of the polymer-modified electrode were developed by Laviron,[116] Saveant.[117] Some factors that complicate the film behaviour are

film swelling, film thickness, electrolyte diffusion phenomena, adsorption, polymer chain motion, and changes in layer structure.[111]

Funt and Hoang synthesised a series of soluble pendant AQ-polystyrene polymers with different AQ spacing.[102] For example, 2-anthraquinone carbonyl chloride reacted with aluminum chloride in dry nitrobenzene to form the soluble poly-[*p*-(9,10-anthraquinone-2-carbonyl)-styrene]-co-styrene (PAQ).[102] Cyclic voltammograms of these polymers showed symmetric reversible peaks at the same potential as for the model compound 2-(*p*-ethylbenzoyl)-9,10-anthraquinone (EBAQ) with a peak current linearly dependant on the square root of the scan rate, indicating the absence of interference between AQ sites.

Another trial by Funt and coworkers was made to stabilize PAQ on a Pt electrode, following deposition from toluene, by irradiating the electrode with ultraviolet (UV) irradiation.[103] The cross-linkage formed in this way stabilized the film and made it inactive in aqueous media. The redox peaks were still identical to the model compound EBAQ with a peak current linearly dependant on the scan rate indicating the behaviour of an adsorbed film. This modified electrode was utilized in the reduction of oxygen in non-aqueous media through a one-electron transfer mechanism. In contrast, Miller prepared a pendant AQ polymer very similar to PAQ but using an amino (-NH-) group instead of the (-CH(phenyl)-) in the main polymer backbone.[115] The presence of the amino group makes the polymer chain more hydrophilic and so the film becomes electroactive in aqueous

media. The reduction of oxygen mediated by AQ that occurs through a $2e^-/2H^+$ mechanism.

The early work done by bonding quinones to polystyrene or polyethyleneimine is only suitable to form thin electroactive films. Gater *et al.* reported an interesting routine electrochemical procedure to form thick electroactive films of 3-2000 monolayers of poly(1,5-diamino anthraquinone) (PDAAQ) on Pt or glassy carbon electrodes.[113] This procedure involves applying a constant potential (1.1 V *vs.* SSCE) for a few minutes in acetonitrile/tetraethyl ammonium perchlorate solution of the DAAQ monomer, with a low speed rotation of the working electrode of 20-70 rpm. Cyclic voltammograms of the polymer film in a monomer-free electrolyte showed the presence of two reversible quinone peaks in addition to the anodic oxidation peaks for the amine polymerization. A linear relation between peak current and scan rates from 20 - 500 mV/s indicates a rapid charge transfer within the polymer film. A prewave was also observed in the cyclic voltammograms.

Gater *et al.* again extended their method to adhere a series of aminonaphthaquinone and aminoanthraquinone polymers, and studied their electroactivity in aqueous solutions over various *p*H ranges.[118] The redox peaks of Q/H_2Q were shifted to negative potentials as the pH increased and electroactivity was maintained only in the acidic aqueous media. Chronoamperometric studies of these polymers showed that reduction of Q was much faster than the corresponding oxidation of H_2Q in aqueous acids.

Yamamoto *et al.* reported the first electro-oxidative polymerization of hydroquinone using a concentration of no less than 50 mM to form poly(dihydroxyphenelene) on a Pt electrode in nitromethane or other solvents with tetraethyl ammonium perchlorate solution using 1.5 V *vs.* Ag/AgCl.[111] Yamamoto proposed that the protonated benzoquinone cation formed electrochemically reacts with hydroquinone to form the polymer. The polymer showed reversible peaks at 0.7 V *vs.* Ag/AgCl in aqueous 70% $HClO_4$ solution. Chemical polymerization to form poly (dihydroxyphenylene) was reported by Sadykh-zade and Razimove, independently.[119]

Organometallic polycondensation of haloaromatic compounds in the presence of zero-valent Ni complexes were successfully used to prepare π-conjugated quinone polymers, including polyanthraquinones.[110] These polymers were soluble in various organic solvents. A series of substituted polyanthraquinone polymers were chemically synthesised by Yamamoto *et al.* starting from certain dichloro monomers, such as dialkoxy AQ, dihydroxy AQ, diamino AQ, and dinitro AQ, using polycondensation with zero-valent Ni complexes.[109] Such polymers were soluble in organic solvents with an average molecular weight of *ca.* 3100-8600 g mol^{-1}. These polymers showed potential applications for electronic and optical devices. Poly(4,8-dinitro-1,5-anthraquinone) was used to construct a photovoltaic cell.

A novel method for preparation of poly(alkylaminoquinones) was reported by Nithianandam and Erhan as anti-corrosive coating. They used a strong oxidizing agent

(i.e. sodium periodate) which permits the use of equimolar quantities of H_2Q and the diamine.[120]

Naoi *et al.* reported their method to design new materials for supercapacitors.[121] Their attempts of electropolymerization of 1,5-DAAQ instead resulted in oligomer. Nevertheless, this oligomer showed promising characteristics. Their method can be explained based on the following findings. Polyaniline is well-known to have high chemical and redox stability in aqueous acidic media[122-125] and it has a high theoretical specific capacitance of 2000 F/g.[38] These advantages make it a useful candidate for use as an electrode material for energy-storage devices, such as supercapacitors and batteries. However, its practical specific capacitance is relatively low, ranging from 160 F g^{-1} to 815 F g^{-1}.[121] The theoretical specific capacitance of benzoquinone, calculated based on a potential range of 0.1 to 0.2 V, ranges from 8934 F g^{-1} to 17870 F g^{-1}.[37] By comparison, the specific capacitance of anthraquinone ranges from 9280 F g^{-1} to 4640 F g^{-1}. Although benzoquinones have the highest specific capacitance they also have serious drawbacks such as instability and the solubility of their corresponding H_2BQ in aqueous media which prevent BQ from having good electrochemical cyclability. Such drawbacks of PANI and BQ can be reduced if a suitable combination of these materials can be made. Another advantage of such a combination was the enhancement of the electron-transfer rate between PANI and BQ due to the H-bond formation between PANI/BQ intermediate complexes. In addition, the composite of PANI and BQ exhibited improved electronic and ionic conductivity in acidic media due to the π-eelectron being free to move in two

dimension and concurrent poroton movment during electron transfer. Consequently enhanced specific power density is obtained.

Li *et al.* synthesised poly(1,5-diaminoanthraquinone) (PDAAQ) chemically using various oxidizing agents (CrO_3, $K_2Cr_2O_7$, K_2CrO_4, or $KMnO_4$ as oxidants in acidic DMF) and various conditions.[114] A novel method was reported to obtain *ca.* 30 nm nanoparticles of PDAAQ. They found that the solubility of various PDAAQ samples was dependent on the polymerization conditions. Consequently, the polymerization could be controlled to match a certain application.

Quinones are naturally-occurring compounds that are very important in photosynthesis and phosphorylation processes since they have the ability to trap the energy of the excited electrons upon exposure to light. Some of these compounds were reviewed by Hodge *et al.*[104] A comparison of some quinone polymers showed that AQ is more likely to be used in electronic devices since it does not contain the active olefin bonds that are present in BQ or NQ. Consequently, AQ has more thermal and chemical stability.

Recently, novel quinone polymers were registered in Japan in a 2009 patent.[126] These polymers were chemically bound to a gel through an aminoacyl group. The gel facilitates a fast electron-transfer reaction when swelling (i.e. there is no electronic interference between quinone groups). Chemically bound aminoacyl groups provide a chemical stability to the polymer and form intramolecular H-bonding with carbonyl groups. In this way, the electron-transfer reaction is not limited by proton diffusion.

Catechol was electropolymerized on ordered mesoporous carbon (OMC) for the first time to form a nano-composite film.[127] This composite was used in sensors to electrocatalyse NADH oxidation. However, such films can be used to catalyze any dehydrogenation processes in biofuel cells and supercapacitors.

Studying the kinetics of electropolymerization is important for investigation of the nature of the polymerization reaction and how the physical properties can be improved.[128] Electropolymerization of 1-AAQ at a Pt electrode in aqueous and nonaqueous solutions was reported by Badawy and coworkers who extensively studied the kinetics. [129,130] In their study the polymerization process was assumed to be primarily due to charge-transfer at the electrode surface. In nonaqueous media the polymerization process was found to be first-order in monomer concentration, while it was zero-order in electrolyte and low levels of water.

So:

$$Rate_{polymerization} = k[AAQ] \qquad \text{Eq. 1.14}$$

Where, k is the heterogeneous rate constant. While in aqueous media, the rate of polymerization was found to also be first-order in the concentration of monomer. Increasing the concentration of sulfuric acid inhibited the rate of polymerization as indicated by the negative slope of the charge density with respect to sulfuric concentration.

1.7.3. Carbon electrodes modified by electrochemical polymerization

Several basic organic monomers and many of their substituted forms can be relatively easily electropolymerized on various electrodes. Examples are pyrroles,[131-133] thiophenes[122] and anilines.[131,134-137] A film is generally produced on the electrode only if the polymerization process is faster than the monomer diffusion process away from the electrode surface.[80] Two types of films can be distinguished based on the nature of the monomer under investigation. These are electroactive and nonelectroactive polymer films.[80]

Electroactive polymer films are usually produced when the polymer remain electroactive at the monomer oxidation potential. Therefore, the polymer/solution interface facilitates further film growth as in the case of polypyrrole films.[80] This type of electropolymerization is important in controlling the film thickness and coating uniformly on the irregular electrode surface. In contrast, polymer films that are nonelectroactive at the monomer oxidation potential are characterized by a rapid growth film at the beginning, followed by a slow electropolymerization until no further film growth can occur due to the passifying effect, as is the case of phenols.[80]

Polyaniline (PANI) is a very attractive conducting polymer because of its chemical stability in air,[137] electrical conductivity,[131] high theoretical specific capacitance *ca.* 2000 F g^{-1} [21,135] and ease of preparation from aqueous solution.[135,137] However, films produced by electropolymerization are thin and brittle[134] which limit their use as electrode materials.[138]

There are two powerful procedures to alter the characteristics of polyaniline. The first is by making a composite with another conducting material such as high surface area carbon.[38,139] The second is by copolymerizing aniline with another substituted aniline monomer.[138,140] Copolymerization is a powerful approach to achieve desirable electrochemical properties that may be very different from the homopolymerization approach.

To facilitate film growth, the addition of a porous conductor is effective.[141] Aniline monomer is efficiently electropolymerized on high porosity carbon electrodes such as activated carbon,[141] carbon nanotubes[39] and graphene.[50] Interestingly, a synergistic effect was reported in the polyaniline/carbon composite in these studies. Faradaic and capacitive currents of the composite were several orders of magnitude larger than for polyaniline alone.[38-40] Moreover, it was found that other conducting polymers such as polypyrrole and polythiophene have no such effect when combined with carbon.[39] The resistance of the PANI/AC was also lower than that of pure PANI or pure activated carbon.[39,141,142]

There are two approaches to electropolymerize aniline onto high surface area carbon, either loading the high surface area carbon onto a glassy carbon electrode followed by electropolymerization of an aniline aqueous acidic solution,[146] or electropolymerization of a dispersed solution mixture of aniline and high surface area carbon.[142] Because the preparation of PANI/CNT composites in organic media is

challenging, the copolymerization of aniline with substituted aniline in organic media may extend the characteristics of PANI/CNTs composite.

Regardless of the above approaches, electropolymerization on carbon can be carried out by three main electrochemical techniques:[143] potentiodynamic, constant current, and constant potential polymerization.[67] The potentiodynamic technique is good for monitoring polymerization of new monomers and for indicating the formal potential of monomer and its polymer[71] while polymerization at constant current allows for better control of the film thickness.[65]

Carbon electrodes have been successfully modified with quinone polymers. For example, 5-hydroxy-1,4-naphthoquinone was electropolymerized on graphite[144,145] while 5-amino-1,4-naphthoquinone was electropolymerized on glassy carbon.[146] The presence of the hydroxyl group in the monomer resulted in the formation of an electroactive polymer film, but it was non-conducting.[144-146] However, the presence of an amino group in the monomer resulted in the formation of an electroactive and conducting polymer film.[146]

1.8. Investigation of porous electrodes

All porous electrodes regardless of their structures can be studied by electrochemical techniques. However, porous electrodes have different characteristics than planar electrodes. As an example, diffusion within porous electrodes depends on the morphology and pore size distribution.[147] Semi-infinite diffusion within porous electrodes

can be observed under certain conditions while under different conditions the porous electrode is considered a series of microelectrodes.[147]

1.8.1. Electrochemical techniques

There are many electrochemical techniques that can be employed to investigate the electrochemical behaviour of porous electrodes. The most widely used techniques in this work are cyclic voltammetry and electrochemical impedance spectroscopy.

1.8.1.1. Cyclic voltammetry (CV)

Cyclic voltammetry is frequently used to acquire qualitative information about a given electrode. Significant thermodynamic and kinetic information of redox species can be rapidly obtained.[63] Single or multiple cycles can be useful to monitor redox positions, coupled chemical reactions and adsorbed species.[63,66] Moreover, specific capacitance and surface concentration can be calculated.[66]

Electropolymerization of a particular monomer was controlled primarily by the cyclic voltammetry in a three-electrode cell. This technique is useful to obtain significant information about the formal potential of the monomer, the onset potential of polymerization and the development of film formation upon cycling can be monitored. Moreover, the CV can be used to monitor the effect of changing any particular experimental condition on the modified electrode.

1.8.1.2. Electrochemical impedance spectroscopy (EIS)

Electrochemical impedance spectroscopy (EIS) is a powerful technique to extract information about chemically-modified electrodes. These information includes: double-layer capacitance, pseudocapacitance, potential-dependant diffusion coefficient, rate of charge transfer, rate of charge transport, and solution resistance. [63,64,148-153] EIS has the ability to distinguish between charge-transfer and charge-transport in conducting polymers and membranes.[151,152] Moreover, a negligible morphology change occurs during the EIS measurements because a small amplitude is used.[63,64,150]

Equivalent circuit models can help to understand the electrochemical behaviour of a given electrode. The transmission line models have been used to explain the electrochemical processes occurring at porous electrodes.[147,151-152] For electrodes with pseudocapacitance character, modified transmission line models have been used.[148,149] Another model called the redox model is accepted to investigate conducting polymers.

1.9. Objectives and thesis outlines

There are several objectives for the work described in this thesis:

1. To explore various methods of quinone attachment to carbon electrodes by:
    a. Chemical and electrochemical modification of different carbon electrodes with anthraquinone, dihydroxybenzene, and dimethoxybenzene precursors through diazonium coupling followed by characterization with electrochemical and non-electrochemical methods.

b. Synthesis and characterization of electrochemically-grafted nitro compounds; and

c. Study the coupling of 1,4-diaminobenzene and 4-aminobenzylamine followed by Michael addition of benzoquinone.

2. Synthesis and characterization of poly(1-aminoanthraquinone).
3. Studying charge trapping in polymer films of poly(1-aminoanthraquinone) in aqueous acids.
4. Synthesis and characterization of copolymers of aniline and 1-aminoanthraquinone.
5. Synthesis and characterization of poly(3,4-dihydroxyaniline).
6. Demonstrate the chemically modified electrodes in asymmetric supercapacitor configuration.

1.10. Thesis outline

1. Introduction
2. Experimental
3. An asymmetric anthraquinone-modified carbon/ruthenium oxide Supercapacitor
4. An asymmetric supercapacitor with anthraquinone and dihydroxybenzene modified carbon fabric electrodes
5. Electrochemical preparation of poly(1-aminoanthraquinone) and its characterization on carbon electrodes

6. Electrochemical copolymerization of aniline with 1-amioanthraqunone on carbon electrodes and its electrocatalytic activity towards O_2 reduction reaction
7. Electrochemical polymerization of dimethoxyaniline on carbon electrodes
8. Miscellaneous methods for modification of carbon electrodes with catechol and benzoquinone moieties
9. Summary and future work

References

(1) Winter, M.; Brodd, R. *Chem. Rev.* **2004**, *104*, 4245-4269.

(2) Simon, P.; Gogotsi Y. *Nat. Mater.* **2008**, *7*, 845-854.

(3) Burke, A. *J. Power Sources* **2000**, *91*, 37-50.

(4) Conway, B. E. In *Electrochemical supercapacitors: scientific fundamentals and technological applications;* Plenum Press: New York, 1999; pp 698.

(5) Miller, J.; Simon P. *Science* **2008**, *321*, 651-652.

(6) Gogotsi, Y.; Simon, P. *Science* **2011**, *334*, 917-918.

(7) Rolison, D. R.; Nazar, L. *Mat. Res. Soc. Bull* **2011**, *36*, 486-493.

(8) Zhao, X.; Sanchez, B.; Dobson, P.; Grant, P. *Nanoscale* **2011**, *3*, 839-855.

(9) Armand, M.; Tarascon, J. *Nature* **2008**, *451*, 652-657.

(10) Cericola, D.; Novak, P.; Wokaun,A.; Kotz, R. *Electrochim. Acta* **2012**, *72*, 1-17.

(11) Pandolfo, A. G. *J. Power Sources* **2006**, *157*, 11-27.

(12) Kötz, R. *Electrochim. Acta* **2000**, *45*, 2483-2498.

(13) Frackowiak, E. *Phys. Chem. Chem. Phys.* **2007**, *9*, 1774–1785.

(14) Frackowiak, E.; Beguin, F. *Carbon* **2001**, *39*, 937-950.

(15) Bard, A.; Inzelt, G.; Fritz, S. In *Electrochemical Dictionary;* Springer: 2008.

(16) Huggins, R. *Solid State Ionics* **2000**, *134*, 179-195.

(17) Verbrugge, M.; Liu, P.. *J. Electrochem. Soc.* **2006**, *153*, A1237-A1245.

(18) Bard, A. J.; Faulkner, L. In *Electrochemical methods: fundamentals and applications;* John Wiley: 2001.

(19) Skotheim, T. A.; Reynolds, J. R. In *Handbook of conducting polymers. Conjugated polymers: processing and applications;* CRC Press: Boca Raton, 2007.

(20) Villers, D. T.; Jobin, D.; Soucy, C.; Cossement, D.; Breau, L.; Belanger, D. *J. Electrochem. Soc.* **2003**, *150*, A747-A752.

(21) Snook, G. A.; Best, A. S. *J. Power Sources* **2011**, *196*, 1-12.

(22) Algharaibeh, Z.; Pickup, P. *Electrochem. Commun.* **2011**, *13*, 147-149.

(23) Duffy, N.; Pandolfo, A. *Electrochim. Acta* **2008**, *54*, 535-539.

(24) Khomenko, V.; Beguin, F. *J. Power Sources* **2010**, *195*, 4234-4241.

(25) Khomenko, V.; Beguin, F. *J. Power Sources* **2006**, *153*, 183-190.

(26) Khomenko, V.; Frackowiak, E.; Beguin, F. *Applied Phys. A* **2006**, *82*, 567-573.

(27) Long, J. W.; Belanger, D.; Brousse, T.; Sugimoto, W.; Crosnier, O. *Mat. Res. Soc. Bull.* **2011**, *36*, 513-522.

(28) Algharaibeh, Z.; Liu, X.; Pickup, P. *J. Power Sources* **2009**, *187*, 640-643.

(29) Sarangapani, S.; Tilak, B.; Chen, C. *J. Electrochem. Soc.* **1996**, *143*, 3791-3799.

(30) Ghosh, A.; Lee, Y. *Chem. Sus. Chem.* **2012**, *5*, 480-499.

(31) Huang, Y.; Liang, J.; Chen, Y. *Small* **2012**, *8*, 1805-1834.

(32) Liu, C.; Cheng, H. *J. Phys. D* **2005**, *38*, R231-R252.

(33) Noked, M. Soffer, A.; Aurbach, D. *J. Solid State Electrochem.* **2011**, *15*, 1563-1578.

(34) Simon, P.; Gogotsi, Y. *Math. Phys. Eng. Sci.* **2010**, *368*, 3457-3467.

(35) Zhang, L. L.; Zhao, X. *Chem. Soc. Rev.* **2009**, *38*, 2520-2531.

(36) Tan, C. W.; Tan, K. H.; Ong, Y. T.; Mohamed, A. R.; Zein, S. H. S.; Tan, S. H. E *Environ. Chem. Lett.* **2012**, *10*, 265-273.

(37) Li, H.; Wang, J.; Chu, Q.; Wang, Z.; Zhang, F.; Wang, S. *J. Power Sources* **2009**, *190*, 578-586.

(38) Hu, C.; Li, W.; Liu, J. *J. Power Sources* **2004**, *137*, 152-157.

(39) Gupta, V.; Miura, N. *Electrochim. Acta* **2006**, *52*, 1721-1726.

(40) Gupta, V.; Miura, N. *J. Power Sources* **2006**, *157*, 616-620.

(41) Lang, X.; Hirata, A.; Fujita, T.; Chen, M. *Nature Nano.* **2011**, *6*, 232-236.

(42) Toupin, M. M.; Brousse, T.; Belanger, D. *Chem. Mater.* **2004**, *16*, 3184-3190.

(43) Liu, X.; Pickup, P. *J. Solid State Electrochem.* **2010**, *14*, 231-240.

(44) Brady, J. In *General Chemistry: Principles and Structure;* 5th; Wiley: 1990.

(45) Dicks, A. *J. Power Sources* **2006**, *156*, 128-141.

(46) Kinoshita, K. Ed.; In *Carbon: electrochemical and physicochemical properties;* Wiley: 1988.

(47) Inagaki, M.; Konno, H.; Tanaike, O. *J. Power Sources* **2010**, *195*, 7880-7903.

(48) Stoller, M.; Park, S.; Zhu, Y.; An, J.; Ruoff, R. *Nano Lett.* **2008**, *8*, 3498-3502.

(49) Wu, Q.; Sun, Y.; Bai, H.; Shi, G. *Phys. Chem. Chem. Phys.* **2011**, *13*, 11193.

(50) Kaiser, A.; Skakalova, V. *Chem. Soc. Rev.* **2011**, *40*, 3786-3801.

(51) Švancara, I.; Vytras, K.; Kalcher, K.; Walcarius, A.; Wang, J. *Electroanalysis* **2009**, *21*, 7-28.

(52) Zima, J.; Barek, J.; Vytras, K. *Crit. Rev. Anal. Chem.* **2009**, *39*, 204-227.

(53) Shamsipur, M.; Golabi, S. M.; Sharghi, H.; Mousayi, M. F. *J. Sold Sate Electrochem.* **2001**, *5*, 68-73.

(54) Pognon, G.; Brousse, T.; Belanger, D. *Carbon* **2011**, *49*, 1340-1348.

(55) Leitner, K. W.; Gollas, B.; Winter, M.; Besenhard, J. *Electrochim. Acta* **2004**, *50*, 199-204.

(56) Futaba, D. D. N.; Hata, K.; Takaeo, Y.; Hiruoka, T.; Hayamizu Y.; Kakadate, Y.; Tanaike, O.; Hatori, H.; Yumura, M. *Nat. Mater.* **2006**, *5*, 987-994.

(57) Liu, X.; Pickup, P. *J. Power Sources* **2008**, *176*, 410-416.

(58) Deng, W.; Ji, X.; Chen, Q.; Banks, C. E. *RSC Adv.* **2011**, *1*, 1171-1178.

(59) Liu, X. ; Trisha, H.; Kopac, M.; Pickup, P. *Electrochim. Acta* **2009**, *54*, 7141-7147.

(60) Liu, X.; Pickup, P. *J. Electrochem. Soc.* **2011**, *158*, A241-A249.

(61) Shirakawa, H.; Edwin, L.; MacDiarmid, A.; Chiange, C.; Heeger, A. *J. Chem. Soc.,Chem. Commun.* **1977**, 578-580.

(62) MacDiarmid, A. *Angew. Chem. Int. Ed.* **2001**, *40*, 2581-2590.

(63) Inzelt , G., Ed.; In *Conducting polymers: A new era in electrochemistry;* Springer; **2005**.

(64) Lyons, M., Ed.; In *Electroactive polymer electrochemistry;* Springer; 1994; Vol. 1.

(65) Stenger-Smith, J. *Prog. Polym. Sci.* **1998**, *23*, 57-79.

(66) Heinze, J.; Frontana, B.; Ludwigs, S. *Chem. Rev.* **2010**, *110*, 4724-4771.

(67) Jagur-Grodzinski, J. *Polym. Adv. Technol.* **2002**, *13*, 615-625.

(68) Jagur-Grodzinski, J. *Polym. Adv. Technol.* **2007**, *18*, 785-799.

(69) Shirakawa, H.; MacDiarmid, A.; Heeger, A. *Chem. Commun.* **2003**, 1-4.

(70) Yin, Z.; Zheng, Q.. *Adv. Energy Mater.* **2012**, *2*, 179-218.

(71) Li, C.; Bai, H.; Shi, G. *Chem. Soc. Rev.* **2009**, *38*, 2397-2409.

(72) Goto, H.; Yoneyama, H.; Togashi, F.; Ohta, R.; Tsujimoto, A; Kita, E.; Ohshima K. *J. Chem. Educ.* **2008**, *85*, 1067-1070.

(73) Inzelt, G.; Pineri,; Schultze, J.; Vorotyntsev, M. *Electrochim. Acta* **2000**, *45*, 2403-2421.

(74) Hatchett, D. W.; Josowicz, M. *Chem. Rev.* **2008**, *108*, 746-769.

(75) Long, Y.; Li, M.; Gu, C.; Wan, M.; Duvall, J.; Liu, Z.; Fan, Z. *Prog. Polym. Sci.* **2011**, *36*, 1415-1442.

(76) Barsan, M. M.; Brett, C. M. A.. *Electrochim. Acta* **2008**, *53*, 3973-3982.

(77) Cheng, Y.; Yang, S.; Hsu, C. *Chem. Rev.* **2009**, *109*, 5868-5923.

(78) Rubinson, J. F.; Koyinamura, Y. *Chem. Soc. Rev.* **2009**, *38*, 3339-3347.

(79) Inzelt, G. *Chem. Biochem. Eng. Q.* **2007**, *21*, 1-14.

(80) Murray, R. *Ann. Rev. Mater. Sci.* **1984**, *14*, 145-169.

(81) Murray, R. *Acc. Chem. Res.* , **1980**, *13*, 135.

(82) Delamar, M.; Pinson, J.; Saveant, J. *J. Am. Chem. Soc.* **1992**, *114*, 5883-5884.

(83) Pinson, J; Podvorica, F. *Chem. Soc. Rev.* **2005**, *34*, 429-439.

(84) Allongue, P.; Desbat, B.; Fagebaume, O.; Hitmi, R.; Pinson, J. *J. Am. Chem. Soc.* **1997**, *119*, 201-207.

(85) Downard, A. *Electroanalysis* **2000**, *12*, 1085-1096.

(86) Griese, S.; Kampouris, D.; Kadara, R.; Banks, C. *Electroanalysis* **2008**, *20*, 1507-1512.

(87) Zhang, G.; Yang, F. *Phys. Chem. Chem. Phys.* **2011**, *13*, 3291-3302.

(88) Tu, X.; Huang, Z.; Jia, X.; Ye, M. *Microchem. Acta* **2008**, *162*, 219-225.

(89) Tu, X.; Huang, Z.; Yang, Q.; Yao, S. *Electroanalysis* **2007**, *19*, 1815-1821.

(90) Toupin, M.; Belanger, D. *J. Phys. Chem. C* **2007**, *111*, 5394-5401.

(91) Toupin, M.; Belanger, D. *Langmuir* **2008**, *24*, 1910-1917.

(92) Zollinger, H. In *Diazo chemistry I: aromatic and heteroaromatic compounds;* VCH Verlagsgesellschaft mbH: **1994**; Vol. I.

(93) Saunders, K. H. In *The aromatic diazo compounds;* Edward Arnold: **1985**.

(94) Mahouche-Chergui, S.; Gam-Derouich, S.; Mangeney, C.; Chehimi, M. M. *Chem. Soc. Rev.* **2011**, *40*, 4143-4166.

(95) Adenier, A.; Cabet-Deliry, E.; Chausse, A.; Griveau, S.; Mercier, F.; Pinson, J.; Vautrin-Ul, C. *Chem. Mater.* **2005**, *17*, 491-501.

(96) Smith, R.; Pickup, P. *Electrochim. Acta* **2009**, *54*, 2305-2311.

(97) Buttry, D.; Donnet, J.; Rebouillat, S. *Carbon* **1999**, *37*, 1929-1940.

(98) Ceccato, M.; Bousquet, A.; Hinge, M..; Pedersen, U.; Daasbjerg, K. *Chem. Mater.***2011**, *23*, 1551-1557.

(99) Mather, B. D.; Viswanathan, K.; Miller, K.; Long, T. *Prog. Poly. Sci.* **2006**, *31*, 487-531.

(100) Lyskawa, J.; Grondein, A.; Belanger, D. *Carbon* **2010**, *48*, 1271-1278.

(101) Fukui, M.; Kitani, A.; Degrand, C.; Miller, L. *J. Am. Chem. Soc.* **1982**, *104*, 28-33.

(102) Funt , B.; Hoang, P. *J. Electrochem. Soc.* **1984**, 131, C328-C328.

(103) Hoang, P. M.; Holdcroft, S.; Funt, B. *J. Electrochem. Soc.* **1985**, *132*, 2129-2133.

(104) Hodge, P.; Gautrot, J. *J. Polym. Int.* **2009**, *58*, 261-266.

(105) Gautrot, J.; Helliwell, M.; Raftery, J.; Cupertino, D. *J. Mater. Chem.* **2009**, *19*, 4148-4156.

(106) Gao, M.; Wang, X.; Zhang, G.; Liu, L. *J. Phys. Chem. C* **2007**, *111*, 17268-17274.

(107) Takada, K.; Ober, C.; Abruna, H. *Chem. Mater.* **2001**, *13*, 2928-2932.

(108) Nishiumi, T.; Yamamoto, K. *Macromolecules* **2003**, *36*, 6325-6332.

(109) Yamamoto, T. *Synlett* **2003**, 425-450.

(110) Yamamoto, T. *Macromolecules* **1998**, *31*, 2683-2685.

(111) Yamamoto, K.; Nishide, H.; Tsuchida, E. *Bull. Chem. Soc. Jpn.* **1990**, *63*, 1211-1216.

(112) Shen, D.; Meyerhoff, M. *Anal. Chem.* **2009**, *81*, 1564-1569.

(113) Gater, V. K. *J. Electroanal. Chem.* **1987**, *235*, 381-385.

(114) Li, X.; Hu, L.; Huang, M. *Chemistry* **2007**, *13*, 8884-8896.

(115) Degrand, C.; Miller, L. *J. Am. Chem. Soc.* **1980**, *102*, 5728-5732.

(116) Laviron, E. A. *J. Electroanal. Chem. Interfacial Electrochem.* **1980**, *112*, 1-9.

(117) Peerce, P. J.; Bard, A. *J. Electroanal. Chem. Interfacial Electrochem.* **1980**, *114*, 89-115.

(118) Gater, V. K.; liu, M.; Love, M.; Leidner, C. *J. Electroanal. Chem. Interfacial Electrochem.* **1988**, *257*, 133-146.

(119) Sadykh-zade, S.; Ragimov, A.; Suleimanova, S.; Liogon'kii, V. *Vyskomol. Soedin. Ser. A* **1972**, 1248.

(120) Nithianandam, V. S.; Erhan S. *Polymer* **1998**, *39*, 4095-4098.

(121) Naoi, K.; Suematsu, S.; Hanada, M.; Takenouchi, H. *J. Electrochem. Soc.* **2002**, *149*, A472-A477.

(122) Zotti, G.; Cattarin, S.; Comisso N. *J. Electroanal. Chem.* **1987**, *235*, 259-273.

(123) Kang, E.; Neoh, K.; Tan, K. *Prog. Polym. Sci.* **1998**, *23*, 277-324.

(124) Huang, J.; Kaner, K. *J. Am. Chem. Soc.* **2004**, *126*, 851-855.

(125) Zengin, H.; Kalayci, G. *Mater. Chem. Phys.* **2010**, *120*, 46-53.

(126) Hiroyuki, N.; Kenichi, K.; Motoshige, S. Quinone Polymer Electrode, Charge Storage Material and Battery Cell. JP 2009217992 (A), Sep 24, 2009.

(127) Bai, J.; Bo, X.; Qi, B.; Guo, L. *Electroanalysis* **2010**, *22*, 1750-1756.

(128) Badawy, W. A.; Medany, S. S. *Int. J. Chem. Kinet.* **2011**, *43*, 141-146.

(129) Ismail, K.; Azzem, M. A.; Badawy, W. A. *Electrochim. Acta* **2002**, *47*, 1867-1873.

(130) Badawy, W. A.; Ismail, K.; Medany, S. S. *Electrochim. Acta* **2006**, *51*, 6353-6360.

(131) Gao, Z.; Ivaska, A. *J. Electroanal. Chem.* **1994**, *364*, 127-133.

(132) Lyons, M.; Fitzgerald, C.; Bannon, T. *Analyst* **1993**, *118*, 361-369.

(133) Wegner, G.; Wernet, W.; Glatzhofer, D.; Ulansk, J.; Krohnke, C.; Mohammadi M. *Synth. Met.* **1987**, *18*, 1-6.

(134) Cao , Y.; Heeger, A. *Synth. Met.* **1992**, *48*, 91-97.

(135) Kang, E.; Tan, K. L.. *Prog. Polym. Sci.* **1998**, *23*, 277-324.

(136) Horvat-Radosevic, V.; Kvastek, K. *J. Electroanal. Chem.* **2008**, *613*, 139-150.

(137) Li, D.; Huang, J.; Kaner, R. *Acc. Chem. Res.* **2009**, *42*, 135-145.

(138) Palaniappan, S.; Manisankar, P. *J. Polym. Res.* **2011**, *18*, 311-317.

(139) Oh, M.; Kim, S. *J. Nanosci. Nanotech.* **2012**, *12*, 519-524.

(140) Lu, J.; Wang, L.; Lai, Q.; Chu, H.; Zhao, Y. *J. Solid State Electrochem.* **2009**, *13*, 1803-1810.

(141) Tamai, H. ; Hakoda, M.; Shono, T.; Yasuda, H. *J. Mater. Sci.* **2007**, *42*, 1293-1298.

(142) Gajendran, P.; Saraswathi, R. *Pure Appl. Chem.* **2008**, 80, 2377

(143) Cosnier, S., Ed.; In *Electropolymerization: concepts, materials and applications;* Weinheim : Wiley-VCH, **2010**.

(144) Pham, M.; Hachemi, A.; Dubois, J. *J. Electroanal. Chem.* **1984**, *161*, 199-204.

(145) Pham, M.; Dubois, J. *J. Electroanal. Chem. Interfatial Electrochem.* **1986**, *199*, 153-164.

(146) Pham, M.; Piro, B.; Bazzaoui, E.; Hedayatullah, M.; Lacroix, J.; Navak, P.; Haas,O. *Synth. Met.* **1998**, *92*, 197-205.

(147) Demenech, A., Ed.; In *Electrochemistry of porous materials; CRC Press;* **2010**.

(148) Gabrielli, C.; Haas, O.; Takenouti, H. *J. Appl. Electrochem.* **1987**, *17*, 82-90.

(149) Ferloni, P.; Matragostino, M.; Meneghello, L. *Electrochim. Acta* **1996**, *41*, 27-33.

(150) Musiani, M. *Electrochim. Acta* **1990**, *35*, 1665-1670.

(151) Pickup, P. *J. Chem. Soc., Faraday Trans.* **1990**, *86*, 3631-3636.

(152) Ren, X.; Pickup, P. *J. Electroanal. Chem.* **1997**, *420*, 251-257.

(153) Albery, W. J.; Chen, Z.; Horrocks, B.; Mount, A.; Wilson, P.; Bloor, D. *Faraday Discuss. Chem. Soc.* **1989**, *88*, 247.

Chapter 2

Experimental

2.1. Introduction

This chapter deals with practical aspects of the work that is considered throughout the entire thesis. In general, a supercapacitor is a device composed of two electrodes, one is designated as the negative electrode while the other as the positive electrode. The negative electrode acts as a cathode during charging but as an anode during discharging, while the positive electrode acts as an anode during charging but as a cathode during discharging.[1,2] However, a new electrode material or modified electrode should be examined in a three–electrode cell configuration to investigate its electrochemical characteristic before its application in a real (two-electrode) device.

2.2. Electrochemical instrumentation

For any electrochemical system there are four basic components that should be present in order to complete the electrochemical process as shown in Scheme 2.1.[3] In general, these include the potentiostat, the function generator, the data-handling system and the electrochemical cell. The first component is the potentiostat which is an analog device that is especially designed to control the potential of the cell instantaneously. The second one is the function generator which is responsible for perturbing the electrochemical cell and converting the signal from digital-to-analog (D/A), as required. Electrochemical techniques can be classified into large amplitude perturbation (e.g. cyclic

voltammetry) or small amplitude perturbation (e.g. electrochemical impedance spectroscopy). The third component is the data handling system in which the signals (e.g. current, potential, time) that resulted from the electrochemical cell according to the perturbation step can be measured and displayed. Data handling along with signal generation are mainly carried out by a microprocessor which is conveniently controlled by suitable software through a personal computer. Before this step the signals from the electrochemical cell should be amplified and converted from analog-to-digital (A/D) signals. The last component is the electrochemical cell where the electrochemical processes take place.

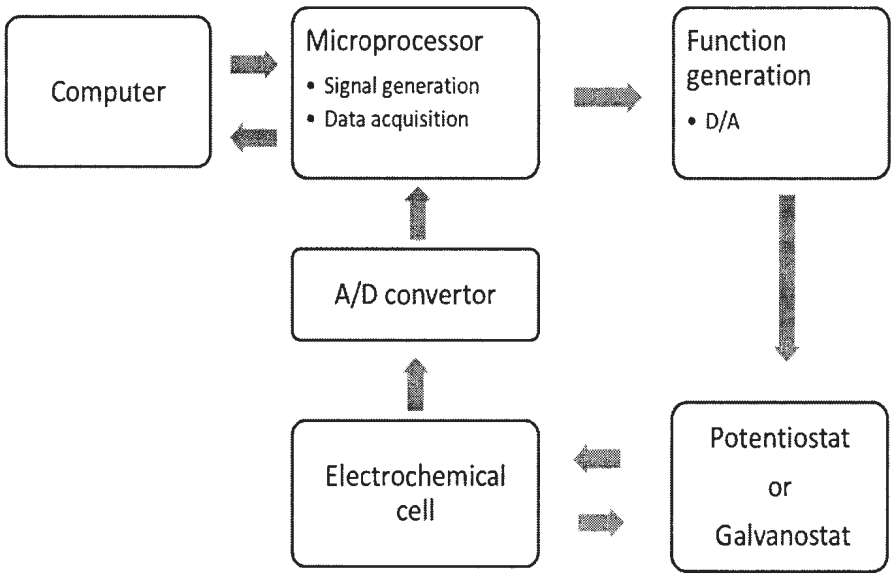

Scheme 2.1: Block diagram of typical electrochemical instrumentation system.

2.3. Electrodes and electrochemical cells

The research described herein has been focused on carbon-based electrode materials. For fundamental studies, glassy carbon (GC) with a flat shiny surface has been used as the working electrode (WE). For this purpose the GC working electrode was polished with an aluminum oxide (alumina; 0.3 μm) slurry on a polishing cloth, then washed with deionized water before being used. A glassy carbon rod (Structure Probe Inc. (SPI); 10 x 3 mm, 0.0707 cm^2) was sealed into a glass tube with epoxy cement. Other glassy carbon electrodes which were sealed in Teflon were also used.

Various types of commercially available carbon materials were examined and/or modified. These include: activated carbon (carbon cloth; Spectrocarb 2225), Vulcan XC 72, Black Pearls 2000, carbon fiber paper (Toray^{TM} TGP-H-090) and glassy carbon. These materials, except GC electrodes, were subjected to modification with some potential redox centres in different ways, without any pretreatment. However, in order to load carbon black (CB) onto carbon fiber paper, a small amount of CB was ground and mixed with appropriate amounts of 5.14% Nafion solution (DuPont) in methanol. Such a mixture was exposed to sonication to form uniform slurry. A drop or two of that slurry was loaded onto the CFP and the solvent (i.e. methanol) was allowed to evaporate.

A platinum wire was used as a counter electrode (CE) in all experiments. In addition, two types of reference electrodes (RE) were routinely used. One was a silver/silver chloride (Ag/AgCl saturated in KCl) electrode which has a potential of 0.197

V vs. normal hydrogen electrode (NHE). The second one was a saturated calomel electrode (SCE), Hg/Hg_2Cl_2 which has a potential of 0.242 V vs. NHE.

Two types of electrochemical cells were used in this work. In each case the electrochemical cell was connected to a potentiostat and was controlled by suitable software using a personal computer. The first type was a two-electrode cell (i.e. analogue to a supercapacitor packaged cell) composed of two working electrodes as shown in Figure 2.1(a). The second type was a three-electrode electrochemical cell which is composed of a working electrode, a reference electrode and a counter electrode as shown in Figure 2.1 (b). As a rule, in the case of the two-electrode setup the whole cell potential was measured while in the case of the three-electrode setup only the half-cell potential (i.e. potential of working electrode vs. potential of the reference electrode) was measured. Therefore, reactions at the working electrode can be best monitored in the three-electrode cell.[4]

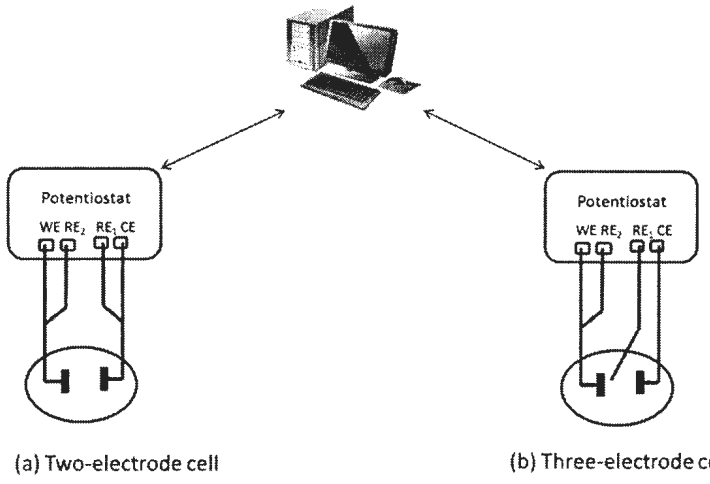

Figure 2.1: Schematic diagram for (a) the two-electrode cell (supercapacitor) and (b) the three-electrode cell.

The three-electrode glass cell was designed in a way that allows close proximity between the working electrode and the reference electrode through a Luggin capillary to minimize the ohmic drop.[3] The flow direction of the inert purge gas (i.e. nitrogen 99.99%) was controlled by a T-shaped stopcock as shown in Figure 2.2. Before any electrochemical measurement, the gas was passed through the electrolyte solution for 20 min to purge off any dissolved oxygen, while during the measurement the T-shaped stopcock was opened in such a way to maintain the inert gas above the solution in order to avoid disturbing the solution and to prevent oxygen gas diffusion from the environment into the electrolyte solution.

Figure 2.2: A photo of a three-electrode electrochemical glass cell. A working electrode was centreed in the middle, a counter electrode was positioned on the left side. A reference electrode was positioned on the right side and was in contact with the electrolyte solution through a Luggin capillary pointed close to the working electrode. A T-shaped stopcock was used to control nitrogen gas flow.

The components of a typical two-electrode cell are shown in Figure 2.3. It was constructed by sandwiching an electrolyte separator (e.g. Nafion™ 112) between two

working electrodes (e.g. two 1 cm^2 carbon cloth electrodes). This separator allows the protons to pass through but not the electrons. Two titanium (Ti) plates that were fixed into polycarbonate blocks were used to make electrical contact. A carbon fiber paper disc (Toray™ TGP-H-090) was placed between each electrode and its Ti current collector to minimize the contact resistance.[5] After assembly of all these parts, the whole cell was immersed in an electrolyte solution such as aqueous 1 M H_2SO_4 containing a reference electrode, and become ready for measurement. Air was not excluded from the cell and all electrochemical measurements were done at room temperature.

For carbon black powder-based electrodes, Nafion solution was used as a binder and to improve the wettability of the electrode which leads to improved electrode capacitance.[5] However, it has lower conductivity within the porous carbons than the conductivity of, for example, aqueous 1 M H_2SO_4 and consequently leads to higher resistance.[5] Therefore, the amount of Nafion solution was optimized.

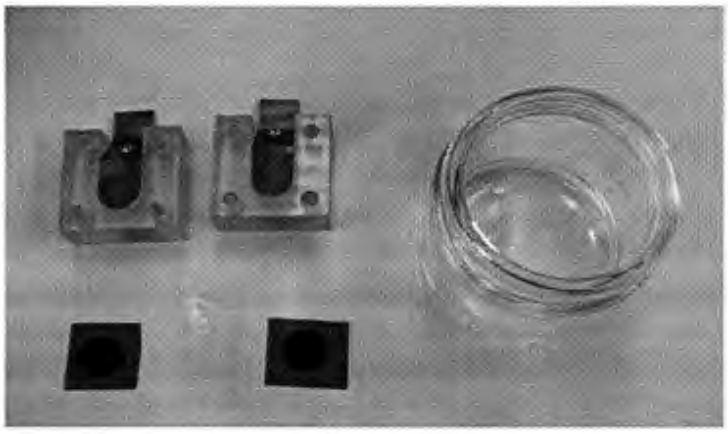

Figure 2.3: Photograph of a typical two-electrode cell consisting of a 50 mL glass jar, two identical polycarbonate square blocks, two titanium plates, two carbon fiber paper discs squares, two carbon electrodes (i.e. carbon cloth) and one colorless Nafion membrane.

2.4. Specific capacitance of two-electrode versus three-electrode configuration

Determination of the specific capacitance in F g^{-1} is crucial to evaluate the effectiveness of an electrode material for supercapacitor applications. Determining C_{sp} based on cyclic voltammetry must be performed after the electrode reaches a steady state cycling response.[4] However, it is unacceptable to report a specific capacitance without referring it to its cell configuration. This is because the calculated values can differ by a factor of four from one another as explained in the following descriptions.[6]

Figure 2.4 (a) shows a schematic diagram for a two-electrode cell in which the two electrodes are connected in series with each other. The total capacitance can be written as in Eq. 2.1.

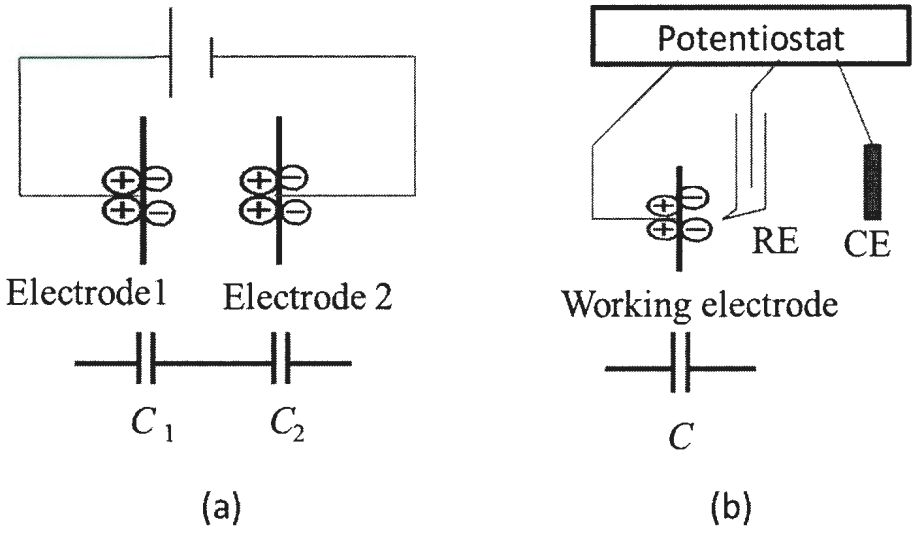

Figure 2.4: Typical electrochemical cell diagrams (a) two-electrode cell and (b) three-electrode cell.

$$\frac{1}{C} = \frac{1}{C1} + \frac{1}{C2} \qquad \text{Eq. 2.1}$$

Assuming that these electrodes are identical and have the same mass (m), their capacitances also will be identical (i.e. $C1 = C2 = C$) and the total capacitance is given as in Eq. 2.2.

$$C_{2E} = \frac{1}{2} C \qquad \text{Eq. 2.2}$$

Therefore, the total specific capacitance ($C_{sp\text{-}2E}$) can be calculated as in Eq. 2.3.

$$C_{sp-2E} = \frac{C_{2E}}{2m} = \frac{1}{4}\left(\frac{C}{m}\right) \qquad \text{Eq. 2.3}$$

However, in case of a three-electrode cell as is shown in Figure 2.4 (b), only one working electrode is considered and the total capacitance is only the capacitance of that working electrode as in Eq. 2.4.

$$C_{3E} = C \qquad \text{Eq. 2.4}$$

Consequently, the total specific capacitance ($C_{sp\text{-}3E}$) can be simply calculated from Eq. 2.5.

$$C_{sp-3E} = \frac{C_{3E}}{m} = \frac{C}{m} \qquad \text{Eq. 2.5}$$

In summary, the specific capacitance calculated based on the three-electrode cell is four times the one calculated based on the two-electrode cell as shown in Eq. 2.6.

$$C_{sp-3E} = 4 \times C_{sp-2E} \qquad \text{Eq. 2.6}$$

2.5. Synthesis of modified carbon electrodes

As a general rule, anthraquinone moieties have been used to modify carbon for use as negative electrodes (anode during discharge) in this work while dihydroxybenzene moieties have been used to modify carbon for use as positive electrodes. In this work, several procedures for modification of carbons as electrode materials for supercapacitors were examined.

A standard three-electrode electrochemical cell was used throughout the experiments. A glassy carbon electrode with a surface area of 0.071 cm^2 was used as the working electrode. Before each experiment the electrode was polished with an aluminium oxide (0.05 μm) slurry on a polishing cloth to obtain a flat shiny surface. A platinum wire was used as the counter electrode while a saturated calomel electrode (SCE) was used as a reference electrode. All electrochemical experiments were conducted under a nitrogen environment after purging the solution with nitrogen gas for 20 min to ensure the absence of oxygen.

2.6. Symmetric and asymmetric cell configuration

It is of major importance to consider which cell configuration is best to use in order to obtain the maximum possible performance out of the electrodes. The energy density of a supercapacitor depends on the capacitance and the square of cell potential.[1,7-9] It is well known that a symmetric cell configuration generally results in a device with a narrow operating cell potential which cannot be extended.[4]

There are two well-known approaches to extend the potential of a supercapacitor. The first approach is to use an organic electrolyte which has a higher potential window than aqueous media. This is useful, but suffers from some practical drawbacks. These include high resistivity which implies lower power density,[4] low capacitance,[10] high cost cells in which moisture must be avoided, and finally, it is not safe to use organic solvents from an environmental prospective.[4, 11] The second approach is to utilize an asymmetric configuration in which two different electrodes that work appropriately over two different potential windows are combined.[4,12-15] This approach is promising since the potential window can be extended and adjusted for aqueous media.[11-13] Moreover, the asymmetric configuration may have lower equivalent series resistance (ESR) than the corresponding symmetric one.[13]

Khomenko *et al.* reported that increasing the cell potential for a manganese oxide/activated carbon capacitor resulted in increase in the specific capacitance but may result in a decrease in the coulombic efficiency and may destroy the capacitive behaviour of the cell.[12] Therefore optimization of the cell potential based on coulombic efficiency is recommended.

2.7. Characterization of modified electrode by electrochemical techniques

The benefits of using an asymmetric configuration over symmetric ones can be recognized by some electrochemical techniques.[4] These include cyclic voltammetry, constant discharge current and electrochemical impedance spectroscopy.

2.7.1. Cyclic voltammetry

Cyclic voltammetry was performed with a RDE4 potentiostat (Pine Instrument company) controlled by CV3 (Colin Cameron) software or alternatively by an EG&G 273A potentiostat controlled by CorrWare software.

In cyclic voltammetry the potential is swept from a certain potential V_1 to another potential V_2 at a specified scan rate, then the potential sweeps in the reverse direction from V_2 to V_1 as shown in Figure 2.5. This waveform can be repeated multiple times where each complete cycle requires 2 t_1. The current response recorded based on this perturbation changes continually according to the electrochemical behavior of the electrode material.

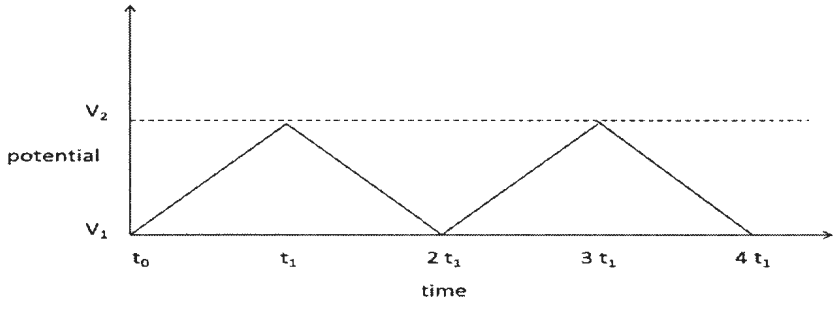

Figure 2.5: Typical waveform of cyclic voltammetry repeated for two cycles.

Because the current response hysteresis depends on the potential, the specific capacitance also depends on the potential window used.

2.7.2. Constant current discharging

Constant current discharge was performed using an EG&G model 273A (Princeton applied research) instrument with CorrWare software as the data acquisition software.

Constant current discharging, also known as chronopotentiometry, is a technique where a constant current is used to fully charge the electrochemical cell to a certain voltage followed by constant current discharging (i.e. voltage decay with time). This technique has been recommended to calculate the cell capacitance using Eq. 2.7.[4]

$$C = \frac{i(t)}{\frac{dV}{dt}} \qquad \text{Eq. 2.7}$$

Where, *i(t)* is the constant discharge current and *dV/dt* is the slope of the discharge curve. Thus, it is used as a proof for the improvement of discharging characteristics after modification. Furthermore, the specific energy and specific power of the supercapacitor device can be calculated from the discharge curve at a particular current. Consequently, Ragone plots can be drawn to evaluate and to compare the performance of the device(s).[1] However, the energy density or the power density of commercial devices depends on the components of the packaged supercapacitors not only the electrode materials.[4]

Typical evaluation of cell resistance can be obtained by constant current discharge by taking into account the initial *i*R drop divided by the applied current as in Eq. 2.8.

$$V = iR \qquad \text{Eq. 2.8.}$$

2.7.3. Electrochemical impedance spectroscopy

Electrochemical impedance spectroscopy (EIS) experiments were performed by combining a Solartron Frequency Response Analyzer (model 1250) with the Solartron Electrochemical interface (model 1286). This combination can provide the appropriate frequency ranges between a low frequency limit up to a frequency higher than the self-resonance frequency (i.e. from *ca.* 0.001 Hz up to *ca.* 5 kHz for electrochemical capacitors).

Data acquisition was done by ZPlot and ZView 2 software (Scribner Associate Inc.). Impedance was used to estimate the cell resistance and consequently evaluate the ability of the cell to provide power through measuring the equivalent series resistance (ESR). However, in commercial supercapacitors (i.e. in the packaged form) the cell resistance depends on all components of the cell not just the electrode resistance. Therefore, the two-electrode cell tested in this work does not fully match the commercial one and validation is necessary.

2.8. Overcharge and overdischarge

There is no problem of overdischarge of a supercapacitor but when it is overcharged it may be destroyed.[4] Although the maximum obtainable energy from a

capacitor is when it is fully discharged, it is practically recommended for a supercapacitor not to be discharged below half of its maximum operating voltage. This is obvious since the energy is directly proportional to the square of the cell voltage. Consequently, only quarter of the total energy will be obtained at half of maximum cell potential.[4] Furthermore, most applications require high voltage.

References

(1) Conway, B. E. In *Electrochemical supercapacitors: scientific fundamentals and technological applications;* Plenum Press: New York, **1999**; pp 698.

(2) Winter, M.; Brodd, R. *Chem. Rev.* **2004**, *104*, 4245-4269.

(3) Bard, A. J.; Faulkner, L. In *Electrochemical methods: fundamentals and applications;* John Wiley: **2001**.

(4) Stoller, M.; Park, S.; Zhu, Y.; An, J.; Ruoff, R. *Nano Letters* **2008**, *8*, 3498-3502.

(5) Liu, X.; Pickup, P. *J. Solid State Electrochem.* **2010**, *14*, 231-240.

(6) Qu, D.; Shi, H. *J. Power Sources* **1998**, *74*, 99-107.

(7) Frackowiak, E.; Beguin, F. *Carbon* **2001**, *39*, 937-950.

(8) Frackowiak, E. *Phys. Chem. Chem. Phys.* **2007**, *9*, 1774–1785.

(9) Pandolfo, A. *J. Power Sources* **2006**, *157*, 11-27.

(10) Burke, A. *J. Power Sources* **2000**, *91*, 37-50.

(11) Khomenko, V.; Beguin, F. *J. Power Sources* **2010**, *195*, 4234-4241.

(12) Khomenko, V.; Beguin, F. *J. Power Sources* **2006**, *153*, 183-190.

(13) Khomenko, V.; Frackowiak, E.; Beguin, F. *Applied Phys. A* **2006**, *82*, 567-573.

(14) Algharaibeh, Z.; Liu, X.; Pickup, P. *J. Power Sources* **2009**, *187*, 640-643.

(15) Villers, D. T.; Jobin, D.; Soucy, C.; Cossement, D.; Breau, L.; Belanger, D. *J. Electrochem. Soc.* **2003**, *150*, A747-A752.

(16) Algharaibeh, Z.; Pickup, P. *Electrochem. Commun.* **2011**, *13*, 147-149.

Chapter 3

An asymmetric anthraquinone-modified carbon/ruthenium oxide supercapacitor

This work has been published in the *J. Power Sources* **2009**, 187, 640-643. This paper was written in part by Dr. Peter Pickup. The work reported was conducted mainly by Zaher Algharaibeh. Ru oxide electrodes and data for the symmetric Ru oxide supercapacitor were provided by Xiaorong Liu.

Abstract

An asymmetric supercapacitor with improved energy and power density, relative to a symmetric Ru oxide device, has been constructed with anthraquinone-modified carbon fabric (Spectracarb 2225) as the negative electrode and Ru oxide as the positive electrode. The performance of the supercapacitor was characterized by cyclic voltammetry and constant current discharging. Use of the anthraquinone-modified electrode extends the negative potential limit that can be used, relative to Ru oxide, and allows higher cell voltages to be used. The maximum energy density obtained was 26.7 Wh kg^{-1} and an energy density of 12.7 Wh kg^{-1} was obtained at a 0.8 A cm^{-2} discharge rate and average power density of 17.3 kW kg^{-1}. The C-AQ/Ru oxide supercapacitor requires 64 % less Ru relative to a symmetric Ru oxide supercapacitor.

3.1. Introduction

Electrochemical capacitors (supercapacitors) are being developed for use in high power electronic devices and electric vehicles.[1-5] Asymmetric or hybrid supercapacitors in which the two electrodes are constructed with different materials are attracting increasing interest because each electrode can be designed and optimized for potential excursions in only one direction.[6,7] This can significantly extend the operating voltage of the device.

We report here on an asymmetric device with an anthraquinone-modified carbon fabric (C-AQ) negative electrode (cathode during charging) and a Ru oxide positive electrode. We have previously shown[8] that anthraquinone-modified carbon fabric is an attractive electrode material for the negative electrode of high power supercapacitors with an aqueous sulfuric acid electrolyte. The redox activity of the AQ provides extra charge at high cell voltages, increasing the energy and power density of the device. Ru oxide is also an excellent electrode material for high power supercapacitors, due to its very high specific capacitance and low resistance.[1,9-17] However, the inferior low potential limit of Ru oxide relative to C-AQ makes AQ-C/Ru oxide asymmetric devices potentially superior to symmetric Ru oxide/Ru oxide devices. The C-AQ/Ru oxide device also has the advantage of lower cost because of the lower mass of Ru required.

3.2. Experimental

3.2.1. AQ-modified carbon fabric electrodes (C-AQ)

AQ-modified Spectracarb 2225 carbon fabric was prepared following a slightly modified version of our previously reported method.[8] Two 1 cm^2 discs (*ca.* 14 mg each) of Spectracarb 2225 carbon fabric (Engineered Fibers Technology) were added to Fast Red Al salt (0.135 g; Acros; anthraquinone-1-diazonium chloride 0.5 $ZnCl_2$) in acetone (15 mL). Water (3 mL) and 50 wt. % hypophosphorous acid (2 mL; Aldrich) that had been cooled in an ice bath were then added. After 30 min in the ice bath with occasional stirring, the Spectracarb discs were collected by filtration, washed well with de-ionized water and then dried at 110 °C for 20 min, and weighed.

Cyclic voltammetry (Pine RDE4 Potentiostat/Galvanostat) was obtained for an AQ-modified electrode in a supercapacitor (see below) by using an Ag/AgCl reference electrode and an unmodified carbon fabric counter electrode.

3.2.2. Ru oxide electrodes

Ru oxide electrodes with a carbon fiber paper support and 5% Nafion binder were prepared by Xiaorong Liu as previously described.[16] Cyclic voltammetry of the Ru oxide on carbon fiber paper was recorded in a conventional glass cell with an EG&G 237A Potentiostat/ Galvanostat.

3.2.3. Supercapacitors

Supercapacitors were constructed by sandwiching an electrolyte separator (Nafion^{TM} 112) between a C-AQ electrode (1cm^2; 15.1 mg) and a Ru oxide electrode (1 cm^2; 8.5 mg Ru oxide + 5.0% Nafion). Ti plates in polycarbonate blocks were used to make electrical contact, and the whole cell was immersed in 1 M H_2SO_4(aq) containing a Ag/AgCl reference electrode. A carbon fiber paper disc (TorayTM TGP-H-090) was placed between the C-AQ electrode and its Ti current collector. Air was not excluded from the cell.

Voltammograms of the C-AQ/Nafion 112/Ru oxide supercapacitor were obtained in two electrode mode (i.e. with the cell acting as a supercapacitor) by connecting the reference lead of the potentiostat (EG&G 273A) to the counter electrode lead. For constant current discharging experiments (EG&G 273A), also in two electrode mode, the supercapacitor was charged for a period of *ca.* 5 min at a cell voltage of 1.3 V.

3.3. Results and discussion

3.3.1. Cyclic voltammetry of the individual electrode materials

Figure 3.1 shows cyclic voltammograms of an AQ-modified carbon fabric electrode, an unmodified carbon fabric electrode, and a Ru oxide electrode in 1M H_2SO_4 (aq). These voltammograms have been normalized with respect to the scan rate and electrode mass to provide a specific capacitance (F g^{-1}) scale. Redox peaks due to the AQ, which are absent in the voltammogram of the unmodified carbon, can be seen at a

formal potential of *ca.* −0.11 V. The average specific capacitance due to the carbon fabric, measured between −0.25 V and 0.8 V, was 199 F g^{-1}, while an average of 482 F g^{-1} was obtained between 0 and −0.25 V for the C-AQ due to enhancement by the redox capacitance of the AQ. Even though this enhanced capacitance occurs over only a narrow potential range, it can provide a disproportionate increase in power and energy density when the C-AQ is used as a negative electrode.[8]

Ru oxide provides a much higher specific capacitance than carbon between 0.0 V and + 1 V, with an average of 770 F g^{-1} seen in Figure 3.1. However, its electrochemistry becomes slow and its capacitance decreases at potentials below 0.0 V. It can be seen from Figure 3.1 that the C-AQ electrode complements the Ru oxide electrode, when used as the negative electrode, by extending the negative potential range and by providing enhanced capacitance at potentials below 0.0 V vs. Ag/AgCl.

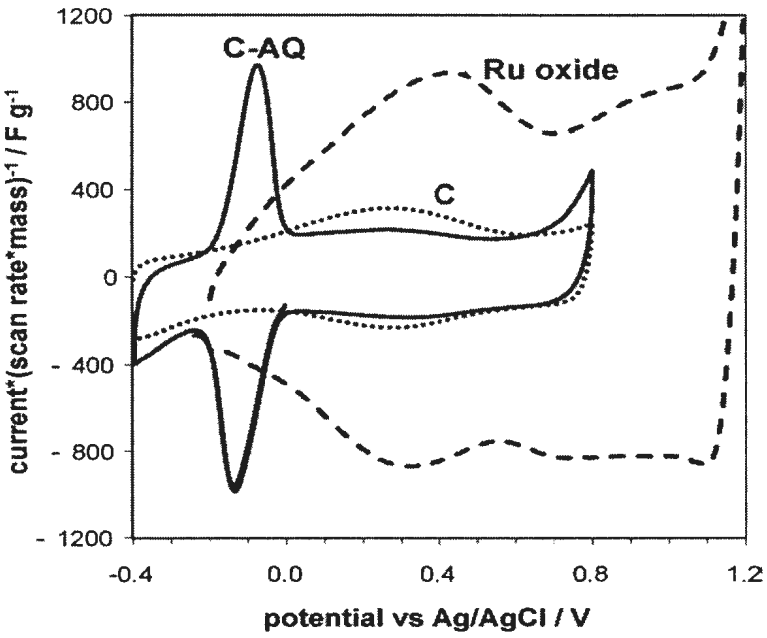

Figure 3.1: Cyclic voltammetry of an AQ-modified Spectracarb electrode (solid line; 14.8 mg; 2 mV s^{-1}), and unmodified Spectracarb electrode (dotted line; 14.3 mg; 20 mV s^{-1}) and a Ru oxide electrode (dashed line; 5.1 mg, 20 mV s^{-1}) in 1 M H_2SO_4 (aq).

3.3.2. Cyclic voltammetry of the supercapacitor

Figure 3.2 shows a cyclic voltammogram of an AQ-C/Ru oxide supercapacitor with the Ru oxide as the working (positive) electrode. Since this voltammogram was recorded in staircase mode, with a long step-time (1 s) determined by the instrument, the currents do not provide an accurate measure of the true specific capacitance. However, the voltammogram does accurately reflect the voltage dependence of the capacitance. The broad peaks centred at *ca.* 0.8 V are due to the reduction (positive scan) and reoxidation (negative scan) of the AQ groups on the surface of the C-AQ electrode that is driven to negative potentials as the supercapacitor is charged. The positions of these peaks can be changed by pre-setting the initial potentials of the electrodes relative to a reference

electrode by employing an external counter electrode. For the experiment reported here, both electrodes were initially set at *ca.* +0.3V vs. Ag/AgCl.

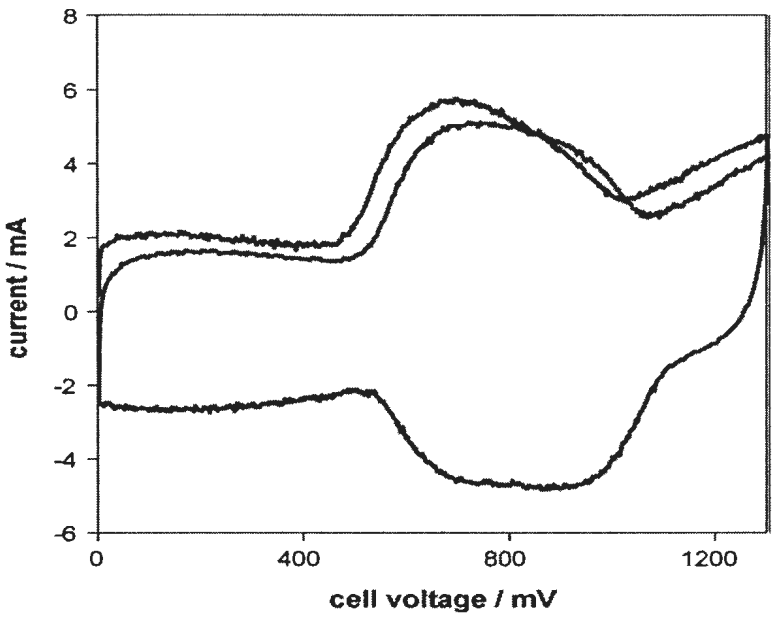

Figure 3.2: Cyclic voltammogram at 2 mV s^{-1} for an AQ-C (15.1 mg)/Nafion 112/Ru oxide (8.5 mg) supercapacitor in 1 M H_2SO_4 (aq).

3.3.3. Constant current discharging

The additional charge storage and release represented by the broad peaks in Figure 3.2 improves the discharge characteristics of the supercapacitor at high cell voltages as shown in Figure 3.3, which compares 10 mA discharge data for an AQ-C/Ru oxide supercapacitor and asymmetric Ru oxide supercapacitor. The slopes of these curves are inversely proportional to the capacitance of the device, and the initial slope is smaller for the AQ-C/Ru oxide device than the symmetric Ru oxide device because of the greater electrode masses employed. This is addressed below in a comparison of the specific capacitances of the two devices.

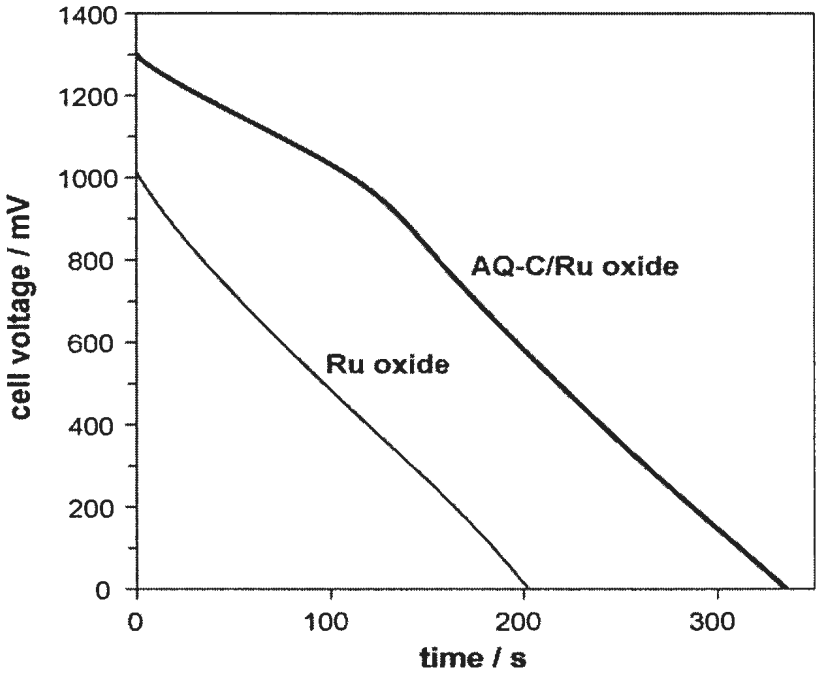

Figure 3.3: Constant current discharge curves at 10 mA for an AQ-C (15.1 mg)/Nafion 112/Ru oxide (8.5 mg) supercapacitor ($V_{initial}$ = 1.3 V) and a Ru oxide (5 mg)/Nafion 112/Ru oxide (5 mg) supercapacitor ($V_{initial}$ = 1.0 V), both in 1 M H_2SO_4 (aq).

The effect of the AQ groups is seen in Figure 3.3 as a lower slope in the discharge curve at high voltages where the AQ groups are being oxidized. The higher slope at potentials below *ca.* 900 mV approximates the slope that would be seen over the full discharge for an asymmetric supercapacitor with an unmodified carbon electrode and a Ru oxide electrode. A key advantage of the AQ-C is that the enhanced capacitance due to the AQ groups maintains a higher cell potential during the first 30% of the discharge and so provides maximum benefit in terms of energy and power density.

The specific capacitance obtained for the C-AQ/Ru oxide supercapacitor from the initial slope (0–100 s) of the 10 mA discharge curve (Figure 3.3) was 159 Fg^{-1}, while the average specific capacitance for discharge to 0V was 109 F g^{-1}. These values are based

on the mass of active materials on both electrodes (i.e. the combined masses of Ru oxide, carbon fabric, and AQ). The symmetric Ru oxide supercapacitor (Figure 3.3) had an average specific capacitance for full discharge of 193 F g^{-1}. Asymmetric carbon fabric device would have a specific capacitance of *ca.* 50 F g^{-1}, based on a specific capacitance of *ca.* 199 F g^{-1} per electrode. An asymmetric unmodified-C/Ru oxide device would have a specific capacitance of *ca.* 95 F g^{-1} based on the slope below 900 mV in Figure 3.3 for the C-AQ/Ru oxide device. It is clear from the comparison of these capacitances that the C-AQ electrode offers an attractive high voltage performance, particularly in light of its much lower cost relative to Ru oxide, and is much better than unmodified carbon.

Discharge curves at higher currents are shown for the C-AQ/Ru oxide supercapacitor in Figure 3.4. The influence of the AQ electrochemistry on the initial slope is still pronounced at 0.1 A and is clear, although less distinct, at 0.8 A. This indicates that the AQ electro-chemistry is sufficiently fast to significantly increase the energy density of the device at high discharge rates.

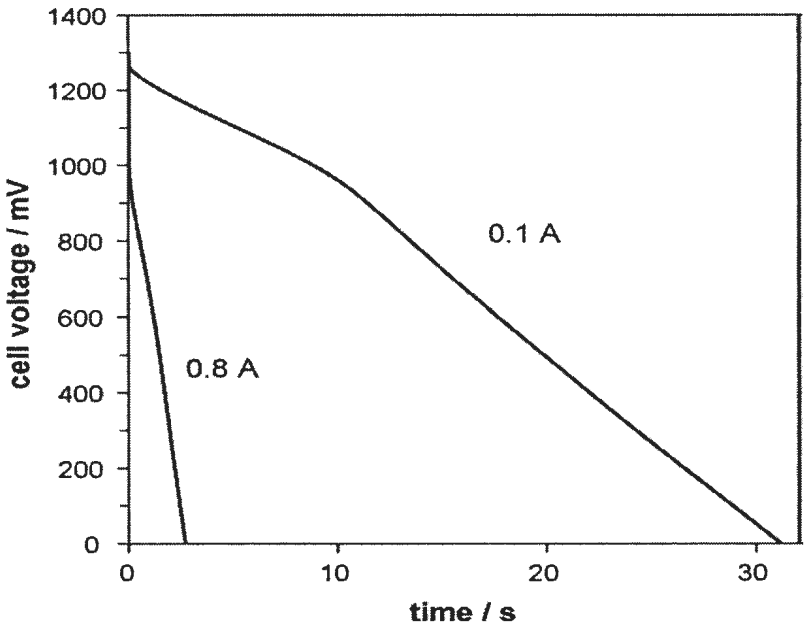

Figure 3.4: Constant current discharge curves for an AQ-C (15.1mg)/Nafion 112/Ru oxide (8.5 mg) supercapacitor in 1 M H_2SO_4 (aq).

Ragone plots for the AQ-C/Ru oxide supercapacitor are shown in Figure 3.4, together with data from Ref.[17] (over a slightly larger range of currents) for a symmetric Ru oxide (10 mg total) device with a Nafion 112 separator. The maximum energy density for the AQ-C/Ru oxide supercapacitor was 26.7 Wh kg^{-1} and an energy density of 12.7 Wh kg^{-1} was obtained at a 0.8 A discharge rate and average power density of 17.3 kW kg^{-1}. The AQ-C/Ru oxide device provided slightly higher energy densities than the Ru oxide device at currents below 0.7 A. It also provided higher power at all currents used.

To properly compare the power densities of the two devices, the results should be scaled to the same mass, since power is theoretically independent of the electrode mass. In practice, the increasing resistance of the electrodes causes the power (and energy density) to drop as the electrode mass is increased, so scaling of the results for the

symmetric Ru oxide device to a mass of 23.6 mg, as shown in Figure 3.5, will overestimate the performance of a 23.6 mg device. However, it is clear from doing this, that both the energy and power densities are higher for the AQ-C/Ru oxide device than they would be for a 23.6 mg symmetric Ru oxide device. Importantly, there would also be a 64% reduction in the mass of Ru required (i.e. 8.5 mg vs. 23.6 mg of Ru oxide).

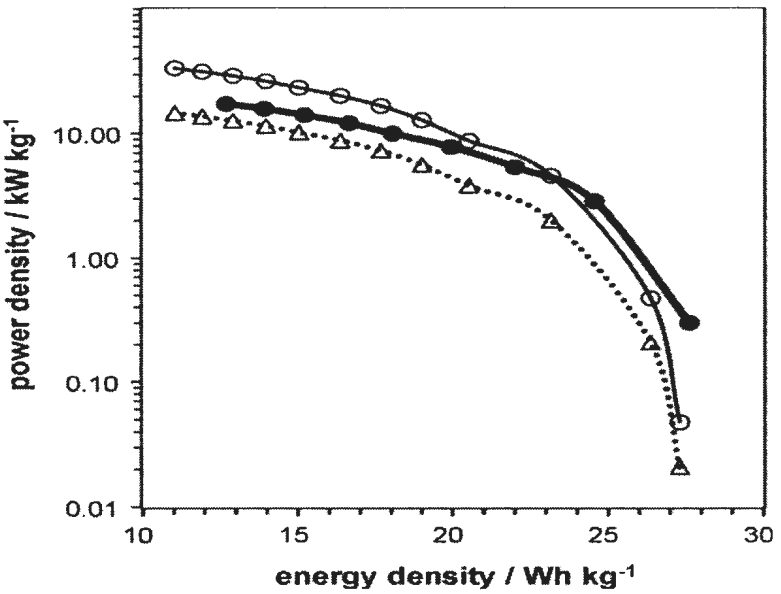

Figure 3.5: Ragone plots for an AQ-C (15.1 mg)/Nafion 112/Ru oxide (8.5 mg) supercapacitor (solid points; $V_{initial}$ = 1.3 V) and a Ru oxide (5 mg)/Nafion 112/Ru oxide (5 mg) supercapacitor (open circles; $V_{initial}$ = 1.0 V; data from Ref. [17]), both in 1 M H_2SO_4 (aq). The open triangles show the data for the symmetric Ru oxide device with the power values divided by a mass of 23.6 mg. All values were calculated for discharge to 0.0 V.

The better performance of the AQ-C/Ru oxide supercapacitor is largely due to its higher operating voltage of 1.3 V relative to 1.0 V for the symmetric Ru oxide supercapacitor. Although it may be possible to operate the symmetric device at higher voltages,[17] the reduced Ru requirement will still make the AQ-C/Ru oxide an attractive alternative. There is also significant scope for improving its performance by use of larger

area electrodes, minimizing contact resistances,[17] and increasing the loading of AQ on the carbon support.

3.4. Conclusions

The AQ-C/Ru oxide supercapacitor described here provides higher energy and power densities than a symmetric Ru oxide device with the same mass, and requires 64% less Ru. In part, the better performance is due to the higher operating voltage. However, the peak shaped redox capacitance of the AQ is also a crucial factor, as is the fact that this capacitance occurs in a potential region close to and beyond the negative potential limit of Ru oxide. Thus the AQ-C electrode has an inherent advantage over Ru oxide as a negative electrode since its negative limit of *ca.* −0.4 V is lower than that of *ca.* −0.2 V for Ru oxide.

Acknowledgments

This work was supported by Defence Research and Development Canada, the Natural Sciences and Engineering Council of Canada (NSERC) and Memorial University.

References

(1) Conway, B. E. In *Electrochemical supercapacitors: scientific fundamentals and technological applications;* Plenum Press: New York, **1999**; pp 698.

(2) Kötz, R. *Electrochim. Acta* **2000**, *45*, 2483-2498.

(3) Winter, M.; Brodd, R. *Chem. Rev.* **2004**, *104*, 4245-4269.

(4) Huggins, R. *Solid State Ionics* **2000**, *134*, 179-195.

(5) Burke, A. *J. Power Sources* **2000**, *91*, 37-50.

(6) Wang, Y.; Xia, Y. *J. Electrochem. Soc.* **2006,** 153, A450.

(7) Khomenko, V.; Frackowiak, E.; Beguin, F. *Applied Phys. A* **2006**, *82*, 567-573.

(8) Kalinathan, K.; DesRoches, D.; Liu, X.; Pickup, X. *J. Power Sources* **2008**, 181, 182.

(9) Zheng, J.; Jow, T. *J. Electrochem. Soc.* **1995**,142, L6.

(10) Zheng, J.; Cygan, P.; Jow, T. *J. Electrochem. Soc.* **1995,** 142, 2699 .

(11) Jang, J.; Kato, A.; Machida, K.; Naoi, K. *J. Electrochem. Soc.* **2006** 153, A321.

(12) Foelske, A.; Barbieri, O.; Hahn, M.; Kotz, R. *Electrochem. Solid State Lett.* **2006**, 9, A 268.

(13) Sugimoto, W.; Iwata, H.; Yokoshima, K.; Murakami, Y.; Takasu, Y. *J. Phys. Chem. B.* **2005** 109, 7330.

(14) Kim, I.; Kim, K. *J. Electrochem. Soc.* **2006**, 153, A383.

(15) Sugimoto, W.; Yokoshima, K.; Murakami, Y.; Takasu, Y. *Electrochim. Acta* **2006** 52, 1742.

(16) Liu, X.; Pickup, P. *J. Power Sources* **2008,** 176, 410.

(17) Liu, X.; Pickup, P. *Energy Environ. Sci.* **2008**, 1, 494.

Chapter 4

An asymmetric supercapacitor with anthraquinone and dihydroxybenzene modified carbon fabric electrodes

This work has been published in the *Electrochem. Commun.* **2011**, 13, 147-149. This paper was written in part by Dr. Peter Pickup. The work reported was conducted by Zaher Algharaibeh.

Abstract

An asymmetric electrochemical capacitor with an enhanced energy density has been constructed by using carbon fabric electrodes modified with complementary functionality: anthraquinone for the negative electrode and 1,2-dihydroxybenzene for the positive electrode. Cyclic voltammetry and constant current discharging were used to evaluate the performance of a supercapacitor with 1 M H_2SO_4 electrolyte and a Nafion separator. Energy densities were found to be double the values obtained for a symmetric device with two unmodified carbon fabric electrodes.

4.1. Introduction

Electrochemical capacitors, also known as supercapacitors, are energy storage devices with the ability to provide higher power densities than batteries.[1-6] Improving the

energy density of such devices without a significant loss in their power density will expand their uses and is essential for some applications such as electric vehicles.[5]

It is now widely recognized that asymmetric supercapacitors, configured from two different electrode materials, provide the best prospects for increasing both energy and power densities.[7-9] In such devices, each electrode can be designed for operation over the optimum potential range to maximize the cell voltage. For example, an asymmetric supercapacitor configured using anthraquinone (AQ) modified high surface area carbon fabric[10] as a negative electrode (anode during discharge) and Ru oxide as a positive electrode provides better energy and power densities than a symmetric Ru oxide device.[11] Although, Ru oxide is considered as an excellent positive electrode material, it is too expensive for commercial applications and suffers from slow kinetics at low potentials.[12,13] We therefore report here on the use of a 1,2-dihydroxybenzene (DHB) modified carbon fabric electrode to replace the Ru oxide positive electrode.

There have been a number of previous reports of the immobilization of 1,2-dihydroxybenzene (DHB; also referred to as o-benzoquinone and catechol) functionality on carbon electrodes.[14-18] The modified electrodes show two reversible two-electron redox processes at standard potentials (pH = 0) of *ca.* 0.4 V and 0.6 V vs. SCE that are well positioned for use in the positive electrode of an asymmetric supercapacitor with an anthraquinone-modified carbon negative electrode. The diazonium coupling of 1,2-dihydroxybenzene to carbon should be more effective than the methods reported in refs.[14-18] and is reported for the first time here.

4.2. Experimental

4.2.1. Materials

Spectracarb 2225 carbon fabric (Engineered Fibers Technologies) and 4-aminocatechol (Tyger Scientific Inc.) were used as received. AQ modified carbon fabric (C-AQ) was prepared as previously described.[11]

4.2.2. DHB-modified carbon fabric electrodes (C-DHB)

To modify Spectracarb 2225 carbon fabric with 1,2-dihydroxybenzene functionality, two 1 cm^2 discs were immersed in 2 ml of 0.25 M HCl and then *ca.* 0.01 g of 4-aminocatechol and water (8 mL) was added. Following cooling in an ice bath, 0.0243 M $NaNO_2$ (2 mL) was slowly added. After a further 30 min in the ice bath, the modified discs were collected, washed well with deionized water, and dried in air overnight. The loading of DHB, determined from the increase in dry mass of the carbon disc, was 3.6 mass %.

4.2.3. Supercapacitors

An asymmetric supercapacitor was configured with an AQ-modified spectrocarb electrode (1 cm^2; ~15.5 mg) and a DHB-modified Spectracarb electrode (1 cm^2; ~15.5 mg) by placing a Nafion™ 112 electrolyte separator between them. Each electrode was separated by a carbon fiber disc (Toray™ TGP-H-090) from a Ti plate current collector in a polycarbonate block in order to minimize the contact resistance.[13] The assembled cell was immersed in 1 M H_2SO_4 (aq) in order to saturate the electrode with the electrolyte.

Air was not excluded since it was found not to have a discernible influence on the voltammetric behaviour of the electrodes.

Cyclic voltammograms for the asymmetric C-AQ/C-DHB supercapacitor were obtained using an EG&G 273A potentiostat in a two electrode mode in which the C-AQ electrode was connected to the reference and counter leads of the potentiostat while the C-DHB electrode was connected to the working electrode lead. The same instrument was used with the same connections in constant current discharging experiments. The supercapacitor was charged for 5 min at 1.2 V before discharging. Cyclic voltammograms of the individual electrodes were obtained in the same cell, with an Ag/AgCl reference electrode immersed in the H_2SO_4 (aq) electrolyte, and the other C-X electrode acting as the counter electrode. Specific capacitances, energy densities, and power densities were calculated by using just the electrode masses, which were summed for both electrodes for measurements in a two-electrode mode.

4.3. Results and discussions

4.3.1. Cyclic voltammetry of the electrode materials

Figure 4.1 shows cyclic voltammograms (CV) of unmodified, AQ-modified, and DHB-modified carbon fabric electrodes. The current axis has been normalised with respect to scan rate and electrode mass to provide the specific capacitance. The DHB-modified carbon cloth electrode shows an average specific capacitance of 201 F g^{-1} between 0.2 and 0.8 V while an average of 141 F g^{-1} was found for the unmodified carbon cloth electrode over the same potential range. The approximately 43% increase in

specific capacitance over the relatively wide positive potential range is due to the reversible DHB redox processes, which produce pseudocapacitance waves at 0.41 V and 0.65 V. The presence of two peaks for DHB is a result of using 4-aminocatechol as a precursor which has two different ways of bonding with carbon fabric, either through a C–C linkage (Structure 1, Scheme 4.1) or a C–N linkage (Structure 2, Scheme 4.1).[14-16]

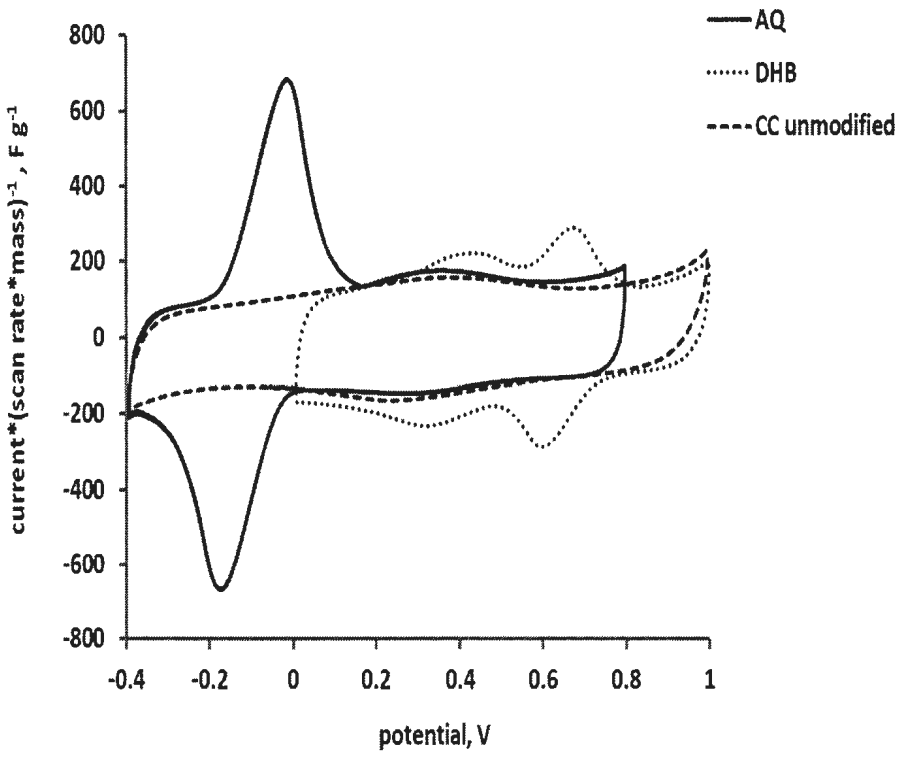

Figure 4.1: Cyclic voltammetry (20 mV/s) of C-AQ (solid line; 15.7 mg), C-DHB (dotted line; 15.6 mg) and unmodified-C (dashed line; 15.3 mg) in (aq) 1 M H_2SO_4. Currents have been normalised with respect to scan rate and electrode mass.

AQ also produces an appreciable enhancement in capacitance over a *ca.* 0.35 V range encompassing the formal potential of the AQ functionality (*ca.* −0.05 V). Over this range the average specific capacitance of the C-AQ electrode was 367 F g^{-1}. Significant peak separations are seen in Figure 4.1 due to the uncompensated resistance of the cell and the large currents involved.

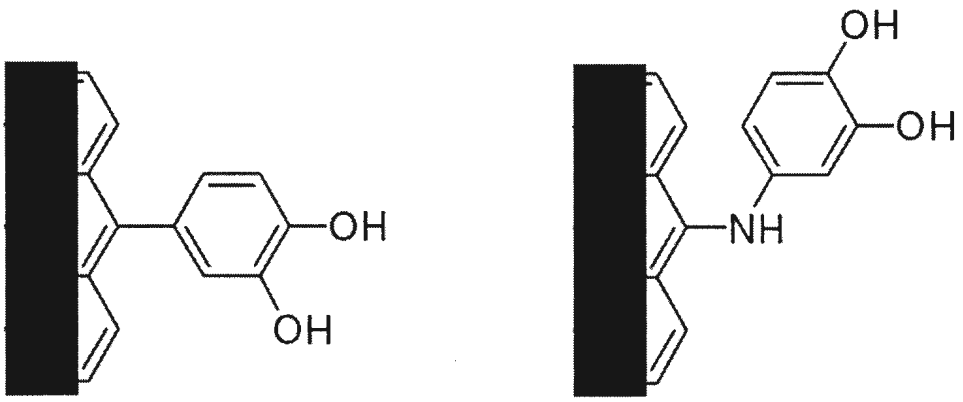

Structure **1** Structure **2**

Scheme 4.1: Possible grafting of 4-aminocatechol to carbon.

The voltammetric responses of the DHB and AQ moieties seen in Figure 4.1 were persistent over many cycles, indicative of covalent immobilization on the carbon surface. In the case of C-AQ, this has been previously documented.[10] For C-DHB, 36 cycles between −0.1 and +0.8 V at 20 mV s^{-1} resulted in only minor changes in the voltammetric behaviour, with no significant change in the average specific capacitance.

4.3.2. Cyclic voltammetry of the asymmetric supercapacitor

Figure 4.2 shows cyclic voltammograms for the asymmetric supercapacitor before and after several charging and discharging cycles. The two broad overlapping peaks between 0.2 and 1.0 V are due to the reversible faradaic processes for both AQ and DHB. Using DHB as the working electrode, AQ is reduced and DHB is oxidized during charging while the AQ is re-oxidized and DHB is re-reduced upon discharging the device. The presence of the reversible redox processes of both AQ and DHB enhance the energy and power densities of the device, which can be regarded as a combination of an electrochemical double layer capacitor and a high power battery.

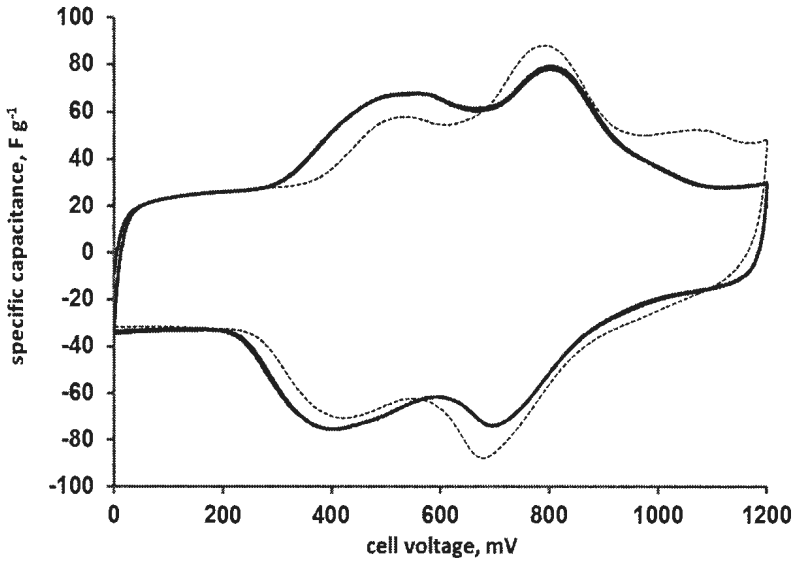

Figure 4.2: Cyclic voltammetry (two-electrode mode) in 1 M H_2SO_4 (aq) of a C-AQ (15.5 mg)/Nafion112/C-DHB(15.6 mg) supercapacitor before (solid) and after (dashed) several charging and discharging cycles, normalised with respect to scan rate (20 mV/s) and the combined mass of the two electrodes.

The differences between the two curves shown in Figure 4.2 are due to drift of the potentials of the electrodes. Since the reference electrode was not used in this experiment, there is no stable reference potential. During repeated charging and discharging, the potential that both electrode return to at full discharge can vary with time. The similarity of the two curves shows that this is a relatively minor effect.

4.3.3. Constant current discharging

Figure 4.3 shows the discharge behaviour of an asymmetric C-AQ/C-DHB supercapacitor and a symmetric unmodified C/C supercapacitor at 0.2 A cm^{-2}. Both capacitors gave similar discharge slopes at high voltages revealing that the asymmetric capacitor has no redox contributions to the charge released at potentials above *ca.* 0.7 V. This is consistent with the cyclic voltammograms shown in Figure 4.2 if the effect of the effective series resistance (ESR) is considered. The redox behaviour of AQ and DHB becomes obvious, however, at cell voltages between 0.7 V and 0.2 V where the slope is much lower for the C-AQ/C-DHB device. In this region, the average specific capacitance was 63 F g^{-1} for the C-AQ/C-DHB capacitor compared to 30 F g^{-1} for the unmodified carbon capacitor. This increase in capacitance leads to enhanced power and energy densities (Table 4.1).

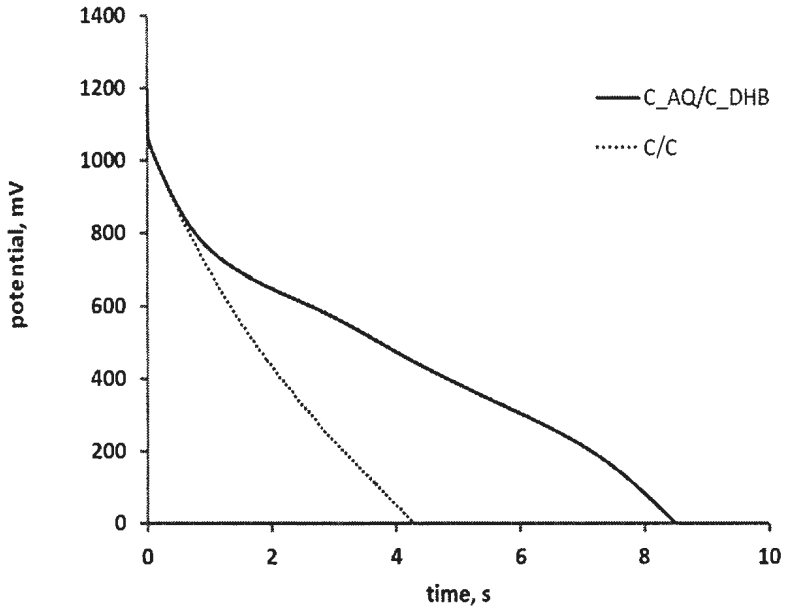

Figure 4.3: Constant current discharging curves at 0.2 A for asymmetric C-AQ(15.5 mg)/ Nafion112/C-DHB (15.6 mg) (thick line) and symmetric C(15.3 mg)/C(15.3 mg) supercapacitors in 1 M H_2SO_4 (aq).

Table 4.1 shows energy and power densities for the two capacitors obtained from constant current discharging in a two-electrode mode. The C-AQ/C-DHB device provided approximately double the energy density of the unmodified carbon device over the current range tested. Power densities (averaged over full discharge) were better for the C-AQ/ C-DHB device at low currents, reflecting its higher average voltage during discharge (Figure 4.3). However, the unmodified carbon device exhibited a lower ESR and therefore better power densities at high currents. The difference in ESR is thought to have been caused by differences in the compression of the two devices rather than the modification of the electrodes. With optimization, the C-AQ/C-DHB supercapacitors should provide higher power densities than C/C supercapacitors at all discharge rates.

Table 4.1: Energy (E_S) and average power (P_S) densities for symmetric C/C and asymmetric C-AQ/C-DHB supercapacitors, for constant current discharging from 1.2 V. The combined electrode masses were 30.6 mg and 31.1 mg, respectively.

Current/ A	C/C		C-AQ/C-DHB	
	E_S/Wh kg^{-1}	P_S/kW kg^{-1}	E_S/Wh kg^{-1}	P_S/kW kg^{-1}
0.01	5.2	0.16	10.0	0.18
0.1	4.2	1.5	8.3	1.7
0.2	3.5	2.9	7.0	3.0
0.3	2.9	4.1	5.9	4.0
0.4	2.5	5.2	4.9	4.8
0.5	2.1	6.2	3.9	5.4
0.6	1.8	7.0	3.2	5.8
0.7	1.5	7.6	2.5	6.2
0.8	1.2	8.2	2.0	6.3
0.9	0.99	8.5	1.5	6.4
1.0	0.80	8.8	1.1	6.3

4.4. Conclusions

The energy density of an aqueous carbon fabric supercapacitor has been doubled by immobilizing different redox species on each electrode to create an asymmetric device. Anthraquinone was used to provide redox pseudocapacitance at negative potentials, while dihydroxybenzene provided redox pseudocapacitance at positive potentials. This results in a combination of battery-like and capacitive behaviour.

Acknowledgments

This work was supported by the Defence Research and Development Canada, the Natural Sciences and Engineering Council of Canada (NSERC) and the Memorial University.

References

(1) Conway, B. E. In *Electrochemical supercapacitors: scientific fundamentals and technological applications;* Plenum Press: New York, **1999**; pp 698.

(2) Kötz, R. *Electrochim. Acta* **2000**, *45*, 2483-2498.

(3) Winter, M.; Brodd, R. *Chem. Rev.* **2004**, *104*, 4245-4269.

(4) Huggins, R. *Solid State Ionics* **2000**, *134*, 179-195.

(5) Burke, A. *Eelectrochem. Acta* **2007** 53, 1083.

(6) Hollenkamp, F.; Pandolfo, A. *J. Power Sources* **2006** 157, 11.

(7) Khomenko, V.; Frackowiak, E.; Beguin, F. *Applied Phys. A* **2006**, *82*, 567-573.

(8) Khomenko, V.; Frackowiak, F.; Beguin, F. *Appl. Phys. A., Mater. Sci. Process.* **2006**, 82, 567.

(9) Duffy, N.; Baldsing, W.; Pandolfo, A. *Electrochim. Acta* **2008** 54, 535.

(10) Kalinathan, K.; DesRoches, D.; Liu, X.; Pickup, X. *J. Power Sources* **2008**, 181, 182.

(11) Algharaibeh, Z.; Liu, X.; Pickup, P. *J. Power Sources* **2009**, 187, 640.

(12) Liu, X.; Pickup, P. *J. Power Sources* **2008**, 176, 410.

(13) Liu, X.; Pickup, P. *Energy Environ. Sci.* **2008**, 1, 494.

(14) Buttry, D.; Peng, J.; Donnet, J.; Rebouillat, S. *Carbon* **1999**, 37, 1929.

(15) Wildgoose, G.; Masheter, A.; Crossley, A.; Jones, J.; Compton, R. *Int. J. Electrochem. Sci.* **2007**, 2, 809.

(16) Uchiyama, S.; Watanabe, H.; Yamazaki, H.; Kanazawa, A.; Hamana, H.; Okabe, Y. *J. Electrochem. Soc.* **2007**, 154, F31.

(17) Siroma, Z.; Ioroi, T.; Yasuda, K.; Tanimoto, K.; Yamazaki, S. *J. Electroanlytical Chem.* **2008**, 616, 64.

(18) Varmagghani, F.; Nematollahi, D. *Electrochim. Acta* **2008**, 53, 3350.

Chapter 5

Electrochemical preparation of poly(1-aminoanthraquinone) and its characterization

Part of this work has been published in *Electrochem. Acta* **2013,** 93, 87-92. This paper was written in part by Dr. Peter Pickup. The work reported was conducted by Zaher Algharaibeh.

5.1. Introduction

Surface modification of carbon materials with redox species has been directed to achieve several goals during the last few decades.[1-10] Chemical[11-15] and electrochemical techniques [1,3,16,17] have been used to covalently attach many diverse redox species with the desired properties.[1,3,6,9,14,16,18,19] Accordingly, a wide range of applications have been explored such as electroanalysis,[6,8,20] electrocatalysis,[5,20,21] fuel cells[20-23] and supercapacitors.[24-33]

Anthraquinones (AQ) are typical examples of quinones for which their electrochemical behaviour has been extensively reported in the literature.[34-38] Their electrochemical activity is highly dependent on the electrolyte composition. A systematic study by Smith and coworkers revealed that there are three different categories.[34] The first category includes AQ in an aqueous solution that is buffered, or has a higher hydrogen ion concentration than the AQ concentration. In this case, the reduction of AQ involves

two electrons and two protons in one step to form the corresponding hydroquinone.[34-40] The second category includes AQ in aprotic solutions. In such a case, the AQ consumes one electron in each of two consecutive steps to form the corresponding dianion.[34,37] The last category includes AQ in unbuffered aqueous solution where the hydrogen ion concentration is lower than that of the AQ. Here, AQ is reduced in the same way as in an aprotic solution. However, due to the strong H-bonding between water and the AQ dianion, a mixture of products is produced. This mixture includes the fully basic dianion (Q^{2-}), the intermediate protonated anion (HQ^{-}) and the hydroquinone (H_2Q).[34]

Anthraquinones (AQ) play a principal role in some biological processes[35] and show potential activity as antitumor drugs,[41] in addition to their potential role in industry.[42] Moreover, a wide range of electrochemical applications involve AQ modified electrodes such as sensors,[43,44] electrocatalysts,[43,45] cation exchange in lithium ion batteries[46] and supercapacitors.[47-51]

The anthraquinone (AQ) moiety has been covalently bonded to carbon electrodes via diazonium coupling and has shown promising characteristics that improve specific energy and specific power as a negative electrode for supercapacitors.[47,48] Unfortunately, covalent bonding of AQ to carbon via diazonium coupling was limited to less than a monolayer.[52] Therefore, a straightforward idea is to modify carbon with an AQ-containing conducting polymer to achieve higher loading and a considerable electronic conductivity.[53,54] Electro-oxidative polymerization of aminoanthaquinones (AAQ) monomers on carbon electrode is expected to be suitable for this purpose.

Recently, a novel hybrid composite of anthraquinone monosulfonate (AQS)/polyaniline on graphite was reported by Zhang and Yang to have electrocatalytic activity towards the oxygen reduction reaction (ORR).[55] Moreover, some polyaniline derivatives[56] show electrocatalytic activity. Therefore, poly(1-AAQ) is expected to have that characteristic as well.

Badawy *et al.* reported that the electropolymerization of 1-AAQ, shown in Figure 5.1 in aqueous 6 M H_2SO_4 on a platinum electrode resulted in the formation of a film that was electroactive in both acidic and neutral solutions between 0.3 and 0.9 V vs. (Ag/AgCl, 3 M KCl).[57] Film degradation occurred below 0.3 V or above 0.9 V. Moreover, the film was also electroinactive in organic media.[57]

In this work, the electrochemical polymerizations of 1-aminoanthraquinone (1-AAQ) monomer in 6 M H_2SO_4 on carbon electrodes were investigated in aqueous and mixed solvents (i.e. aqueous/non-aqueous) under various experimental conditions. The monomer structure is expected to be maintained within the polymer chains because the radical cation formed on the primary amine activates the *ortho* and *para* positions on the aromatic ring.[58]

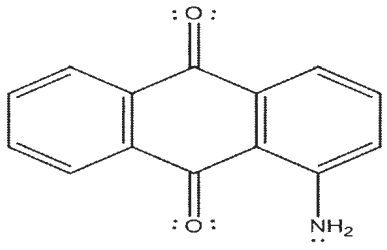

Figure 5.1: 1-aminoanthraquinone (1-AAQ).

5.2. Experimental

5.2.1. Chemicals

1-Aminoanthraquinone (1-AAQ, 97%; Aldrich) was dissolved in hot 6 M H_2SO_4 (aq) with stirring before use. Deionized water was used in all experiments. Sulfuric acid (ACP chemicals Inc.) was diluted before use as required. HPLC grade acetonitrile (Aldrich) was used as received.

5.2.2. Instrumentation

A standard three-electrode electrochemical cell was used throughout the experiments. A glassy carbon electrode with a surface area of 0.071 cm^2 was used as the working electrode. Before each experiment the electrode was polished with aluminum oxide (0.05 μm) slurry on a polishing cloth to obtain a flat shiny surface. A platinum wire was used as the counter electrode while a saturated calomel electrode (SCE) was used as a reference electrode. All electrochemical experiments were conducted under a nitrogen environment after purging the solution with nitrogen gas (99.99%) for 20 min to ensure the absence of oxygen.

Cyclic voltammograms were recorded using an analog RDE4 potentiostat (Pine Instruments) while impedance measurements were conducted using a Solartron model 1286 potentiostat connected to a model 1250 frequency response analyzer. The impedance of poly(1-AAQ), was initially run at 0.0 V versus the open circuit potential (OCP) followed by impedance at the specified potentials by scanning the frequency from

10000 Hz down to 0.1 Hz. The resulting impedance data were recorded and analyzed by ZView software (Scribner Associates Inc.). The infrared spectra of the solid 1-AAQ monomer and a solid poly(1-AAQ) film were directly measured using an attenuated total reflectance Fourier transform infrared spectrometer (ATR FTIR) from Bruker (model Alfa) while OPUS software was used to analyze the spectra. Scanning electron microscope (SEM) images were taken using a Quanta 400 FEG model from FEI Company.

5.3. Results and discussion

5.3.1. Electrochemical polymerization

There are many factors that affect film formation when a particular electrochemical polymerization technique is used. These include: potential limits, type and amount of solvent(s) and electrolyte(s), concentration of monomer, pH, temperature, and impurities.[56] In addition, polymer properties differ according to the technique with which electropolymerization is carried out.[53] There are three general electrochemical procedures to prepare conducting polymers. These are potentiodynamic (i.e. cyclic voltammetry), potentiostatic (i.e. constant potential), and galvanostatic (i.e. constant current).[53,59,60]

5.3.2. Solubility of the 1-aminoanthraquinone monomer

A proper solvent is required to dissolve both the monomer and the electrolyte before carrying out electropolymerization. The 1-aminoanthraquinone (1-AAQ) monomer

is insoluble in pure water and has limited solubility in dilute aqueous acids even after stirring or when sonication is used. Solubility was enhanced by stirring the mixture and heating it in a water bath. The effect of temperature on solubility was examined through comparison of the anodic peak current of the monomer and the shape of the cyclic voltammogram obtained from electropolymerization using the same working electrode and identical experimental conditions except changing the temperature used during preparation of the 1-AAQ solution. The increase in the anodic peak current of 1-AAQ upon increasing the solubilisation temperature indicates increased solubility of the monomer. Almost complete solubility of 22.3 mg of 1-AAQ was obtained in 20 mL of 6 M H_2SO_4 when it was heated up to 90 °C, see Figure 5.2. However, heating the solution may produce unfavourable side reactions that affect the electropolymerization process. Therefore, two 1-AAQ samples were solubilized in 6 M H_2SO_4 at 75 °C and 90 °C before potentiodynamic polymerization at room temperature, as seen in Figure 5.3. This figure shows that there is no significant change in the polymerization process upon heating the 1-AAQ monomer solution up to 75 °C or 90 °C.

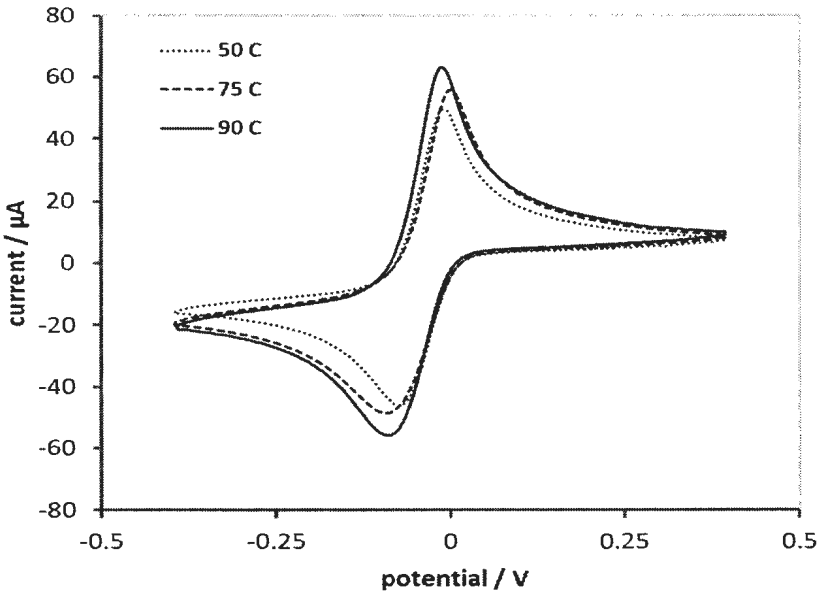

Figure 5.2: Cyclic voltammograms of 1-AAQ solubilized in 6 M H_2SO_4 at three different temperatures, at a scan rate of 50 mV/s, using the same glassy carbon working electrode. A constant amount of 0.0223 g 1-AAQ to 20 mL 6 M H_2SO_4 was used for each test.

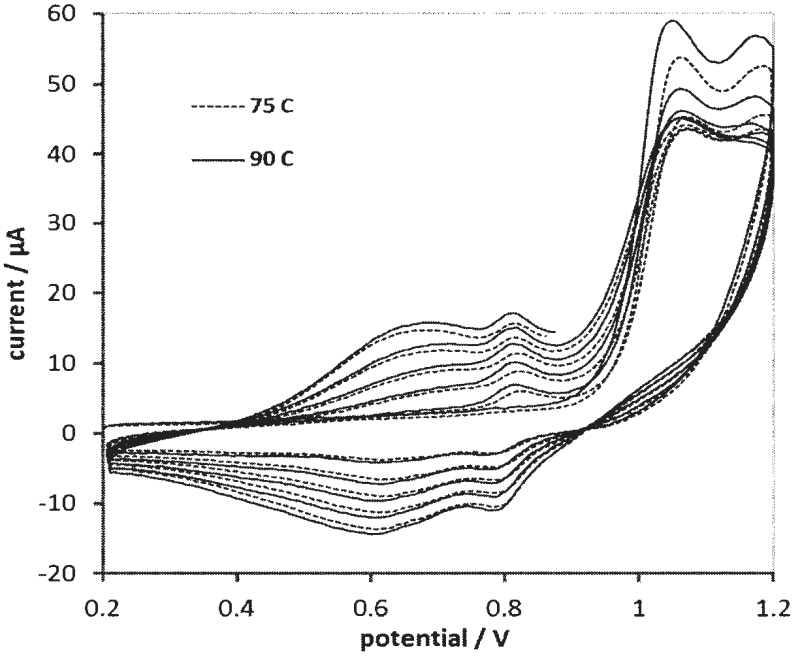

Figure 5.3: Comparison of electropolymerization of the same amount of 1-AAQ monomer (0.0223 g) solubilized at two different temperatures 75 °C (dotted line) and 90 °C (solid line) in 6 M H_2SO_4.

The actual amount of 1-AAQ monomer soluble in aqueous 6 M H_2SO_4 at room temperature is shown in Figure 5.4. The mass of soluble 1-AAQ increased linearly with respect to the added mass of 1-AAQ. These values were calculated after an appropriate suction filtration of that solution through a glass frit at room temperature followed by washing of the residue with deionized water and drying in an oven at 70 °C for 10 min, before weighing. In order to accomplish this study, three amounts of 1-AAQ in 6 M H_2SO_4, were stirred and solubilized by gentle heating in a water bath and were removed from it when its temperature just reached 90 °C. It can be concluded that the insoluble fraction collected at each temperature must have been an impurity in the purchased 1-AAQ.

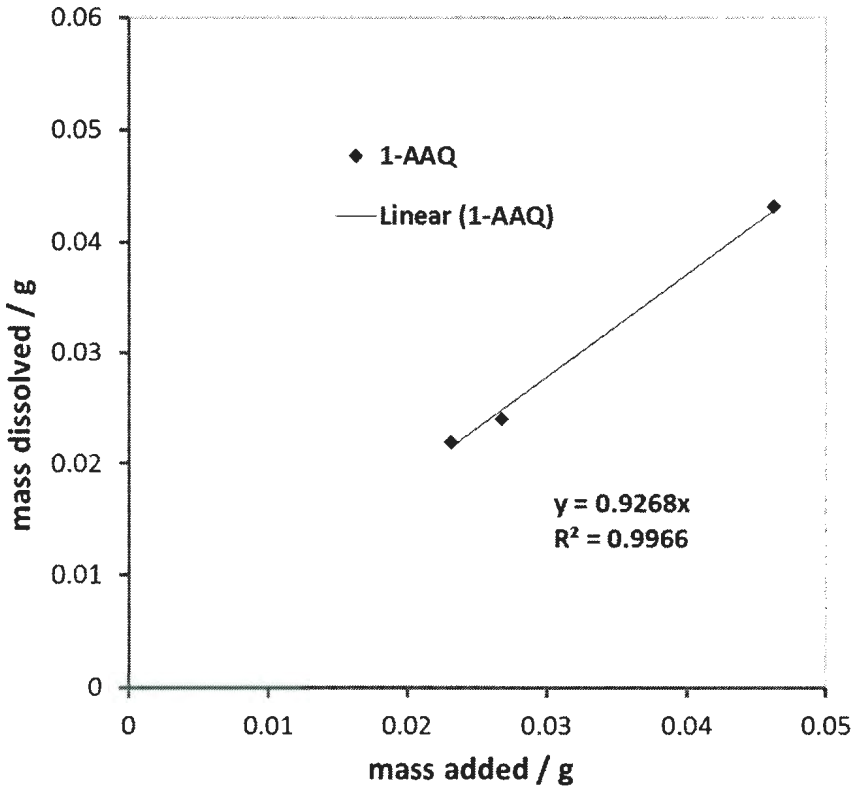

Figure 5.4: Mass of 1-AAQ dissolved versus mass added at room temperature.

1-AAQ is also soluble in a number of organic solvents and in mixtures of aqueous/organic media. Tetraalkylammonium salts are appropriate electrolytes whenever acetonitrile is used alone.[62] In the case of mixtures of 6 M H_2SO_4 (aq) and acetonitrile the monomer 1-AAQ was dissolved in 6 M H_2SO_4 (aq) first followed by the addition of a clear aliquot of that solution to acetonitrile. It is notable that the order of addition is crucial for the electropolymerization process. This might be explained by considering some organic impurities that are soluble in acetonitrile but not in aqueous acid interfere with the initiation step.

5.3.3. Potentiodynamic polymerization of 1-AAQ

5.3.3.1. Effect of potential window on potentiodynamic polymerization of 1-AAQ

For this study, electro-oxidative polymerization of 1-AAQ on glassy carbon (GC) was examined under two different potential windows (0.2 to 1.2) V and (-0.45 to 1.0) V vs. SCE keeping other experimental conditions the same. These conditions involve preparing the polymerization solution from 0.0223 g of 1-AAQ in 20 mL 6 M H_2SO_4 (aq) under stirring and heating the solution up to 90 °C.

5.3.3.1.1. Potentiodynamic polymerization of 1-AAQ at 0.2 to 1.2 V

Figure 5.5 represents cyclic voltammograms for 1-AAQ polymerization over a potential range of 0.2 V to 1.2 V vs. SCE. The current remained close to zero during the first cycle up to *ca.* 0.95 V where it sharply increased indicating the oxidation of 1-AAQ monomers forming radical cations followed by dications as shown in Scheme 5.1.[57,61,62]

These species are highly reactive and can initially form dimers in a fast chemical step. This is indicated by the absence of reduction peaks corresponding to the monomer oxidation peaks. According to the resonance structures of the monomer radical cation, some examples of which are shown in Scheme 5.2 various types of coupling can be inferred such as N-N′, N-C4′, C4-C4′, C4-C2 and C2-C2′. [57] These couplings may form soluble dimers that diffuse away from the electrode or can be adsorbed on its surface. In the latter case, dimers can continue coupling to form a poly(1-AAQ) film. The presence of two new redox couples at *ca.* 0.6 V and 0.8 V indicates that the film is electroactive and is more easily oxidized than the monomer itself. The polymer film is conductive clearly because the anodic oxidation current of 1-AAQ increases with cycling after the first few cycles. These results are similar to those reported by Badawy *et al.* on platinum or gold electrodes.[57]

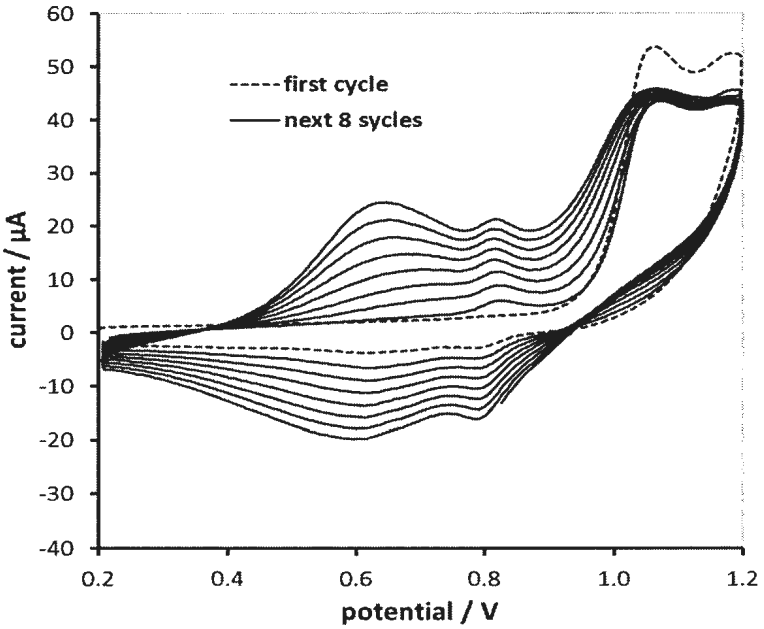

Figure 5.5: Electro-oxidative polymerization of *ca.* 5 mM 1-AAQ in 6 M H_2SO_4 on glassy carbon electrode scanned from 0.2 to 1.2V vs. SCE at a rate of 50 mV/s.

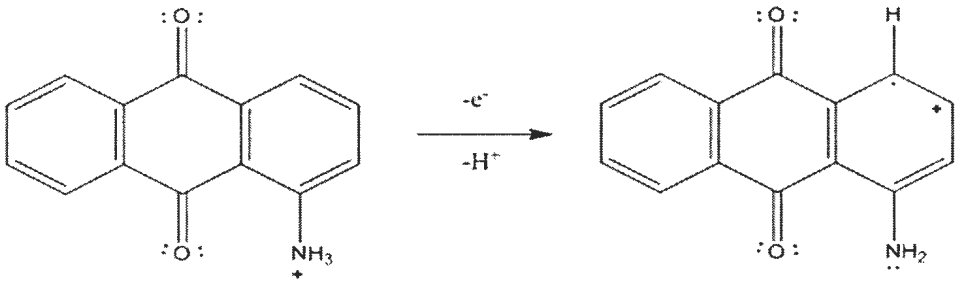

Scheme 5.1: Oxidation step of 1-AAQ to form a radical cation.

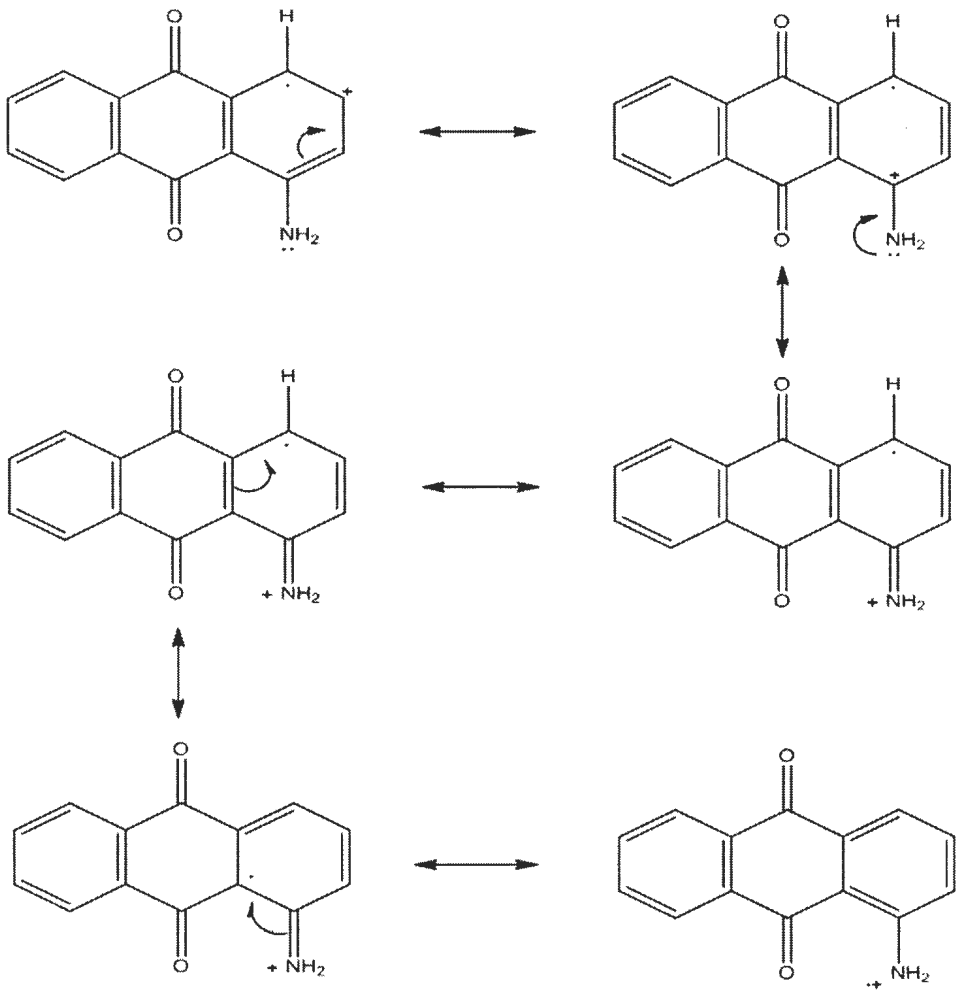

Scheme 5.2: Some resonance structures of 1-AAQ monomer radical cation.

5.3.3.1.2. Potentiodynamic polymerization of 1-AAQ at -0.45 V to 1.0 V

The polymerization of 1-AAQ from 0.2 to 1.2 V described in section 5.3.3.1.1 did not show the behaviour at negative potentials where the quinone functionality of the 1-AAQ monomer is electroactive. Moreover, the upper oxidation limit was not optimized. Therefore, 1-AAQ was electropolymerized by scanning the potential between -0.45 and 1.0 V vs. SCE as shown in Figure 5.6. The potential was first scanned around the formal potential of the 1-AAQ monomer at about -0.08 V vs. SCE (dotted line) and then the anodic oxidation potential was increased to the minimum oxidative polymerization potential at 1.0 V (solid line). At this potential a small increase in the current indicates the oxidation of the monomer to form the radical cation as expected. Interestingly, sweeping the potential repeatedly between -0.45 V to 1.0 V shows unexpected cyclic voltammograms. However, polymer formation is clearly revealed by the presence of two redox peaks, at *ca.* 0.8 V and 0.6 V, which increased upon cycling similar to those seen in Figure 5.5. When the potential was extended down to -0.45 V the cathodic peak current increased gradually upon cycling with a slight shift in the reduction peak potential of the anthraquinone (AQ) moiety to more negative potentials. On the other hand the oxidation of the reduced form of AQ did not appear at the same oxidation potential as for the monomer. Instead, large shifts from 0.01 V to 0.35 V were observed for the first four cycles similar to the way that polymerization of some phenazines proceeds.[76] Such a shift in anodic peak potential (E_{pa}) can be explained based on the increase in the film resistance as the film thickness increases. After that, the oxidative current for AQ developed into a peak similar to the reduction peak but at a much higher potential, as seen in Figure 5.6(b).

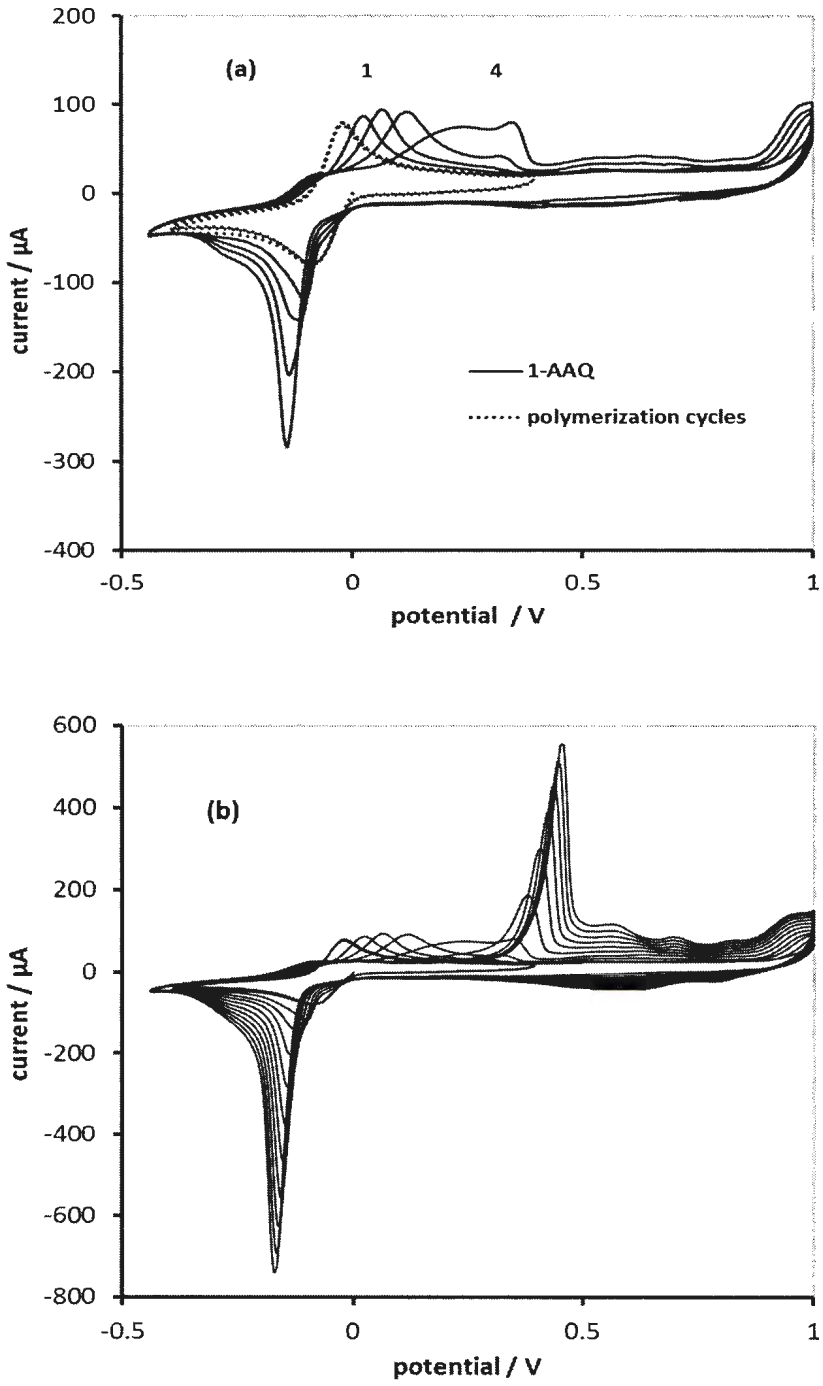

Figure 5.6: Electro-oxidative polymerization of 1-AAQ (0.0223 g in 20 mL of 6 M H_2SO_4) on a glassy carbon electrode scanned from -0.45 to 1.0 V vs. SCE at a rate of 100 mV/s. The experiment was done under a nitrogen atmosphere, (a) first four cycles, and (b) ten cycles.

5.3.3.1.3. Scanning electron microscopy (SEM) of a poly(1-AAQ) film

Figure 5.7 shows a scanning electron micrograph (SEM) of a dry poly(1-AAQ) film on a glassy carbon electrode after potentiodynamic electropolymerization from -0.45 V to 1.00 V in 6 M H_2SO_4. This figure reveals an incomplete coverage of the electrode surface with a rough film and a non-uniform deposition. A thin film of less than 1 μm, based on polymerization deposition of poly(1-AAQ) for ten cycles, can be seen from the image. Moreover, the SEM images support the local deposition of the oligomers followed by nucleation and film growth formation in which the rate determining step is supposed to be the diffusion of the 1-AAQ towards the oxidized oligomer[64,65] to form an island-like structure.[65]

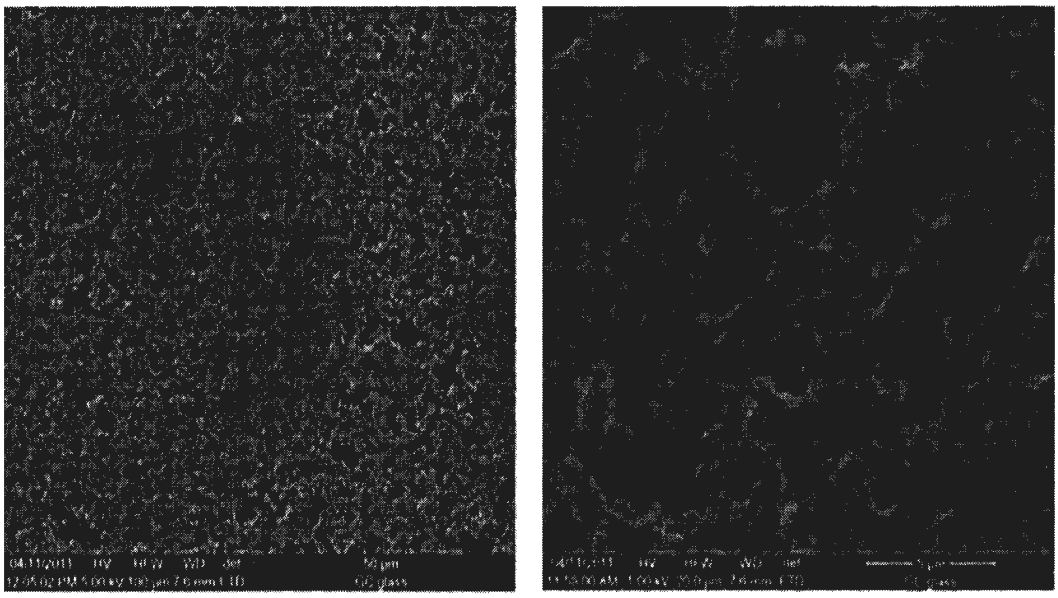

Figure 5.7: Scanning electron microscopy (SEM) of GC/poly(1-AAQ).

5.3.3.2. Cyclic voltammetry of poly(1-AAQ) in 6 M H_2SO_4 (aq)

Poly(1-AAQ) formed potentiodynamically was then examined in a monomer-free 6 M H_2SO_4 solution, as shown in Figure 5.8. The potential was scanned between -0.45 V and 0.8 V instead of 1.0 V to avoid over-oxidation[66,67] or degradation of the polymer film.[66,68] The main cathodic peak at *ca.* -0.2 V can be attributed to the reduction of the quinone moieties in the polymer, while the much smaller and broader cathodic wave between +0.8 and +0.3 V can be attributed to reduction of the polyaniline-like backbone. Curiously, there is no reoxidation wave for the quinone close to its reduction wave. Moreover, scaning the potential between -0.45 V and 0.3 V revealed the absence of the large AQ reduction peak. That is to say that the electrochemistry of the poly(1-AAQ) film was unusal.

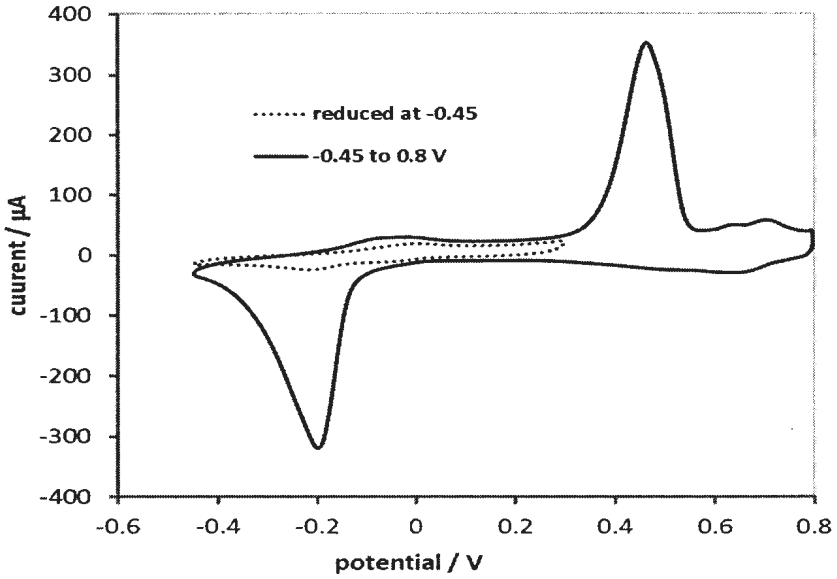

Figure 5.8: Steady state cyclic voltammogram (after three cycles) of GC/poly(1-AAQ) in monomer-free 6 M H_2SO_4 solution at 5 mV/s. Poly(1-AAQ) was prepared by cycling from -0.45V to 1.0 V vs. SCE.

Figure 5.9(a) shows cyclic voltammograms of a poly-AAQ coated electrode in 6 M H_2SO_4 (aq) at various scan rates, in the absence of AAQ in solution. These voltammograms show a broad region of electrochemistry at potentials above +0.3 V, with major anodic peaks at *ca.* +0.4 V and +0.5 V, and a major cathodic peak at *ca.* -0.2 V. Peaks currents increased linearly with the square root of scan rate indicating that they were due to diffusion (or migration)-limited as shown in Figure 5.9(b). The first anodic peak at *ca.* +0.4 V (ranging from +0.36 V at 5 mV s^{-1} and +0.44 V at 400 mV s^{-1}) is presumably due to its reoxidation, since the cathodic peak at -0.2 V did not diminish with cycling, and quinone re-oxidation should occur before oxidation of the polymer backbone. This assignment was confirmed by variation of the potential limits (section 5.3.3.4).

The behavior of the quinone electrochemistry in Figure 5.9 is very unusual, and the very large peak separation cannot be accounted for by slow electron transfer kinetics, or an uncompensated resistance. Both of these would lead to a much stronger dependence of the peak separation on scan rate. However, the observed characteristics are similar to those for charge trapping in bilayer electrodes (electrodes modified with two discrete electroactive polymer films).[69,70] Moreover, such charge trapping phenomena can also occur in homopolymer films where changes in conductivity can cause sites in the film to be trapped in either reduced or oxidized states.[71]

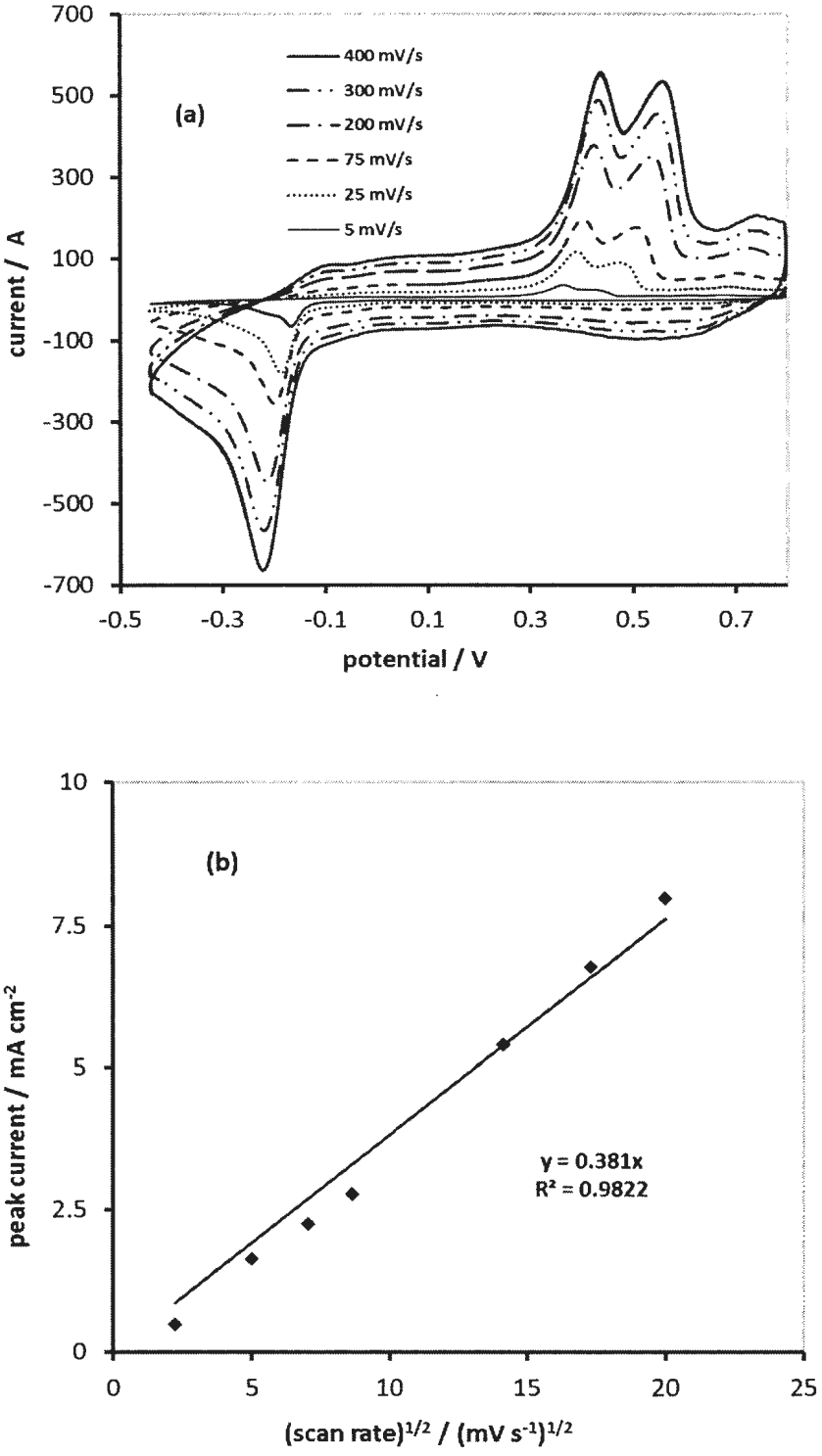

Figure 5.9: (a) Cyclic voltammograms of GC/poly(1-AAQ) in 6 M H_2SO_4 at various scan rates from 5 mV/s to 400 mV/s, (b) Plot of anodic peak current at *ca.* + 0.4 V vs. square root of scan rate.

In the case of poly-AAQ, there is not expected to be a bilayer structure but there are two distinguishable redox moieties in the homopolymer film. The first one results from the polymerization of the aromatic amine and is analogous to the electrochemistry of polyaniline, which occurs over a wide potential range. The second one is the anthraquinone redox centres which have a formal potential close to −0.1 V. The observation of a charge trapping phenomenon in Figure 5.9 therefore suggests that the electrochemistry of the quinone is mediated by the conductivity due to the polyaniline like backbone, and that it becomes trapped in the reduced state (H_2AQ in Eq. 1.5) because the backbone becomes non-conductive at sufficiently low potentials.

$$AQ + 2e^- + 2H^+ \rightleftharpoons H_2AQ \qquad \text{Eq. 5.1}$$

Impedance spectroscopy was therefore applied in order to explore this possibility and measure the magnitudes of any conductivity changes that may occur.

5.3.3.3. Impedance and charge trapping: Bilayer-like electrode behavior

Impedance is a powerful technique to investigate charge transport in electroactive polymers.[74-76] Accurate measurement of parameters related to charge transfer and charge transport in a film coated electrode from its equilibrium state can be achieved by using a wide range of frequency. Two forms of impedance presentation are used in this section to facilitate the study of charge trapping in poly(1-AAQ). These are complex impedance (Nyquist) plots and series capacitance versus real impedance plots. Each can be used to resolve some of the important parameters.

A typical Nyquist plot for a conducting polymer modified electrode is shown in Figure 5.10. and a corresponding equivalent circuit is shown in Figure 5.11. Three main regions, according to their frequency range, can be distinguished. The first region is the high frequency region where charge transfer processes dominate. The semi-circle at high frequencies can be used to determine the double layer capacitance (C_{dl}) and the charge transfer resistance (R_{ct}) of the polymer film. The highest frequency intercept with the real impedance axis can be taken as the solution resistance (R_s), also known as uncompensated resistance (R_{un}). The second region is observed at medium frequencies where diffusion and/or migration processes of ions in the polymer film dominate and appears as a straight line with 45° slope also known as the Warburg impedance (modeled as an open Warburg element, W_o).[75,76] The final region is the low frequency region where the actual film thickness limits the diffusion process within the film and leads to a vertical line.

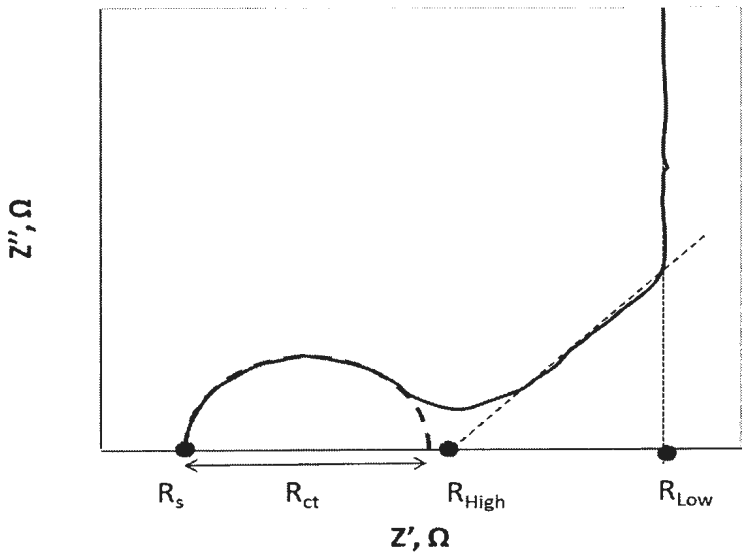

Figure 5.10: Typical Nyquist plot, imaginary impedance (Z") versus real impedance (Z'), of a conducting polymer.

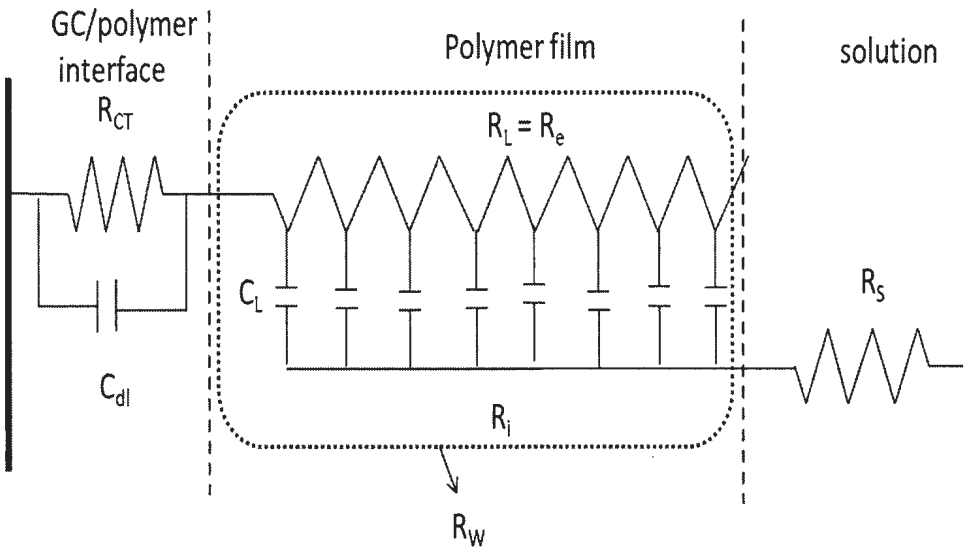

Figure 5.11: Equivalent circuit for a typical conducting polymer.[77]

The resistance of the Warburg element consists of a combination of the film's electronic resistance (R_e) and ionic resistance (R_i) although these cannot be distinguished from a single Nyquist plot. To estimate R_e and R_i, impedance measurements at various potentials are essential.[72,75,78] Albery *et al.* derived some useful theoretical equations that are related to experimental values R_{High} and R_{Low} from a Nyquist plot, typically as shown in Figure 5.12(a).[78] These are summarized as follows:

If R_{ct} is negligible, (as in Figure 5.12.).

$$R_{High} = R_s + R_\infty \qquad \text{Eq. 5.2}$$

Where $R_{\infty,}$ is the resistance at infinite frequency.

with $$(R_\infty)^{-1} = (R_e)^{-1} + (R_i)^{-1} \qquad \text{Eq. 5.3}$$

Therefore, $(R_\infty)^{-1}$ is dominated by the lowest value of R_e or R_i.

Moreover,

$$R_{Low} = R_s + R_\Sigma/3 \qquad \text{Eq. 5.4}$$

and

$$R_\Sigma = R_e + R_i \qquad \text{Eq. 5.5}$$

Changing the potential of poly(1-AAQ), as expected for all conducting polymers, results in a significant change in electronic resistance while a smaller change in the ionic resistance is expected. Consequently, R_e and R_i can be resolved. Moreover, for a conducting polymer (or redox polymer), the length of Warburg, or Warburg-like, region (R_W) corresponds to one third of the film resistance ($R_L = 3R_W$).[79] On the other hand, the film capacitance (C_L) can be obtained by plotting the imaginary impedance (Z'') versus the reciprocal of frequency $(2\pi f)^{-1}$ at low frequencies as shown in Figure 5.12(b).

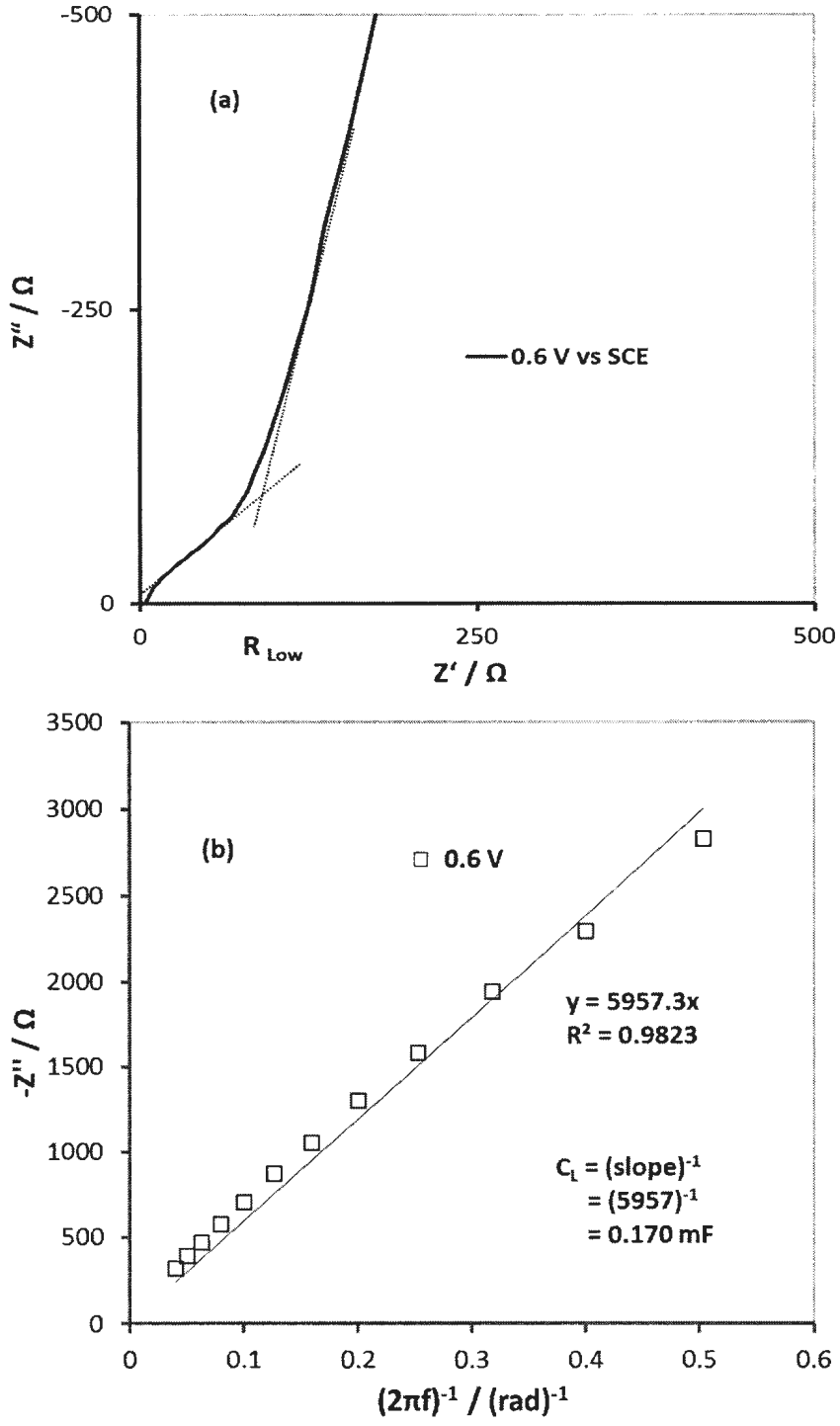

Figure 5.12: (a) Typical Nyquist plot of GC/poly(1-AAQ) at +0.60 V vs. SCE in 6 M H_2SO_4; (b) determining the film capacitance (C_L) from Nyquist plot.

The second useful plot is the series capacitance versus real impedance plot. In this case, the Warburg region is seen as an approximately linear increase in capacitance from close to zero.[80] Compared to Figure 5.12, it is most convenient and objective to measure the length of this region, along the real impedance axis, from a capacitance plot as shown in Figure 5.13 for data at 0.2 V.[80] The capacitance value at the intercept shown in Figure 5.13 provides a good estimate of the film capacitance (C_L). It is a useful tool to monitor changes in the film capacitance and film resistance as a function of potential.[80]

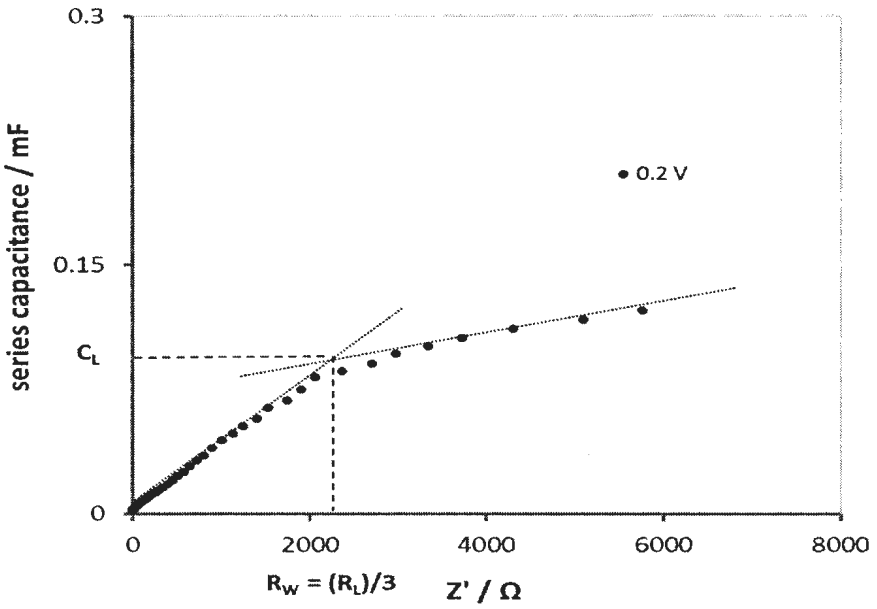

Figure 5.13: Selected plot of series capacitance versus real impedance of poly(1-AAQ) at 0.2 V vs. SCE. C_L is the polymer film capacitance; R_W and R_L are the Warburg and the film resistances, respectively.

Figure 5.14(a) shows impedance (Nyquist) plots at selected potentials for a poly(1-AAQ) coated GC electrode in 6 M H_2SO_4 (aq). These experiments were run in order of decreasing potential over a range that encompasses the quinone formal potential. It was inferred from the cyclic voltammetry in Figure 5.9 that the conductivity of the film

irreversibly decreased over this range, since the quinone groups could be reduced at the formal potential on the cathodic scan, but could not be reoxidized at this potential on the anodic scan. However, the Nyquist plots in Figure 5.14(a) do not appear to show any evidence for this. The problem here appears to be due to dominance of the Nyquist plots by the effects of background currents, the origin of which is unclear but could due the reduction of trace oxygen or other impurities.

Figure 5.14(b) shows that Warburg-type (i.e. 45° straight line) impedance at high frequencies was clear at a potential of -0.1 V which indicates that the reduction of AQ and polyaniline-like backbone was limited by migration and/or diffusion processes.

In addition, the Nyquist plot for the bare GC electrode in 6 M H_2SO_4 (aq) revealed large semicircles at -0.1 V to -0.4 V as shown in Figure 5.15 which support the dominance of the background current. Because the impedance measurements of the bare GC were performed over a frequency range (1000 Hz to 0.01 Hz) different from those of GC/poly(1-AAQ), a comparison of their Nyquist plots is not informative.

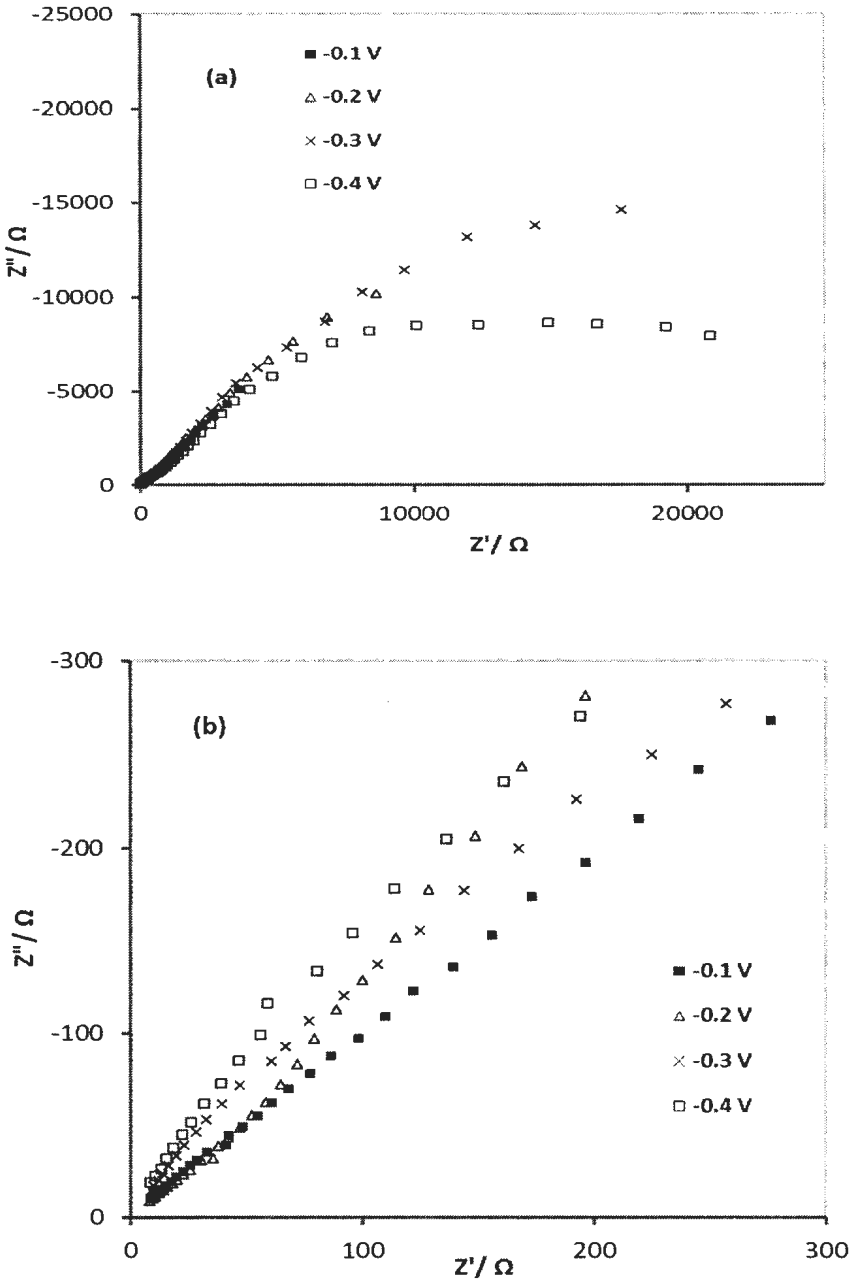

Figure 5.14: Nyquist plots for GC/poly(1-AAQ) in 6 M H_2SO_4 (aq) at potentials of -0.1 V, -0.2 V, -0.3 V and -0.4 V vs. SCE. (a) Full range and (b) narrow range of impedances.

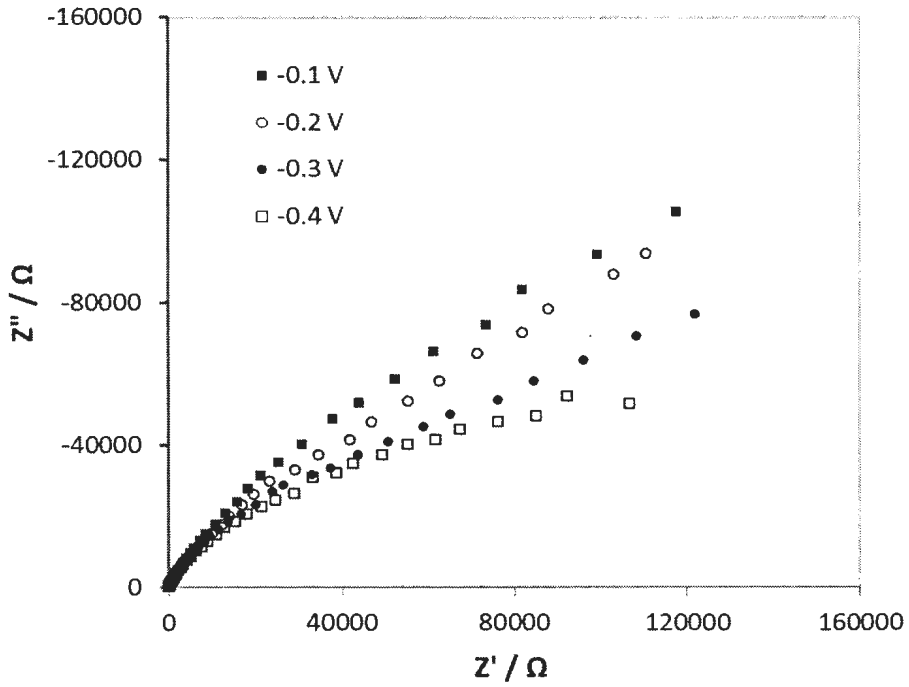

Figure 5.15: Nyquist plots for bare GC in 6 M H_2SO_4 (aq) at potentials of -0.1 V, -0.2 V, -0.3 V and -0.4 V vs. SCE.

The dominance by the background current can be minimized by plotting the data as series capacitance *vs.* real,[80] and such capacitance plots are shown in Figure 5.16. Here it can be seen that at -0.1 V the poly(1-AAQ) coated GC electrode exhibited a much larger capacitance than the bare GC electrode, and that its capacitance decreased to a value close to that of bare GC as the potential was decreased. The large capacitance of the poly-AAQ at -0.1 V (and -0.2 V) indicates that the polyaniline-like backbone was still partially oxidized, and explains why the quinone group could be reduced at its thermodynamic (formal) potential. The loss of capacitance (electroactivity) may explain why it could not be reoxidized at this potential.

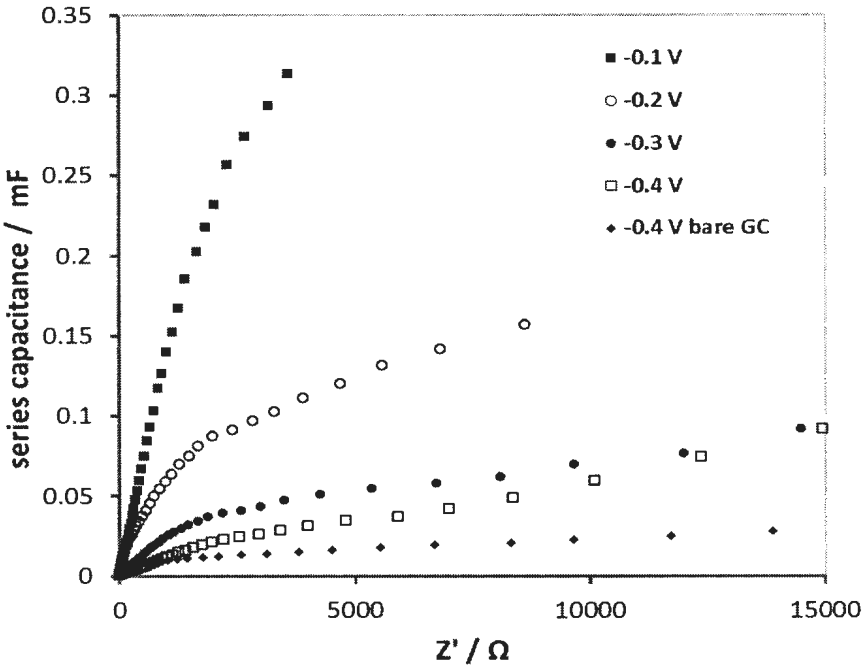

Figure 5.16: Series capacitance versus real impedance plots for poly(1-AAQ) at -0.1 V to -0.4 V and at potentials of -0.4 V for bare GC.

Having established that the reduction of the quonine groups in the polymer can be mediated by the electrochemisty (redox or electronic conductivity) of the polymer backbone, the next step was to understand why the reoxidation is not also mediated at the quinone formal potential. To this end, impedance measurements were made from 0.1 V to 0.7 V in the order of increasing potential, following reduction of the film at -0.4 V. The results are shown in Nyquist (Figure 5.17) and capacitance plots (Figure 5.18).

At +0.1 V, the impedance of the electrode was similar to that at -0.4 V (see Figure 5.16 and Figure 5.18), with low capacitance and high resistance. The low doping level and consequent high resistance of the polymer backbone can thus explain why the quinone groups were not reoxidized at this potential during cyclic voltammetry. Since thermodynamically they should be oxidized, they can be said to be trapped in the reduced

state because they are electronically insulated from the GC electrode. This is essentially a meta-stable state resulting from hysteresis in the electrochemistry of the backbone.

As the potential was increased from +0.1 V, the data in Figure 5.18 show only minor changes until +0.4 V. At this potential, there was a significant increase in capacitance and the resistance clearly began to decrease. Significantly, this potential approximately matches that of the first anodic peak in cyclic voltammetry (Figure 5.8). The position of this peak, which is due predominantly to the reoxidation of the quinone groups, can thus be explained by the observed turn-on of the backbone conductivity between +0.3 and +0.4 V. At higher potentials, the capacitance of the film continued to increase, and its resistance decreased, as expected for electrochemical doping of a conjugated (conducting) polymer.

The Nyquist plots in Figure 5.17 all show medium frequency regions at *ca.* 45° corresponding to a Warburg, or Warburg-like, impedance where the length of this region (R_W) corresponds to one third of the film resistance ($R_L = 3R_W$) for a conducting polymer (or redox polymer).[79] It is notable that the capacitive line at low frequencies is not ideally vertical as expected for a pure capacitor. This behavior can be explained by considering the following factors: non smooth film morphology[81] (as is shown in the SEM in Figure 5.7), various charge transfer rates at the microscopic level,[81] and/or different adsorption processes.[81]

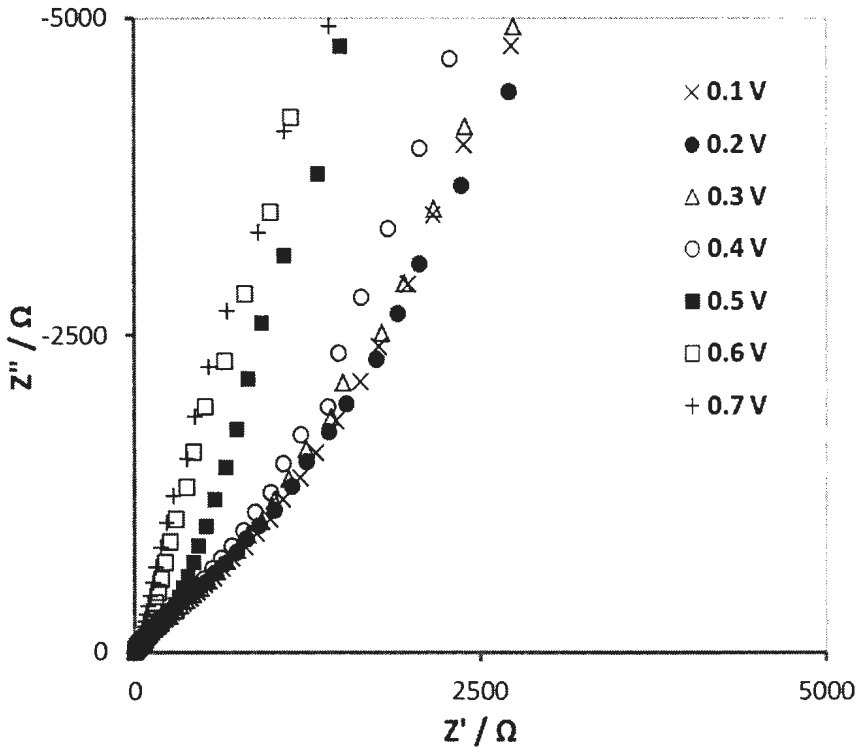

Figure 5.17: Nyquist plots for GC/poly(1-AAQ) immersed in 6 M H_2SO_4 at potentials of +0.1 V, +0.2 V, +0.3 V +0.4 V, +0.5 V, +0.6 and +0.7 V vs. SCE, respectively.

It is qualitatively clear from Figure 5.18 that the film resistance decreases and the film capacitance increases as the potential increases. No flat plateau for series capacitance at low frequencies were observed because of the inhomogeneous morphology of the film, and/or the background current.

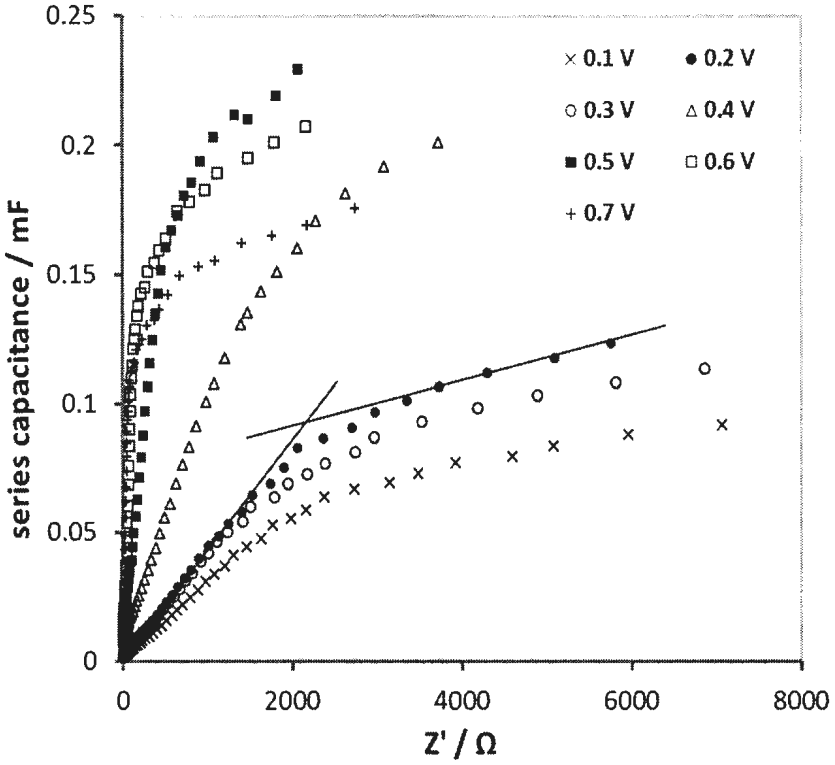

Figure 5.18: Series capacitance versus real impedance at potentials of +0.1 V, +0.2 V, +0.3 V, +0.4 V, +0.5 V, +0.6 and +0.7 V vs. SCE.

The film capacitances and film resistances at potentials from -0.4 V to 0.7 V obtained from Figure 5.16 and Figure 5.18 are presented in Table 5.1. Compared with the typical exponential dependence on potential of the conductivity of other conducting polymers[82,83] the results in Table 5.1. are unusual in that no significant changes in resistance were observed between -0.4 V and +0.3 V. This points to some other form of conduction through the film, which could be due to the electrolyte in pores. It cannot be due to redox conduction due to the AQ/H_2AQ couple, which would peak at the formal potential (*ca.* -0.1 V) and be much smaller at higher and lower potentials.

The fact that the reducedformof anthraquinone (H_2AQ) did not undergo oxidation at the proper potential (i.e. close to -0.1 V) on the subsequent forward scan may be attributed to the high resistivity of the polymer film. That is to say, the charge was trapped in the reduced form and cannot be released unless the film becomes sufficiently conducting at E > +0.3 V where the untrapping reaction (i.e. oxidation of both the polyaniline-type backbone and H_2AQ) occurs. The shift in the anodic peak potential (E_{pa}) can be roughly predicted based on the following equation.

$$E_{pa} = E^{\circ\prime} + \frac{0.029}{n} + iR \qquad \text{Eq. 5.6}$$

Applying Eq. 5.6 to the un-trapping peaks in Figure 5.9 yields resistances ranging from 13 kΩ at 5 mV s^{-1} to 0.9 kΩ at 400 mV s^{-1}. The decrease in the apparent film resistance with increasing scan rate can be attributed to the lower amount of time spent at low potentials during trapping of the H_2AQ sites. The resistances in Table 5.1 at potentials below 0.6 V fall within this range, but do not appear to be high enough to fully account for the voltammetric results, especially those at the lowest scan rates. This may be due to the differences in the time scales of the impedance and voltammetry experiments and the effects of hysteresis in the conductivity changes, as illustrated in section 5.3.3.4.

Table 5.1: Resistances and capacitances of poly(1-AAQ) film in 6 M H_2SO_4 (aq) from series capacitance data in Figure 5.16 and Figure 5.18.

Potential (V)	Film resistance (kΩ)	Film capacitance (mF)
-0.4	6.2	0.023
-0.3	5.3	0.042
-0.2	4.9	0.099
-0.1	4.9	0.232
0.1	7.0	0.070
0.2	6.8	0.090
0.3	6.9	0.097
0.4	5.0	0.172
0.5	1.6	0.186
0.6	0.66	0.175
0.7	0.36	0.148

Figure 5.19 shows that measuring impedance at various potentials is useful to discriminate between electronic resistance (R_e) and ionic resistance (R_i). From this figure, R_{High} is relatively independent of potential and remains at values less than 10 Ω. Therefore, R_∞ values remain small and are dominated by the smallest value of R_e or R_i. On the other hand, R_{Low} values increase significantly from 50 Ω to 1600 Ω with decreasing potential due to significant increase in R_e as expected for any conducting polymer. Consequently, R_i is considered as the smallest resistance in order to explain the small R_∞. This is reasonable because of the high electrolyte concentration (i.e. 6 M H_2SO_4 (aq)) used.

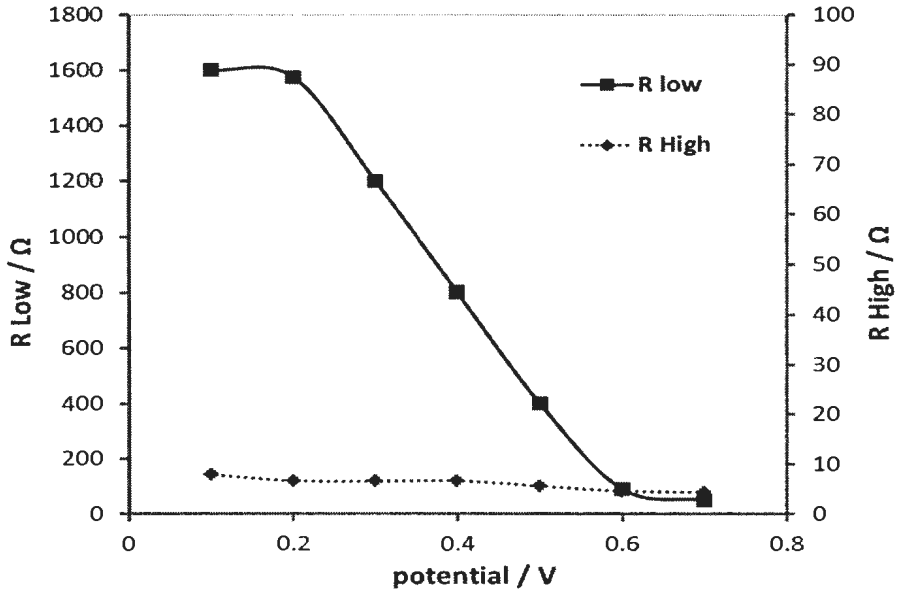

Figure 5.19: Changing of R_{High} and R_{Low} with potential.

Based on Eq. 5.2 to Eq. 5.5, values of electronic resistance (R_e) of poly(1-AAQ) range from 0.014 kΩ to 4.8 kΩ for potentials from 0.7 V down to 0.1 V as shown in Table 5.2.

Table 5.2: Estimated resistances of poly(1-AAQ) from Nyquist impedance plots at positive potentials (+ 0.1 V to + 0.7 V) in 6 M H_2SO_4(aq), assuming that R_{ct} and R_i are negligible, and $R_{High} = R_s$.

Potential (V)	**R_s (Ω)**	**R_{Low} (kΩ)**	**R_e (kΩ)**
0.1	7.9	1.6	4.8
0.2	6.7	1.6	4.7
0.3	6.6	1.2	3.6
0.4	6.7	0.80	2.4
0.5	5.6	0.40	1.2
0.6	4.6	0.090	0.26
0.7	4.4	0.050	0.14

5.3.3.4. Dependance on switching limits and preconditioning potentials

Potential-hold and reverse cyclic voltammograms over various potential windows were recorded at 50 mV/s in 6 M H_2SO_4 solution in order to understand the behaviour of the charge trapping in GC/poly(1-AAQ). In Figure 5.20(a) the potential was scanned initially over the full potential window (i.e. -0.45 V to 0.8 V) to ensure the existence of the charge trapping phenomenon. Then it was scanned between 0.2 V and 0.8 V to release any trapped charges. This is obvious from the absence of an untrapping peak between 0.3 V and 0.6 V. After that the potential was scanned between 0.0 V and 0.8 V and revealed again that there was no release of the charge. The same was observed when the potential was scanned between -0.05 V and 0.8 V. However, when the potential was scanned between -0.1 V and 0.8 V or between -0.15 V and 0.8 V a small pre-peak was observed at *ca.* 0.3 V on the forward scan which indicates a small release of the trapped charge. At these potentials (i.e. -0.1 V or -0.15 V) the AQ group is electroactive and the film becomes redox conducting because oxidized and reduced forms coexist (mixed valence). Holding the potential at -0.15 V for 2 min resulted in more charge trapping and consequently more charge recovery at *ca.* 0.3 V. The above results indicate that the redox site that is responsible for the trapping reaction (i.e. AQ) has a formal potential that lies in a conducting region not in the insulating one. In other words, the charge trapping due to AQ reduction has a kinetic-trapping origin.

Figure 5.20(b) shows voltammograms of a poly-AAQ electrode with various upper potential limits and preconditioning potentials. The potential was initially scanned

between -0.45 V and +0.3 V to produce the steady state voltammogram displayed as the solid line in the figure. This almost featureless (see below) response shows that the film had been fully reduced and that the upper limit of +0.3 V was insufficient to oxidize either the hydroquinone groups or the polymer backbone. Subsequent holding of the potential at +0.5 V for 1 min produced a small reduction wave at *ca.* -0.25 V on the next scan (dotted line), and a significant anodic peak at *ca.* +0.4 V. Thus the hydroquinone groups can be slowly oxidized at +0.5 V, but reduction of the quinone is still inhibited. This slow electrochemistry of the hydroquinone groups is consistent with the high resistance of the film measured at +0.5 V by impedance (1200 Ω in Table 5.1), which would have presumably become much higher during the scan from +0.5 V to the quinone formal potential. When the potential was held at +0.7 V for 1 min, the subsequent voltammetric scan Figure 5.20(b) showed a full size quinone reduction peak at -0.2 V and a large reoxidation peak at *ca.* +0.4 V, consistent with the lower film resistance generated at +0.7 V (360 Ω in Table 5.1).

These results reveal a complexity in the conductivity changes of the polymer beyond those documented by the impedance experiments. Based on other studies of conductivity changes in conducting polymers[53,84] and the results in Figure 5.20, it can be surmised that there is considerable hysterisis in the potential dependence of the conductivity of poly(1-AAQ) due to conformational or other[84] changes during its reduction and oxidation. Thus, a potential of +0.7 V is required to fully reset the polymer to its original conformation, electroactivity, and conductivity.

Comparing the voltammograms in Figure 5.20 with those in Figure 5.6 and Figure 5.9, it can be seen that the splitting of the anodic wave into two peaks as seen in Figure 5.9 depends on the conditions of the experiment. For freshly prepared films, the 2nd peak was small (Figure 5.6) or not resolved (Figure 5.20). However, the 2nd peak became more pronounced/resolved with use, and with increasing scan rate Figure 5.9. These changes were most likely due to conformational and or morphological changes within the film during its repeated reduction and oxidation.

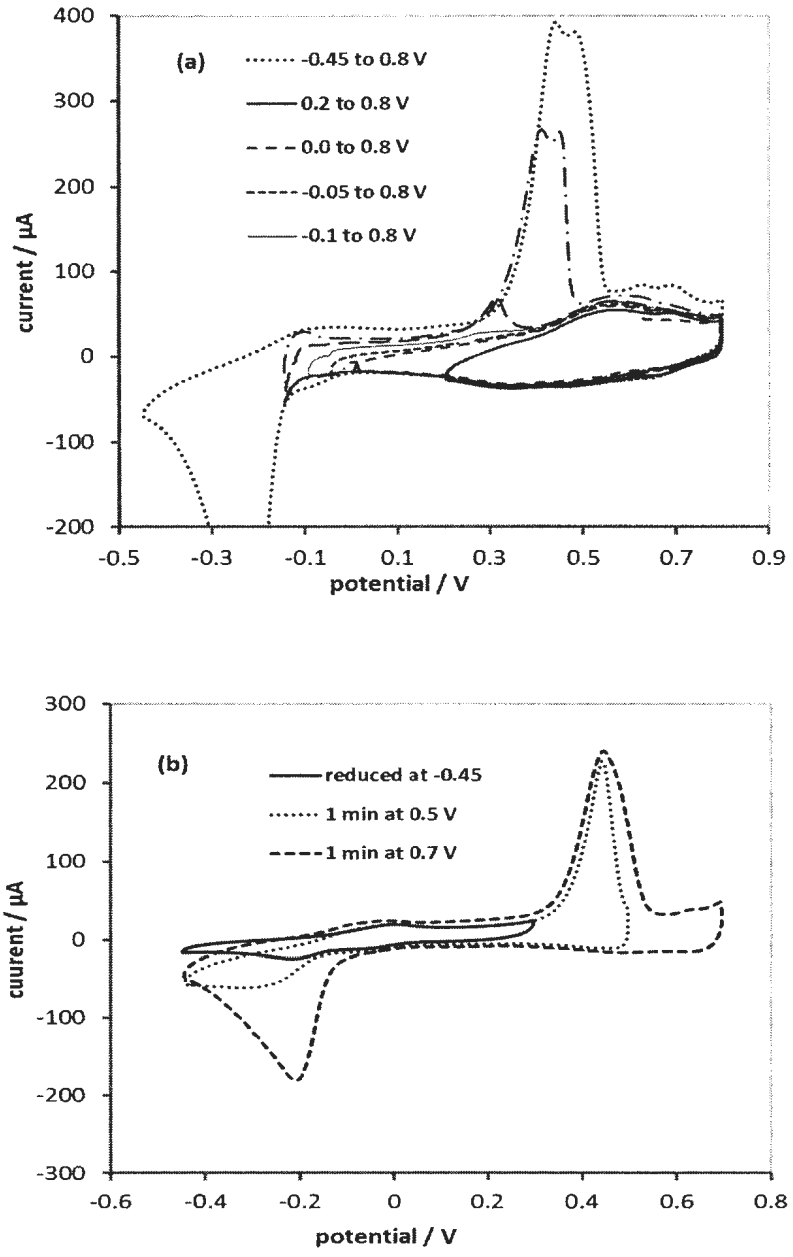

Figure 5.20: Hold and reverse study of cyclic voltammetry of poly(1-AAQ) deposited on a glassy carbon electrode in 6 M H_2SO_4 and scanned at a rate of 50 mV s^{-1}. (a) Potential was scanned initially between -0.45 and 0.8 V then it was scanned in the following order: between 0.2 and 0.8 V, between 0.0 V and 0.8 V, between -0.05 V and 0.8 V, between -0.1 V and 0.8 V, between -0.15 V and 0.8 V, and finally hold for 2 min at -0.15 before scan to 0.8 V. (b) Potential was scanned initially between 0.3 and -0.45 V and stopped at -0.45 V then it was scanned in the following order: hold for 1 min at 0. 5 V before scan to -0.45 V and finally hold for 1 min at 0. 7 V before scan to -0.45 V.

5.3.3.5. Capacitive properties of poly(1-AAQ)

Figure 5.22 shows capacitance values of poly(1-AAQ) determined from impedance (i.e. from Series capacitance vs. Z') compared to capacitance for poly(1-AAQ) and bare glassy carbon electrode calculated from their cyclic voltammograms by dividing the current by the scan rate which was 5 mV/s. Impedance measurements were recorded with a small sine wave amplitude (*ca.* 10 mV) over a frequency range of 10000 Hz to 0.1 Hz. Film capacitance was obtained from series capacitance versus real impedance plots recorded in the following potential order (-0.1 V to -0.4 V) followed by (+0.1 V to +0.7 V) with 0.1 V potential step increments. Combining data from impedance and cyclic voltammetry is useful to understand the electrochemical behavior of conducting polymers.

Figure 5.21 shows that, at any given potential, the capacitance value calculated from impedance was much lower than the corresponding one calculated from cyclic voltammetry, as expected for any conducting polymer.[86-88] The reason for that could be the difference in potential perturbation amplitudes in the two techniques.[86-89] Such expectation was further confirmed for another conducting polymer by running the cyclic voltammetry experiment over a narrow potential window (i.e. 10 mV) which resulted in a 30% decrease in capacitance compared to the capacitance obtained when the full potential window is used.[86,88] Moreover, the capacitance in Figure 5.21, calculated from the cyclic voltammogram, was not accurate because the film was not prepolarized before running the potential sweep in order to obtain a redox equilibrium as proposed by

Rossberg[89] and Genies.[90] In addition, conformational changes in the polymer chains are more significant in the case of cyclic voltammetry.[88] The large apparent peak capacitances at -0.1 V and +0.4 V were attributed earlier to trapping (reduction) and untrapping (oxidation) of AQ groups present in the polymer film. However, the charge trapped in the reduction reaction is not fully recovered in the oxidation reaction. This is clear from the difference in the sizes of the peaks. This difference can be attributed to charge trapping leakage.[69]

In other words, some of the AQ groups present within the polymer chains can be oxidized slowly before the untrapping peak is reached. The polymer film reveals high capacitance with diffusion control within the low conductivity region (i.e. between 0.0 V and 0.3 V) which is not fully understood. However, it can probably be explained by considering the film as an AQ redox polymer instead of as a conducting polymer. In such a case, electron transport within the film occurs via electron hopping (electron exchange) between adjacent AQ centres which is governed by Fick's diffusion law.[91] This process is facilitated by slight movement of AQ centres and diffusion of a sufficient amount of counter ions to ensure electroneutrality. Therefore, the overall diffusion process is controlled by the slowest step of the following processes: electron hopping, redox centre movement and counter ion diffusion.[91]

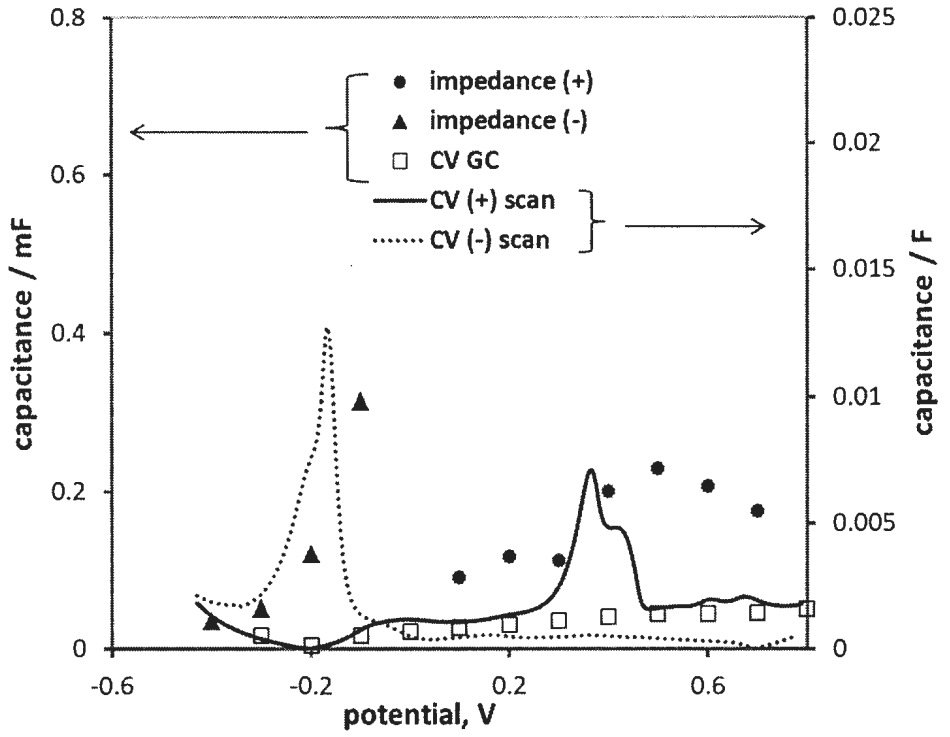

Figure 5.21: Limiting capacitance (from impedance) of GC/poly(1-AAQ) versus electrode potential compared with the capacitance of bare GC and GC/poly(1-AAQ) (from cyclic voltammogram at 5.0 mV/s) in 6 M H_2SO_4 (aq). Absolute values are presented for the negative scan cyclic voltammogram.

The ability of poly(1-AAQ) to hold the charges when a potential is applied across it is shown in Figure 5.22 by plotting the charge versus the potential between -0.2 V to 0.8 V . When charging the polymer over the 1 V potential window (i.e. from -0.2 V to 0.8 V) the charge increases linearly with potential except at the untrapping potential where the charge sharply increased with potential. Moreover, at the end of charging the accumulated charge provide the average capacitance as in Eq. 5.7.

$$Q = CV \qquad \text{Eq. 5.7}$$

Q is the total charge that the polymer film can hold when a certain potential V is applied across the electrode and C is the proportionality constant which is equal to the film capacitance.

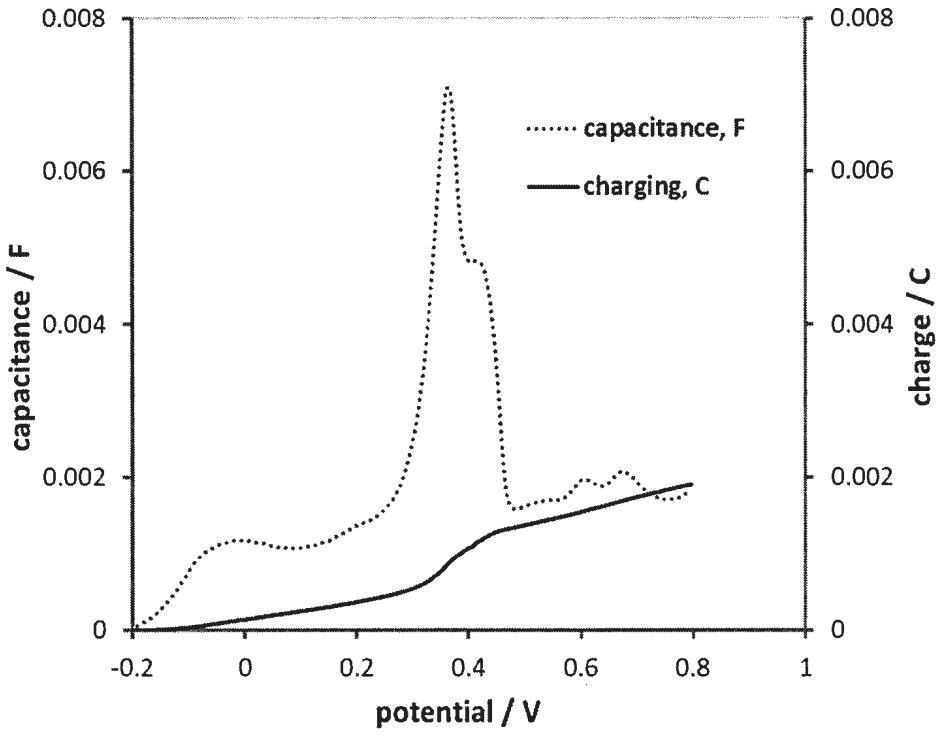

Figure 5.22: Comparison of capacitance and charge versus potentials for GC/poly(1-AAQ) in 6 M H_2SO_4 (aq).

5.3.3.6. Charging/discharging properties of poly(1-AAQ)

A current-potential plot obtained from cyclic voltammetry of poly(1-AAQ) at 5 mV s^{-1} was utilized to study its charging/discharging properties as shown in Figure 5.23. The total amount of charge that the polymer film can hold depends on potential. In general, the charge accumulation, during the positive scan, was linearly dependent on the potential except at potentials where the AQ is electroactive. The charge reached a

maximum value of 0.002 C at the end of charging step. Only 25% of the total charge was stored in the film over potentials where the film is highly resistive (i.e. from -0.45 V to 0.2 V). On the other hand, during the negative potential scan, the polymer film undergoes discharging in which the charge that has already been stored decreases linearly with potential. About 80% of the total charge stored during the charging process was maintained over a potential window between 0.8 V down to -0.1 V followed by a sharp decrease in the film charge over the potential window where the AQ reduction reaction occurs (i.e. between -0.1 V and -0.4 V). This hysteresis in charge/discharge profile would be a problem for practical electrochemical capacitaor application.

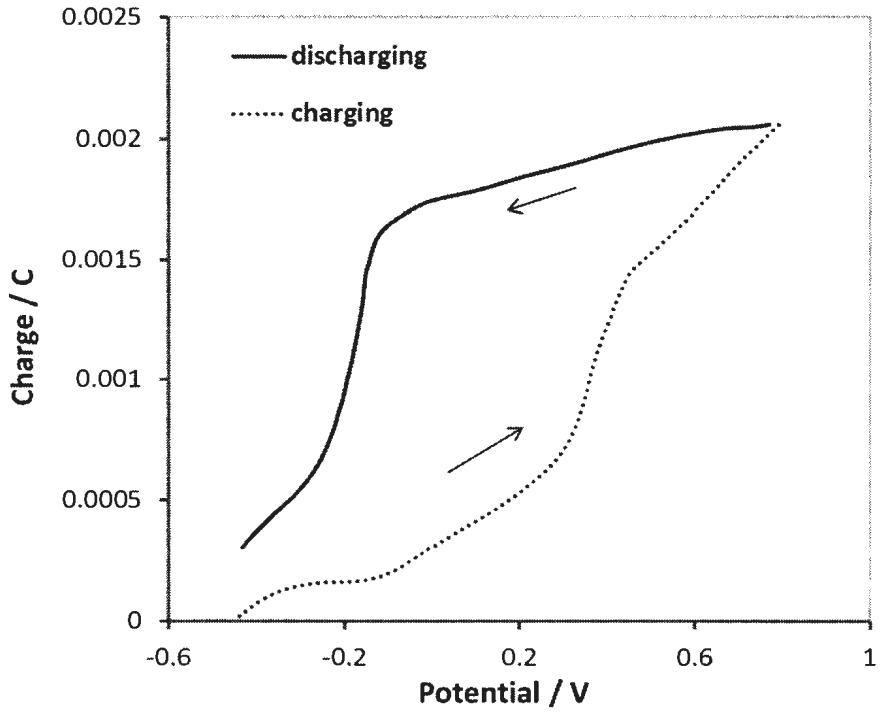

Figure 5.23: Charging/discharging plot of GC/poly(1-AAQ) in 6 M H_2SO_4 (aq) over a potential range between -0.45 V to 0.8 V.

5.3.3.7. The nature of poly(1-AAQ) film capacitance at -0.1 V

The poly(1-AAQ) film was further investigated by impedance spectroscopy at -0.1 V compared to the impedance of a bare GC electrode as shown in Figure 5.24. High capacitance and low resistance was observed only when measuring impedance without an equilibrium time. However, repeating the experiment with a 5 min equilibration time at -0.1 V or -0.2 V before measuring the impedance at -0.1 V resulted in a huge decrease in capacitance. These results reveal slow loss of polyaniline type capacitance.

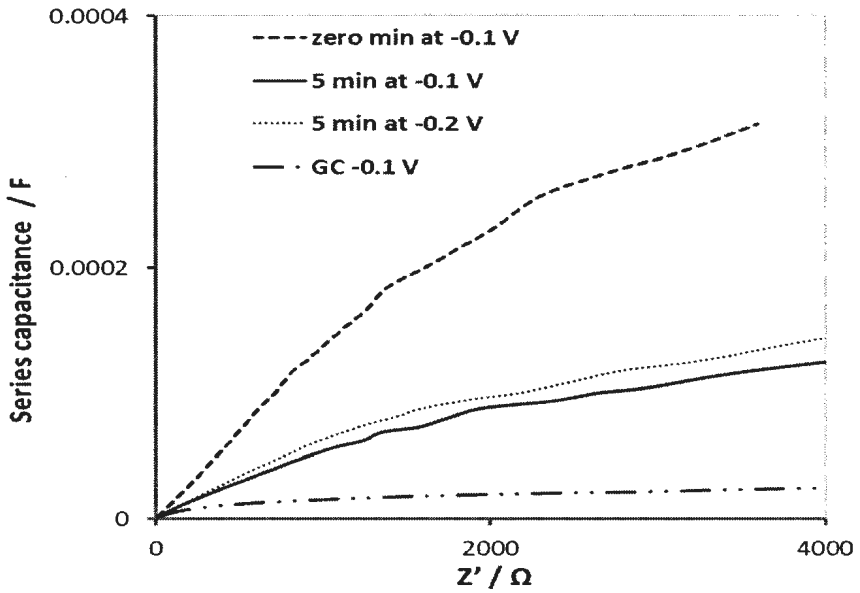

Figure 5.24: Series capacitance versus real impedance of GC/poly(1-AAQ) in 6 M H_2SO_4 (aq) compared to bare GC. All measurements were at -0.1 V vs. SCE. Various equilibrium time and potential were used as indicated.

5.3.3.8. Impedance data fitting for poly(1-AAQ)

Experimental and simulated Nyquist plots of GC/poly(1-AAQ) at - 0.3 V, + 0.1 V and + 0.6 V are shown in Figure 5.25(a) and (b). These two different potentials were chosen to explore the behavior of the film at different oxidation states and consequently at

different conductivity and resistance. Parameters from experimental data were obtained from the dimensions of the plot at the appropriate frequency range. Using circuit fitting for a selected narrow high frequency range gives the charge transfer resistance (R_{ct}). The film resistance (R_L) designated from the Warburg impedance was calculated from R_Σ based on Eq. 5.5. Finally, the film capacitance (C_L) was calculated from the slope of Z" vs. $1/(2\pi f)$ at low frequency since C_L = 1/slope.

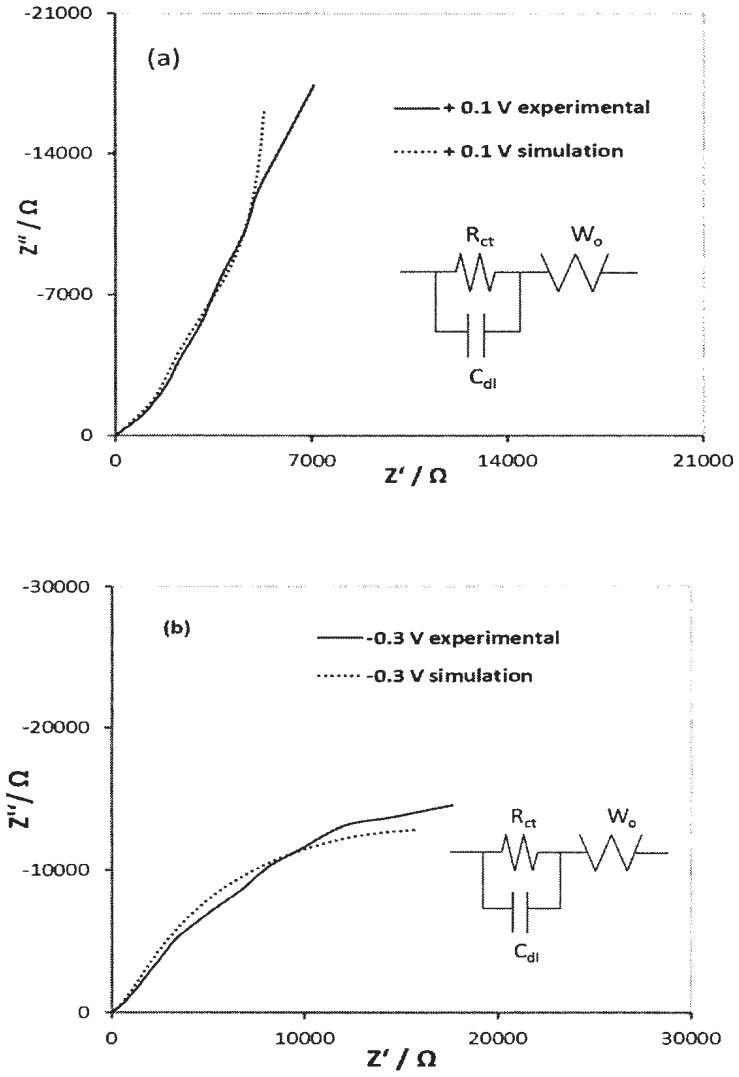

Figure 5.25: Experimental and fitting of Nyquist plots for poly(1-AAQ) in 6M H_2SO_4 (aq) over the frequency range 10000 Hz to 0.01 Hz. (a) at 0.1 V (b) and at -0.3 V.

The fitting parameters along with the experimental ones for poly(1-AAQ) at + 0.1 V and – 0.3 V are summarized in Table 5.3. Relatively good agreements between the experimental and fitted impedance data were obtained. The observed significant discrepancies indicate that both the experimental and fitted data should be considered as semiquantitative descriptions of the film. The non-ideal behavior of the film probably resulted from the uneven film thickness and changes in morphology across the film.[77]

The trend for the charge transfer resistance (R_{ct}) (i.e. the electronic charge transfer resistance) is to decrease with increasing potential where the electron transfer at the GC/polymer interface becomes more facilitated and the polymer becomes more conducting. Even though, the R_{ct} values are considered significantly high. The film resistance (R_L) also was found to decrease with increasing potential. This is expected because as the potential increases the polymer film becomes partially oxidized and thus more electronically conducting. However, the C_L increases with increasing potential where the film becomes partially oxidized.

Table 5.3: Experimental and fitting parameters for the impedance of poly(1-AAQ) in 6 M H_2SO_4. (-) in this table denotes that the value cannot be measured from the plot.

	R_{ct} / Ω		R_L / Ω		C_L / F	
E / V	**semicircle**	**fit**	**45°**	**fit**	**-1/(2πf Z'')**	**fit**
+ 0.1	3384	4184	4776	4681	6.30×10^{-5}	1.28×10^{-4}
- 0.3	11597	14232	-	33178	-	7.79×10^{-5}

5.3.3.9. FTIR spectra of poly(1-AAQ)

Figure 5.26 shows Fourier transform infra-red (FTIR) spectra for the solid monomer 1-AAQ while Figure 5.27 shows the corresponding poly(1-AAQ) which was deposited as a thin film on a GC electrode by potentiodynamic polymerization from 6 M H_2SO_4 solution. FTIR experiments may, but not necessarily, provide additional support for the polymer formation and the possible ways of coupling. The evidence for polymer formation is mainly the presence of imine (i.e. (C=N) at 1558 cm^{-1}), amine (i.e. (N-H) deformation of secondary amine at 1504 cm^{-1}) and HSO_4^- (i.e. S-O at 1028 cm^{-1}) moieties, respectively.[51,57] This suggest coupling at the 1,4 positions in the 1-AAQ. In addition, the absorption band of the α,β-unsaturated carbonyl group in 1-AAQ at 1663 cm^{-1} was shifted to lower energy at 1644 cm^{-1} due to polymer formation. These findings indicate that the polymer has the essential functional groups that are responsible for its electroactivity. It is also notable from these figures that some bands were very small (e.g. 1557 cm^{-1}) and sometimes cannot be distinguished from the noise.

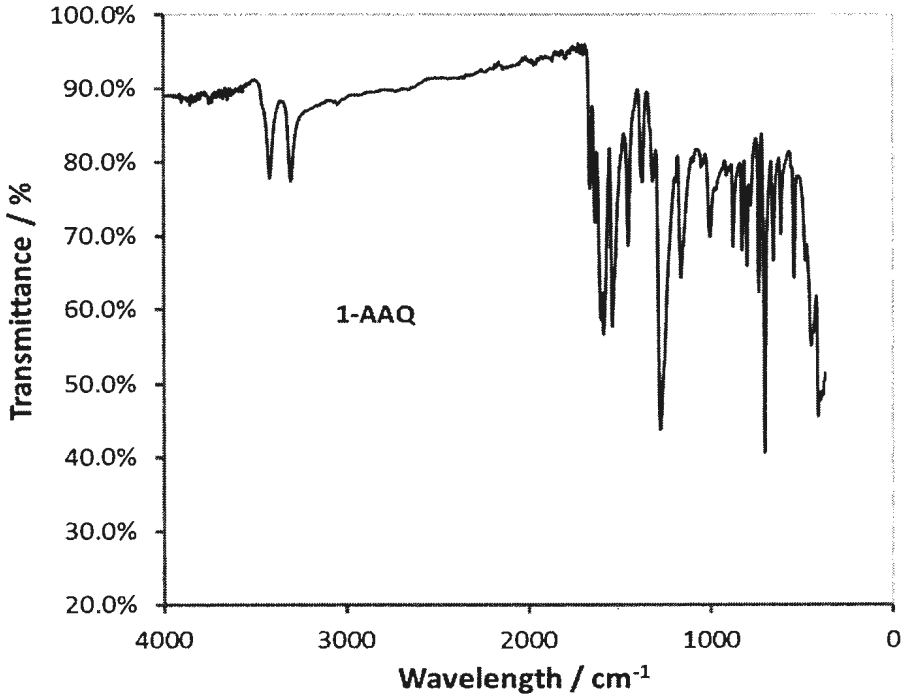

Figure 5.26: ATR-FTIR spectrum of solid 1-AAQ monomer.

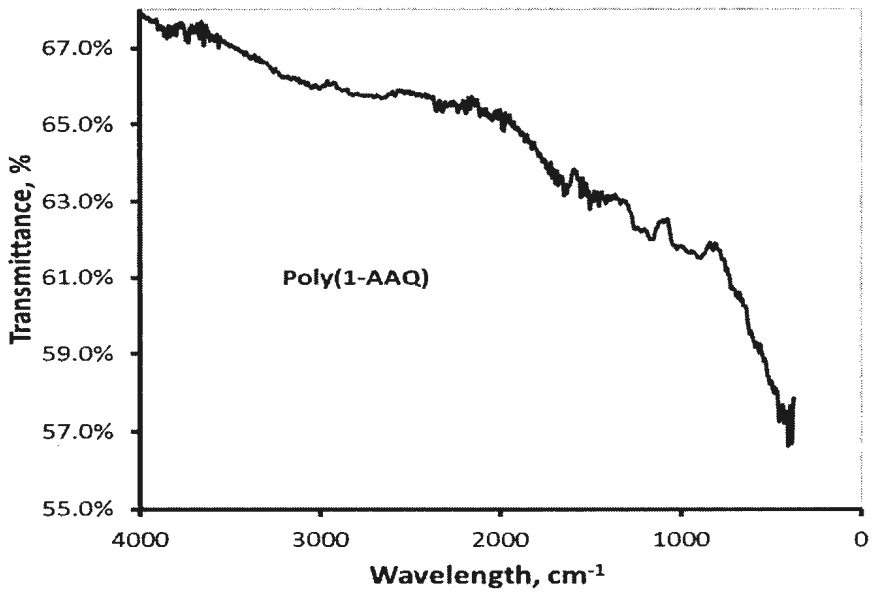

Figure 5.27: ATR-FTIR spectrum of poly(1-AAQ) deposited on GC electrode by potentiodynamic polymerization from 6 M H_2SO_4 (aq).

The main FTIR transmission bands proposed for both 1-AAQ and poly(1-AAQ) with comparisons from the literature are given in Table 5.4.

Table 5.4: Proposed FTIR assignments for poly(1-AAQ) compared with the literature.

Possible assignments	1-AAQ (Literature)	Poly(1-AAQ) (literature)
C=O (quinone)	1602 (1596)[57]	1644 (1631)[57]
C=N str. imine	-	1558 (1580)[51]
N-H deformation	1540 (1550)[51] 1° amine	1504 (1500)[51] 2° amine
C-N str.	1218 (1290)[51]	1258 (1250)[51]
N-H str.		
ϒ asym. (NH2)	3417 (3410)[51] strong	-
ϒ sym. (NH2)	3302 (3310))[51] strong	3167 (3170)[51] weak
N-H str. 2 amine	-	3425 (3430)[51]
C-H out of plane bend. vibration		
of 2H	829 (850)[51]	828 (830)[51]
of 3H	706-801 (710-810)[51]	697-828 (710-820)[51]
HSO_4^-	-	1028 (1050)[92]

5.3.3.10. Proposed structure for poly(1-AAQ)

From SEM images, it can be seen that a porous solid film was deposited on glassy carbon electrodes by potentiodynamic polymerization. This film, based on cyclic voltammetry and impedance measurements, shows various electroactive sites with conducting properties depending on the potential. Furthermore, FTIR spectra of the monomer and the polymer reveal that the polymer has been electrodeposited in a manner similar to polyaniline derivatives without losing the AQ structure. The probability of coupling between monomer units depends on the presence of the highest stable radical.

Stability of the various radical cations that are formed electrochemically which may be located at NH_2, C1, or C4 positions in 1-AAQ, respectively, as reported by Naoi *et al.*[92] However, it has been found that for 1,5-diaminoanthraquinone the radical at the α position has the highest spin density.[90] By analogy, it is expected that a radical at the α position will be the most stable one for 1-AAQ. Therefore, the most probable coupling of two monomer units will be at 1,4 and 5,8 positions.[51,57,90,93] Accordingly, the proposed polymer structure for poly(1-AAQ) in the fully reduced and fully oxidized forms are drawn in Figure 5.28. Naoi *et al.* reported that potentiodynamicaly prepared crystalline structural oligomers of 1,5-diaminoanthraquinone have a π-π interaction which reduces chain movement to the minimum which enable them to attain high electrochemical cyclability.[92] This characteristic may be found in poly(1-AAQ) prepared potentiodynamically but needs further investigation by X-ray diffraction (XRD).

(a)

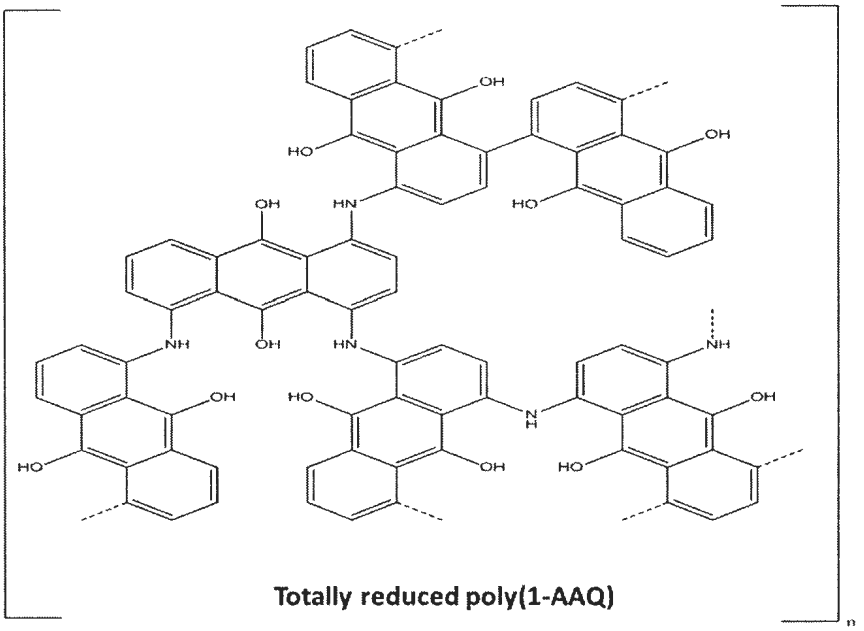

(b)

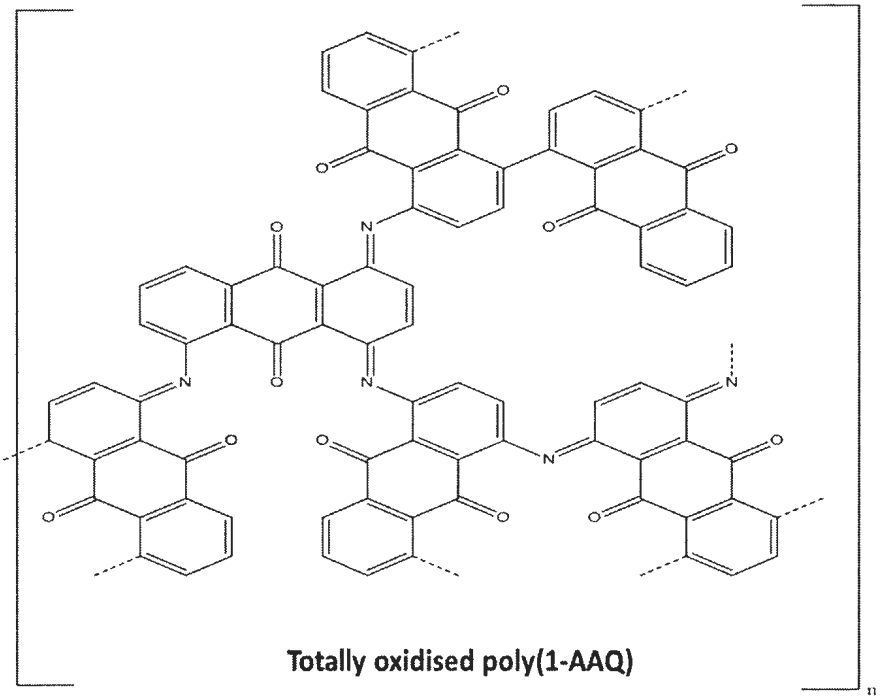

Figure 5.28: Proposed structures of poly(1-AAQ) (a) in the totally reduced form and (b) totally oxidized form.

5.3.3.11. Electropolymerization in mixed solvents

In this section potentiodynamic polymerization of 1-AAQ in a mixture of solvents (i.e. aqueous/organic) is reported. It is notable that dissolving 1-AAQ in acetonitrile before adding H_2SO_4 did not produce a polymer film during potential cycling. This might be attributed to some unwanted impurities that inhibit the polymerization process or form soluble products. The following is a suitable way to deposit poly(1-AAQ) films from mixed solvents. Initially 0.0223 g 1-AAQ was dissolved in 20 mL of 6 M H_2SO_4 (aq) through stirring and heating to 80 °C. Then 10 mL of this solution was diluted with 10 mL of acetonitrile. Therefore, the concentration of 1-AAQ was 2.5 mM and the concentration of H_2SO_4 was 3 M with an overall aqueous to organic volume ratio of 1:1. This solution was used to deposit poly(1-AAQ) films on glassy carbon electrodes by cycling at 50 mV s^{-1} between -0.6 V and 1.4 V vs. SCE, as shown in Figure 5.29. Again the AQ reoxidation peak was shifted to more positive potential which reveals the trapping phenomenon.

The first few cycles (not all of them are shown for clarity) were scanned over a potential regime where the redox peaks of the 1-AAQ monomer appears (i.e. $E_{1/2}$ = -0.090 V vs. SCE). The peak separation for the 1-AAQ monomer was 180 mV which indicates a quasireversible redox peak on glassy carbon.[94] The potential was then extended to initiate polymerization through the formation of radical cations upon anodic oxidation of 1-AAQ which is indicated by a sharp increase in the anodic current at *ca.* 1.0 V vs. SCE. Actually, the onset potential for 1-AAQ oxidation (i.e. 0.925 V vs. SCE) was

estimated from extrapolating this sharply increasing current to the potential axis. When the potential was switched back to the negative direction, a small cathodic peak appeared at *ca.* 0.8 V which can be attributed to reduction of the dimer.[46,57] On subsequent cycles, the current for the AQ reduction increased with small shifts in the peak potential to more negative values. Again the AQ reoxidation peak was shifted to more positive potential which reveals the trapping phenomenon or can be explained based on the formation of a porous polymer film which is more resistive than the bare glassy carbon electrode.[74,95] As the film thickness increased with cycling, the film resistance also increased.[46] Accordingly, the monomer oxidation peak is expected to shift to more positive potentials.

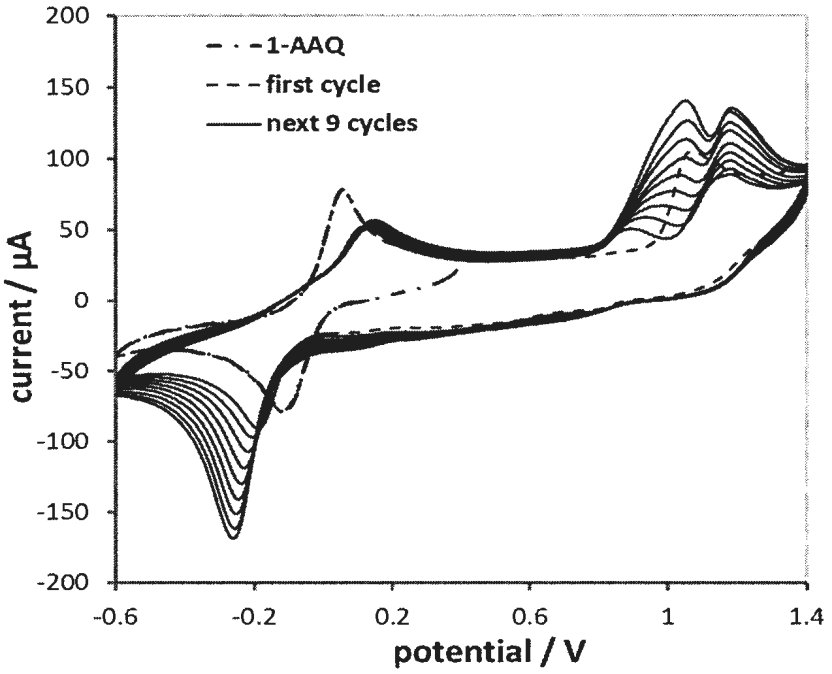

Figure 5.29: Potentiodynamic polymerization at 50 mV s^{-1} of 1-AAQ on a glassy carbon electrode in mixed solvents, where 0.0223 g of 1-AAQ was preheated initially in 6 M H_2SO_4 (aq) then 10 mL it was diluted with 10 mL of acetonitrile (1:1).

Poly(1-AAQ) prepared in the mixed solvent was then immersed in acetonitrile and deionized water multiple times, before testing the polymer in a monomer–free solution, to remove any soluble monomers and or oligomers. Figure 5.30 shows cyclic voltammograms of poly(1-AAQ) in 6 M H_2SO_4 (aq) over a narrow potential window from -0.4 V to 0.4 V, to avoid polymer overoxidation, and at scan rates ranging from 5 mV s^{-1} to 40 mV s^{-1}. Two small redox couples due to AQ activity are clearly identified at formal potentials of 0.20 V and -0.09 V. This finding reveals that these redox peaks are related to AQ sites close to the GC surface. The former redox peak (i.e. at 0.20 V) may be related to the formation of a complex between AQ and an aniline-type structure through hydrogen bonding, as shown in Figure 5.31.[85,92,96]

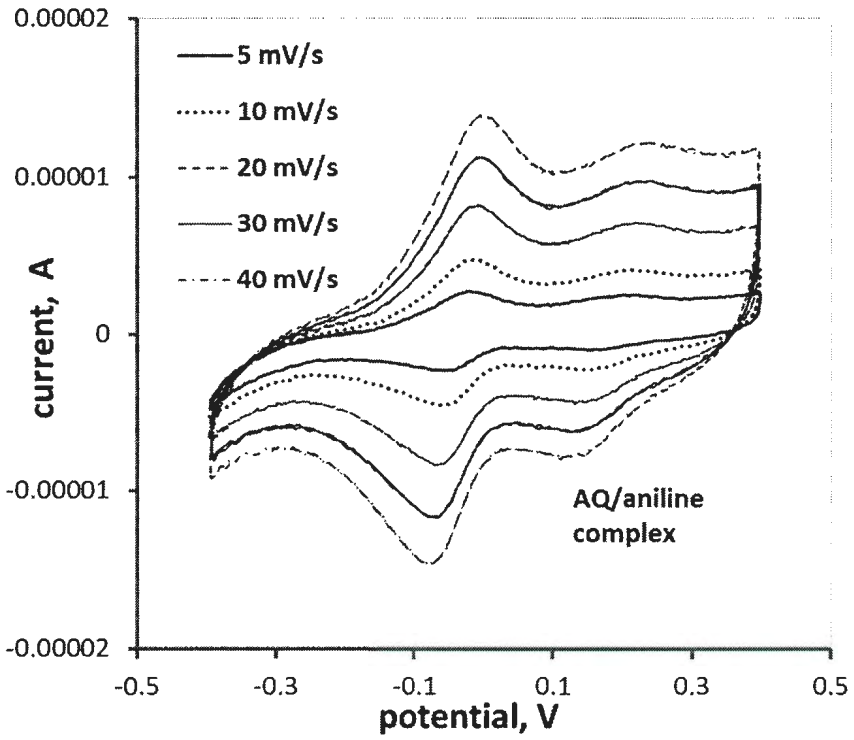

Figure 5.30: Scan rate effect on poly(1-AAQ) in 6 M H_2SO_4 (aq) following CV in Figure 5.29.

The peak potential difference ($E_{anodic} - E_{cathodic}$) for the couple at -0.09 V was greater than zero which indicates a significant change in chain conformation.[97] Moreover, the peak width at half height (PWHH) of the -0.09 V couple, scanned at 40 mV s^{-1} was 136 mV (i.e. > 90/n). This can be explained by repulsive interaction between the AQ redox centres in the film.[98]

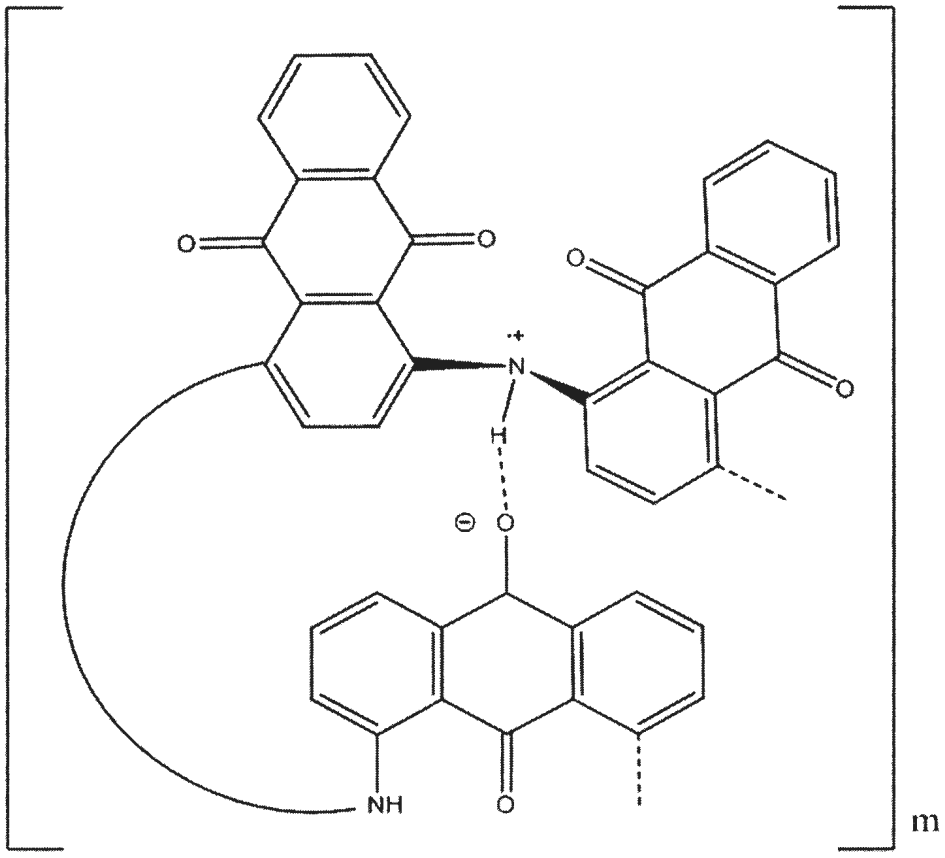

Figure 5.31: Schematic representation of the complex proposed between AQ and a bridging nitrogen.

The potentiodynamic polymerization of 1-AAQ from the mixed solvent system did not solve the charge trapping issue which is not useful for supercapacitor applications. There are some differences in electrochemistry of poly(1-AAQ) prepared from mixed

solvents which can be attributed to different conducting properties, inner film structure and porosity.[53,71,74,76] Naoi *et al.* reported highly conducting characteristics of poly 1,5-diaminoanthraquinone over a 2.3 V potential window.[51] They explained that high film conductivity in the reduced state is based on the presence of the two oxygen atoms in the AQ centres which improve the conductivity within the film through a "tunneling bridge".[51,92,96]

Previously reported voltammograms for the polymerization of 1-AAQ from a 1:1 mixture of acetonitrile and 6 M H_2SO_4 (aq) show charge trapping that is similar to that shown Figure 5.6 but without the progressive shifting of the quinone reoxidation peak.[47] However, the charge trapping phenomenon was not discussed in that work. Small reversible quinone waves were reported at *ca.* +0.05 V, and we have been able to reproduce these (see Figure 5.32) by depositing poly-AAQ from a mixture of acetonitrile and 6 M H_2SO_4 (aq). Similar small waves are also seen in the -0.45 V to +0.3 V voltammograms in Figure 5.20, which is expanded in Figure 5.32. It is clear from Figure 5.20 that these small reversible or quasi-reversible waves at the quinone formal potential involve only a small fraction of the quinone sites in the film and so do not represent the bulk behavior. They are presumably due to quinone sites close to the interface with the glassy carbon electrode.

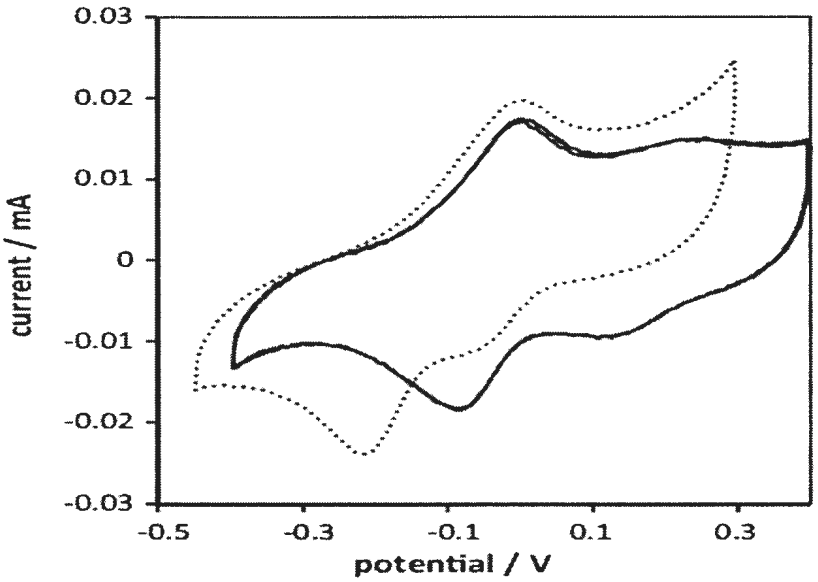

Figure 5.32: Cyclic voltammetry of poly(1-AAQ) coated GC electrodes in 6 M H_2SO4 (aq) at 50 mV s^{-1}. The poly(1-AAQ) was deposited from 6 M H_2SO_4 (• • • •) or a 1:1 mixture of acetonitrile and 6 M H_2SO_4 (—).

Charge trapping can also be seen in a literature voltammograms of poly(5-amino-1,4-naphthoquinone).[99] In that case, quasi-reversible electrochemistry of the quinone was observed at 0.07/0.15 V, and it was thought that the polymer backbone was oxidized at 0.69 V and reduced at about 0.03 V. In a more recent report on poly(2-methyl-5-amino-1,4-naphthoquinone),[85] similar partial charge trapping peaks were attributed to interactions between the quinone and amine groups whereby $NH^{+\cdot}$ generated on the anodic scan oxidized trapped hydroquinone sites and hydroquinone sites generated during the cathodic scan reduced trapped $NH^{+\cdot}$ sites.

5.3.3.12. Potentiodynamic polymerization of 1-AAQ on porous carbon materials

In the preceding sections, electropolymerization of 1-AAQ was reported for a flat carbon surface (i.e. the glassy carbon electrode). However, electrodeposition of this

polymer on porous high surface area carbon is important for practical applications.[100-105] Here, the same experimental conditions described in sections 5.3.3.1.1 and 5.3.3.1.2 were used to electropolymerize 1-AAQ on carbon fiber paper (CFP; Toray TGP-H-090), (CFP). Nearly the same voltammetric characteristics during polymerization were found; compare Figure 5.33 and Figure 5.34 with Figure 5.5 and Figure 5.6. However, preliminary potentiodynamic polymerization results on high surface area carbon black (Vulcan X72 and Black Pearls 2000) were not successful. This can be attributed to the weak binding between the carbon black powder and the substrate (i.e. glassy carbon) as some flakes were seen to fall away from the electrode into the electrolyte solution. Therefore, more work needs to be done to optimize loading and adhesion of carbon black on glassy carbon.

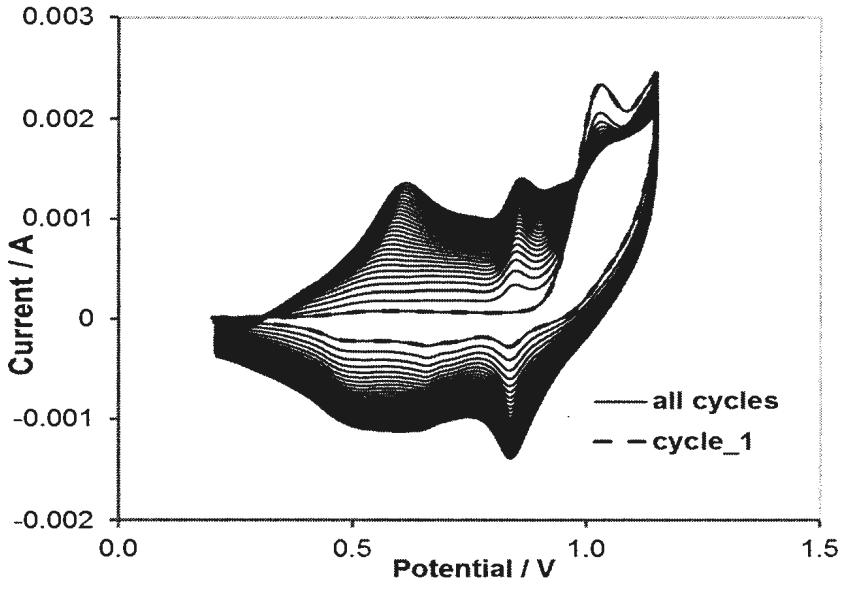

Figure 5.33: Electro-oxidative polymerization of *ca.* 5 mM 1-AAQ dissolved in 6 M H_2SO_4 (aq) on carbon fiber paper (CFP) electrode scanned from 0.2 to 1.2 V vs. SCE at a rate of 100 mV/s.

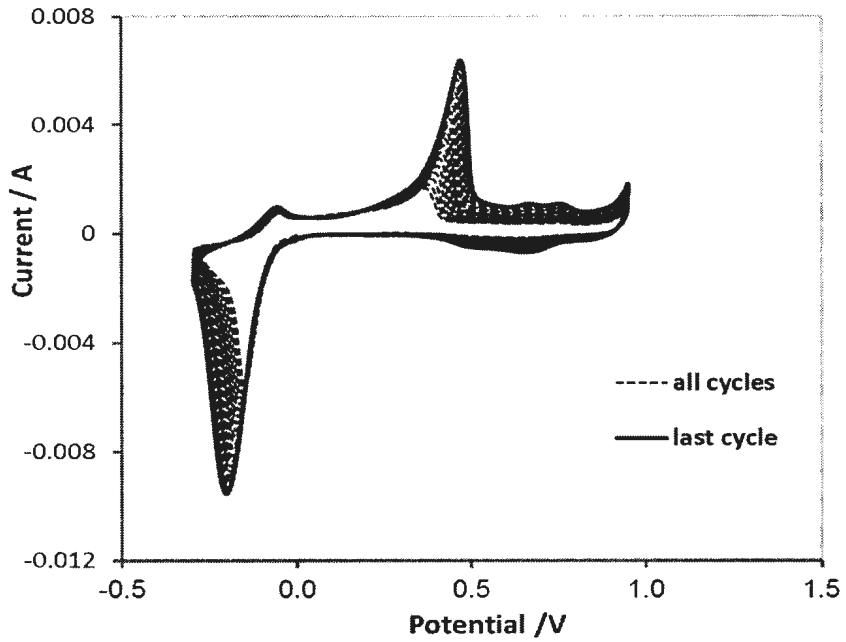

Figure 5.34: Electro-oxidative polymerization of *ca.* 5 mM 1-AAQ dissolved in 6 M H_2SO_4 (aq) on carbon fiber paper (CFP) electrode scanned from -0.45 to 1.0 V vs. SCE at a rate of 50 mV/s. for ten cycles.

5.4. Conclusions

The electrochemical activity of the quinone couple in poly-AAQ is dependent upon the conductivity due to the polyaniline-like backbone. During cyclic voltammetry the polymer retains sufficient conductivity on the cathodic scan for the quinone groups to be reduced at potentials close to the formal potential of *ca.* −0.1 V vs. SCE. However, the conductivity of the reduced film becomes insufficient to allow re-oxidation at the thermodynamic potential, except for sites close to the interface between the polymer film and the electrode. Sufficient conductivity is only recovered at potentials above *ca.* +0.3 V, leading to trapping of the quinone sites in their reduced state over the −0.1 V to +0.36 V region of the anodic scan. The peak current for reoxidation of the quinone groups is shifted to +0.36 V at 5 mV s^{-1} and +0.44 V at 400 mV s^{-1}.

Although this charge trapping effect may have some value in electronic devices,[106] for example, it will limit performance in most applications. It is therefore important that it is fully understood so that kinetic limitations on the quinone electrochemistry in electrochemically deposited polyanthraquinones and related materials can be minimized.

References

(1) Delamar, M.; Pinson, J.; Saveant, J. *J. Am. Chem. Soc.* **1992**, *114*, 5883-5884.

(2) McCreery, R. *Chem. Rev.* **2008**, *108*, 2646-2687.

(3) Pinson, J; Podvorica, F. *Chem. Soc. Rev.* **2005**, *34*, 429-439.

(4) Shamsipur, M.; Golabi, S. M.; Sharghi, H.; Mousayi, M. F. *J. Solid Sate Electrochem.* **2001**, *5*, 68-73.

(5) Murray, R. *Acc. Chem. Res.* , **1980**, *13*, 135.

(6) Wring, S. A.; Hart, J. *Analyst* **1992**, *117*, 1215-1229.

(7) Solak, A.; Eichrst, L.; Clark, W.; McCreery, R. *Anal. Chem.* **2003**, *75*, 296-305.

(8) Hatchett, D. W.; Josowicz, M. *Chem. Rev.* **2008**, *108*, 746-769.

(9) Švancara, I.; Vytras, K.; Kalcher, K.; Walcarius A.; Wang, J. *Electroanalysis* **2009**, *21*, 7-28.

(10) Burkhardt, S.; Lowe, M.; Conte,S.; Zhou, W.; Qian, H.; Rodriguez, G.; Gao, J.; Hennig,R.; Abruna, H. *Energy Environ. Sci.* **2012**, *5*, 7176-7187.

(11) Ghanem, M.; Kocak, I.; Al-Mayouf, A.; AlHoshan, M.; Bartlett, P. *Electrochim. Acta* **2012**, *68*, 74-80.

(12) Toupin, M.; Belanger, D. *Langmuir* **2008**, *24*, 1910-1917.

(13) Toupin, M.; Belanger, D. *J. Phys. Chem. C* **2007**, *111*, 5394-5401.

(14) Mahouche-Chergui, S.; Gam-Derouich, S.; Mangeney, C.; Chehimi, M. M. *Chem. Soc. Rev.* **2011**, *40*, 4143-4166.

(15) Zollinger, H. In *Diazo Chemistry I: Aromatic and Heteroaromatic Compounds;* VCH Verlagsgesellschaft mbH: **1994**; Vol. I.

(16) Bélanger, D.; Pinson, J. *Chem. Soc. Rev.* **2011**, *40*, 3995-4048.

(17) Downard, A. *Electroanalysis* **2000**, *12*, 1085-1096.

(18) Liu, G. Chckalingham, M.; Khor, S.; Gui, A. *Catal. Sci. Tech.* **2011**, *1*, 207-217.

(19) Wildgoose, G.; Banks, C.; Leventis, H.; Compton, R. *Mikrochim. Acta* **2006**, *152*, 187-214.

(20) Griese, S.; Kampouris, D.; Kadara, R.; Banks, C. *Electroanalysis* **2008**, *20*, 1507-1512.

(21) Dicks, A. *J. Power Sources* **2006**, *156*, 128-141.

(22) Wu, G.; More, K.; Johnston, C.; Zelenay, P. *Science* **2011**, *332*, 443-447.

(23) Zhou, Y.; Neyerlin, K.; Olson, T.; Pylypenko, S.; Bult, J.; Dinh, H.; Gennett, T.; Shao, Z.; O'Hayre, R. *Energy Environ. Sci.* **2010**, *3*, 1437-1446.

(24) Leitner, K. W.; Gollas, B.; Winter, M.; Besenhard, J. *Electrochim. Acta* **2004**, *50*, 199-204.

(25) Zhao, X.; Sanchez, B.; Dobson, P.; Grant, P. *Nanoscale* **2011**, *3*, 839-855.

(26) Simon, P.; Gogotsi Y. *Nat. Mater.* **2008**, *7*, 845-854.

(27) Frackowiak, E. *Phys. Chem. Chem. Phys.* **2007**, *9*, 1774–1785.

(28) Conway, B. E. In *Electrochemical supercapacitors: Scientific fundamentals and technological applications;* Plenum Press: New York, **1999**; pp 698.

(29) Burke, A. *J. Power Sources* **2000**, *91*, 37-50.

(30) Miller, J.; Simon P. *Science* **2008**, *321*, 651-652.

(31) Schnorr, J. M. *Chem. Mater.* **2011**, *23*, 646-657.

(32) Zhang, Y.; Wu, X.; Wang, L.; Zhang, A.; Xia, T. *Int J. Hydrogen Energy* **2009**, *34*, 4889-4899.

(33) Li, C.; Bai, H.; Shi, G. *Chem. Soc. Rev.* **2009**, *38*, 2397-2409.

(34) Quan, M.; Sanchez, D.; Wasylkiw, M. F.; Smith, D. K. *J. Am. Chem. Soc.* **2007**, *129*, 12847-12856.

(35) Katsumi, J.; Nakayama, T.; Esaka, Y.; Uno, B. *Anal. Sci.* **2012**, *28*, 257-265.

(36) Batchelor-McAuley, C.; Li, Q.; Dapin, S.; Compton, R. *J. Phys. Chem. B* **2010**, *114*, 4094-4100.

(37) Gupta, N.; Linschitz, H. *J. Am. Chem. Soc.* **1997**, *119*, 6384-6391.

(38) Costentin, C.; Loualt, C.; Robert, M.; Saveant, J. *Chem. Rev.* **2008**, *108*, 2145-2179.

(39) Allongue, P.; Desbat, B.; Fagebaume, O.; Hitmi, R.; Pinson, J. *J. Am. Chem. Soc.* **1997**, *119*, 201-207.

(40) Lafitte, V.; Wang, W.; Yashina, A.; Lawrence, N. *Electrochem. Commun.* **2008**, *10*, 1831-1834.

(41) Schinazi, R.; Chu, C.; Babu, J.; Oswald, B.; Saalmann, V.; Cannon, D.; Eriksson, B.; Nasr, M. *Antiviral Res.* **1990**, *13*, 265-272.

(42) Campos-Martin, J.; Blanco-Brieva, G.; Fierro, J. *Angew. Chem. Int. Ed.* **2006**, *45*, 6962-6984.

(43) Watkins, J.; Lawwrance, K.; Tylor, J.; James, T.; Bull, S.; Marken, F.. *Electroanalysis* **2011**, *23*, 1320-1324.

(44) Badawy, W. A.; Medany, S. S. *Int. J. Chem. Kinet.* **2011**, *43*, 141-146.

(45) Manisankar, P.; Gomathi, A.; Velayutham, D. *J. Solid State Electrochem.* **2005**, *9*, 601-608.

(46) Ramiz, M. M.; Khudaish, E. A.; Deronzier, A.; Chardon-Noblat, S. *J. Electroanal. Chem.* **2010**, *647*, 35-42.

(47) Kalinathan, K.; DesRoches, D.; Liu, X.; Pickup, P. *J. Power Sources* **2008**, *181*, 182-185.

(48) Algharaibeh, Z.; Liu, X.; Pickup, P. *J. Power Sources* **2009**, *187*, 640-643.

(49) Algharaibeh, Z.; Pickup, P. *Electrochem. Commun.* **2011**, *13*, 147-149.

(50) Pognon, G.; Brousse, T.; Belanger, D. *Carbon* **2011**, *49*, 1340-1348.

(51) Naoi, K.; Suematu, S.; Manago, A. *J. Electrochem. Soc.* **2000**, *147*, 420-426.

(52) Smith, R.; Pickup, P. *Electrochim. Acta* **2009**, *54*, 2305-2311.

(53) Heinze, J.; Frontana, B.; Ludwigs, S. *Chem. Rev.* **2010**, *110*, 4724-4771.

(54) Pauliukaite, R.; Barsan, M.; Brett, C. *Anal. Lett.* **2010**, *43*, 1588-1608.

(55) Zhang, G.; Yang, F. *Phys. Chem. Chem. Phys.* **2011**, *13*, 3291-3302.

(56) Yano, J.; Kokura, M.; Ogury, K. *J. Appl. Electrochem.* **1994**, *24*, 1164-1169.

(57) Badawy, W.; Ismail, K.; Medany, S. *Electrochim. Acta* **2006**, *51*, 6353-6360.

(58) Barsan, M.; Brett, C. *Electrochim. Acta* **2008**, *53*, 3973-3982.

(59) Inzelt, G., Ed.; In *Conducting polymers: A new era in electrochemistry;* Springer; **2005**.

(60) Cosnier, S., Ed.; In *Electropolymerization: concepts, materials and applications;* Weinheim: Wiley-VCH, **2010**.

(61) Oyama, N.; Sato, M.; Ohsaka, T. *Synth. Met.* **1989**, *29*, E501-E506.

(62) Inzelt, G.; Pineri,; Schultze, J.; Vorotyntsev, M. *Electrochim. Acta* **2000**, *45*, 2403-2421.

(63) Algharaibeh, Z.; Pickup, P. *Electrochim. Acta* **2013**, 93, 87-92.

(64) Wang, X.; Tang, X.; Li, X.; Hua, X. *Inter. J. Mol. Sci.* **2009**, *10*, 5257-5284.

(65) Choi, S.; Park, S. *J. Electrochem. Soc.* **2002**, *149*, E26-E34.

(66) Zotti, G.; Schiavon, G.; Zecchin, S. *Synth. Met.* **1995**, *72*, 275-281.

(67) Beck, F.; Braun, P.; Oberst, M. *Ber. Bunsenges. Phys. Chem.* **1987**, *91*, 967-974.

(68) Wegner, G.; Wernet, W.; Glatzhofer, D.; Ulansk, J.; Krohnke, C.; Mohammadi, M. *Synth. Met.* **1987**, *18*, 1-6.

(69) Denisevich, P.; Willman, K.; Murray, R. *J. Am. Chem. Soc.* **1981**, *103*, 4127.

(70) Hillman, A.; Mallen E. *J. Electroanal. Chem.* **1990**, 281, 109.

(71) Paulson, S.; Elliott, C. *J. Phys. Chem. B* **2001**, *105*, 8718-8724.

(72) Pickup, P. *J. Chem. Soc., Faraday Trans.* **1990**, *86*, 3631-3636.

(73) Musiani, M. *Electrochim. Acta* **1990**, *35*, 1665-1670.

(74) Inzelt, G. *Chem. Biochem. Eng. Q.* **2007**, *21*, 1-14.

(75) Ren, X.; Pickup, P. *J. Phys. Chem.* **1993**, *97*, 3941-3943.

(76) Rubinson, J. F.; Koyinamura, Y. *Chem. Soc. Rev.* **2009**, *38*, 3339-3347.

(77) Ren, X. ; Pickup, P. *J. Electroanal. Chem.* **1997**, *420*, 251-257.

(78) Albery, W. J.; Chen, Z.; Horrocks, B.; Mount, A.; Wilson, P.; Bloor, D. *Faraday Discuss. Chem. Soc.* **1989**, *88*, 247.

(79) Albery, W.; Elliott, C.; Mount, *A. J. Electroanal. Chem.* **1990**, 288, 15.

(80) Lefebvre, M.; Martin, R.; Pickup, P. *Electrochem. Solid-State Lett.* **1999**, 2, 259.

(81) Kötz, R. *Electrochim. Acta* **2000**, *45*, 2483-2498.

(82) Mao, H.; Pickup, P. *J. Am. Chem. Soc.* **1990**, 112, 1776.

(83) Ofer, D.; Crooks, R.; Wrighton, M. *J. Am. Chem. Soc.* **1990**, 112, 7869.

(84) Paul, E.; Ricco, A.; Wrighton, M. *J. Phys. Chem.* **1985**, 89, 1441.

(85) Pham, M.; Hubert, S.; Maurel, F.; Dao, H.; Takenouti, H. *Synth. Met.* **2004**, *140*, 183-197.

(86) Dinh, H.; Birss, V. *J. Electroanal. Chem.* **1998**, *443*, 63-71.

(87) Dinh, H.; Birss, V. *J. Electrochem. Soc.* **2000**, *147*, 3775-3784.

(88) Ren, X.; Pickup, P. *J. Electroanal. Chem.* **1994**, *372*, 289-291.

(89) Roßberg, K.; Paasch, G.; Dunsch, L.; Ludwig, S. *J. Electroanal. Chem.* **1998**, *443*, 49-62.

(90) Genies, E.; Penneau, J.; Vieil, E. *J. Electroanal. Chem. Interfac. Electrochem.* **1990**, *283*, 205-219.

(91) Gabrielli, C.; Haas, O.; Takenouti, H. *J. Appl. Electrochem.* **1987**, *17*, 82-90.

(92) Naoi, K.; Suematsu, S.; Hanada, M.; Takenouchi, H. *J. Electrochem. Soc.* **2002**, *149*, A472-A477.

(93) Kang, E.; Neoh, K.; Tan, K. *Prog. Polym. Sci.* **1998**, *23*, 277-324.

(94) Kinoshita, K. Ed.; In *Carbon: electrochemical and physicochemical properties;* Jiohn Wiley & Sons: **1988**.

(95) Demenech, A., Ed.; In *Electrochemistry of porous materials; CRC Press;* **2010**.

(96) Matveeva, E. *Synth. Met.* **1996**, *83*, 89-96.

(97) Schwartz, B. *Annu. Rev. Phys. Chem.* **2003**, *54*, 141-172.

(98) Lyons, M., Ed.; In *Electroactive polymer electrochemistry;* Springer; **1994**; Vol. 1.

(99) Pham, M.; Piro, B.; Bazzaoui, E.; Hedayatullah, M.; Lacroix, J.; Navak, P.; Haas,O. *Synth. Met.* **1998**, *92*, 197-205

(100) Coffey, B.; Madsen, P.; Poehler, T.; Searson, P. *J. Electrochem. Soc.* **1995**, *142*, 321-325.

(101) Dalmolin, C.; Canobre, S.; Biaggio, S.; Rocha-Filho, R.; Bocchi, N. *J. Electroanal. Chem.* **2005**, *578*, 9-15.

(102) Tamai, H. ; Hakoda, M.; Shono, T.; Yasuda, H. *J. Mater. Sci.* **2007**, *42*, 1293-1298.

(103) Zengin, H.; Kalayci, G. *Mater. Chem. Phys.* **2010**, *120*, 46-53.

(104) Moghaddam, R.; Pickup, P. *Phys. Chem. Chem. Phys.* **2010**, *12*, 4733-4741.

(105) Oh, M.; Kim, S. *J. Nanosci. Nanotech.* **2012**, *12*, 519-524.

(106) Kaake, L.; Barbara, P.; Zhu, X. *J. Phys. Chem. Lett.* **2010**, *1*, 628-635.

Chapter 6

Electrochemical copolymerization of aniline with 1-aminoanthraquinone and its electrocatalytic activity towards O_2 reduction

6.1. Introduction

Since their discovery in the 1970s, intrinsically conducting polymers, also known as synthetic metals, have been extensively investigated.[1-6] Due to their unique chemical, optical, mechanical and electrochemical characteristics a wide range of applications have been developed such as electroanalysis,[7,8] batteries,[9-11] electrochromic devices[7,12] and supercapacitors.[4,5,13-15] Many conducting polymers are derived from simple monomers like aniline, pyrrole, and thiophene and their derivatives[16,17]

Conducting polymers are promising for supercapacitor applications since they have higher specific capacitances than carbon electrodes and a relatively lower cost compared to some metal oxides.[4,5] Moreover, thin or thick polymer films can be readily oxidized or reduced.[18] Interestingly, they can be altered and modified to obtain many diverse physical, chemical and electrochemical characteristics.[7]

There are four different methodologies that can be used to modify a particular conducting polymer to achieve the desired properties.[19] These include using a substituted

monomer,[19] adjusting the polymerization conditions,[20] modifying the polymer by post treatment[19,21] or by copolymerizing two or more monomers.[22]

By utilizing the last methodology (i.e. copolymerization), a number of benefits can be obtained. For example, polyaniline is not electrochemically active in solutions of pH >4.[19,23] Therefore it is normally copolymerized with another pH dependent functional group in order for polyaniline to be useful over a wider pH range.[23] For example, polymerization of 1-aminoanthraquinone (1-AAQ) with aniline produces aniline-co-1-AAQ copolymer which is electroactive up to pH 7.[24] In addition, copolymerization of aniline with an alkylaniline leads to tunable conductivity.[19,22] Better stability and solubility was reported by copolymerizing aniline with butylaniline.[25]

Copolymerization of two monomers which have a large difference in their oxidation potentials is difficult.[16] Therefore, it is recommended to select monomers of similar oxidation potentials for copolymerization such as the copolymerization of aniline with a substituted aniline.[19,24] Fortunately, aniline and 1-AAQ have relatively similar oxidation potentials and are readily copolymerized on GC.[24] The AQ functionality has been utilized for supercapacitors either through covalent bonding to carbon[26,27] or in a polymer deposited onto a carbon electrode.[28,29] It has also been used for catalytic reactivity towards the oxygen reduction reaction (ORR).[30-33] Moreover, conducting polymers are also potential candidates for ORR.[34-36] The ORR is a very important reaction. Until now, platinum (Pt) is the best catalyst that is widely used in fuel cells, even though it is very expensive ($1830 per ounce).[34] Therefore, it is highly desirable to

replace Pt with a less expensive and available material as a catalyst for fuel cell applications especially at the cathode where the ORR is slow and needs a larger amount of Pt than that is needed for hydrogen oxidation at the anode.[34]

For electrochemical devices, materials which have a synergistic effect when combined are highly desirable to maximize the benefit of the desired characteristics such as the specific capacitance and the electrocatalytic activity.[37] A synergistic effect implies that the overall response resulting from the combination of two different materials will be greater than the sum of the responses of the two materials individually. Recently, Xu *et al.* reported a synergistic effect in terms of specific capacitance from combining a hierarchical nanowire polyaniline with graphene oxide which resulted in improving the energy storage ability in supercapacitors.[37] Moreover, a synergistic effect between a polyaniline film and quinone/hydroquinone in solution towards the ORR was observed.[39] Therefore, the copolymers prepared from these monomers are expected to have favorable characteristics for supercapacitors applications and for electrocatalysis of the oxygen reduction reaction.[35,36,40]

There are some additional benefits resulting from the copolymerization of aniline and 1-AAQ on high surface area carbons. For supercapacitor applications under some conditions the polymer film thickness, and consequently the pseudocapacitance, can be increased without increasing the film resistance.[41] On the other hand, the electrocatalytic ORR using confined AQ in a film is more favorable than using AQ in solution.[31]

The electrochemistry of polyaniline has been extensively studied and reported in the literature. The deposition of polyaniline from highly acidic aqueous media is well known to produce two reversible peaks at *ca.* 0.1 and 0.7 V vs. SCE.[17] A total charge of 0.6 to 0.7 e^-/aniline was observed.[17] Conductivity was observed over the potential range of 0.1 V to 0.7 V.[17] It was found that the rate determining step of electropolymerization depends on the anion concentration and not on the proton concentration.[42] The type of anion determines whether a porous or compact morphology will be deposited.[42]

1-Aminoanthraquinone (1-AAQ) was homopolymerized in aqueous acid,[43] nonaqueous[33] conditions and in mixed aqueous/nonaqueous media.[44] Polymerization of 1-AAQ in aqueous acid leads to charge trapping phenomena which are not useful for supercapacitor applications as discussed in chapter 5.

Recently, 1-AAQ was co-polymerized with aniline in 4 M H_2SO_4 solutions by Palaniapan and Manisankar.[24] However, the cyclic voltammograms of the modified electrode showed no electroactivity of 1-AAQ in a monomer free solution.[24] Therefore, the objective of this work was to prepare the copolymer under slightly different conditions and to examine the electroactivity of the copolymer for supercapacitor applications and for electrocatalytic activity of ORR.

6.2. Experimental

1-Amino-9,10-anthraquinone (AAQ, 97%; Aldrich) was dissolved in hot 6 M H_2SO_4 with stirring and the solution cooled to ambient temperature before use. Aniline (99.99 %; Aldrich) was purified twice by passing it through an aluminum oxide (neutral

507 C) column before use. Sulfuric acid (98%; ACP chemicals Inc.) was used as received. An acetate buffer solution which contains 0.5 M Na_2SO_4 has been prepared from 0.05:0.02 M (CH_3COOH/CH_3COONa) and adjusted to pH = 3.03. Methanol (ACS) grade and Nafion^{TM} solution (DuPont; 5.14%) were used to disperse carbon black samples. Deionized water was used in all experiments and acetone (ACS) grade was used for the washing step. A Nafion membrane (DuPont; Nafion^{TM} 112) was used as separator between the two electrodes in an asymmetric supercapacitor.

Glassy carbon electrodes (0.071 cm^2) were polished to a mirror-like shiny surface with 0.3 micron alumina paste (micro metallurgical LTD) and washed with deionized water before use.

A carbon black electrode was prepared according to the following procedure. About 0.09 g of Vulcan XC72 (Cabot Corporation) was mixed with 0.01 g of Nafion solution (DuPont; Nafion^{TM} 5.14%) and 5 mL of methanol solution and dispersed via sonication for 20 min. After that few drops of that slurry were loaded onto the end of carbon fiber paper (CFP; Toray^{TM} TGP-H-090) strip and allowed to dry before use.

A conventional three-electrode cell was used to deposit polyaniline, poly(1-AAQ) or poly(ani-co-1-AAQ) onto the working electrode (i.e. either a GC or CFP/Vulcan XC72) or to examine the modified electrode. A platinum wire was used as the counter electrode while a saturated calomel electrode (SCE) was used as a reference electrode. The electrochemical experiments were conducted generally under a gaseous nitrogen

environment; a gaseous oxygen environment was used for experiments where the electrocatalytic effect towards the oxygen reduction reaction was investigated.

A typical two-electrode cell was constructed as a prototype for a supercapacitor device. The negative electrode (i.e. CFP/Vulcan-poly(ani-co-1-AAQ)) was separated from the positive electrode (i.e. CFP/Vulcan-polyaniline) by a typical electrolyte separator (e.g. Nafion^{TM} 112) sheet. Two titanium plates fixed in polycarbonate blocks were used to make the electrical contacts between the modified electrodes and the potentiostat. Each modified electrode was separated from the titanium plate with a disc of CFP to minimize the contact resistance.[45] The whole cell was immersed in the appropriate electrolyte solution (e.g. 1 M H_2SO_4).

6.2.1. Instrumentation

Cyclic voltammograms were recorded using an analog RDE4 potentiostat instrument (Pine Instruments) using CV3 (Colin Cameron) software.

6.3. Results and discussion

6.3.1. Potentiodynamic polymerization of aniline and aniline with 1-AAQ

It was reported that electropolymerization of *ca.* 5 mM equimolar of 1-AAQ and aniline in 4 M H_2SO_4 showed a stable copolymer with a relatively high conductivity of 10.21×10^{-3} S cm^{-1} compared to a conductivity *ca.* 3×10^{-2} S cm^{-1} for polyaniline.[24] However, electropolymerization of 1-AAQ in 4 M H_2SO_4 was unsuccessful, which might be due to the limited solubility of the monomer even after heating the solution up to 90

°C. The best solubility of 1-AAQ was obtained after heating a mixture of *ca.* 5 mM 1-AAQ in 6 M H_2SO_4 up to 90 °C. Therefore, all homo/copolymerizations in this work were conducted in 6 M H_2SO_4 using potentiodynamic polymerization to follow the polymerization process, as seen in Figure 6.1 and Figure 6.2.

The effect of using a higher concentration of acid on the electropolymerization of aniline was investigated by cyclic voltammetry (CV). Fig 6.1 (a) and (b) show the polymerization of aniline in 4 M H_2SO_4 and 6 M H_2SO_4, respectively. Figure 6.1 (a) shows potentiodynamic polymerization of 5 mM aniline in 4 M H_2SO_4 on a glassy carbon electrode at a scan rate 100 mV/s over a potential range of -0.1 to 1.2 V vs. SCE, starting from zero potential. The inset shows the first cycle of aniline monomer oxidation where the current sharply increased at an onset potential of 0.91 V. The shape of this cyclic voltammogram indicates several stages of polyaniline formation which is in good agreement with what was reported previously by Palaniappan and Manisankar.[24] Although aniline was completely soluble in 4 M H_2SO_4, the 1-AAQ was poorly soluble in 4 M H_2SO_4. Therefore, the stock aniline solution was also prepared in 6 M H_2SO_4. Using such a high acid concentration resulted in a notable color change of the solution from light orange to yellow. In addition, the electropolymerization of aniline in 6 M H_2SO_4 showed a less featured and suppressed CV as seen in Figure 6.1 (b). Using such a high acid concentration might affect the solubility of the nucleation centres, the degradation processes and the rate of electropolymerization.[46] Zotti *et al.* concluded that the most important factor that determines the rate of electropolymerization is the anion concentration and not the proton concentration.[42] Morales *et al.* reported that the rate of

aniline polymerization in aqueous 4 M hydrochloric (HCl) acid was more than in 6 M HCl solution.[47] In addition, the amount of benzoquinone by-product increases with increasing the concentration of the acid.[48]

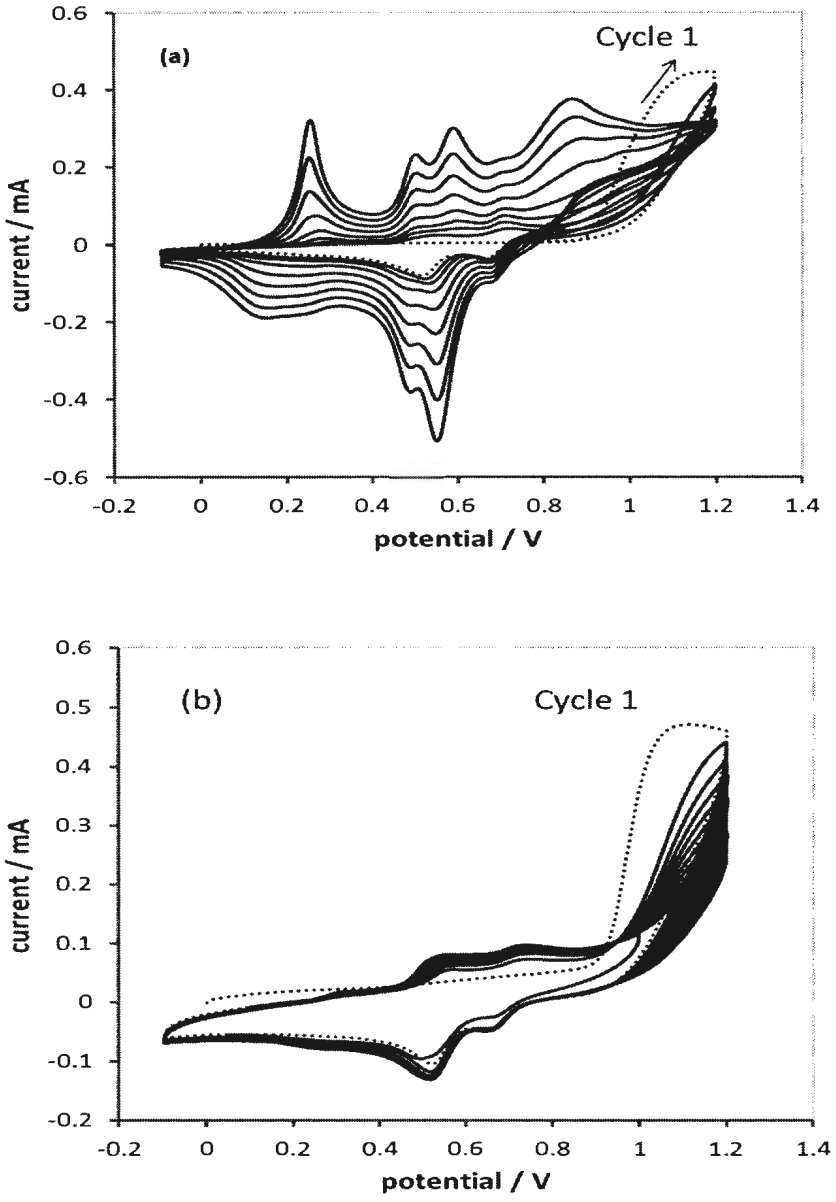

Figure 6.1: Potentiodynamic polymerization at 100 mV/s from -0.1 V to 1.2 V vs. SCE of aniline (a) in 4 M H_2SO_4 and (b) in 6 M H_2SO_4.

The upper oxidation potential limit may affect the electropolymerization process as overoxidation and/or degradation processes become more likely. For comparison, aniline has been potentiodynamically electropolymerized between -0.1 V and 1.2 V vs. SCE instead of -0.1 and 1.3 V vs. SCE as reported by Palaniappan and Manisankar.[24] Both potential ranges gave almost the same CV characteristics. However, it is notable that using a lower anodic potential for the electropolymerization of aniline (i.e. 1.2 V instead of 1.3 V) resulted in a shift of all redox pair potentials during polymerization to less positive potentials, as summarized in Table 6.1.

Table 6.1: Peak potentials for anodic and cathodic peaks from electropolymerization of 5 mM aniline in 4 M H_2SO_4 at 100 mV/s using a potential window of -0.1 to 1.2 V vs. SCE on GC. Numbers between brackets were acquired over potentials of -0.1 to 1.3 V vs. SCE, see reference.[24]

(-0.1 to 1.2) V $E_{p,a}$ / V	Δ E (Shift) / V	(-0.1 to 1.2) V $E_{p,c}$ / V	Δ E (shift) / V
0.25 (0.35)	0.10	0.15 (0.24)	0.09
0.51 (0.60)	0.09	0.49 (0.56)	0.07
0.60 (0.70)	0.10	0.55 (0.61)	0.06
0.70 (0.81)	0.10	0.68 (0.75)	0.07

Figure 6.2(a) shows potentiodynamic polymerization of 1-AAQ in 6 M H_2SO_4 on glassy carbon electrode at a scan rate of 100 mV/s over a potential range of -0.1 to 1.2 V vs. SCE, starting from zero potential. The first cycle (inset) shows a sharp increase in the anodic current at 0.94 V. The current increased upon cycling indicating the formation of

conducting poly(1-AAQ). Two anodic peaks at 0.64 V and 0.82 V and two cathodic peaks at 0.60 V and 0.79 V were observed. A significant reduction current was observed below zero which was not observed in the case of the polymerization of aniline. This is most probably due to reduction of the anthraquinone. Figure 6.2(b) shows potentiodynamic copolymerization of a 0.2:0.8 mole ratio mixture of aniline:1-AAQ in which the solution had a final concentration of 1 mM aniline and 4 mM 1-AAQ. The first cycle (inset) shows a gradual increase of the anodic current before the sharp increase in anodic current at 0.97 V which is different from the oxidation potentials of pure aniline or pure 1-AAQ of 0.91 V and 0.94 V, respectively. Moreover, the shape of the cyclic voltammogram has characteristics close but not identical to that of polymerization of 1-AAQ especially the reduction current below zero. Figure 6.2(c) shows potentiodynamic copolymerization of a 0.4:0.6 mole ratio of aniline:1-AAQ in which the solution had a final concentration of 2 mM aniline and 3 mM 1-AAQ. The first cycle (inset) shows an oxidation potential at 0.91 V which is close to the oxidation potential of pure aniline. However, the presence of cathodic current below zero shows that 1-AAQ was involved in the polymerization process. Figure 6.2(d) shows potentiodynamic copolymerization of 0.6:0.4 mole ratio of aniline:1-AAQ in which the solution has a concentration of 3 mM aniline and 2 mM 1-AAQ. The first cycle (inset) shows a gradual increase in the anodic current preceding the sharp increase in the anodic current at 0.98 V. A reduction current below zero also observed in the first cycle as well as the following cycles. Finally, Figure 6.2(e) shows potentiodynamic copolymerization of 0.8:0.2 mole ratio of aniline:1-AAQ in which the solution has a concentration of 4 mM aniline and 1 mM 1-AAQ.

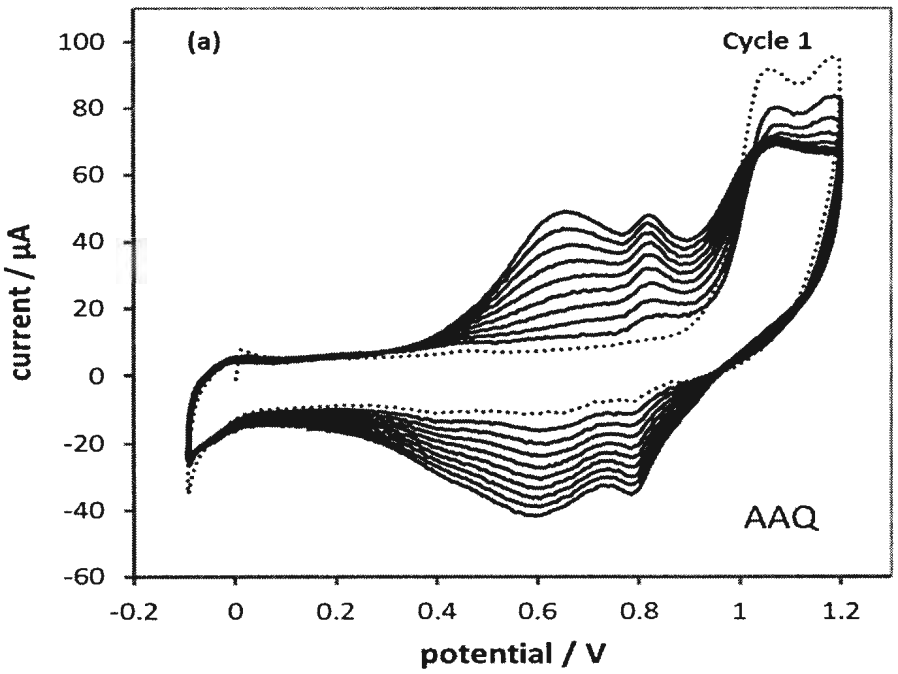
(a)
Cycle 1
AAQ
current / µA
potential / V
100
80
60
40
20
0
-20
-40
-60
-0.2
0
0.2
0.4
0.6
0.8
1
1.2

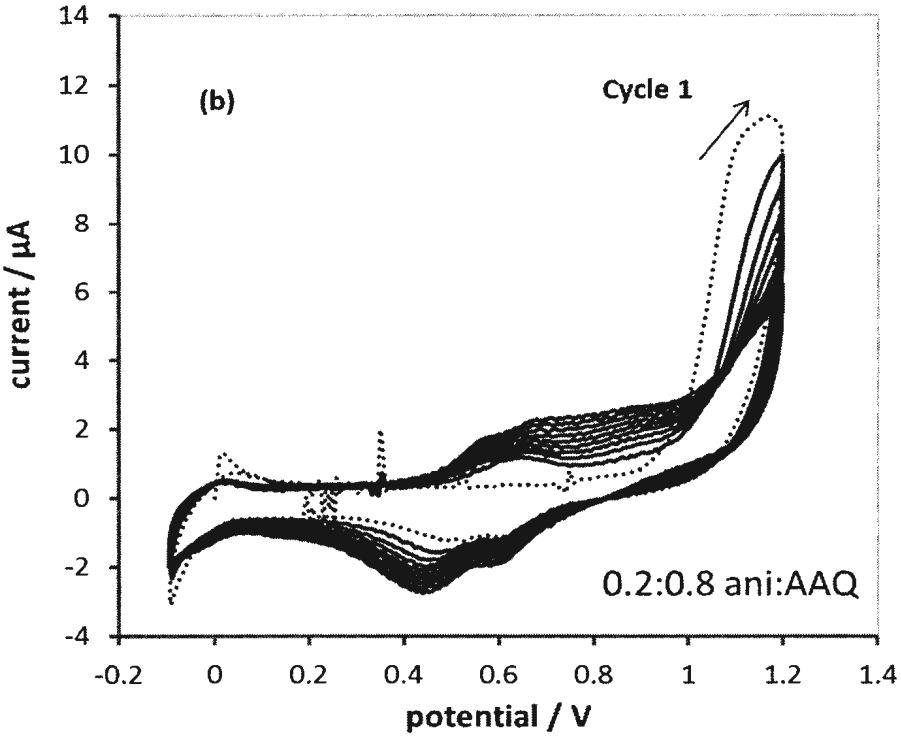
(b)
Cycle 1
0.2:0.8 ani:AAQ
current / µA
potential / V
14
12
10
8
6
4
2
0
-2
-4
-0.2
0
0.2
0.4
0.6
0.8
1
1.2
1.4

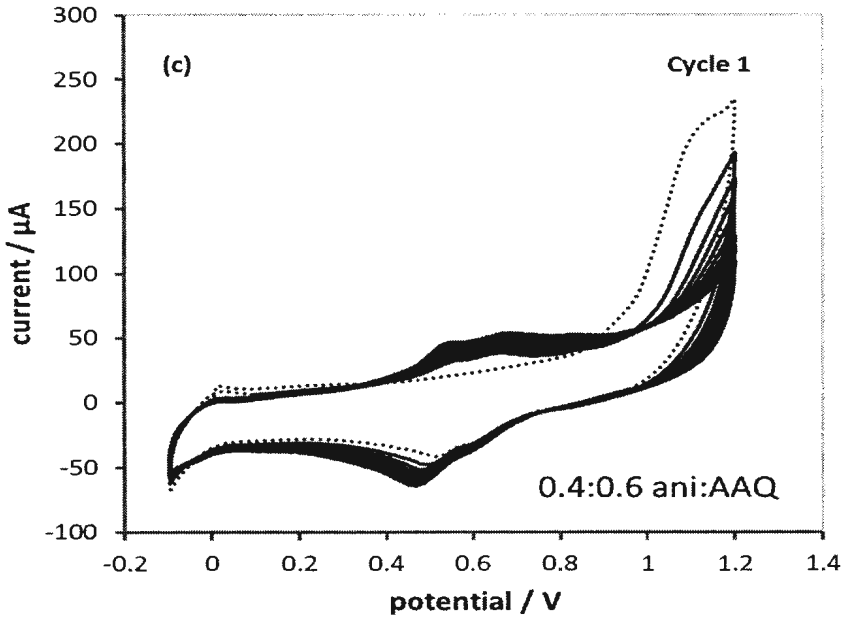
(c)
Cycle 1
0.4:0.6 ani:AAQ
current / µA
potential / V
300
250
200
150
100
50
0
-50
-100
-0.2
0
0.2
0.4
0.6
0.8
1
1.2
1.4

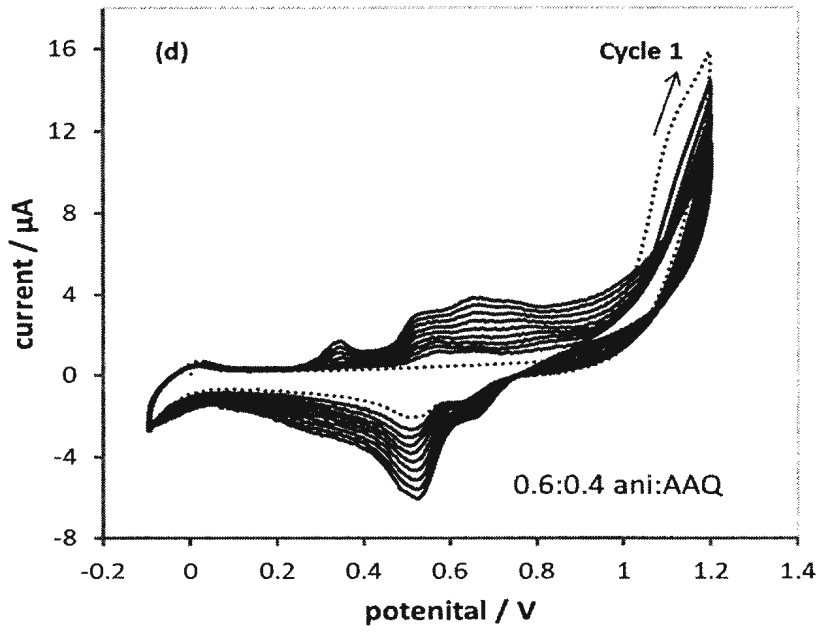
(d)
Cycle 1
0.6:0.4 ani:AAQ
current / µA
potenital / V
16
12
8
4
0
-4
-8
-0.2
0
0.2
0.4
0.6
0.8
1
1.2
1.4

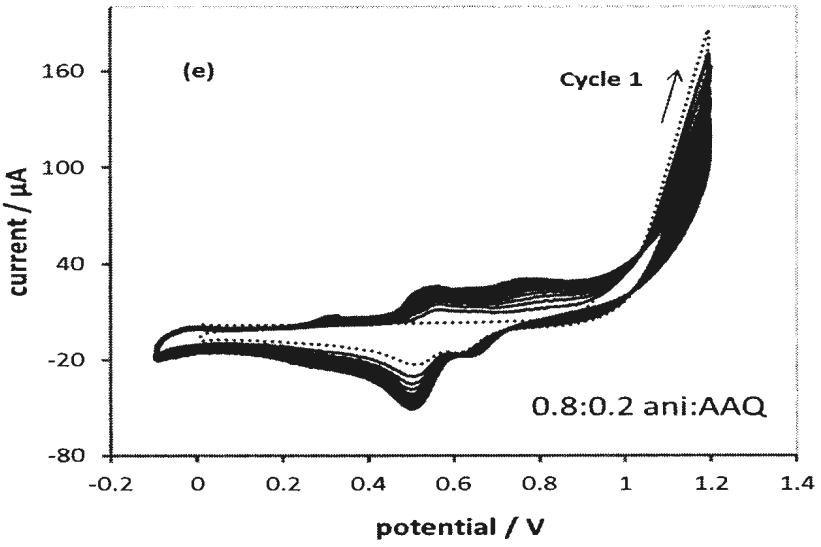

Figure 6.2: Potentiodynamic polymerization at 100 mV/s on GC in 6 M H_2SO_4 of the following feed ratios of aniline:1-AAQ (a) 0.0:1.0, (b) 0.2:0.8, (c) 0.4:0.6, (d) 0.6:0.4, (e) 0.8:0.2.

6.3.2. Study of scan rate effect

6.3.2.1. Scan rate effect on polyaniline

Figure 6.3(a) and (b) show cyclic voltammograms of polyaniline film deposited on a GC electrode at various scan rates in 4 M H_2SO_4. At such high acid concentration the polyaniline film is remarkably electroactive over the potential window of 0.0 V to 0.8 V vs. SCE. A symmetric reversible redox couple at *ca.* 0.5 V with a negligible potential peak separation between the anodic and cathodic peaks (i.e. E_{pa}-E_{pc}), which is independent of scan rate, was observed. The anodic peak current at 0.5 V was linear with scan rates from 10 mV s^{-1} to 600 mV s^{-1} as shown in Figure 6.3(c). This behavior along with the negligible peak separation indicates that the redox sites of polyaniline were adhering to the GC and in equilibrium with the applied potential, exhibiting thin layer behavior.[16,49] A peak shifts with increasing scan rate was only observed for the first

oxidation peak at *ca.* 0.3 V vs. SCE which might be due to structural rearrangement below this potential.[50]

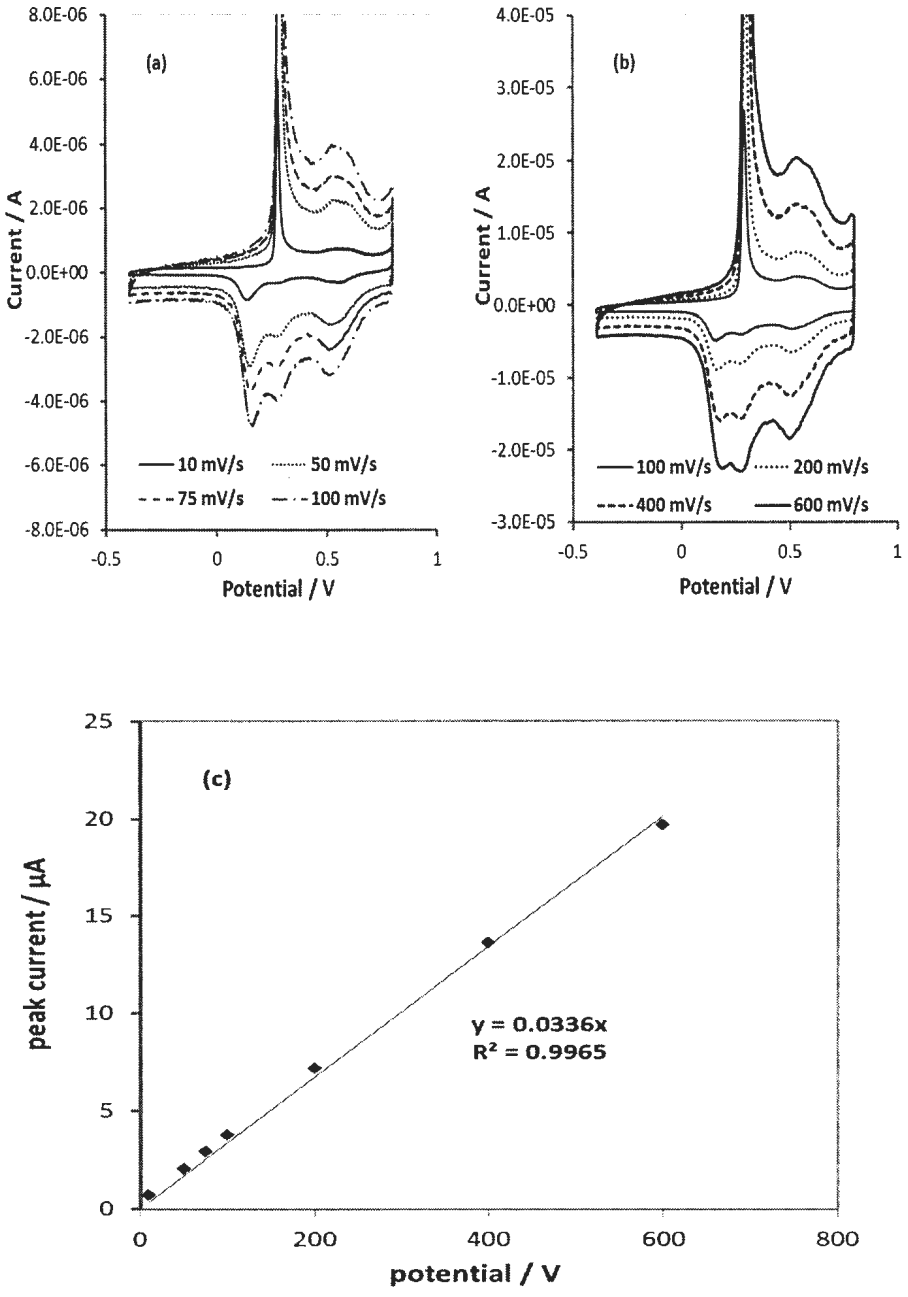

Figure 6.3: Cyclic voltammograms of GC/polyaniline in 4 M H_2SO_4 at scan rates (a) 10 to 100 mV s^{-1} and (b) 100 to 600 mV s^{-1}, and (c) the corresponding peak current vs. scan rate at 0.5 V vs. SCE.

6.3.3. The voltammetry of the ani-co-1-AAQ copolymer

In principle, the characteristics of the copolymer deposited on the electrode should be essentially dependent on the feed ratio of the two monomers used if all other conditions are kept the same. Figure 6.4 shows CVs at 75 mV/s for two poly(ani-co-1-AAQ) films compared to bare GC in 1 M H_2SO_4(aq). Both of the copolymers showed distinguishable CVs from the bare GC. However, a slight change in the feed ratio (i.e. 0.8:0.2 compared to 0.6:0.4) resulted in a significant change in the CV. The higher the aniline content in the feed ratio, the closer the CV is to the pure polyaniline CV.

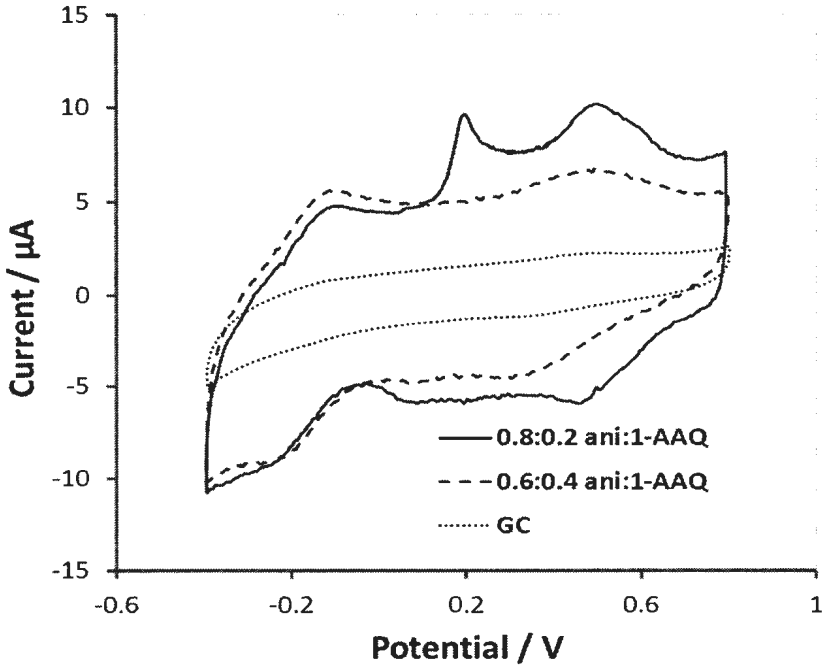

Figure 6.4: Cyclic voltammograms at 75 mV/s of ani-co-1-AAQ copolymers in 1 M H_2SO_4(aq) prepared from two different feed ratio of 0.8:0.2 and 0.6:0.4 aniline:1-AAQ compared to bare GC.

6.3.3.1. Study scan rate effect of 0.6:0.4 aniline:1-AAQ copolymer

Figure 6.5(a) clearly shows that the copolymer deposited from 6:4 aniline:1-AAQ feed ratio is electroactive between -0.4 V and 0.8 V vs. SCE where AQ electroactivity appears at a negative potential between 0.0 down to -0.4 V vs. SCE. A quasireversible behavior of AQ was observed with peak separation of 75 mV measured at 10 mV s^{-1} (i.e. > 59/n, n= 2 for AQ). Redox couple corresponding to polyaniline segments is still present with less symmetric anodic and cathodic peaks at 0.5 V, compared to pure polyaniline.

Figure 6.5(b) shows that the peak current of the copolymer at 0.5 V vs. SCE increased linearly with the scan rate with a potential independent of scan rates.

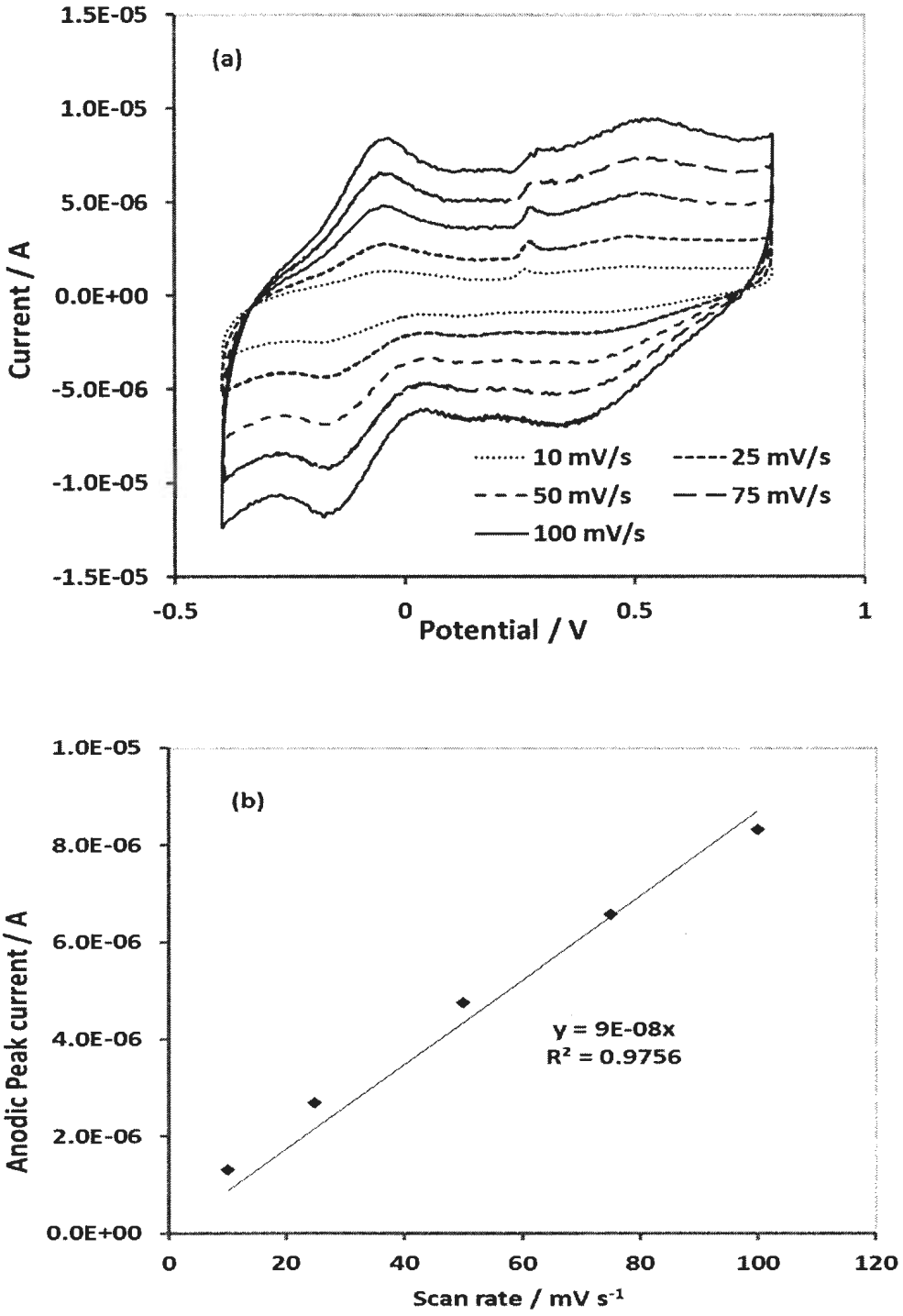

Figure 6.5: (a) Cyclic voltammograms of 0.6:0.4 aniline:1-AAQ copolymer in 4 M H_2SO_4 (aq) from 10 to 100 mV s^{-1}. (b) The corresponding peak current vs. scan rate at potential 0.5 V vs. SCE.

6.3.4. Comparison of ani-co-1-AAQ polymer versus polyaniline

Figure 6.6 shows the electrochemical response of polyaniline compared to a 6:4 aniline:1-AAQ copolymer in monomer-free 4 M H_2SO_4 (aq). It is clear from the figure that the polyaniline film showed electroactivity between *ca.* 0.0 and 0.8 V vs. SCE while the copolymer showed electroactivity over wider potential window between *ca.* -0.4 V and 0.8 V vs. SCE indicating the presence of the AQ functionality in the copolymer film. This is interesting because it means that the copolymer film will be much more suitable as a negative electrode for asymmetric supercapacitors.

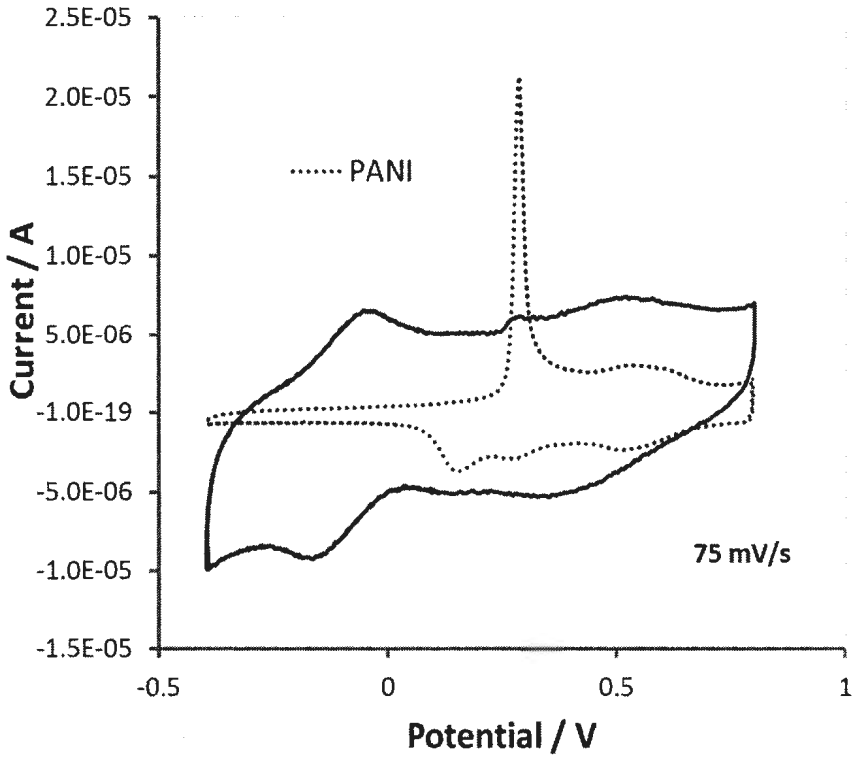

Figure 6.6: Cyclic voltammograms of GC/polyaniline (dotted line) and a 6:4 aniline:1-AAQ feed ratio GC/copolymer (solid line) in 4 M H_2SO_4 at 75 mV s^{-1}.

6.3.5. The electrocatalytic reduction of O_2 by the ani-co-1-AAQ copolymer

The electrocatalytic effect of a GC electrode modified with ani-co-1-AAQ copolymer has been investigated primarily by cyclic voltammetry.

6.3.5.1. Cyclic voltammetry

The oxygen reduction reaction on GC or any modified carbon can be easily observed in cyclic voltammetry although its mechanism is complicated and still not fully understood.[51] Two working electrodes have been examined in a solution of 0.5 M H_2SO_4(aq) saturated with O_2 to illustrate the electrocatalytic effect of ani-co-1-AAQ copolymer as shown in Figure 6.7. A cathodic peak was observed at -0.6 V vs. SCE when using bare GC, whereas the same peak was observed at higher potential (i.e. at -0.5 V vs. SCE) when using a GC/ani-co-1-AAQ copolymer as the working electrode indicating a lowering in the O_2 reduction overpotential. The reduction peak current was not significantly higher from that of the bare GC. This might be due to the small coverage of the AQ functionality in the copolymer film.

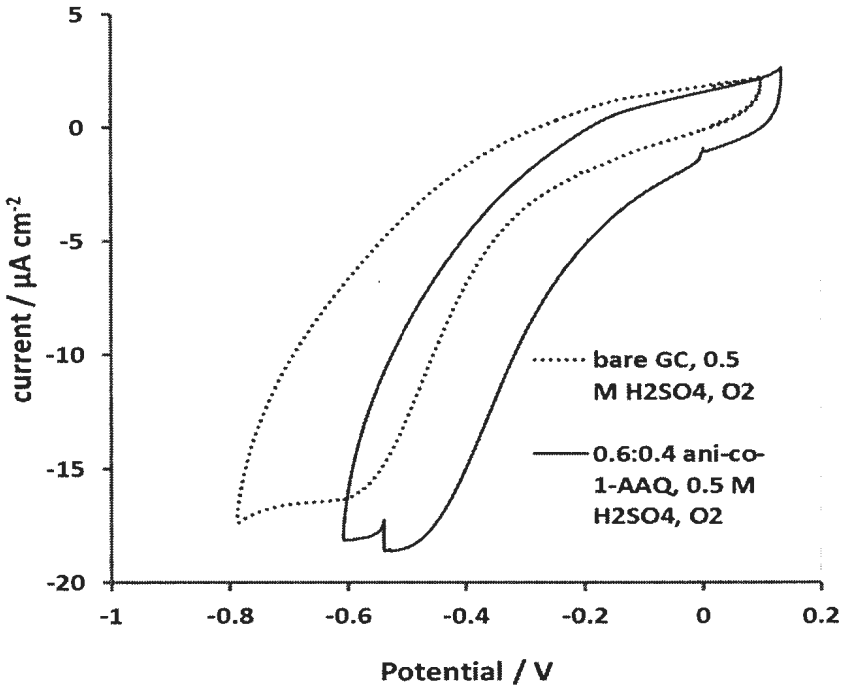

Figure 6.7: The cyclic voltammograms of the reduction of O_2 by 0.6:0.4 aniline-co-1-AAQ copolymer modified GC in aqueous 0.5 M H_2SO_4 (solid line) compared to bare GC in aqueous 0.5 M H_2SO_4 (dotted line). All solutions were saturated with O_2.

6.4. Conclusions

Electrochemical copolymerization of aniline:1-AAQ at various feed ratios was successfully employed to deposit copolymer films on glassy carbon and vulcan XC72 carbon black from 6 M H_2SO_4 (aq). The characteristics of the copolymer films were sensitive to the monomer ratio. The films are electroactive over a potential window of -0.4 V to 0.8 V vs. SCE with no charge trapping. This finding demonstrates that the copolymers are potential candidates to be used as negative electrodes for supercapacitors.

A poly(ani-co-1-AAQ) film also showed electrocatalytic activity towards oxygen reduction in 0.5 M H_2SO_4 (aq) solution as indicated by a preliminary studies via cyclic voltammetry.

Further work is required to optimize, characterize and evaluate poly(ani-co-1-AAQ) copolymers on porous carbon materials for applications in supercapacitors and other applications that depend on electrocatalytic activity for oxygen reduction reaction.

References

(1) MacDiarmid, A. *Angew. Chem. Int. Ed.* **2001**, *40*, 2581-2590.

(2) Inzelt, G., Ed.; In *Conducting polymers: A new era in electrochemistry; Springer;* **2005**.

(3) Cosnier, S., Ed.; In *Electropolymerization: concepts, materials and applications;* Weinheim : Wiley-VCH, **2010**; 280.

(4) Snook, G.; Kao, P.; Best, A. *J. Power Sources* **2011**, *196*, 1-12.

(5) Conway, B. E. In *Electrochemical supercapacitors: scientific fundamentals and technological applications;* Plenum Press: New York, 1999; pp 698.

(6) Gurunathan, K.; Murugan, V.; Marimuthu, R.; Mulik, U.; Amalnerkar, D. *Mater. Chem. Phys.* ***1999****, 61, 173-191.*

(7) Li, C.; Bai, H.; Shi, G. *Chem. Soc. Rev.* **2009**, *38*, 2397-2409.

(8) Hatchett, D.; Josowicz, M. *Chem. Rev.* **2008**, *108*, 746-769.

(5) Conway, B. E. In *Electrochemical supercapacitors: scientific fundamentals and technological applications;* Plenum Press: New York, 1999; pp 698.

(6) Gurunathan, K.; Murugan, V.; Marimuthu, R.; Mulik, U.; Amalnerkar, D. *Mater. Chem. Phys.* ***1999****, 61, 173-191.*

(7) Li, C.; Bai, H.; Shi, G. *Chem. Soc. Rev.* **2009**, *38*, 2397-2409.

(8) Hatchett, D.; Josowicz, M. *Chem. Rev.* **2008**, *108*, 746-769.

(9) Aricò, A.; Bruce, P.; Scrosati, B.; Tarascon, J.; Schalkwijk, W. *Nat. Mater.* **2005**, *4*, 366-377.

(10) Goto, H.; Yoneyama, H.; Togashi, F.; Ohta, R.; Tsujimoto, A.; Kita, E.; Ohshima, K. *J. Chem. Educ.* **2008**, *85*, 1067-1070.

(11) Armand, M.; Tarascon, J. *Nature* **2008**, *451*, 652-657.

(12) Liu, G. Chckalingham, M.; Khor, S.; Gui, A. *Catal. Sci. Technol.* **2011**, *1*, 207-217.

(13) Simon, P.; Gogotsi, Y. *Nat. Mater.* **2008**, *7*, 845-854.

(14) Zhao, X.; Sanchez B.; Dobson, P.; Grant, P. *Nanoscale* **2011**, *3*, 839-855.

(15) Zhang, Y.; Wu, X.; Wang, L.; Zhang, A.; Xia, T. *Int J. Hydrogen Energ.* **2009**, *34*, 4889-4899.

(16) Heinze, J.; Frontana, B.; Ludwigs, S. *Chem. Rev.* **2010**, *110*, 4724-4771.

(17) Zotti, G.; Cattarin, S.; Comisson, N. *J. Electroanal. Chem.* **1987**, *235*, 259-273.

(18) Inzelt, G. *Chem. Biochem. Eng.* **2007**, *21*, 1-14.

(19) Chen, C.; Sun, C.; Gao, Y. *Electrochim. Acta* **2008**, *53*, 3021-3028.

(20) Beadle, P.; Banka, E.; Rannou, P.; Djurado, D. *Synth. Met.* **1998**, *95*, 29-45.

(21) Yue, J.; Wang, Z.; Cromack, K.; Epstein, A.; MacDiarmid, A. *J. Am. Chem. Soc.* **1991**, *113*, 2665-2671.

(22) Wei, Y.; Ramakrishnan, R.; Sandeep, A.; Patel, S. *Macromolecules* **1990**, *23*, 758-764.

(23) Zhang, J.; Shan, D.; Mu, S. *Polymer* **2007**, *48*, 1269-1275.

(24) Palaniappan, S.; Manisankar, P. *J. Polym. Res.* **2011**, *18*, 311-317.

(25) Ye, S.; Do, N.; Da, L.; Vijh, A. *Synth. Met.* **1997**, *88*, 65-72.

(26) Pognon, G.; Brousse, T.; Demarconnay, L.; Belanger, D. *J. Power Sources* **2011**, *196*, 4117-4122.

(27) Algharaibeh, Z.; Liu, X.; Pickup, P. *J. Power Sources* **2009**, *187*, 640-643.

(28) Naoi, K.; Suematu, S.; Manago, A. *J. Electrochem. Soc.* **2000**, *147*, 420-426.

(29) Naoi, K.; Suematu, S.; Hanada, M.; Takenouchi, H. *J. Electrochem. Soc.* **2002**, *149*, A472-A477.

(30) Holdcroft, S.; Funt, L. *J. Electroanal. Chem. Interf. Electrochem.* **1987**, *225*, 177-186.

(31) Griese, S.; Kampouris, D.; Kadara, R.; Banks, C. *Electroanal.* **2008**, *20*, 1507-1512.

(32) Hodge, P.; Gautrrot, J. *Polym. Int.* **2009**, *58*, 261-266.

(33) Ismail, K.; Azzem, M.; Badawy, W. *Electrochim. Acta* **2002**, *47*, 1867-1873.

(34) Wu, G.; More, K.; Johnstein, C.; Zelenay, P. *Science* **2011**, *332*, 443-447.

(35) YANO, J.; Kokura, M.; Ogury, K. *J. Appl. Electrochem.* **1994**, *24*, 1164-1169.

(36) Malinauskas, A. *Synth. Met.* **1999**, *107*, 75-83.

(37) Xu, J.; Wang, K.; Zu, S.; Han, B.; Wei, Z. *Nano* **2010**, *4*, 5019-5026.

(38) Wan, Q.; Fan, S.; Yue, X.; Lang, X.; Xu, W.; Li, J.; Feng, C. *Wuli. Huaxue Xuebao* **2010**, *26*, 2951-2956.

(39) Matveeva, E. *Synth. Met.* **1996**, *83*, 89-96.

(40) Zhang, G.; Yang, F. *Phys. Chem. Chem. Phys.* **2011**, *13*, 3291-3302.

(41) Moghaddam, R.; Pickup, P. *Phys. Chem. Chem. Phys.* **2010**, *12*, 4733-4741.

(42) Zotti, G., Cattarin, S.; Comisso, N. *J. Electroanal. Chem. Int. Electrochem.* **1988**, *239*, 387-396.

(43) Badawy, W.; Ismail, K.; Medany, S. *Electrochim. Acta* **2006**, *51*, 6353-6360.

(44) Ramiz, M.; Khudaish, E.; Deronzier, A.; Chardon-Noblat, S. *J. Electroanal. Chem.* **2010**, *647*, 35-42.

(45) Liu, X.; Pickup, P. *J. Solid State Electrochem.* **2010**, *14*, 231-240.

(46) Stilwell, D. E.; Park, S. *J. Electrochem. Soc.* **1988**, *135*, 2254-2262.

(47) Morales, G.; Llusa, M.; Miras, M.; Barbero, C. *Polymer* **1997**, *38*, 5247-5250.

(48) Lux, F. *Polymer* **1994**, *35*, 2915-2936.

(49) Murray, R. *Ann. Rev. Mater. Sci.* **1984**, *14*, 145-169.

(50) Grzeszczuk, M.; Poks, P. *Synth. Met.* **1998**, *98*, 25-29.

(51) Yang, H.; McCreery, R. *J. Electrochem. Soc.* **2000**, *147*, 3420-3428.

(52) Quan, M.; Sanchez, D.; Wasylkiw, M.; Smith, D. *J. Am. Chem. Soc.* **2007**, *129*, 12847-12856.

(53) Dalmolin, C.; Canobre, S.; Biaggio, S.; Rocha-Filho, R.; Bocchi, N. *J. Electroanal. Chem.* **2005**, *578*, 9-15.

(54) Yamazaki, S.; Ioroi, T.; Yasuda, K.; Tartimoto, K. *J. Electroanal. Chem.* **2008**, *616*, 64-70.

Chapter 7

Electropolymerization and hydrolysis of dimethoxyaniline on carbon electrodes

7.1 Introduction

Porous carbon materials have been widely utilized in energy conversion and energy storage devices such as batteries,[1] fuel cells[2] and supercapacitors.[3-9] Their natural availability and the possibility of synthesizing new carbons with diverse physical, chemical and electrochemical properties with high purity at a relatively low cost make them potential candidates for modern electrochemical devices.[4,6,9] Typical examples of such materials are graphite, activated carbon, carbon black, carbon nanotubes, graphene and fullerene.[2,4-7]

For supercapacitor applications with high power capability, highly reversible electrostatic adsorption/desorption of the electrolyte ions is required. To achieve this goal, high surface area carbons with adjustable pore sizes that facilitate the access of the ions are typically used.[3,5,7,9] Recently, activated carbon with a surface area > 2000 $m^2 g^{-1}$ was applied.[9] However, carbon black (CB) materials of moderate surface area (i.e. 10 to 1500 $m^2 g^{-1}$) are promising.[6,9,10] Because CB exsists in powder form it needs a binder to fix it onto the substrate surface. Polyvinylidene difluoride (PVDF) may be used as a binder.[9]

Devices configured from pure carbon materials normally have high power density but suffer from low energy density.[3,6,7]

In order to enhance the energy density of CB electrodes, modification of the electrode with a reversible redox species that provides additional pseudocapacitance can be used.[9,11-18] The appropriate redox moiety can be covalently attached to the carbon surface via diazonium coupling[14,19-22] or can be noncovalently bonded to carbon such as the modification with conducting polymers.[23-27]

We reported in previous work a novel covalent modification of carbon cloth via chemical diazonium coupling starting from 3,4-dihydroxyaniline (i.e. 4-aminocatechol) precursor.[18] Such modification enabled us to use the immobilized dihydroxybenzene (DHB) as a novel positive electrode to compliment an anthraquinone (AQ) modified carbon which works well as a negative electrode.[17,18,28] It is of great importance that DHB can be used in energy storage devices since it has a lower mass to charge ratio (*ca.* 55 g mol^{-1} of electrons) compared to AQ (*ca.* 104 g mol^{-1} of electrons).

Direct electropolymerization of dihydroxyaniline has not been reported in the literature. However, indirect methods have been used to obtain polydihydroxyaniline modified electrodes. For example, Morita *et al.* reported the electrochemical polymerization of 2,5-dimethoxyaniline on a Pt electrode in mixed aqueous/organic media followed by a hydrolysis step in a monomer free aqueous acid to convert the methoxy groups into hydroxyl groups which were utilized for their electrocatalytic activity towards the oxidation of Fe(II) and Co(II)[29,30] and towards the oxidation of

hydroquinone as well.[31] Recently, Liu *et al.*, using the same method, managed to electropolymerize 2,5-dimethoxyaniline on activated carbon and examined the modified electrode in aqueous media for use in supercapacitor applications.[32] On the other hand, Sun *et al.* examined the electrochemistry of poly(2,5-dihydroxyaniline) modified activated carbon electrode in a nonaqueous media.[33] The polymer was electroactive over a potential range of -0.1 V to 0.6 V *vs.* Ag/AgCl. The polymer formed (i.e. poly(2,5-dihydroxyaniline)) showed nanoscale dimensions with high specific capacitance of 959 F g^{-1}, calculated at 3 mA/cm^2 in aqueous media.[32] Interestingly, Jain *et al.* reported a novel green pathway to prepare a nanoscale poly(2,5-dimethoxyaniline) in a highly ionic strength condition using a mild oxidizing agent (i.e. $NaCl/HCl/H_2O_2$) without any catalyst.[34] This polymer has a specific capacitance of 205 F g^{-1}.[34]

In this work the electrochemical polymerization of both 3,4-dihydroxyaniline and 3,4-dimethoxyaniline (shown in Figure 7.1) was examined. Direct and indirect routes to poly(3,4-dihydroxyaniline) were explored on carbon black electrodes. Successful polymerizations were further examined by cyclic voltammetry, impedance and galvanostatic charging/discharging to investigate the suitability of the modified electrodes for supercapacitors.

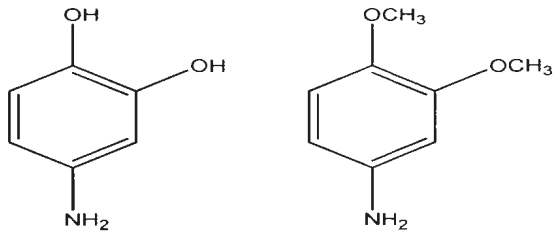

3,4-dihydroxyaniline 3,4-dimethoxyaniline

Figure 7.1: Structures of 3,4-dihydroxyaniline and 3,4-dimethoxyaniline.

7.2 Experimental

7.2.1 Preparation of GC/Vulcan-PVDF and GC/BP-PVDF electrodes

N-pyrrolidine (2 mL) was added to 0.05 g of Vulcan XC72 powder and sonicated for 15 min. Polyvinylidene difluoride (PVDF; 0.05 g) was then added and the mixture was heated in an oil bath to dissolve the PVDF (m.p. 177 °C). Once a uniform slurry was obtained a drop of it was loaded onto a bare GC electrode and dried under vacuum overnight.

7.2.2 Electrochemical polymerization of 3,4-dimethoxyaniline

Electropolymerization of 0.2 M of 3,4-dimethoxyaniline was carried out in 0.5 M H_2SO_4 at a scan rate of 5 mV s^{-1} in a three compartment cell under nitrogen gas. The working electrode was GC/Vulcan-PVDF while the reference was a saturated calomel electrode (SCE) and the counter electrode was a platinum wire. After completion of the electropolymerization process the working electrode was immersed in 0.5 M H_2SO_4 followed by deionized water and finally in acetone before being allowed to dry.

7.2.3 Hydrolysis of methoxy groups in the film

The polymer modified electrode (i.e. GC/Vulcan-PVDF/polydimethoxyaniline or GC/BP-PVDF/polydimethoxyaniline) was then subjected to another cyclic voltammetric experiment under the same experimental conditions as the electropolymerization step but in monomer free 0.5 M H_2SO_4 to hydrolyse the dimethoxy groups into the corresponding hydroxyl groups. The hydrolysis step was stopped when a stable cyclic voltammogram was observed.

7.2.4 Instrumentation

All electrochemical measurements were conducted in a three-electrode cell configuration. Cyclic voltammograms were recorded using an analog RDE4 potentiostat (Pine Instruments) using CV3 (Colin Cameron) software or by using an EG&G 273A potentiostat controlled by CorrWare software. Impedance measurements were conducted using a Solartron model 1286 potentiostat connected to a model 1250 frequency response analyzer. All impedance measurements are performed at 10 mV amplitude and a frequency change from 1000 Hz to 0.05 Hz. The resulting impedance data were recorded and analyzed by ZView software (Scribner Associates Inc.).

7.3 Results and discussion

7.3.1 Electropolymerization of dimethoxyaniline on GC/CB-PVDF

Direct electrochemical polymerization of 5 mM of 3,4-dihydroxyaniline in 1 M H_2SO_4 on glassy carbon (GC) was studied at different potential windows as in Figure

7.2(a) and (b). The peak currents due to the hydroxyl groups decreased as the potential was swept between 0.0 V and 0.9 V vs. SCE, see Figure 7.2(a). This is may be due to the instability of the monomer itself since different CVs were obtained at 20 min and 60 min after preparation of the solution as shown in Figure 7.2(a) and (b) or it may be due to the formation of a non-conduction polyphenol film.[35-37]

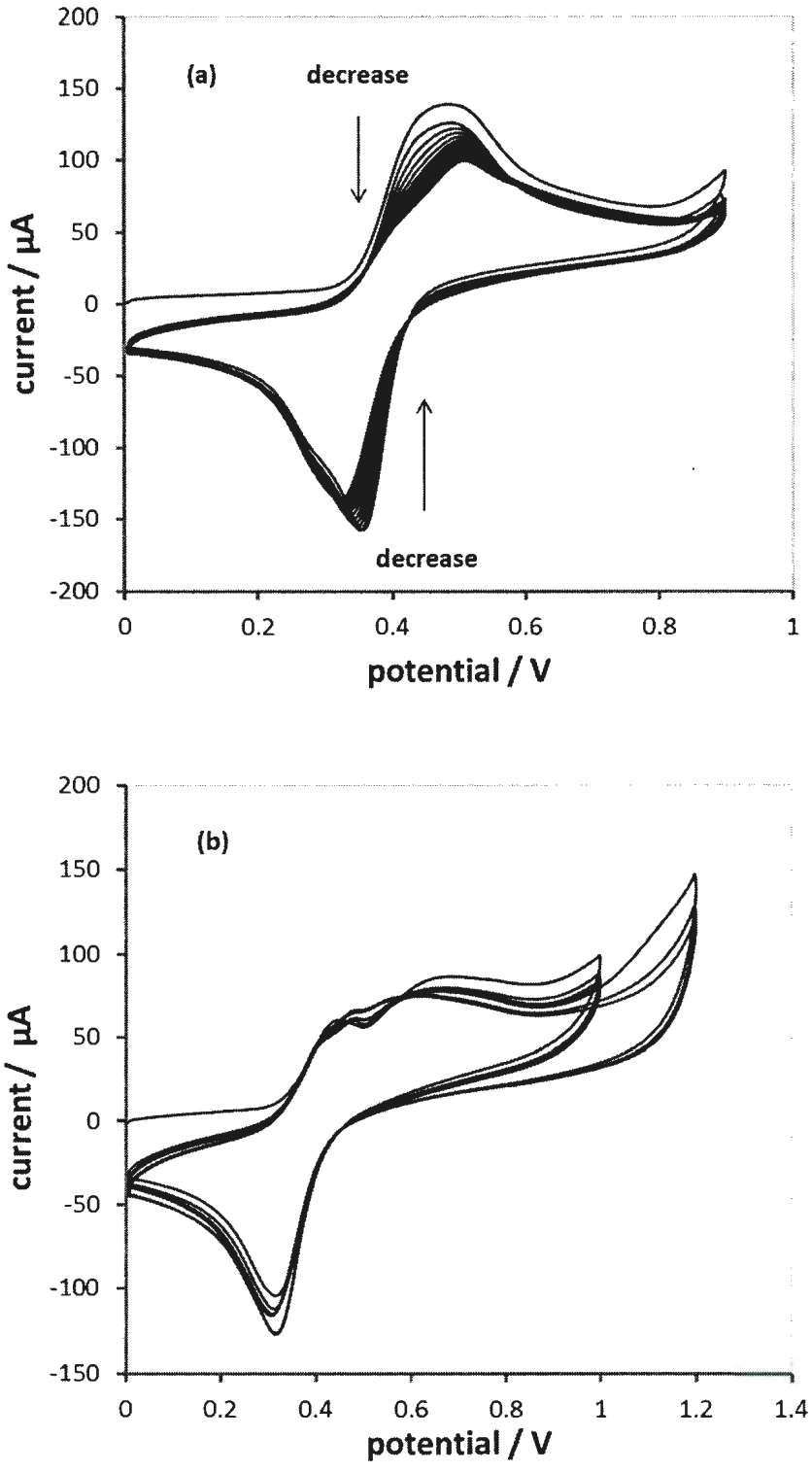

Figure 7.2: Cyclic voltammograms at 50 mV s^{-1} of 5 mM 3,4-dihydroxyaniline in 1 M H_2SO_4 (aq) on GC at (a) 20 min and (b) 60 min after preparation of the solution.

Based on the above results the modification of the carbon electrode was performed, using an indirect procedure, by initial electrochemical polymerization of 3,4-dimethoxyaniline in aqueous acid followed by hydrolysis of the dimethoxy groups to the corresponding hydroxyl groups, based on a procedure from the literature with little modification.[32]

Figure 7.3(a) shows the first two cycles of potentiodynamic polymerization of *ca.* 0.2 M dimethoxyaniline on a GC/Vulcan-PVDF electrode in 1 M H_2SO_4. The potential was swept between -0.15 V and + 0.85 V vs. SCE at 5 mV s^{-1}. As expected, no anodic current was observed at potentials below the onset potential (i.e. at 0.6 V) of the monomer. At 0.6 V there was a sharp increase in the anodic current indicating the oxidation of the monomer followed by a small anodic peak. When the potential was switched back at 0.85 V, a crossover point was observed at *ca.* 0.65 V in the first cycle indicating an autocatalytic nucleation step. This behaviour is normally observed in the potentiodynamic deposition of conducting polymers.[38] Two new redox couples were observed at 0.27 V and 0.37 V and their peak currents increased upon cycling due to the film formation process.

Figure 7.3(b) shows selected cycles of the potentiodynamic polymerization of 3,4-dimethoxyaniline in 0.5 M H_2SO_4 for a maximum of 10 cycles. It is notable that no more crossover points were observed. In addition, the peak current of the oxidation of the monomer did not change significantly. That is, for these ten cycles the deposited film has little effect on the oxidation of the monomer.

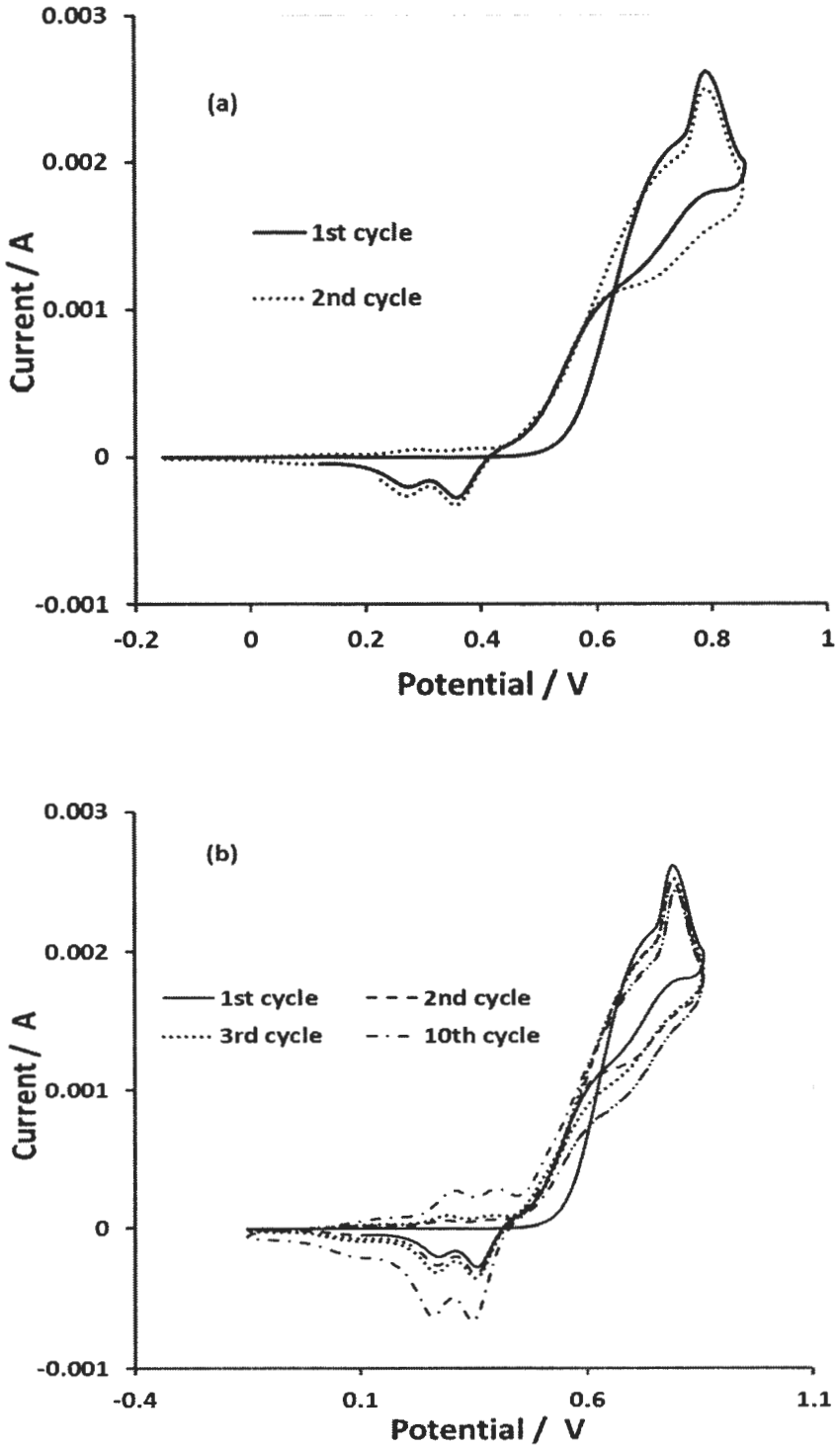

Figure 7.3: (a) Cyclic voltammetry of electropolymerization of 0.2 M dimethoxyaniline on GC/Vulcan-PVDF in 0.5 M H_2SO_4 (aq) at 2 mV s^{-1}, first two cycles. (b) Same as (a) for 10 cycles.

Following the polymerization step, the dimethoxy groups in the polymer film were hydrolysed into the dihydroxy groups by sweeping the potential at 5 mV s^{-1} between 0.0 V and 0.9 V vs. SCE for several cycles as shown in Figure 7.4. It is clear that a steady state was rapidly reached after few potential sweeps. This is probably because hydrolysis step concomitantly occurred with the polymerization step.[29]

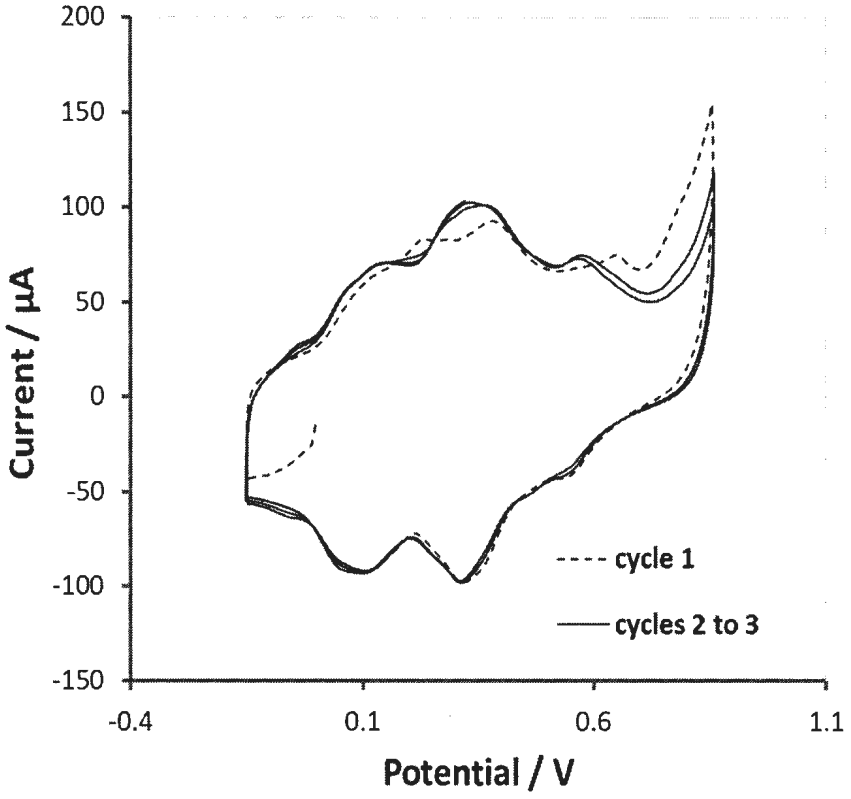

Figure 7.4: The hydrolysis of GC/ Vulcan-PVDF/ polydimethoxyaniline film by potential sweep at 5 mV s^{-1} in 0.5 M H_2SO_4 (aq).

Figure 7.5(a) shows cyclic voltammograms following hydrolysis of GC/Vulcan-PVDF/polydihydroxyaniline in 0.5 M H_2SO_4 (aq) at 5 mV s^{-1} and of an unmodified GC/Vulcan-PVDF electrode under the same conditions. The current for the unmodified electrode is plotted on a second y-axis because it is not for the same working electrode

before modification. The CV of the polymer modified electrode does not show the rectangular behaviour of Vulcan XC72. Instead, it shows three reversible couples at *ca.* 0.10 V, 0.32 V and 0.6 V which significantly enhance the capacitance of the electrode. In other words, the electrochemical behaviour of the modified electrode is dominated by the electroactivity of the conducting polymer. The presence of more than one peak might indicate the presence of mixed polymers where coupling through oxygen is not excluded. The specific capacitance for these experiments was not calculated because the mass of the electrodes was not measured before and after modification. Figure 7.5(b) shows that the peak current increased with increasing the scan rate with a slight shift of the anodic peak potential to more positive potentials and the cathodic peak to more negative potentials even at low scan rates.

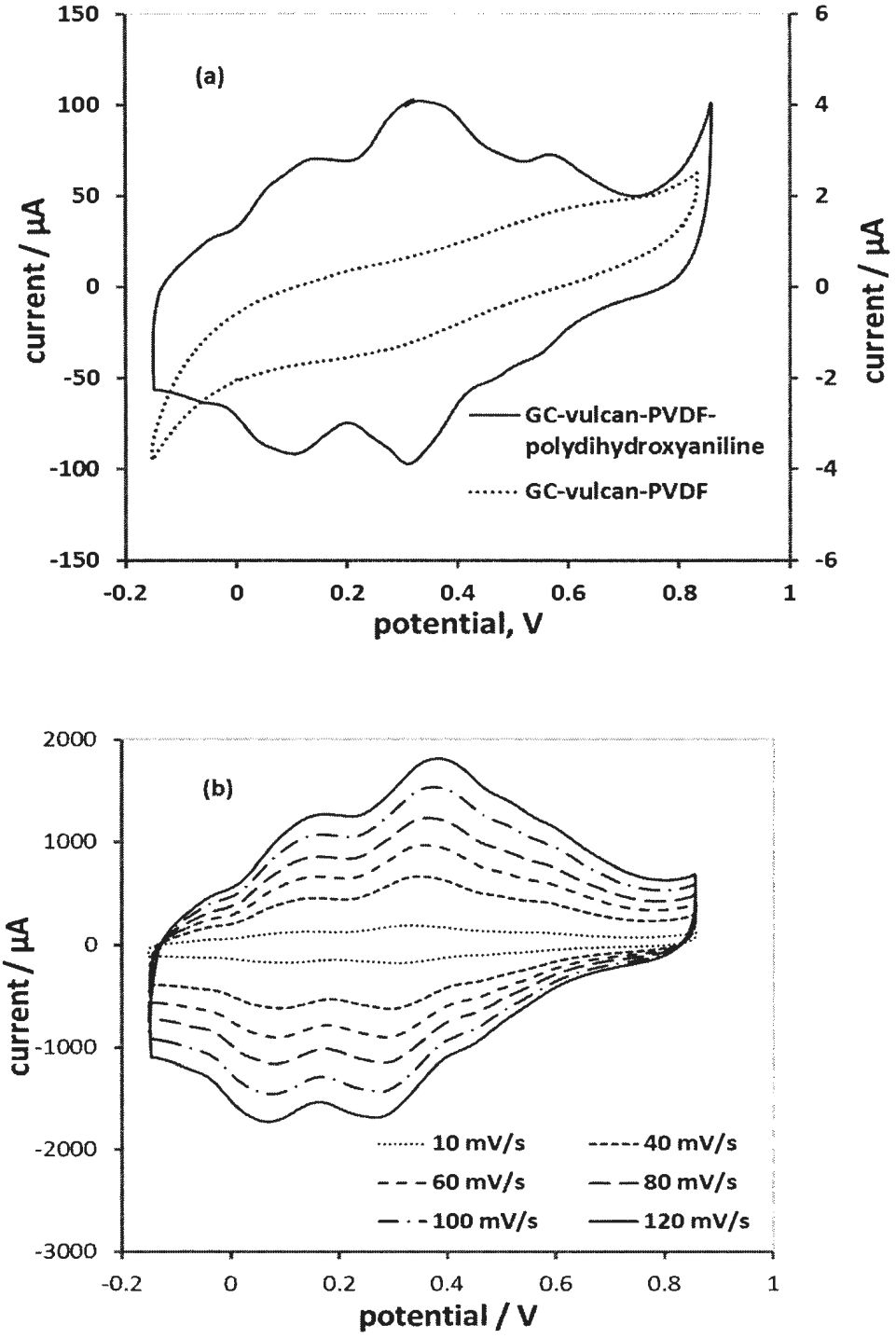

Figure 7.5: (a) Cyclic voltammogram of GC/Vulcan-PVDF/polydihydroxyaniline *vs.* GC/Vulcan-PVDF in 0.5 M H_2SO_4 (aq) at 5 mV s^{-1}. (b) Scan rate effect on the polymer at rate of 10 mV s^{-1} to 120 mV s^{-1}.

Modification of Black Pearls 2000 (BP) with 3,4-dimethoxyaniline generally resembled the modification of Vulcan XC72 as shown in Figure 7.6(a) and (b).

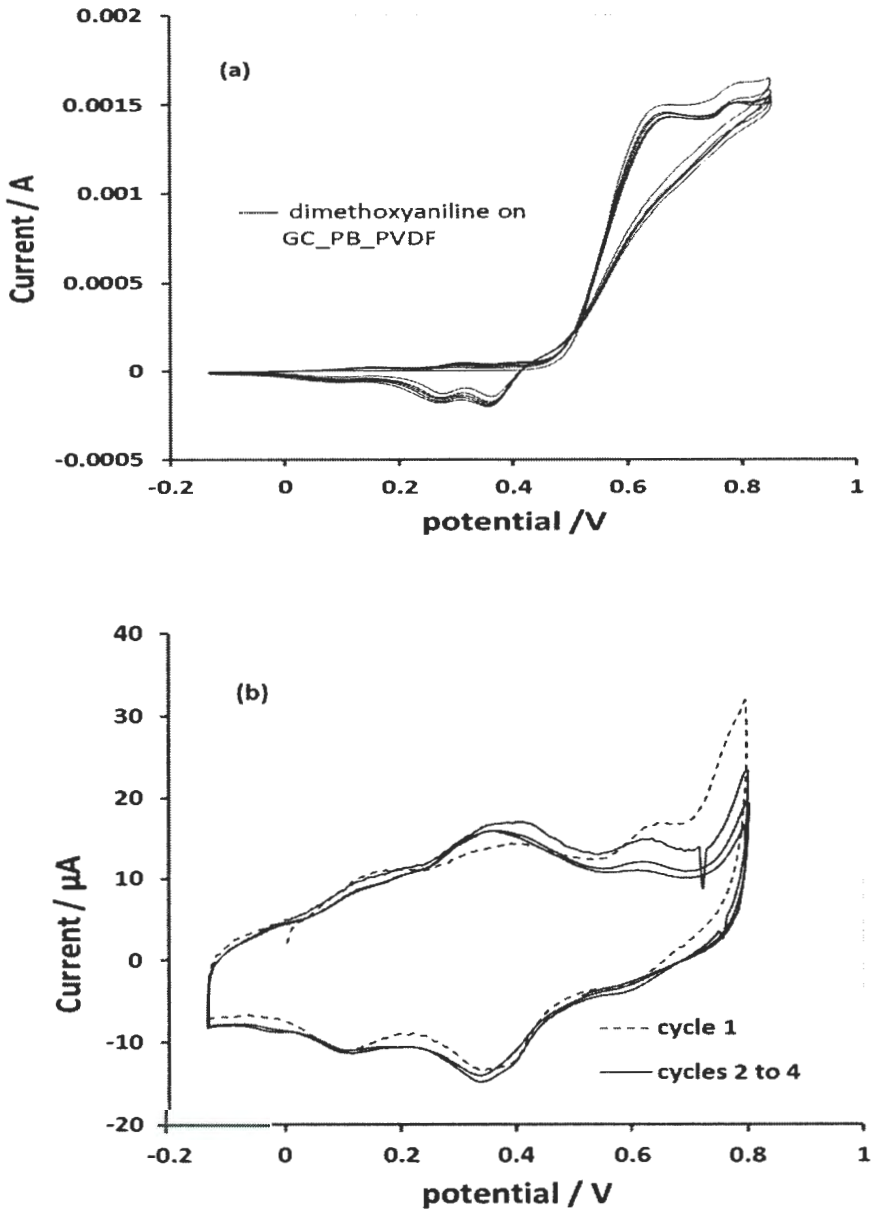

Figure 7.6: (a) Cyclic voltammetry of electropolymerization of 0.2 M dimethoxyaniline on GC/BP-PVDF in 0.5 M H_2SO_4 (aq) at 2 mV s^{-1}. (b) The hydrolysis of GC/ BP-PVDF/ polydimethoxyaniline film by potential sweep at 5 mV s^{-1} in 0.5 M H_2SO_4 (aq).

Scan rate effect of the modified Black Pearls 2000 (BP) with 3,4-dimethoxyaniline in 0.5 M H_2SO_4 (aq) was shown in Figure 7.7.

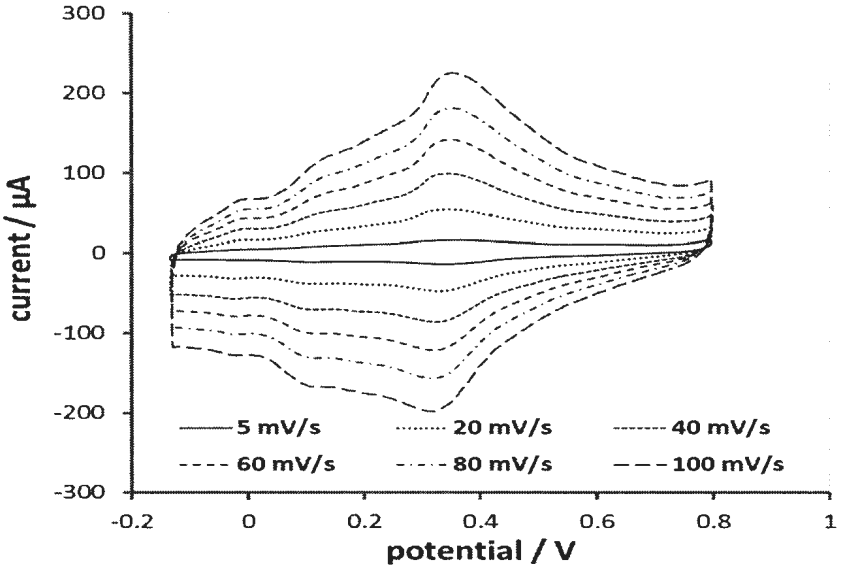

Figure 7.7: Cyclic voltammogram of GC/BP-PVDF/polydihydroxyaniline in 0.5 M H_2SO_4 (aq) at scan rate from 5 mV s^{-1} to 100 mV s^{-1}.

7.3.2 Impedance of GC/BP-PVDF/polydihydroxyaniline

Based on the cyclic voltammogram shown in Figure 7.6, where significant differences in peak currents were observed over the potential range from -0.15 V and +0.85 V, the impedance of the modified electrode was measured at 0.0 V and 0.35 V, respectively. However, at these potentials, the Nyquist plots recorded at frequency ranges from 1000 Hz to 0.05 Hz revealed a non-ideal vertical line as seen in Figure 7.8(a) and (b). The polymer film showed no charge transfer resistance at either potential as revealed from the absence of a semicircle plot at high frequencies (i.e. 1000 Hz). Moreover, the modified electrode showed no mass transfer resistance since no Warburg line was observed at medium frequencies. However, converting the Nyquist plot into the series

capacitance versus the real impedance plot seen in Figure 7.8(c) revealed that the film has a capacitance of *ca.* 17.5 mF cm^{-2} (i.e. considering 0.071 cm^2 GC electrode) at + 0.35 V which is comparable to 12.0 mF cm^{-2} at 0.3 V (anodic peak potential) reported by Liu *et al.* for poly(2,5-dihydroxyaniline) via cyclic voltammetry at 1 mV s^{-1}.[32] Moreover, the film resistance (R_{film}) was determined to be 8.1 Ω cm^2 at 0.35 V and 4.3 Ω cm^2 at 0.0 V.

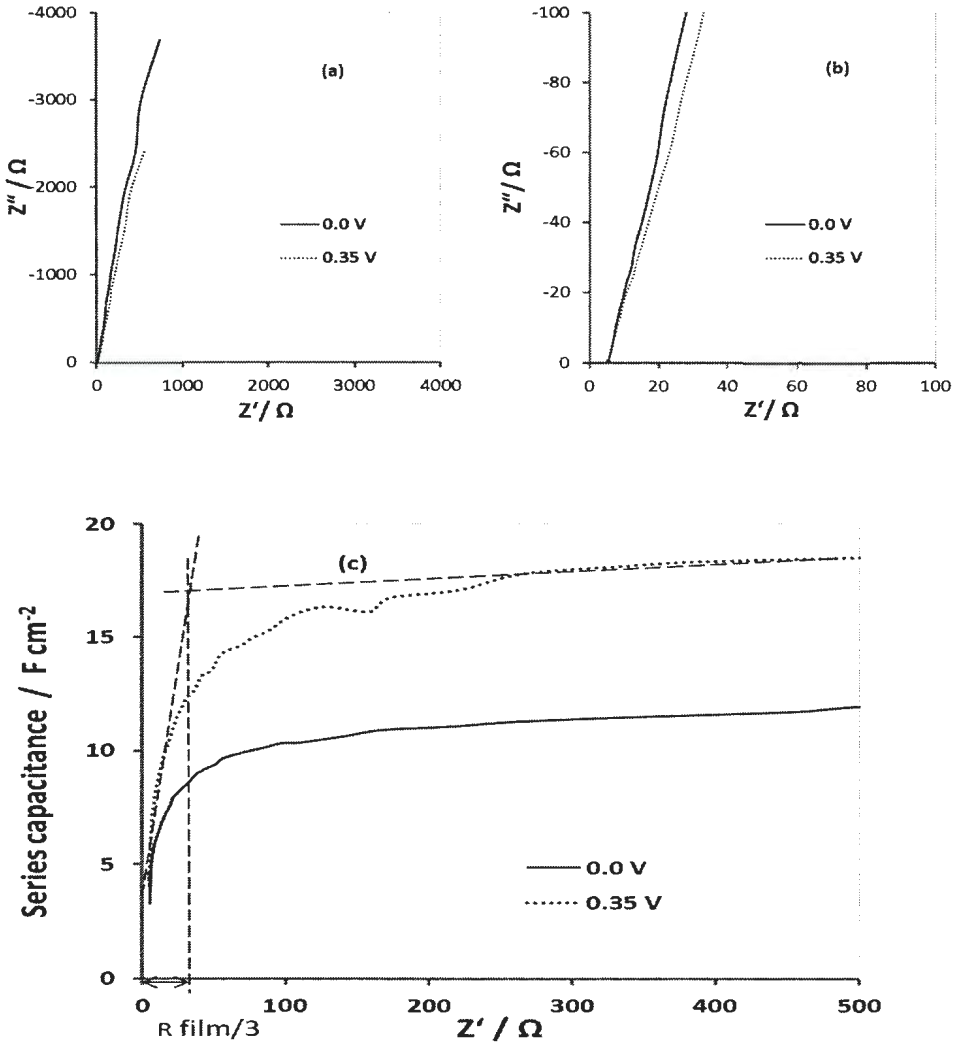

Figure 7.8: Nyquist plots for of GC/BP-PVDF/polydihydroxyaniline in aqueous 1 M H_2SO_4 (a) at 0.0 V (solid line) vs. SCE and +0.35V (dotted line). (b) Enlarged scale of (a). (c) Series capacitance versus real impedance.

7.3.3 Galvanostatic charging/discharging stability

Figure 7.9(a) shows the charging/discharging cycles of the GC/Vulcan-PVDF/polydihydroxyaniline electrode in 1 M H_2SO_4 (aq) at $1.0x10^{-4}$ A. The charging or the discharging plot was not linear over the whole potential range as excpected for the double layer behaviour of carbon materials (i.e. Black Pearls 2000). The lower the slope the higer the capacitance that can be obtained. This can be related to the additional pseudocapacitance participation of the conducting polymer (i.e. polydihydroxyaniline).

Figure 7.9(b) shows the capacitance of the GC/Vulcan-PVDF/polydihydroxyaniline calculated based on the discharge plots from 0.8 V to 0.0 V at a discharging current of $1.0x10^{-4}$ A. After less than a hundered of cycles the capacitance remain relatively constant at about *ca.* 15.5 mF cm^{-2} for 400 cycles which is in good agreement with the calculated capacitance from impedance experiments *ca.* 17.5 mF cm^{-2}, see Figure 7.8. No significant loss of the polymer electroactivity after 500 cycles indicating the stability of the charging/discharging process of the modified electrode.

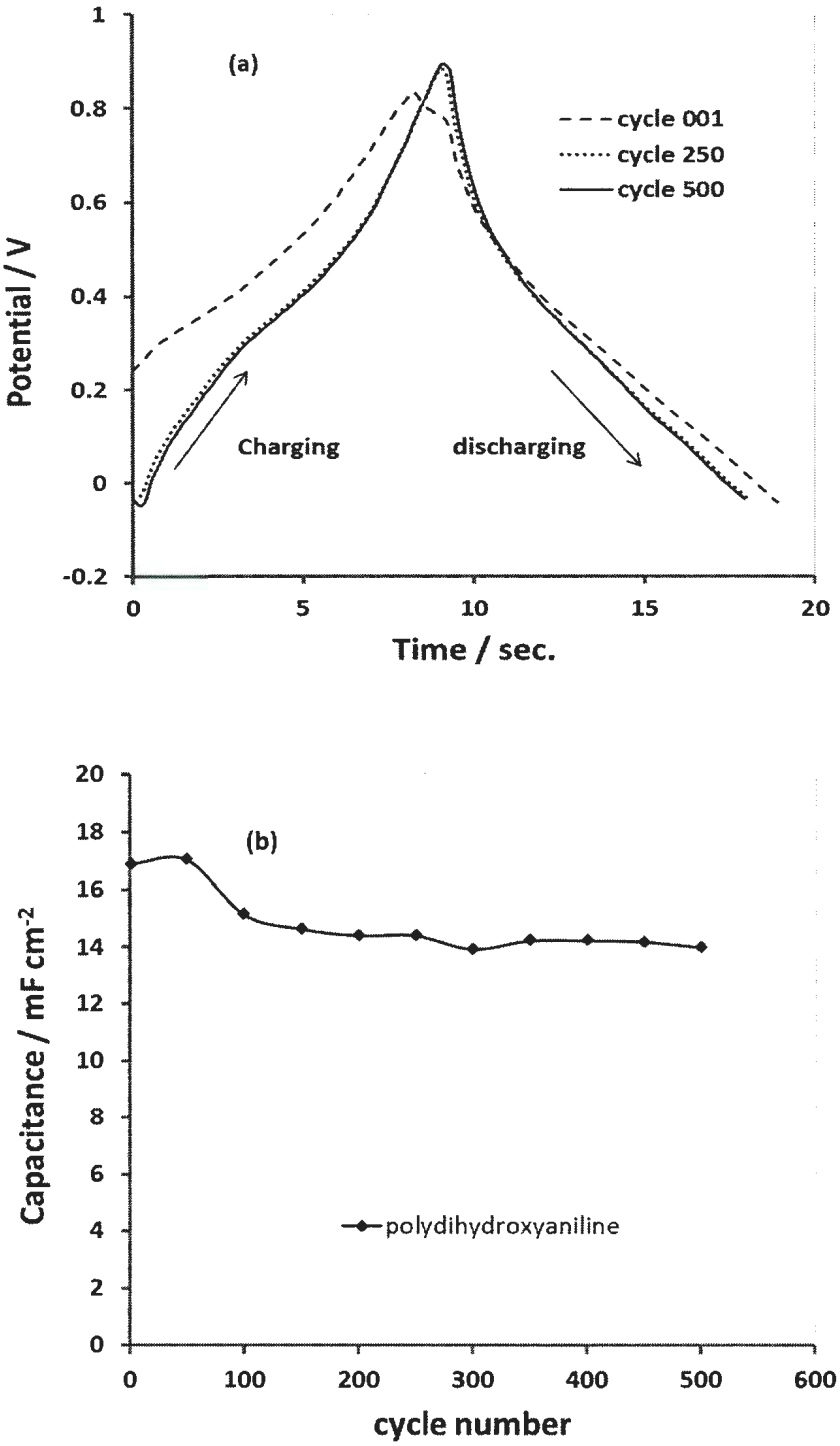

Figure 7.9: (a) Stability of a GC/BP-PVDF/polydihydroxyaniline electrode during charge/discharge in 1 M H_2SO_4 (aq), under N_2 for 500 cycles. (b) Capacitance versus cycle number calculated from the discharge current of $1.0x10^{-4}$ A.

7.4 Conclusion

Modification of two types of carbon black electrodes with polydihydroxyaniline was obtained by electropolymerization of the dimethoxyaniline precursor (i.e. 3,4-dimethoxyaniline) in aqueous acid followed by a hydrolysis step to convert the dimethoxy substituent into the corresponding hydroxyl groups. The electrochemical activity of this modified electrode over a positive potential range 0.0 V to 0.7 V along with its stability in aqueous media for at least 500 cycles reveals the possibility of utilizing this electrode as a positive electrode in supercapacitor applications, especially in the asymmetric cell configuration. For example, real examination of this modified electrode as a positive electrode along with anthraquinone modified carbon black as a negative electrode will be promising. In addition, it may have useful redox activity in neutral and nonaqueous media which needs further investigations.

Additional information is still required to fully understand the electrochemical behavior of this polymer. The presence of multiple reversible peaks suggests the presence of mixed polymers in the film where additional spectroscopic studies are needed to investigate a proposed structure of this polymer. Elemental analysis (i.e. CH analysis) is required to prove the occurrence of the hydrolysis step. Further investigation of poly(3,4-dihydroxyaniline) modified carbon black by SEM is also needed to show the nano dimensions of such polymers.

References

(1) Armand, M.; Tarascon, J. *Nature* **2008**, *451*, 652-657.

(2) Dicks, A. *J. Power Sources* **2006**, *156*, 128-141.

(3) Conway, B. E. In *Electrochemical supercapacitors: scientific fundamentals and technological applications;* Plenum Press: New York, **1999**.

(4) Frackowiak, E.; Beguin, F. *Carbon* **2001**, *39*, 937-950.

(5) Pandolfo, A.; Hollenkamp, A. *J. Power Sources* **2006**, *157*, 11-27.

(6) Frackowiak, E. *Phys. Chem. Chem. Phys.* **2007**, *9*, 1774–1785.

(7) Simon, P.; Gogotsi, Y. *Nat. Mater.* **2008**, *7*, 845-854.

(8) Inagaki, M.; Konno, H.; Tanaike, O. *J. Power Sources* **2010**, *195*, 7880-7903.

(9) Noked, M.; Soffer, A.; Aurback, D. *J. Solid State Electrochem.* **2011**, *15*, 1563-1578.

(10) Kim Kinoshita, Ed.; In *Carbon: electrochemical and physicochemical properties;* Jiohn Wiley & Sons: 1988.

(11) Delamar, M.; Pinson, J.; Saveant, J.; *J. Am. Chem. Soc.* **1992**, *114*, 5883-5884.

(12) Wring, S.; *Analyst* **1992**, *117*, 1215-1229.

(13) Leitner, K. W.; Winter, M.; Besenhard, J.; *Electrochim. Acta* **2004**, *50*, 199-204.

(14) Pinson, J.; Podvarica, F.; *Chem. Soc. Rev.* **2005**, *34*, 429-439.

(15) Bélanger, D.; Pinson, J. *Chem. Soc. Rev.* **2011**, *40*, 3995-4048.

(16) Pognon, G.; Brousse, T.; Belanger, D.; *Carbon* **2011**, *49*, 1340-1348.

(17) Algharaibeh, Z.; Liu, X.; Pickup, P.; *J. Power Sources* **2009**, *187*, 640-643.

(18) Algharaibeh, Z.; Pickup, P.; *Electrochem. Commun.* **2011**, *13*, 147-149.

(19) Downard, A. *Electroanalysis* **2000**, *12*, 1085-1096.

(20) Mahouche-Chergui, S.; Gam-Derouich, S.; Mangeney, C.; Chehimi, M. *Chem. Soc. Rev.* **2011**, *40*, 4143-4166.

(21) Toupin, M.; belanger, D.; *J. Phys. Chem. C* **2007**, *111*, 5394-5401.

(22) Smith, R.; Pickup P. *Electrochim. Acta* **2009**, *54*, 2305-2311.

(23) Dhand, C.; Arya, S.; Monika, M.; Malhotra, B. *Anal. Biochem.* **2008**, *383*, 194-199.

(24) Frackowiak, E.; Khomenko, V.; Jurewicz, K.; Lota, K.; Beguin, F. *J. Power Sources* **2006**, *153*, 413-418.

(25) Villers, D.; Jobin, D.; Chantal, C.; Cossement, D.; Chahine, R.; Breau, L.; Belanger, D. *J. Electrochem. Soc.* **2003**, *150*, A747-A752.

(26) Kaiser, A. B.; Skakalova, V. *Chem. Soc. Rev.* **2011**, *40*, 3786-3801.

(27) Snook, G. A.; Kao, P.; Best, A. S. *J. Power Sources* **2011**, *196*, 1-12.

(28) Kalinathan, K.; Derrick, P.; Liu, X.; Pickup, P. *J. Power Sources* **2008**, *181*, 182-185.

(29) Morita, M.; Takase, H.; Ishakawa, M.; Matsuda, Y. *Chem. Lett.* **1994**, 1645-1648.

(30) Morita, M.; Takase, H.; Ishakawa, M.; Matsuda, Y. *Bull. Chem. Soc. Jpn.* **1995**, *68*, 2207-2213.

(31) Wang, W.; Yamagushi, T.; Takahashi, K.; Komura, T. *Denkikagaku* **1998**, *66*, 1032-1033.

(32) Liu, L.; Wang, W.; Zou, W.; He, B.; Sun, M.; Wang, M.; Xu, X. *J. Solid State Electrochem.* **2010**, *14*, 2219-2224.

(33) Sun, M.; Wang, W.; He, B.; Sun, M.; Liu, W.; Ge, H.; Zhang, Q.; Sun, F. *J. Appl. Polym. Sci.* **2012**, 1-9.

(34) Jain, S.; Surwade, S.; Agnihorta, S.; Dua, V.; Eliason, P.; Gregory, J.; Morose, G.; Manohar, S. *Green Chemistry* **2010**, *12*, 585-589.

(35) Yuqing, M.; *Trends Biotechnol.* **2004**, *22*, 227-231.

(36) Vieira, S. N.; Ferreira, L.; Franco, D.; Afonso, A.; Goncalves, R.; Madurro, A.; Madurro, J. *Macromol. Sympos.* **2006**, *245-246*, 236-242.

(37) Cosnier, S.; *Electroanalysis* **1997**, *9*, 894-902.

(38) Heinze, J.; Ludwigs, S. *Chem. Rev.* **2010**, *110*, 4724-4771.

Chapter 8

Miscellaneous methods for modification of carbon electrodes with catechol and benzoquinone moieties

8.1. Introduction

Modified carbon materials have been extensively utilized in a wide range of potential applications. These include environmental,[1,2] electroanalytical,[3-6] corrosion protection[5] and for electrochemical devices such as batteries,[7] fuel cells[8] and supercapacitors.[9-15] In general, high surface area carbons have been utilized in these applications.

The vast majority of commercially available high surface area carbon black (e.g. Vulcan XC72) can be considered relatively pure materials (*ca.* > 95 % C) with some unavoidable functionality on the surface depending on the raw materials and the experimental conditions used in their synthesis.[16] Accordingly, limited applications of carbon black in electrochemical devices have been found. Fortunately, carbons can be readily functionalized with many diverse organic modifiers that can alter the chemical, physical and electrochemical properties as desired. Such organic modifiers have been extensively reported in the literature.[2-5,15,17-24] Moreover, transition metal complexes can be attached to the carbon surface once its organic ligand can be attached.[5,25,26]

The formation of strong covalent bonds between the substrate and the organic modifier is highly desired in many applications. Aryl diazonium coupling is one of the best methodologies for that and consequently becomes increasingly interesting.[4,5,18,26-30] It is applicable for modification of a wide range of surfaces including metals,[19,31] carbon,[4,5,26,30] semiconductors and even non-conductors.[19,26] Moreover, in most cases it is an easy, rapid reaction and can be carried out in aqueous, nonaqueous or ionic liquid media,[26,32,33] to modify bulk,[22-24,31] or nanosurfaces as well.[6,34,35]

There have been various approaches developed to utilize diazonium coupling to modify carbon surfaces.[5,6,26,36] The simplest way is to start with the diazonium salt precursor directly which is spontaneously coupled to the carbon.[18,22-24,37,38] However, in most cases the diazonium salt of the desired redox modifier is not readily available and/or suffers from instability.[5] Therefore, one can instead start from another aryl precursor, that contains an amine[36,39-42] or nitro[40,43] group as a substituent, which produces a diazonium cation *in situ* as an intermediate step.[24,40] This is very useful since there is no need to synthesize and purify the diazonium salt precursor.[5,40] Gooding and coworkers showed that the modified surfaces based on the *in situ* approach resemble those prepared from isolated diazonium salt which reveals the effectiveness of the *in situ* approach.[44]

Additional advantages from the *in situ* formation of diazonium cation can be achieved by using nitro precursors. The electrochemical reduction of the nitro group can be performed separately from the diazotization step to enhance the preparative aspect of the coupling and in some cases it is necessary to separate the diazotization step to

preserve the precursor from any side reaction with the reducing agent.[40,43] Alternatively, the diazotizing reagent (i.e. $NaNO_2$) can coexist with the nitro precursor in the electrochemical cell during the nitro group electroreduction process.[40,43] Because the diazotization reaction is fast, local diazonium coupling can be achieved.[40,43]

In chapter four, we reported a novel modification of the carbon cloth with 1,2-dihydroxybenzene (DHB) functionality starting from 3,4-dihydroxyaniline (DHA) also known as 4-aminocatechol and shown as structure (I) in Figure 8.1.[24] Two reversible peaks were observed at 0.4 V and 0.6 V vs. SCE in aqueous 1 M H_2SO_4. The resultant modified electrode was promising as a positive electrode especially when it was configured with anthraquinone modified carbon as a negative electrode in an asymmetric supercapacitor.[23,24] Practically, the device showed a two fold increase in the energy density compared to a symmetric device with unmodified carbon electrodes.[24]

The diazonium salt of 1,2-dihydroxybenzene was not commercially available. Several trials to synthesis dihydroxybenzene diazonium salt or its amine (i.e. aminocatechol) from 4-nitrocatechol precursor failed. This pathway is promising because 4-nitrocatechol is much less expensive (10 $/g) compared to 500 $/g for 4-aminocatechol. However, recently Belanger and coworkers successfully prepared 4-aminocatechol from 3,4-dimethoxyaniline.[45]

The objective of this work was devoted to explore the covalent attachment of dihydroxybenzene (DHB) and dimethoxybenzene (DMB) moieties to carbon black substrates starting from 3,4-dihydroxyaniline and from other less expensive and readily

available precursors such as 3,4-dimethoxyaniline or 1,2-dihydroxy-4-nitrobenzene as shown in Figure 8.1 structure (I), (II) and (III), respectively. The DMB functionality can either be used in a positive electrode in nonaqueous media[46] or can be converted into the corresponding DHB following a demethylation step with a demethylating agent such as boron tribromide.[47] Moreover, the DMB moiety can be used to protect lithium ion batteries from overcharging.[46,48]

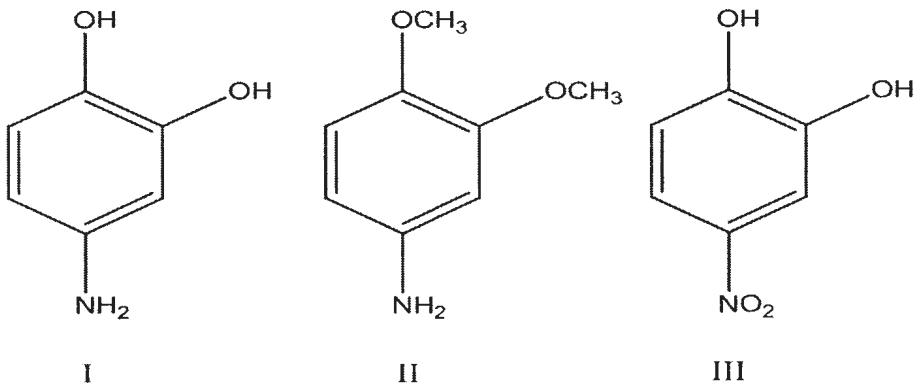

I II III

Figure 8.1: Structures of (I) 3,4-dihydroxyaniline (4-aminocatechol), (II) 3,4-dimethoxyaniline (4-aminoveratrole) and (III) 1,2-dihydroxy-4-nitrobenzene (4-nitrocatechol).

In principle, aryl amines and aryl-aliphatic amines can form a covalent bonding by routes other than diazonium coupling, such as Michael addition.[49-51] This idea encourages the use of aryl-diamine precursors. The modification of carbon with an aryl-diamine or aryl-aliphatic amine is important when the attachment of more than one redox modifier is required.[50,52] One amine terminal might be covalently bonded to the substrate via diazonium coupling while the other terminal becomes free for further modifications.[51, 53] Moreover, the redox centres (e.g. quinone) can be built layer-by-layer with different linkers and spacers.[18,51] The redox behaviour of free quinone in aqueous media was

systematically studied by Quan *et al.* and found to be dependent on the electrolyte composition.[54] Recently, a set of fundamental studies of the proton/electron transfer processes for aminobenzoquinone self-assembled monolayer modified gold electrode was reported by Zhang and Burgess.[55-57]

8.2. Experimental

Vulcan XC72 carbon black (Cabot Corporation), 3,4-dimethoxyaniline (Sigma Aldrich, 98 %), Boron tribromide (Sigma Aldrich), 4-aminocatechol (Tyger Inc.), sodium nitrite (Aldrich, 99.5%), benzoquinone (Aldrich, 98 %), 4-aminobenzylaniline (Aldrich, 98 %), acetone (ACS grade), acetonitrile HPLC grade (Aldrich), sulfuric acid (ACP chemicals Inc., 98%) and hydrochloric acid (Anachemia, 37%) were used as received.

All electrochemical cells were constructed in a three-electrode cell with the modified electrode as a working electrode, platinum (Pt) wire as a counter electrode and Ag/AgCl or saturated calomel electrode (SCE) as a reference electrode.

8.2.1. Modification of carbon black with 3,4-dihydroxyaniline

Diazonium coupling was used to modify carbon black (e.g. Vulcan CX-72) with 1,2-dihydroxybenzene moiety according to the following procedure. About 0.1 g of Vulcan and 0.01 g of 3,4-dihydroxyoxyaniline were mixed in 10 mL of 0.01 M HCl and kept cold in an ice bath (0.0 °C). About 10.0 mL of 0.1 M sodium nitrite ($NaNO_2$) was then added slowly and the mixture was allowed to react for further 30 min with frequent

stirring. Finally, the product was filtered and washed with deionized water and allowed to dry under air.

The modification was then investigated by cyclic voltammetry. The modified Vulcan was sonicated with methanol for 30 min. A small amount of the slurry was loaded on carbon fiber paper (CFP) and allowed to dry before using it as a working electrode in a three-electrode cell.

8.2.2. Modification of carbon black with 3,4-dimethoxyaniline followed by demethylation

Another way to use diazonium coupling to modify carbon black (e.g. Vulcan XC72) with 1,2-dihydroxybenzene moiety is described in the following procedure. About 0.1 g of Vulcan and 0.03 g of 3,4-dimethoxyaniline were mixed in 10 mL of 0.25 M HCl and kept cold in an ice bath (0.0 °C). About 10.0 mL of 0.2 M sodium nitrite ($NaNO_2$) was then added slowly and the mixture was allowed to react for a further 30 min. Finally, the product was filtered and washed with deionized water and was allowed to dry under air.

For demethylation, about 15 mL of dry dichloromethane (CH_2Cl_2) was added to 0.1 g of Vulcan (which was modified with 3,4-dimethoxyaniline in the previous step) in a round bottom flask which was sealed with a septum and kept under an inert environment through a permanent contact with a balloon of argon. The mixture was kept under stirring in a dry ice/acetone bath (-78 °C). About 0.4 mL of boron tribromide (BBr_3) solution (1 M in CH_2Cl_2) was then added with a syringe and the reaction was kept under stirring

overnight during which the temperature gradually reached room temperature. Finally, the product was filtered and washed with a mixture of deionized water/methanol and was allowed to dry under air.

The modified carbon was then dispersed in methanol by sonication for 30 min. A small portion of the modified carbon was loaded (i.e. 0.00026 g after drying) onto the end of a 3 cm piece of carbon fiber paper (CFP). This electrode was then examined by cyclic voltammetry in 1 M H_2SO_4 (aq).

8.2.3. Exploring nitrocatechol as a precursor for the modification of carbon with 1,2-dihydroxyaniline

To explore the usefulness of using nitrocatechol as a precursor for modifying carbon black the following cyclic voltammetry experiments were carried out. A three electrode cell was configured using carbon fiber paper (CFP) loaded with 0.00105 g of Vulcan XC72 as working electrode. The electrolyte solution was 0.001 M of 4-nitrocatechol dissolved in 1 M H_2SO_4 (aq). The potential was scanned for two cycles then the working electrode was transferred from the nitrocatechol solution into a 1 M H_2SO_4 (aq) reactant-free solution where another cyclic voltammetric study was performed.

8.2.4. The electroreduction of 4-nitrocatechol followed by *in situ* diazonium coupling

To modify a glassy carbon electrode by an *in situ* diazonium coupling from a 4-nitrocatechol the following procedure was followed. An electrolyte solution was prepared by dissolving 0.1 M of tetrabutylammonium hexafluorophosphate (Bu_4NPF_6) in a (18+2) mL mixture of acetonitrile and 1 M HCl. To this solution $1.03x10^{-4}$ mole of

4-nitrocatechol and $2.00x10^{-4}$ mole of sodium nitrite ($NaNO_2$) were added. Therefore, the final mixture has a mole ratio of (1.03:20.00:2.00) of 4-nitrocatechol: HCl:$NaNO_2$. The electrochemical reduction of the nitro group to an amine group was carried out under nitrogen using cyclic voltammetry in a three-electrode cell by sweeping the potential between 0.0 V and -1.2 V vs. SCE at 50 mV s^{-1}. A glassy carbon working electrode was used.

The modified electrode was then immersed in acetonitrile, dried and tested using cyclic voltammetry in 1 M H_2SO_4 in a three-electrode cell.

8.2.5. Chemical modification of diamine followed by benzoquinone

To modify Vulcan with 4-aminobenzylaniline (ABA) the following procedure was used.[58] About 0.05 g of Vulcan was dispersed in 5 mL of deionized water by sonication for 10 min. To this mixture 1.14 mL (0.01 moles) of ABA and 0.69 g (0.01 moles) of $NaNO_2$ was added and allowed to dissolve overnight under stirring. After that 0.5 mL of concentrated HCl was added and the mixture kept under reflux overnight. Finally, the mixture was filtered with a 0.2 μm Nylon membrane (Millipore) and washed with deionized water, dimethylformamide (DMF), methanol and acetone and allowed to dry under vacuum overnight to obtain the Vulc-ABA.

To modify the Vulc-ABA with benzoquinone (BQ) the following procedure was used.[55] 20 mL of 95% ethanol/water solution was heated to 50 °C in a water bath. 0.0138 g BQ was added to obtain a solution of 6.3 mM. This solution was kept for three min then

filtered with a 0.2 μm Nylon membrane (Millipore) and washed with 95% ethanol/water, deionized water and allowed to dry under vacuum to obtain the Vulc-ABA-BQ.

8.3. Results and discussion

8.3.1. Modification of carbon black with 3,4-dihydroxyaniline

The cyclic voltammogram of the Vulcan after its reaction with 4-aminocatechol via diazonium coupling is shown in Figure 8.2. There are two main reversible peaks at 0.41 V and 0.65 V, respectively. The latter is expected to be observed as a result of carbon-carbon coupling as shown in structure 1 in Figure 8.3.[59,60] However, the former peak may be due to the coupling of the dihydroxybenzene through the NH_2 group as shown in structure 2 in Figure 8.3[60,61] or may be due to some polymerization.[59] The reversibility of these peaks was maintained over 100 cycles. In addition, they show significantly higher specific capacitance compared to the unmodified Vulcan (i.e. < 20 F g^{-1}). On the other hand, Pognon *et al.* recently used a slightly different procedure than ours to modify Black Pearls 2000 carbon black with 4-aminocatechol which resulted in the formation of three reversible peaks at 0.2 V, 0.4 V and a small one at 0.6 V.[45]

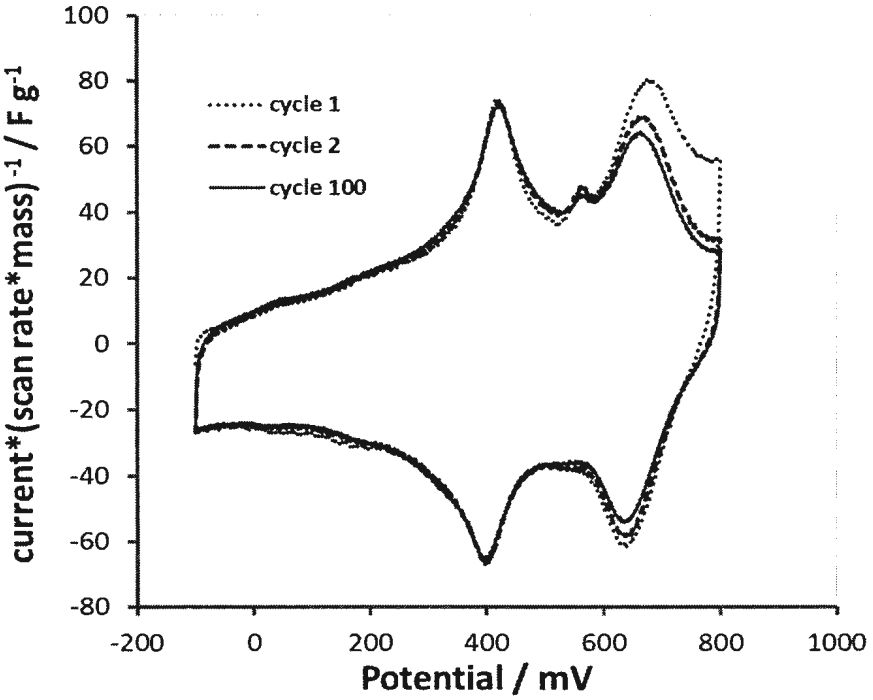

Figure 8.2: Cyclic voltammetry of Vulcan XC72 modified with 3,4-dihydroxyaniline (0.00094 g) at 50 mV/s in 1 M H_2SO_4 (aq).

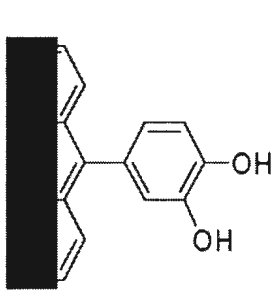

Structrure 1

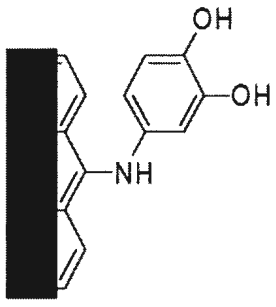

Structrure 2

Figure 8.3: Possible coupling of the dihydroxybenzene moiety.

8.3.2. Modification of carbon black with 3,4-dimethoxyaniline followed by demethylation

Figure 8.4 shows cyclic voltammogram at 20 mV/s of Vulcan that had been reacted initially with dimethoxyaniline followed by demethylation with boron tribromide. Again two small reversible peaks at *ca.* 0.34 V and 0.67 V vs. Ag/AgCl were observed. Based on the finding of diazonium coupling of 3,4-dihydroxyanilne to Vulcan XC72 presented in section 8.3.1 the former peak (i.e. 0.34 V) can be attributed to structure 2 while the latter peak (i.e. 0.67 V) can be attributed to structure 1 as shown in Figure 8.3.

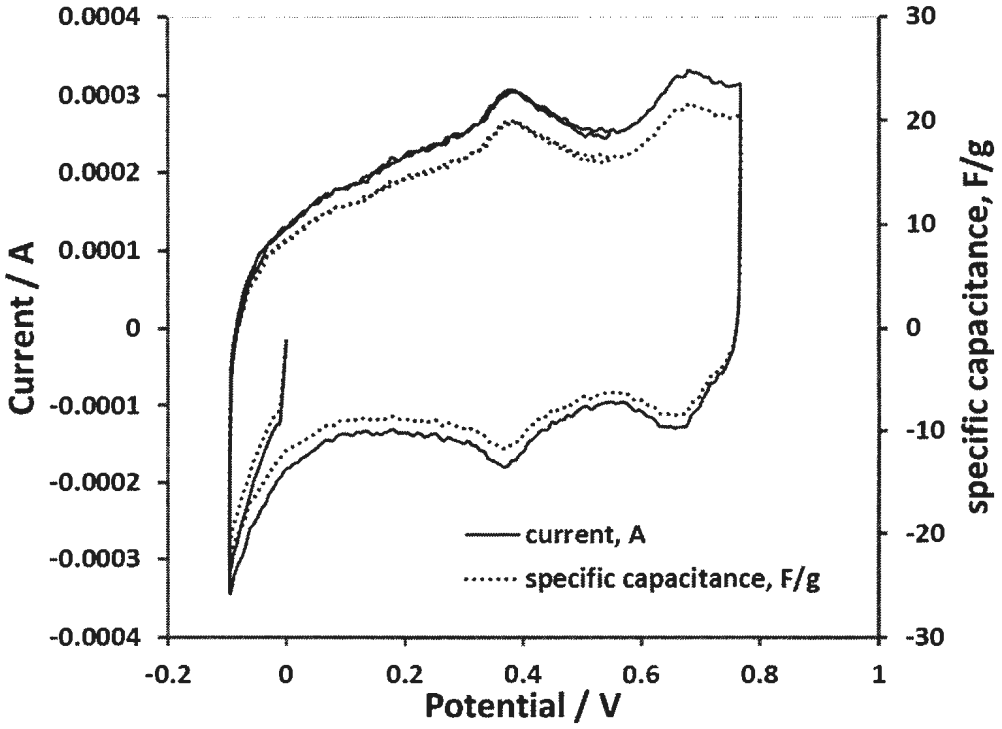

Figure 8.4: Cyclic voltammograms of Vulcan XC72 modified with 3,4-dimethoxyaniline followed by demethylation into 3,4-dihydroxyaniline at a scan rate of 20 mV s^{-1} in 1 M H_2SO_4 (aq), 0.26 mg of modified Vulcan XC72 was loaded.

8.3.2.1. Elemental analysis

Table 8.1 shows elemental analysis results for unmodified Vulcan XC72 and the corresponding Vulcan-DHB. The unmodified Vulcan XC72 contains insignificant amounts of oxygen and nitrogen atoms. However, after diazonium coupling of 4-aminocatechol to Vulcan the modified Vulcan-DHB had a mole ratio of 4/1 for O/N. These results were in good agreement with the cyclic voltammograms shown in Figure 8.2 where the two reversible peaks have approximately the same area under the curve. In other words, half of the modification was performed through coupling according to structure 1 and the other half was done according to structure 2, resulting in approx. 4 O atoms per N atom.

For Vulcan XC72 modified with dimethoxyaniline followed by demethylation the H % and N % (as seen in Table 8.1) were both below 0.3 % which resembles the unmodified Vulcan XC72. This finding is expected since the amount of DHB on the carbon was small as indicated by the cyclic voltammogram shown in Figure 8.4. However, the O % in the modified Vulcan XC72 along with cyclic voltammetry revealed the grafting with 1,2-dimethoxybenzene functionality. It seems that the diazonium coupling was efficient but the hydrolysis was not.

Table 8.1: Elemental analysis of unmodified Vulcan XC72 compared to samples modified with DHB and indirectly with DMB followed by demethylation to form DHB.

Elemental Analysis %	Unmodified Vulcan XC72	Vulcan-DHB	Vulcan-DHB via DMB
C	96.48	96.19	95.83
H	< 0.3	< 0.3	< 0.3
N	< 0.3	0.37	< 0.3
O	< 0.3	1.83	1.87

8.3.3. Exploring nitrocatechol as a precursor for the modification of carbon with 1,2-dihydroxyaniline

The possibility of utilizing nitrocatechol as a precursor for the modification of porous carbons was investigated by cyclic voltammetry as shown in Figure 8.5 and Figure 8.6. In Figure 8.5 the electrochemical behaviour of 4-nitrocatechol in 1 M H_2SO_4 is shown at a carbon fiber paper loaded with Vulcan XC72 as the working electrode. The potential was initially scanned at a rate of 50 mV s^{-1} from + 0.6 V down to -0.4 V vs. Ag/AgCl which shows no electrochemical activity at positive potentials since the catechol was already present in the reduced form. However, an irreversible wave at -0.26 V was observed probably due to the reduction of nitro group into the corresponding amine group, analogous to the reduction of nitrobenzene in which 6 e^- and 6 H^+ are consumed as shown in Scheme 8.1.[62,63] As the potential was scanned in the reverse direction (i.e. anodic scan) followed by a second cycle a $2e^-$ reversible couple was observed at *ca.* +0.4 V due to the formation of 4-aminocatechol at the vicinity of the electrode.

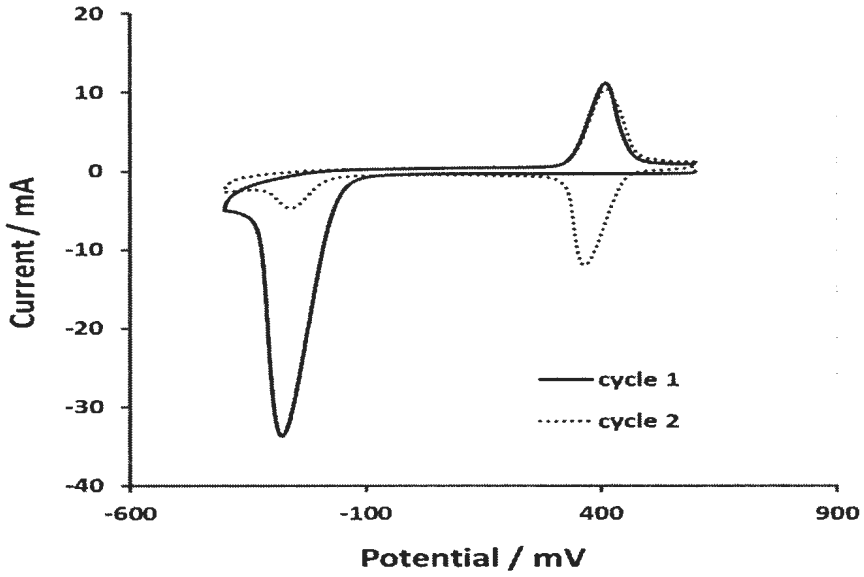

Figure 8.5: Cyclic voltammogram of 4-nitrocatechol on GC in 1 M H_2SO_4 (aq) at 50 mV/s.

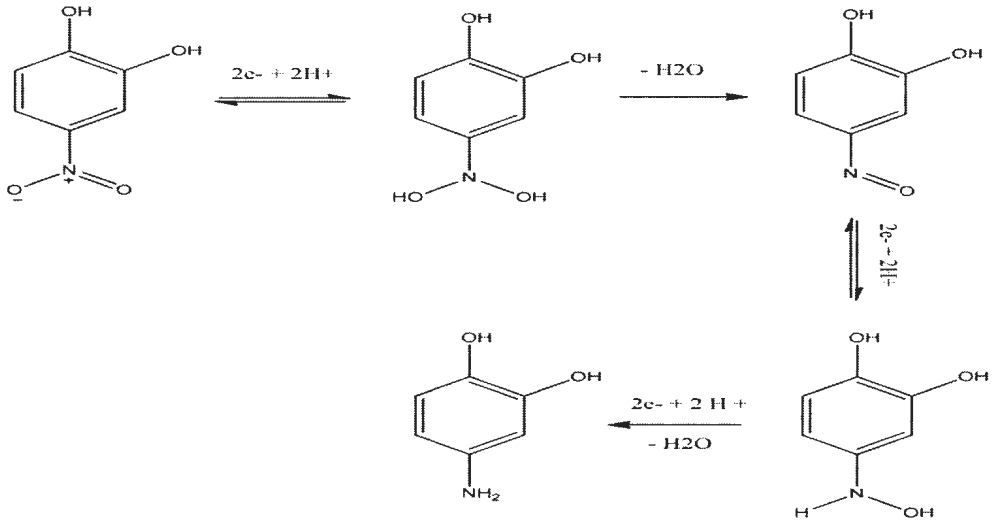

Scheme 8.1: Proposed reduction pathway of 4-nitrocatechol in aqueous acid.

The Vulcan XC72 electrode was then removed from the previous electrochemical cell and placed in a new cell containing fresh 1 M H_2SO_4 (aq) with no 4-nitrocatechol. Two cycles were carried out at 50 mV s^{-1} between +0.6 V and –0.4 V as seen in Figure

8.6. A small reduction peak at *ca.* +0.4 V was observed initially indicating that some 4-aminoaminocatechol was adsorbed on the electrode surface. However, a large reduction peak at – 0.31 V revealed that a large amount of nitrocatechol was entrapped within the Vulcan pores. This reduction peak is more cathodic than the initial one observed in Figure 8.5 which may be due to the interaction of some redox functional group on the carbon with the amine group generated from the reduction of the nitro group.[43] Some new reversible peaks can also be seen which may result from hydroxylation[62] or dimerization.[62]

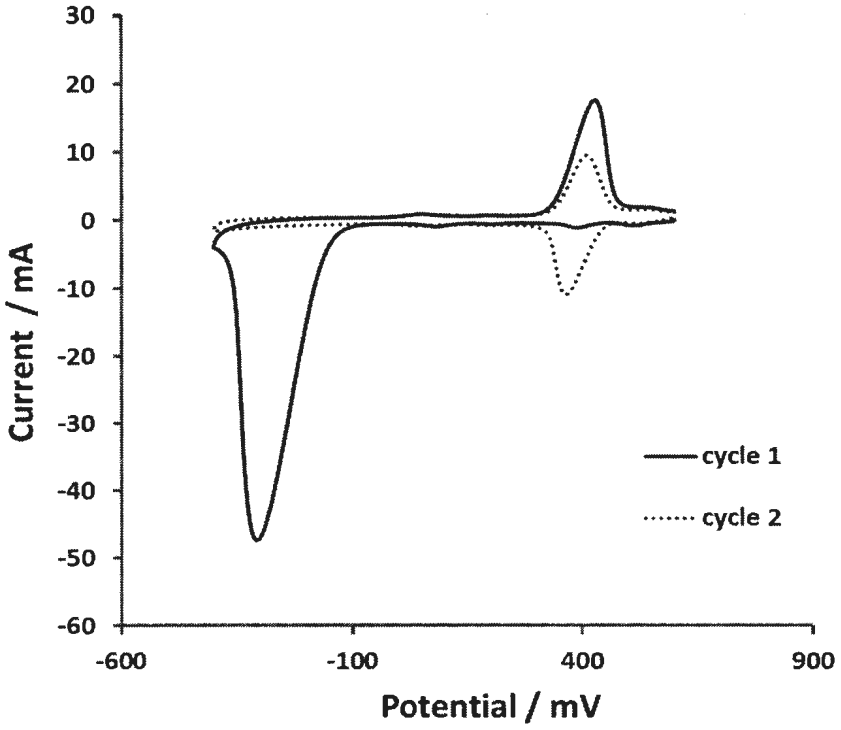

Figure 8.6: Cyclic voltammetry of a Vulcan carbon electrode in 1 M H_2SO_4 at 50 mV s^{-1} following the cyclic voltammetry in a 4-nitrocatechol solution shown in Figure 8.5.

8.3.4. Electroreduction of 4-nitrocatechol in presence of nitrite

Figure 8.7 shows cyclic voltammograms of the electroreduction of 4-nitrocatechol in the presence of sodium nitrite and 0.1 M tetrabutylammonium hexafluorophosphate dissolved in (9:1) acetonitrile:1 M HCl, between 0.0 V and -1.2 V at 50 mV/s. A reduction peak was observed initially at -0.75 V due to the reduction of nitro group. As sweeping was continued this peak current diminished as a result of nitro group consumption. Moreover, a cathodic peak shift was observed which could have resulted from an interaction between the amine group and the oxygenated groups on the bare carbon electrode.[43] It was reported that three equivalents of nitrite is needed to complete the reaction.[43] A reduction tail was recognized at negative potentials (i.e. -1.0 V) after seven cycles which may be due to the use of only two equivalents of nitrite.[43]

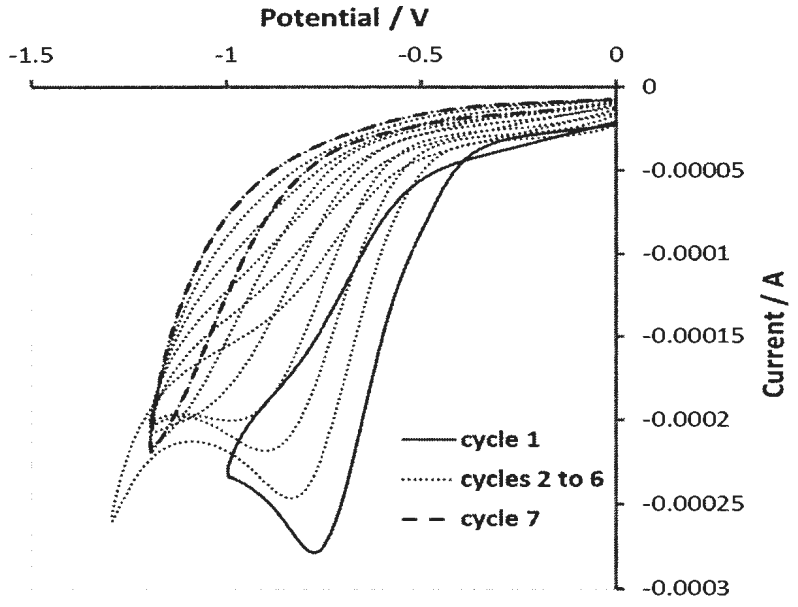

Figure 8.7: Cyclic voltammogram at 50 mV s^{-1} of electrochemical reduction of $1.03x10^{-4}$ mole of 4-nitrocatechol on GC electrode in a solution contains $2.00x10^{-4}$ mole of $NaNO_2$, ((18 + 2) mL; acetonitrile + 1 M HCl) and 0.1 M Bu_4NPF_6.

Figure 8.8(a) and (b) show cyclic voltammograms of DHB-Vulcan electrode in 1 M H_2SO_4 (aq) at different scan rates. The potential was scanned between 0.0 V and 0.8 V and reveals the presence of two reversible peaks at 0.4 V and 0.6 V as in the case of modification with 4-aminocatechol, (see section 8.3.1). However, these peaks behave differently with respect to scan rate. The former peak showed an increase in the peak separation with increasing scan rate while the latter did not. The peak at 0.6 V is consistent with the attachment of DHB to the carbon via C-C bond while the less reversible peak at 0.4 V might be due adsorbed or entrapped 4-aminocatechol since its potential matches that of 4-aminocatechol in Figure 8.5 to the adsorbed or entrapped DHB.[45]

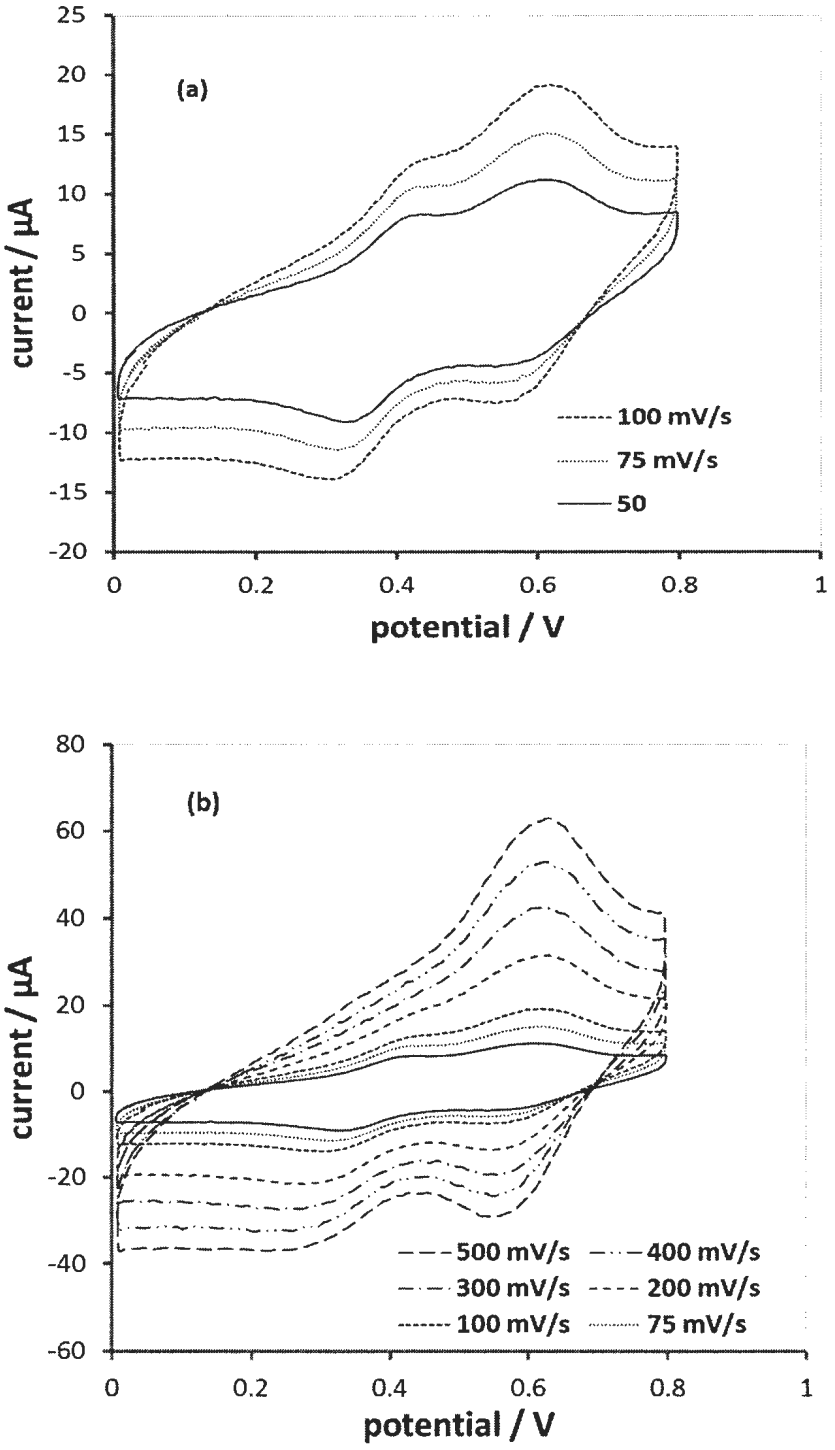

Figure 8.8: Cyclic voltammograms in 1 M H_2SO_4 (aq) for GC/Vulcan following grafting with nitrocatechol. (a) Scan rates are from 50 to 100 mV s^{-1}. (b) Scan rates are from 50 to 500 mV s^{-1}.

Figure 8.9 shows that the cathodic peak current of the modified Vulcan XC72 carbon measured at 0.56 V vs. SCE was linearly dependent on scan rate which indicates that DHB was attached to the Vulcan XC72 surface.

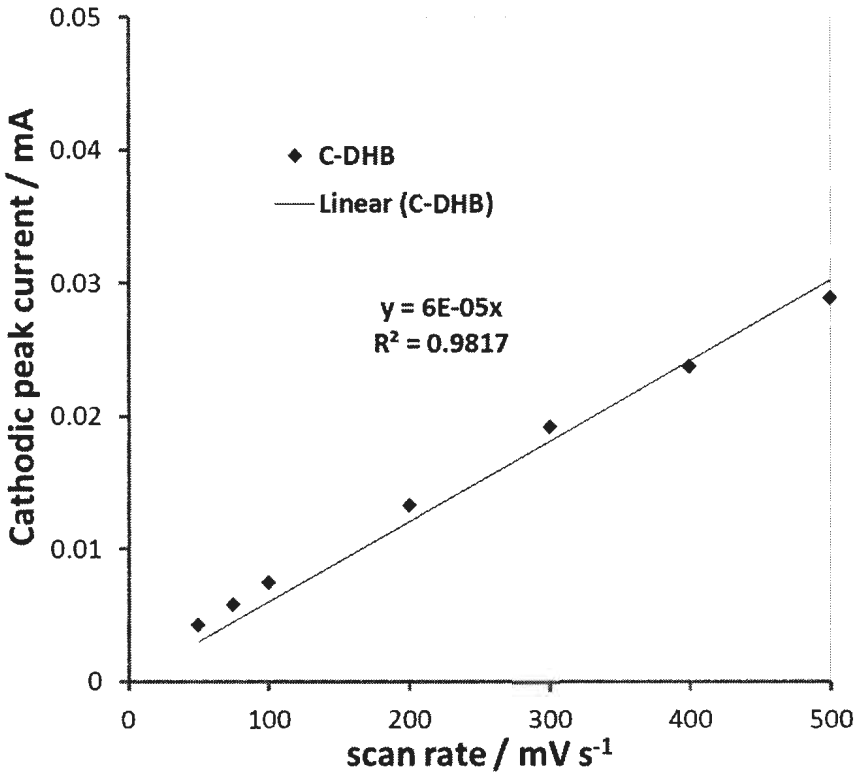

Figure 8.9: Linear plot of cathodic peak current at *ca.* 0.56 V versus scan rates for Vulcan XC72 following grafting with nitrocatechol, measured in 1 M H_2SO_4 (aq).

8.3.5. Modification of carbon black with aryl diamine followed by Michael addition of benzoquinone

Figure 8.10 shows the cyclic voltammogram at 50 mV/s of Vulcan XC72 modified initially with 4-aminobenzylaniline (ABA) via diazonium coupling followed by

a covalent attachment of benzoquinone (BQ) to the amine terminals via a Michael addition reaction. The figure reveals three main closely spaced redox couples at *ca.* 0.16 V, 0.28 V and 0.43 V vs. SCE as an indication of multiple binding modes of the BQ to the surface.[51] The BQ can be singly bound to the amine through position 2 (i.e. 0.28 V) and/or doubly bound through positions 2 and 5 with a cathodic shift of the BQ formal potential for the additional binding (i.e. 0.16 V).[51,55] The peak at 0.43 V might be assigned to some sort of noncovalent bonding between ABA and BQ.[51,55]

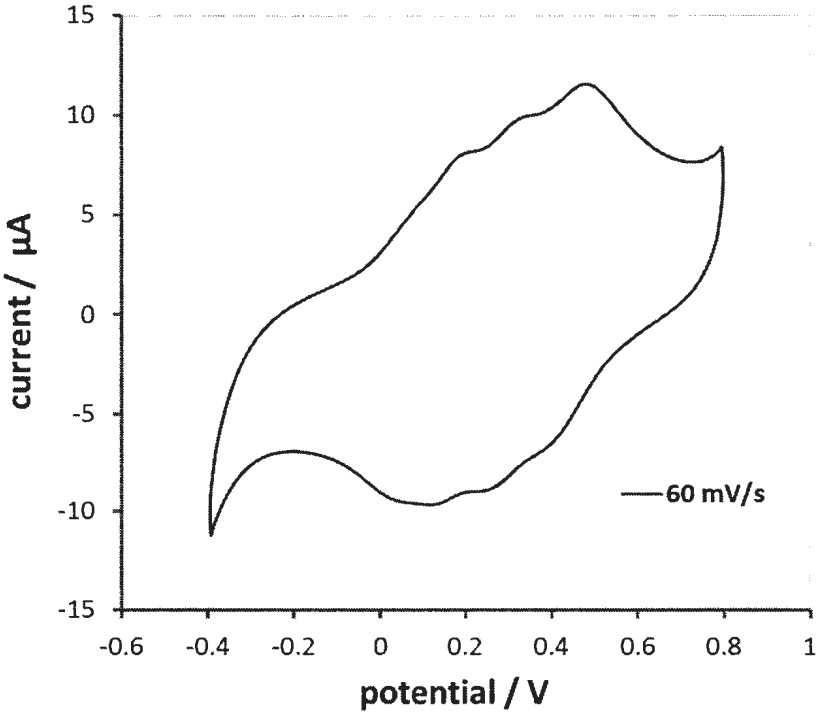

Figure 8.10: Cyclic voltammogram at 50 mV/s of GC/Vulcan-ABA-BQ in 1 M H_2SO_4 (aq).

Figure 8.11 shows the effect of scan rate on the electroactivity of GC/Vulcan-ABA-BQ in 1 M H_2SO_4 (aq). The peak potential was independent of scan rate for the range chosen and the peak current increased with increasing scan rate. The

electrochemical behaviour of the BQ was not ideal since the BQ sites were not sufficiently separated from each other. Therefore, to systematically study the modification of Vulcan XC72 carbon black with ABA-BQ an electroinactive spacer should be used.[55]

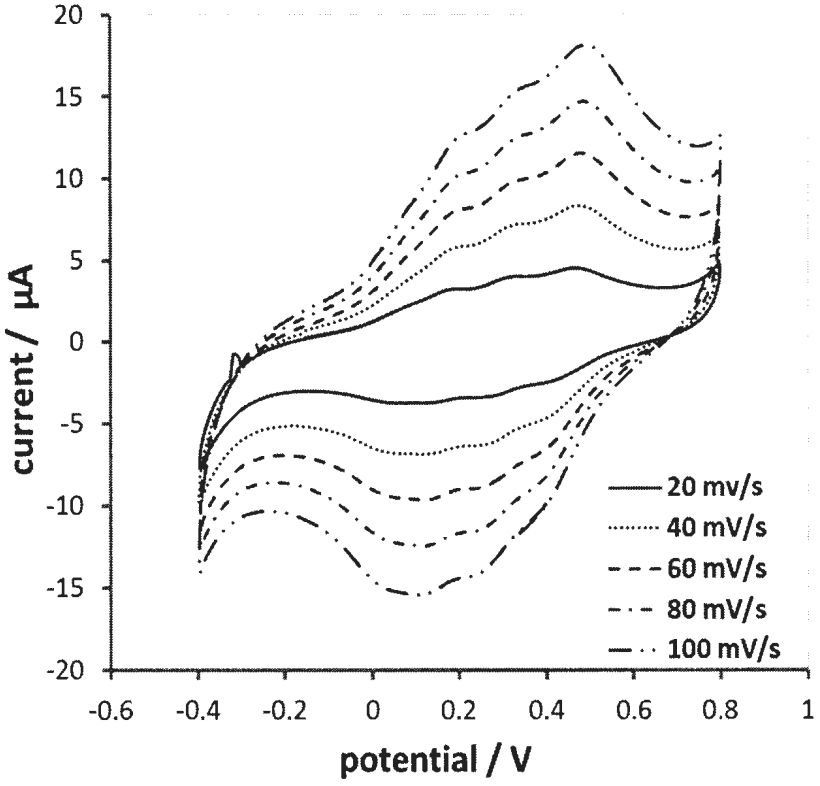

Figure 8.11: Cyclic voltammogram of GC/Vulcan-ABA-BQ in 1 M H_2SO_4 (aq) at scan rate from 20 mV/s to 100 mV/s.

8.4. Conclusions

A number of different *in situ* diazonium coupling methods to graft the 1,2-dihydroxybenzene moiety onto Vulcan XC72 carbon black have been demonstrated. In all cases the modified carbons resulted in the formation of two redox peaks instead of

three as reported by Belanger and coworkers.[45] The reasons for this discrepancy are not fully understood and emphasize the sensitivity of the coupling of quinones to slight differences in the preparation conditions. These modified carbons are promising as positive electrode materials for supercapacitors in aqueous media.[24,45] The modification of Vulcan with 1,2-dimethoxybenzene was also successful but needs further examination as a positive electrode material for supercapacitors in nonaqueous media.

An interesting new approach for the *in situ* diazonium coupling was to start from the nitrocatechol precursor as a potential alternative to the diazonium salt or the amine precursors for 1,2-DHB. It is available at low cost and has higher stability. Moreover, local diazonium coupling becomes possible when the electroreduction of the nitro precursor is performed in the presence of nitrite in the cell.

The modification of Vulcan carbon black with 4-aminobenzylaniline (ABA) followed by a Michael addition reaction with benzoquinone (BQ) is also reported. Further work is required for all these systems in order to fully understand the bonding modes, stability and electrochemistry. Their characteristics should also be further assessed for applications in supercapacitors and other possible applications such as electrocatalysis.

References

(1) Yin, C.; Aroua M.; Daud W. *Separation and Purification Technology* **2007**, *52*, 403-415.

(2) Solak, A.; Eichorst, L.; William J. Clark, W.; McCreery R. *Anal. Chem.* **2003**, *75*, 296-305.

(3) Wring, S. *Analyst* **1992**, *117*, 1215-1229.

(4) Delamar, M.; Pinson, J.; Saveant, J. *J. Am. Chem. Soc.* **1992**, *114*, 5883-5884.

(5) Bélanger, D.; Pinson, J. *Chem. Soc. Rev.* **2011**, *40*, 3995-4048.

(6) Wildgoose, G.; Banks, C.; Leventis, H. *Mikrochimica Acta* **2006**, *152*, 187-214.

(7) Armand, M.; Tarascon, J. *Nature* **2008**, *451*, 652-657.

(8) Dicks, A. *J. Power Sources* **2006**, *156*, 128-141.

(9) Conway, B. E. In *Electrochemical supercapacitors: scientific fundamentals and technological applications;* Plenum Press: 1999.

(10) Frackowiak, E.; Beguin, F. *Carbon* **2001**, *39*, 937-950.

(11) Frackowiak, E. *Phys. Chem. Chem. Phys.* **2007**, *9*, 1774–1785.

(12) Pandolfo, A.; Hollinkamp, A. *J. Power Sources* **2006**, *157*, 11-27.

(13) Simon, P.; Gogotsi, Y. *Nat. Mater.* **2008**, *7*, 845-854.

(14) Inagaki, M.; Konno, H.; Tanake, O. *J. Power Sources* **2010**, *195*, 7880-7903.

(15) Noked, M.; Soffer, A.; Aurbach D. *J. Solid State Electrochem.* **2011**, *15*, 1563-1578.

(16) Kim Kinoshita, Ed. In *Carbon: electrochemical and physicochemical properties;* Jiohn Wiley & Sons: 1988.

(17) Leitner, K.; Winter, M.; Besenhard, J. *Electrochim. Acta* **2004**, *50*, 199-204.

(18) Chrétien, J.; Ghanem, M.; Bartlet, P.; Kilburn, J. *Chem.Eur. J.* **2009**, *15*, 11928-11936.

(19) Pinson, J.; Podvarica, F. *Chem. Soc. Rev.* **2005**, *34*, 429-439.

(20) McCreery, R. *Chem. Rev.* **2008**, *108*, 2646-2687.

(21) Pognon, G.; Brousse, T.; Demarconnay L.; Belanger, D. *J. Power Sources* **2011**, *196*, 4117-4122.

(22) Smith, R.; Pickup, P. *Electrochim. Acta* **2009**, *54*, 2305-2311.

(23) Algharaibeh, Z.; Liu, X.; Pickup, P. *J. Power Sources* **2009**, *187*, 640-643.

(24) Algharaibeh, Z.; Pickup, P. *Electrochem. Commun.* **2011**, *13*, 147-149.

(25) Yeşildağ, A.; Ekinci, D. *Electrochim. Acta* **2010**, *55*, 7000-7009.

(26) Mahouche-Chergui, S.; Gam-Derouich, S.; Mangeney, C.; Chehimi, M. *Chem. Soc. Rev.* **2011**, *40*, 4143-4166.

(27) Saunders, K. H. In *The aromatic diazo compounds;* Edward Arnold: 1985.

(28) Zollinger, H. In *Diazo Chemistry I: Aromatic and Heteroaromatic Compounds;* VCH Verlagsgesellschaft mbH: 1994; Vol. I.

(29) Barbero, C.; Sereno, L. *J. Electroanal. Chem.* **1990**, *291*, 81-101.

(30) Allongue, P.; Desbat, B.; Fagebaume, O.; Hitmi, R.; Pinson, J. *J. Am. Chem. Soc.* **1997**, *119*, 201-207.

(31) Bernard, M.; Chausse, A.; Cabet-Deliry E.; Chehimi M.; Pinson, J.; Podvorica, F.; Vautrin-Ul C. *Chem. Mat.* **2003**, *15*, 3450-3462.

(32) Ghilane, J.; atin, P.; Fontaine O.; Lacroix, J.; Randriamahazaka, H. *Electrochem. Commun.* **2008**, *10*, 1060-1063.

(33) Agullo, J.; Canesi, S.; Schaper, F.; Morin, M.; Belanger, D. *J. Electrochem. Soc.* **2012**, *159*, H758-H764.

(34) Dyke, C. A.; Tour, J. *Nano Letters* **2003**, *3*, 1215-1218.

(35) Mirkhalaf, F.; Paprotny, J.; Schiffrin, D. *J. Am. Chem. Soc.* **2006**, *128*, 7400-7401.

(36) Toupin, M.; Belanger, D. *Langmuir* **2008**, *24*, 1910-1917.

(37) Kalinathan, K.; DesRoches, D.; Liu, X.; Pickup, P. *J. Power Sources* **2008**, *181*, 182-185.

(38) Barrière, F. Downard, A. *J. Solid State Electrochem.* **2008**, *12*, 1231-1244.

(39) Toupin, M.; belanger, D. *J. Phys. Chem. C* **2007**, *111*, 5394-5401.

(40) Cougnon, C.; Gohier, F.; Belanger, D.; Mauzeroll, J. *Angew. Chem. Int. Ed.* **2009**, *121*, 4066-4068.

(41) Baranton, S.; Belanger, D. *J. Phys. Chem. B* **2005**, *109*, 24401-24410.

(42) Corgier, B.; Marqutte, C.; Blum, L. *J. Am. Chem. Soc.* **2005**, *127*, 18328-18332.

(43) Cougnon, C.; Nguyen, N.; Dabos-Seignon, S.; Mauzeroll, J.; Belanger, D. *J. Electroanal. Chem.* **2011**, *661*, 13-19.

(44) Liu, G.; Chckalingham, M.; Khor, S.; Gui, A.; Gooding, J. *Electroanalysis* **2010**, *22*, 918-926.

(45) Pognon, G.; Cougnon, C.; Mayilukila, D.; Belanger, D. *ASC Appl. Mater. Interfaces* **2012**, *4*, 3788-3796.

(46) Buhrmester, C.; Chen, J.; Moshurchak, L.; Jiang, J.; Wang, R.; Dahn, J. *J. Electrochem. Soc.* **2005**, *152*, A2390-A2399.

(47) McOmie, J.; Watts, M.; West, D. *Tetrahedron* **1968**, *24*, 2289-2292.

(48) Chen, Z.; Qin, Y.; Amine, K. *Electrochim. Acta* **2009**, *54*, 5605-5613.

(49) Mather, B.; Kalpana, V.; Miller, K.; Long, T. *Progress Polym. Sci.* **2006**, *31*, 487-531.

(50) Nguyen, N.; Esnault, C.; Gohier, F.; Belanger, D.; Cougnon, C. *Langmuir* **2009**, *25*, 3504-3508.

(51) Budavári, V.; Szucs, A.; Oszko, A.; Novak, M. *Electrochim. Acta* **2003**, *48*, 3499-3508.

(52) Breton, T.; Belanger, D. *Langmuir* **2008**, *24*, 8711-8718.

(53) Budavári, V.; Szucs, A.; Somali, Cs.; Novak, M. *Electrochim. Acta* **2002**, *47*, 4351.

(54) Quan, M.; Wasylkiw, M.; Smith, D. K. *J. Am. Chem. Soc.* **2007**, *129*, 12847-12856.

(55) Zhang, W.; Burgess, I. *J. Phys. Chem. C* **2010**, *114*, 2738-2745.

(56) Zhang, W.; Burgess, I. *Phys.Chem. Chem. Phys.* **2011**, *13*, 2151-2159.

(57) Zhang, W.; Burgess, I. *J. Electroanal. Chem.* **2012**, *668*, 66-72.

(58) Lyskawa, J.; Grondein, A.; Belanger, D. *Carbon* **2010**, *48*, 1271-1278.

(59) Wildgoose, G.; Crossley, A.; Jones, J.; Compton, R. *J. Electrochem. Sci.* **2007**, *2*, 809-819.

(60) Uchiyama, S.; Yamazaki, H.; Kanazawa, A.; Hamana, H.; Okabe, Y. *J. Electrochem. Soc.* **2007**, *154*, F31-F35.

(61) Buttry, D.; Donnet, J.; Rebouillat, S. *Carbon* **1999**, *37*, 1929-1940.

(62) Nematollahi, D.; Varmaghani, F. *Electrochim. Acta* **2008**, *53*, 3350-3355.

(63) Wain, A.; Lawrence, N.; Greene, P.; Wadhawan, J.; Compton, R. *Phys. Chem. Chem. Phys.* **2003**, *5*, 1867-1875.

Chapter 9

Summary and future work

9.1. Summary

Although high surface area carbon materials having an excellent power density are well known as electrode materials for supercapacitors, they have limited energy density. The theme of this work was to study the modification of carbon electrode materials with anthraquinone (AQ) and dihydroxybenzene (DHB) functionality to improve their energy density without sacrificing their excellent power density.

These quinone redox groups were chosen for two fundamental reasons. First, their electrochemical activities were utilized to add an extra pseudocapacitance charging to the inherently double layer capacitance charging found in the unmodified carbons. Second, their redox potentials were chosen to increase the useful cell potential limits in an asymmetric capacitor to maximize the performance.

Two methodologies were examined in this work for modification of carbon. The first one utilized diazonium chemistry to form covalently bound quinone to the carbon electrode. The second one explored the anodic polymerization of quinone amine derivatives onto carbon electrodes.

The following techniques were used to characterize the modified carbons: cyclic voltammetry (CV), electrochemical impedance spectroscopy (EIS), galvanic cycle, scanning electron microscopy (SEM), attenuated total reflectance Fourier transform infrared (ATR FTIR) spectroscopy and elemental analysis (EA).

The performances of the supercapacitors constructed in this work were evaluated by cyclic voltammetry and constant current discharging chronopotentiometry. The energy density and the power density of the supercapacitors were determined based on the constant current discharging experiments and evaluated based on their Ragone plots.

Searching for new materials with excellent performance and reasonable cost has been challenging for the supercapacitor industry. Ruthenium oxide is considered as one of the best known materials for supercapacitors but suffers from limited availability and high cost. AQ and DHB modified carbon electrodes are reported in this work as potential candidates to minimize the dependence on the usage of Ru oxide or even to replace it in the future with relatively low cost materials.

Compared to a symmetric Ru oxide supercapacitor, the asymmetric device constructed from AQ carbon cloth as a negative electrode and Ru oxide as a positive electrode required 64% less Ru and provided better energy and power densities. These findings were related to the high specific capacitance of the AQ modified carbon (i.e. 482 F/g compared to 199 F/g for the unmodified carbon) over a potential region close to and more negative than the Ru oxide negative potential limit.

Following this result, a novel method for grafting the DHB moiety was reported and shown to provide a promising alternative positive electrode to replace the Ru oxide electrode. The argument here is that the DHB has a low mass to charge ratio (i.e. 55 g/mol of electrons) which is even better than that of AQ (i.e. 104 g/moles of electrons). A double in energy density compared to the symmetric unmodified carbon cloth device was achieved by constructing an asymmetric device with DHB modified carbon cloth as a positive electrode and AQ modified carbon cloth as a negative electrode. This results in a combination of battery-like and capacitive behaviour.

When trying to increase the loading of the AQ onto the carbon electrode via the electrochemical oxidative polymerization of the 1-aminoanthraquinone (1-AAQ), an unexpected result was obtained. The polymer film was deposited but the redox activity of AQ was distorted. The AQ reduction peak was observed at the usual thermodynamic potential (i.e. -0.1 V vs. SCE) while the reoxidation peak was shifted to more positive potential (e.g. +0.36 V vs. SCE) at 50 mV/s. This unusual behavior was extensively investigated by cyclic voltammetry and impedance spectroscopy. The redox activity of AQ was found to be complicated by the conductivity of the polyaniline-like backbone. As the potential was scanned cathodically the conductivity of the film gradually decreased but remained sufficient to allow the AQ reduction reaction to occur at its formal potential. However, scanning the potential anodically after reaching -0.45 V resulted in a re-oxidation of the H_2AQ at a potential of +0.36 V instead of *ca.* -0.1 V. In other words, the AQ sites in the film are trapped in the reduced state until the film becomes sufficiently conducting at +0.3 V. These results may open new prospective research avenues to

overcome or to minimize this kinetic limitation of the AQ redox activity in the electrochemically deposited poly(1-AAQ) films.

Following these results the 1-AAQ was successfully copolymerized with aniline and found to form a film which is electroactive over the potential range (i.e. -0.45 to 0.8 V vs. SCE) compared to the electroactivity of polyaniline (i.e. 0.0 to 0.8 V) in 4 M H_2SO_4 (aq). A small redox peak of AQ was observed at its thermodynamic potential with the absence of charge trapping.

The electrochemical polymerization of 3,4-dihydroxyaniline was met with limited success for unknown reasons. Therefore, the electrochemical polymerization of DHB functionality was performed from a 3,4-dimethoxyaniline precursor followed by a hydrolysis step after the film formation. Three reversible redox couples extended between 0.0 V and 0.7 V vs. SCE.

The diazonium coupling was revisited and various recent approaches were examined. The *in situ* diazonium coupling was found to be more suitable for diazonium coupling than the *ex situ* approach since a number of diverse redox functionalities could be attached to carbon electrodes without the need for preparing and purifying the diazonium salt or worrying about its stability. 3,4-dihydroxyamine, 3,4-dimethoxyamine and 4-nitro-1,2-dihydroxyamine were attached to carbon electrodes and their electrochemical activities were studied.

Finally, the modification of Vulcan carbon black with 4-aminobenzylaniline (ABA) followed by a Michael addition reaction with benzoquinone (BQ) is reported. Studying the electrochemistry of BQ modified Vulcan-ABA was incomplete and should be studied in more systematic way to obtain the interaction-free BQ centres.

9.2. Future work

Based on the work that was done in this thesis the following future work is proposed.

1- Studying the dimethoxybenzene (DMB) modified carbon in nonaqueous media and ionic liquids for supercapacitors.

2- Monitoring and controlling the location of electrochemical deposition of poly(1-AAQ) on high surface area carbons and extending their application in fuel cell reactions.

3- Re-examine the electropolymerization of other mono and diamino-anthraquinones on carbon black.

4- Extend the use of diazonium coupling and electrochemical polymerization of quinones methodologies to modify other nanostructured carbon materials such as carbon nanotubes, graphene sheets and onion-like carbon for supercapacitors.

5- Studying the copolymerization of 4-aminocatechol with aniline and its usefulness for supercapacitors and electrocatalytic effect.